

Seasonal thermal energy storage of solar heat

Its role in the clean heating transition in China



Tianrun Yang

Seasonal thermal energy storage of solar heat
Its role in the clean heating transition in China

Tianrun Yang

Seasonal thermal energy storage of solar heat: Its role in the clean heating transition in China

Tianrun Yang

杨天润

Seasonal thermal energy storage of solar heat: Its role in the clean heating transition in China

PhD dissertation, Copernicus Institute of Sustainable Development, Utrecht University, the Netherlands

This research was funded by the China Scholarship Council (CSC).

ISBN: 978-90-393-7629-4

Print: Ridderprint, www.ridderprint.nl

Copyright © 2024 Tianrun Yang

All rights reserved. No parts of this publication may be reproduced, stored in a retrieval system, or transmitted in any form or by any means without permission of the author and the publisher holding the copyright of the published articles.

Seasonal thermal energy storage of solar heat: Its role in the clean heating transition in China

Seizoensgebonden warmte opslag van zonnewarmte: De rol van opslag in de warmte transitie in China

(met een samenvatting in het Nederlands)

Proefschrift

ter verkrijging van de graad van doctor aan de
Universiteit Utrecht
op gezag van de
rector magnificus, prof. dr. H.R.B.M. Kummeling,
ingevolge het besluit van het college voor promoties
in het openbaar te verdedigen op

maandag 29 januari 2024 des ochtends te 10.15 uur

door

Tianrun Yang

杨天润

geboren op 11 juli 1992
te Liaoning, China

Promotor:

Prof. dr. G.J. Kramer

Copromotor:

Dr. W. Liu

Beoordelingscommissie:

Dr. ir. W.H.J. Crijns-Graus

Prof. dr. W. Hu

Prof. dr. H. Lund

Prof. dr. E. Worrell

Prof. dr. X. Zhang

What's past is prologue.

— William Shakespeare (The Tempest)

欲买桂花同载酒，

终不似，少年游。

— 刘过《唐多令·芦叶满汀洲》

(Even if I can buy laurel wine for you and get afloat as before, could our youth renew?)

SUMMARY

Since the adoption of the Paris Agreement, countries and regions have been submitting their climate action plans, aiming to achieve carbon neutrality in the coming decades to combat climate change. A transition from a fossil fuel-based to a renewable energy-based energy system is essential to achieve these goals. Action is being taken in the power generation sector. However, the transition in the heating sector, which is the focus of this thesis, has received relatively less attention.

Space and water heating are essential energy services, accounting for nearly half of global energy use in buildings, 63% of which is provided by fossil fuel combustion. Since fossil fuels are fundamentally storable and renewables almost invariably less so, the seasonality of heat demand in the built environment provides a real challenge for the decarbonization of this sector. Seasonal thermal energy storage (STES) can harvest and store solar thermal energy in summer and use it for heating in winter, and could thereby be an enabler for the transition to fossil fuel-free heat supply.

This thesis aims to conduct an in-depth analysis and optimization of STES technologies employing solar heat from technical, economic, environmental, and implementation feasibility perspectives to identify their overall attractiveness in the heating market and to assess their benefits in the clean heating transition and renewable power integration. Since heat demand is climate-dependent and building stocks and building traditions differ between nations and regions, such an analysis must necessarily be regionally specific. The analysis in this thesis focuses on the heat transition in the built environment in China. China is the world's largest heat consumer with a CO₂ emission intensity 30% higher than the world average and faces significant challenges for a carbon-neutral future.

We first conduct a comprehensive techno-economic review analysis of STES technologies based on previous research and projects worldwide to provide a general overview of the development status, barriers, and economic competitiveness of STES technologies in the current heating market. The results show that latent and thermochemical heat storage technologies are advantageous in terms of technical performance, such as high energy density and few geological requirements, while sensible heat storage is more mature and has a lower levelized cost of heat. Configuration parameters and technical performance have a significant impact on economic performance. We find that only pit and aquifer storage applications are economically competitive with decentralized natural gas boilers and solar heating.

Second, we study STES technologies at four locations in China to assess how the local context impacts the optimal configuration planning, techno-economic-environmental performance, and feasibility of STES applications. The results show that the prospects for STES of solar heat vary across China. In northern China, the implementation of STES

technologies can increase the renewable energy penetration in fossil fuel-based district heating at a low CO₂ avoidance cost. In southern China, where electric heating dominates, electricity system decarbonization is a more cost-effective route to heat decarbonization than STES technologies. STES implementation is attractive in locations with rich solar resources, high heating loads, and current coal-based heating systems. The key technical parameters for achieving optimal techno-economic-environmental performance and determining the configuration planning of STES technologies in different climate zones are also investigated. We conclude that solar collector area and borehole number are the most influential variables in system configurations. Appropriately reducing the borehole number for the STES system in cold climates and increasing the solar collector area in warm climates is conducive to achieving a lower CO₂ avoidance cost.

Third, we zoom in on the most promising regions for STES to compare the technical, economic, and environmental performance of STES with other sustainable heating technologies and their implementation feasibility at the local level. It is found that STES of solar heat is attractive with competitive levelized cost of heat and CO₂ avoidance cost compared to natural gas boiler, biomass boiler, electric boiler, and solar-assisted ground source heat pump. It is a promising technology with a decreasing levelized cost of heat and increasing CO₂ emission reduction ability, although its residential acceptance in China is relatively low and requires a long investigation and underground construction period.

Finally, we study STES in the context of the regional energy system. We specifically evaluate the impact of replacing (coal-based) district heating systems with STES on the regional power and heat supply and the effects that the introduction of STES has on renewable power integration. We conclude that replacing fossil fuel-based district heating systems with STES technologies can reduce fossil fuel consumption and CO₂ emissions across the combined heat and power systems at an affordable cost. STES in fact facilitates the integration of wind and solar power into power grids by reducing curtailment. As more solar and wind power is added to the grid, the benefits of such substitution increase. Thus, STES of solar heat offers an attractive option for realizing a sustainable heating transition in line with the carbon-neutral target.

SAMENVATTING

Nadat de klimaat overeenkomst van Parijs was ondertekend, hebben landen en regio's hun klimaatactieplannen ingediend, met als doel om in de komende decennia een koolstofarme maatschappij te creëren. Een overgang van een op fossiele brandstoffen gebaseerd energiesysteem naar een op hernieuwbare energie gebaseerd energiesysteem is essentieel voor het bereiken van deze maatschappij. Het opwekken van elektriciteit krijgt al jaren aandacht. De transitie in de warmte sector, waar dit proefschrift zich op richt, heeft echter relatief minder aandacht gekregen.

Het gebruik van verwarming is een belangrijke levensbehoefte. De helft van het energiegebruik van gebouwen wordt gebruikt voor verwarming, waarvan 63% door verbranding van fossiele brandstof wordt gegenereerd. Fundamenteel gezien zit er heel veel energie opgeslagen in fossiele brandstof, terwijl energie gegenereerd uit hernieuwbare bronnen extra stappen vereist om opgeslagen te worden. De seizoensgebondenheid van de warmtevraag creëert een uitdaging, waardoor het verminderen van de broeikasgas uitstoot van deze sector vermoeilijk wordt. Seizoensgebonden Warmte Opslag (SWO) kan zonnewarmte opslaan gedurende de zomer, deze warmte kan herbruikt worden in de winter en kan daarmee een sleutelrol vervullen in de transitie naar een fossiel vrije warmte generatie.

Dit proefschrift beoogt een analyse en optimalisatie van SWO technologieën in combinatie met zonnewarmte te doen. Hierbij wordt zowel gefocust op de technologische, economische en milieutechnische aspecten als op de haalbaarheid van de implementatie. Waardoor de waarde van deze SWO technologieën voor de warmte transitie bepaald kan worden. Omdat warmte gebruik klimaatafhankelijk is en architectuur van gebouwen verschilt tussen regio en landen moet de focus van deze analyse specifiek op een regio zijn. In dit geval is gekozen om de focus op China te leggen. China is grootste warmte gebruiker op aarde met een koolstof uitstoot intensiteit die 30% hoger ligt dan het gemiddelde op aarde. Daarmee ligt er een grote uitdaging voor China in het verschiep om CO₂ neutraal te worden.

Als eerste maken we een uitgebreide technisch economische overzicht van de SWO technologieën. Dit is gebaseerd op eerdere onderzoeken en projecten en heeft als doel om een breed overzicht te geven van de ontwikkeling, barrières en economische rendabiliteit van SWO technologieën gezien de huidige warmte markt. De resultaten tonen aan dat latente en thermochemische warmteopslagtechnologieën beter presteren wat betreft de technische aspecten. Zij hebben namelijk een hoge energiedichtheid en hebben weinig geologische vereisten. “Sensible” warmte opslag is daarentegen volwassener en heeft een lagere genivelleerde kosten. Hierbij is aangetoond dat configuratieparameters en technische prestatie van groot belang zijn voor de economische rentabiliteit. Alleen van bodem energie

in de vorm van een kuil of een watervoerende laag is aangetoond dat deze economisch gezien kunnen concurreren met individuele gas ketels en zonnewarmte.

Als tweede zijn de SWO technologieën op vier locaties in China bestudeerd om vast te stellen hoe de optimale configuratieplanning, technisch-economische-milieuprestaties en haalbaarheid van SWO-toepassingen beïnvloedt wordt door de lokale context. De resultaten laten zien dat het toekomstperspectief voor SWO van zonnewarmte in China varieert. In het noorden van China kan de implementatie van SWO-technologieën het aandeel van hernieuwbare energie in een warmtenetwerk, dat opereert op basis van fossiele brandstoffen, verhogen. In het zuiden van China, waar veel gebouwen verwarmt worden met elektriciteit, is het vanuit een milieuperspectief effectiever om te kijken naar het uitstoot vrij maken van de elektriciteit in plaats van de warmte. De implementatie van SWO is aantrekkelijk op locaties met veel zonne-energie, een hoge warmtevraag en een bestaand warmtenetwerk dat gevoed wordt met warmte gegenereerd door de verbranding van kolen. De belangrijkste technische parameters voor het bereiken van optimale technisch-economische en milieuprestaties en het bepalen van de configuratieplanning van SWO-technologieën in verschillende klimaatzones worden ook onderzocht. De conclusie hiervan is dat het oppervlak van de zonnecollector en het aantal boorgaten de meest invloedrijke variabelen zijn het configureren van een systeem. Door het aantal boorgaten voor het SWO-systeem in koude klimaten te verminderen en het oppervlak van de zonnecollector in warme klimaten te vergroten, kan voor minder geld de reductie in CO₂ uitstoot vergroot worden.

Als derde duiken we dieper in de meest veelbelovende regio's voor SWO om de technische, economische en milieuprestaties van SWO te vergelijken met andere duurzame verwarmingstechnologieën en hun haalbaarheid van implementatie. Hieruit is gebleken dat SWO kan concurreren met gas ketel, biomassa ketels, elektrische ketel en een warmte koude opslag systeem gekoppeld met zonne-energie op basis van de genivelleerde kosten en de kosten per kg CO₂ uitstoot. SWO is een veelbelovende technologie waarvan de genivelleerde kosten dalen en waardoor de CO₂ uitstoot daalt. Een kanttekening is echter dat de bereikbaarheid voor installatie van een SWO in de Chinese woonwijken relatief laag is daarbovenop is er veel onderzoek nodig en kost het veel tijd om een SWO aan te leggen.

Tot slot bestuderen we SWO in de context van het regionale energiesysteem. We evalueren de impact van het vervangen van (op kolen gebaseerde) warmtenetwerk door een SWO op de regionale elektriciteits- en warmtevoorziening en de effecten die de introductie van SWO heeft op de integratie van duurzame elektriciteit in het elektriciteitsnetwerk. We concluderen dat het vervangen van het warmtenetwerk op basis van fossiele brandstoffen door SWO-technologieën het verbruik van fossiele brandstoffen en de CO₂-uitstoot tegen een betaalbare prijs kan verminderen voor zowel het elektriciteitsnetwerk als het warmtenetwerk. SWO vergemakkelijkt de integratie van wind- en zonne-energie in elektriciteitsnetten, omdat het de belemmeringen voor uit hernieuwbare energiebronnen geproduceerde elektriciteit tot een minimum beperkt. Naarmate er meer zonne- en windenergie in het net wordt opgewekt,

nemen de voordelen van een dergelijke vervanging toe. SWO van zonnewarmte biedt dus een aantrekkelijke optie voor het realiseren van een duurzame verwarmingstransitie in lijn met de koolstofneutrale doelstelling.

CONTENTS

CHAPTER 1	Introduction	17
CHAPTER 2	Seasonal thermal energy storage: A techno-economic literature review	31
CHAPTER 3	Techno-economic-environmental analysis of seasonal thermal energy storage with solar heating for residential heating in China	75
CHAPTER 4	Integrated assessment on the implementation of sustainable heat technologies in the built environment in Harbin, China	115
CHAPTER 5	Seasonal thermal energy storage employing solar heat: A case study of Heilongjiang, China, exploring the transition to clean heating and renewable power integration	155
CHAPTER 6	Conclusions	185
BIBLIOGRAPHY		197
ACKNOWLEDGMENTS		221
CURRICULUM VITAE		225
PUBLICATIONS		227



1

Introduction

Climate change is one of the greatest threats to human well-being and planetary health that modern humans have ever faced, potentially causing rising sea levels, extreme weather events, and declining biodiversity [1]. The main driver of observed climate change is greenhouse gas emissions from human activities, of which CO₂ is the main contributor [2]. Energy accounts for more than two-thirds of global greenhouse gas emissions, with half coming from fuel combustion for electricity and heat generation [3].

The Paris Agreement was signed by 195 parties at the United Nations Climate Change Conference in Paris, France, in 2015 to hold the increase in the global average temperature to well below 2 °C and to pursue efforts to limit the temperature increase to 1.5 °C above pre-industrial levels [4].

1.1. The global energy transition and in the special case of China

Since 2020, countries have been submitting their national climate action plans, aiming to achieve carbon neutrality in the following decades. The adoption of the Paris Agreement highlights the urgent need for an energy transition from a fossil fuel-based to a renewable energy-based energy system. Actions in electricity generation are observed [5] (Figure 1.1). The share of fossil fuels in global electricity generation fell by 6% over the last decade, while the percentage of wind and solar power increased from 1.6% and 0.1% to 6.0% and 3.1%, respectively.

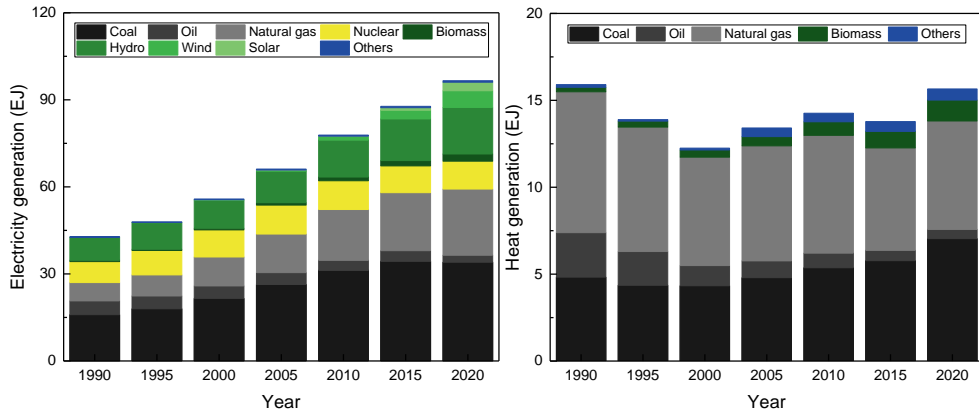


Figure 1.1. Electricity (left) and heat (right) generation in the world by source between 1990 and 2020 [5].

However, there is a lack of effective change in the heating sector. Fossil fuels meet almost 90% of heat demand. Space and water heating are essential energy services, accounting for almost half of global energy use in buildings, leading to around 4100 Mt CO₂ emissions in 2022 [6]. Around 40% of households worldwide require space heating during part of the year,

with heating being a major component of residential energy expenditure, particularly in colder climates.

China is the world's largest consumer of primary energy, consuming about 157.7 EJ in 2021, 64.7 EJ more than was consumed by the United States, which ranks second [7] (Figure 1.2). Most primary energy is still derived from fossil fuels, especially coal, making China the largest emitter of CO₂, accounting for nearly 31% of global emissions in 2021 [8]. China has committed to peak CO₂ emissions before 2030 and achieve carbon neutrality before 2060 [9]. Reducing CO₂ emissions in China would be an unparalleled contribution to climate change mitigation [10].

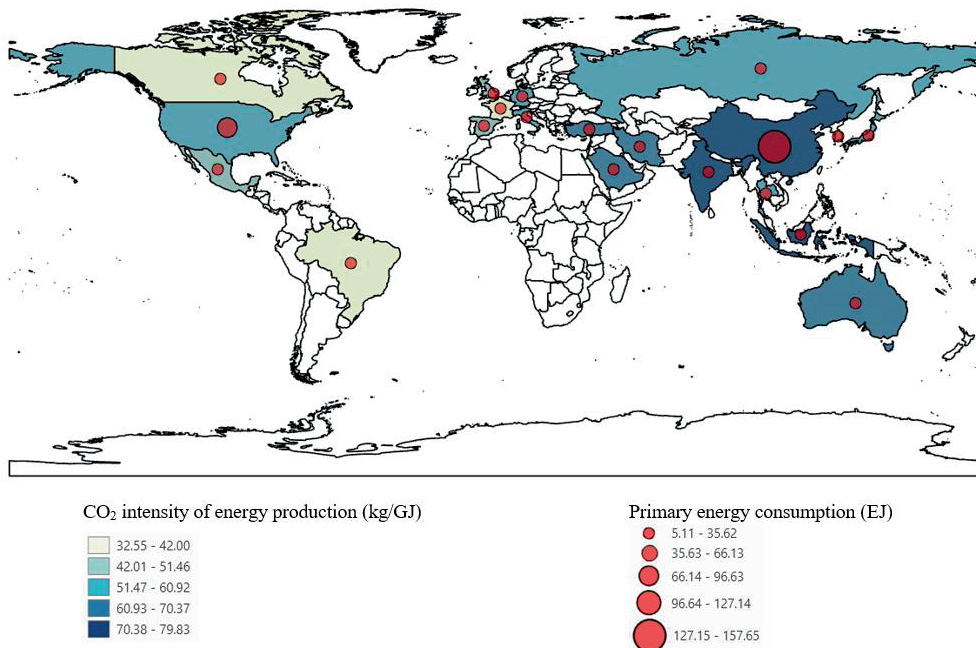


Figure 1.2. Primary energy consumption and CO₂ intensity of energy production by country in 2021 (Top 20 energy consumer) [7, 11].

China is shifting its power generation structure faster than the world average (Figure 1.3). The share of fossil fuels in electricity generation fell by 13% over the last decade, while the percentage of wind and solar power increased from 1.1% and 0 to 6.0% and 3.4%, respectively [5]. However, fossil fuels still dominate heat generation (99%). China has set a target to double the amount of wind and solar power generation by 2025 and to increase the share of non-fossil sources in energy consumption to 25% by 2030 and more than 50% by 2050 [12, 13]. In addition to decarbonizing the electricity sector, a clean transition in the heating sector is essential to achieve the carbon-neutral goal.

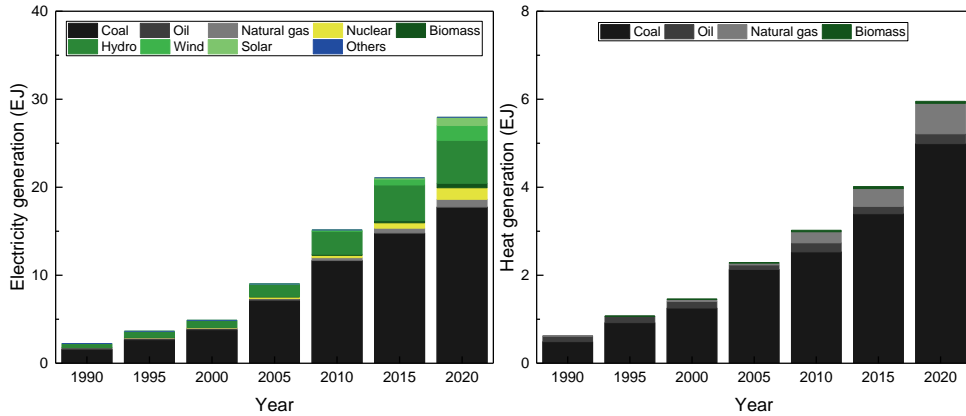


Figure 1.3. Electricity (left) and heat (right) generation in China by source between 1990 and 2020 [5].

1.2. Heat in the built environment in China

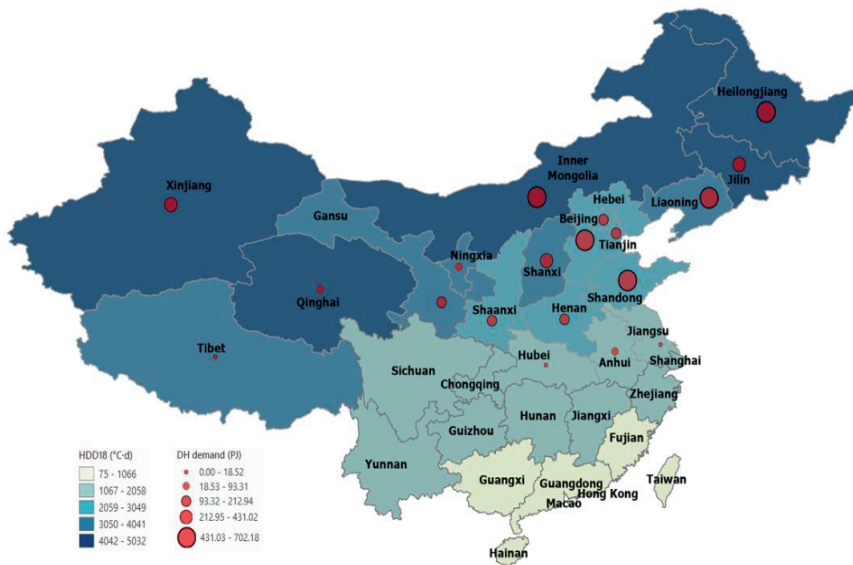


Figure 1.4. Heating degree day and district heating demand in China [14, 15].

The climate varies widely across China, with the country's latitude ranging from 4°N to 53°N, which has a significant impact on the demand for space heating. The heating degree day (HDD) and district heating demand in China are shown in Figure 1.4, where HDD18 refers to the number of degrees that a day's average temperature is below 18 °C. District heating systems are widely used in northern cities, where coal-fired cogeneration units and boilers are the primary heating sources due to the abundant supply and low price of coal [16].

Chapter 1

In rural areas, residents mainly use decentralized coal and biomass stoves. In southern regions, decentralized residential space heating systems, including air conditioners (highest share), electric heaters, and gas boilers, are widely used [17].

China has the largest district heating system in the world, accounting for 40% of global district heating production, with a CO₂ emission intensity 30% higher than the world average [18]. The length of the district heating network increased from 954 km in 1985 to over 461,493 km in 2021, with an average annual growth rate of 19% [19]. In 2021, the total heated area was 10.6 billion m², covering about 203 million people in northern China. The heating sector consumed 441.8 million tons of coal (equivalent to 7.9 EJ), accounting for 10.3% of China's total coal demand. As the heating industry in China uses coal as its primary fuel source, it causes severe air pollution and health damage [20].

To alleviate environmental pollution and carbon emissions caused by coal-dominated heating, China issued the *Clean Winter Heating Plan in Northern China (2017–2021)*, clarifying the definition of clean heating for the first time [21]. Clean heating in the plan refers to the use of natural gas, electricity, geothermal energy, biomass, solar energy, industrial waste heat, and nuclear energy to achieve low-emission and low-energy-consumption heating methods through highly efficient heating systems. The implementation of this plan requires local authorities to comprehensively evaluate and select appropriate sustainable heating technologies based on local conditions.

Among these measures, natural gas is not preferred for a long-term transition to fully renewable energy. Electric heating generates more carbon emissions than coal-fired heating due to the current power structure in China, which is dominated by coal-fired power [22]. With the goal of rapidly developing renewable power generation, electric heating could be a favorable alternative heating method in the coming decades.

China has rich geothermal resources, equivalent to 825.2 YJ [23]. However, the distribution of resources is uneven (Figure 1.5). The high-temperature geothermal resources are mainly scattered in the Mediterranean-Himalayan tropical zone (southern Tibet, southern Yunnan, and western Sichuan) and the Pacific Rim tropical zone (Taiwan). The low-medium temperature geothermal resources are mainly distributed in the southeastern coastal area and Cenozoic large and medium sedimentary basins.

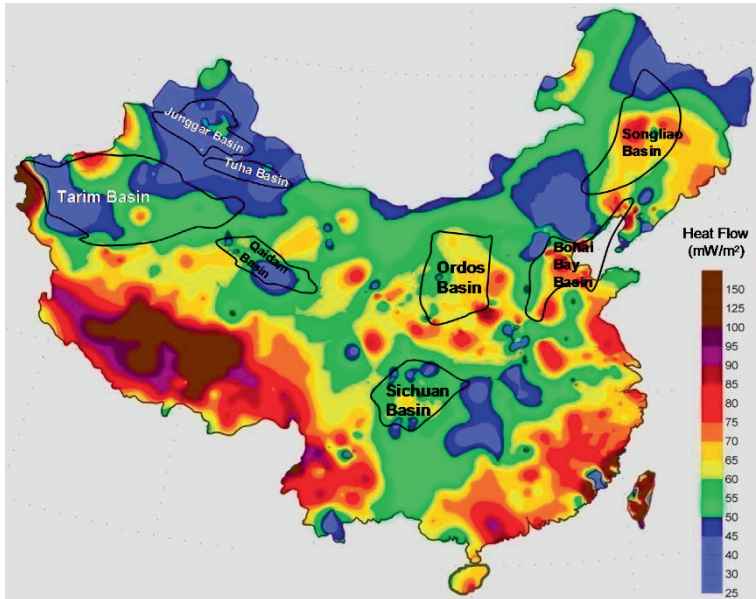


Figure 1.5. Geothermal resources in China [24].

The waste heat potential in China is estimated to be 58.4 EJ, mainly from the electricity generation and industry sectors [25]. Cogeneration units have been widely implemented in northern China, and industrial waste heat sources are located far away from the urban heat load center [26]. Like geothermal energy, the use of waste heat for heating depends on the local availability of heat sources; therefore, it is not universally feasible in all regions.

As the largest agricultural country, China has abundant biomass resources (Figure 1.6). The theoretical reserve of biomass resources in China is 22.7 EJ, including agricultural waste, forestry waste, municipal solid waste, and sewage sludge [27]. Biomass can exist as a solid, liquid, or gaseous fuel that can be used in the electricity, heating, and transport sectors. The energy demand for the electricity and transport sectors in China in 2020 was 28.0 EJ and 12.1 PJ, respectively [28]. Local biomass resources are insufficient to sustain the electricity sector. As suggested in previous studies, the use of biomass for heating is not socio-economically optimal [29]. The heating sector should reduce its biomass consumption, leaving biomass for other sectors to support decarbonization transitions [30, 31].

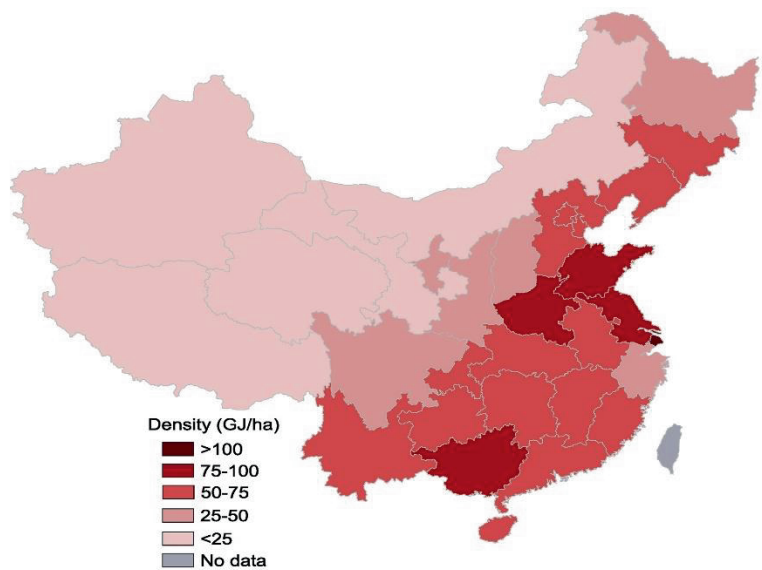


Figure 1.6. Biomass resource density in China [27].

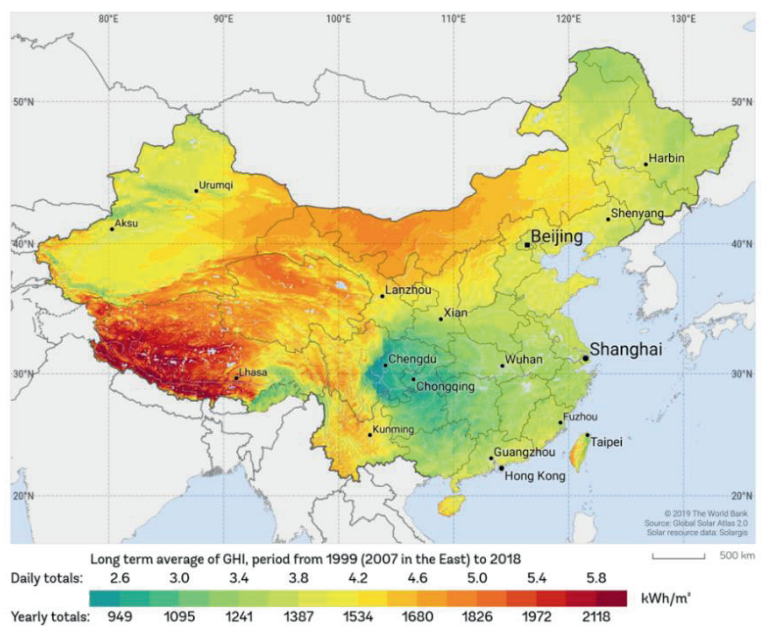


Figure 1.7. Average global horizontal irradiation in China [32].

Generally, solar radiation is abundant in China (Figure 1.7), with more than two-thirds of the country receiving more than 5000 MJ/m² of irradiance and more than 2200 hours of sunshine per year [33]. Although China accounts for more than 70% of the global solar collector installations, solar thermal has contributed little to space heating in China (less than 0.3%)

[34]. The majority is used as individual water heaters for domestic hot water. With abundant solar resources and favorable policies, solar heating holds broad application prospects in China.

The demand for district heating in the built environment in China does not match the distribution of sustainable heat resources (**Figure 1.8**). Northern areas have high heat demand, but sustainable heat resources are located in southern regions. Especially for the northeastern provinces, there is a need for a universally applicable method to contribute to the clean heating transition. Among the presented sustainable heat resources, the use of biomass, geothermal, and waste heat for heating purposes is highly dependent on the local availability of heat sources. Solar heating can be a universally feasible method for all of China except the Sichuan Basin. The inherent intermittency of solar energy can be overcome by applying seasonal storage to effectively balance the mismatch between high solar gains in summer and high heat demand in winter. In this thesis, we focus on seasonal thermal energy storage (STES) of solar heat, exploring its role in the clean heating transition in China.

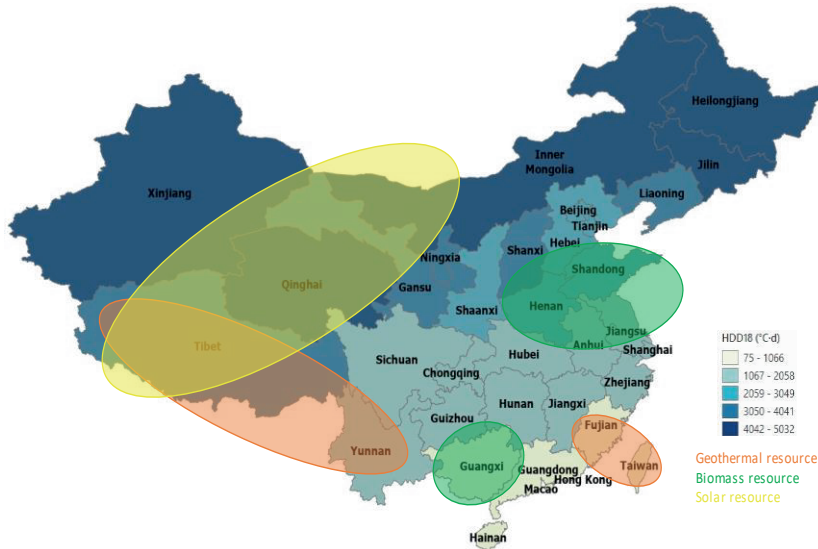


Figure 1.8. Heating degree day and sustainable heating resources in China.

1.3. Seasonal thermal energy storage

Heating in the built environment is, by definition, seasonal. A challenge for decarbonizing heating in the built environment is the seasonal mismatch between heat demand and generation from sustainable sources. Many sustainable heat supply systems are characterized by high initial investment and low operating costs [22]. Therefore, an installed capacity tailored at peak demand is not cost-effective. Extending the operating period to an annual level can help meet energy demand, reduce costs, and achieve decarbonization. Optimal use

Chapter 1

of sustainable heat requires long-term storage to accommodate seasonal demand and supply variations.

STES technologies can harvest and store solar thermal energy in the summer and use it for heating in the winter, facilitating the replacement of fossil fuel-based heat supply and coordinating the magnitude of the seasonal mismatch between heat supply and demand [35]. As the combustion of fossil fuels dominates global residential heating demand, STES of solar heat offers an attractive option for achieving a sustainable heating transition.

The technical feasibility of STES technologies employing solar heat has been widely demonstrated. It has been researched and implemented in Europe [36, 37], Asia [38, 39], North America [40, 41], and Oceania [42, 43]. Applications include buildings [44], greenhouses [45], campuses [46], communities [40], and large-scale district-level systems [47]. However, their overall attractiveness compared with other sustainable heating options, economic and environmental performance, and implementation feasibility at the local level remain unclear. Insight into how the local context (climate conditions and existing heating infrastructure) impacts the technical, economic, and environmental performance of STES technologies is limited.

In addition to reporting the technical performance of STES applications, previous studies have introduced methods for STES system optimization [48-52]. However, they either ignored the environmental aspect or failed to draw a general conclusion on identifying the key parameters and quantifying their influence on the optimization results. There is a need for a better understanding of the optimal economic and environmental performance of STES applications and the conditions to achieve it in different climate zones. It requires an integrated optimization criterion and method to select the optimal solution.

From an energy system perspective, the scope of previous studies has been limited to individual projects, whereas the impact of STES applications on power and district heating systems remains unknown. Knowledge of the ability of STES technologies to facilitate the integration of renewable energy is limited. There is a need to assess the feasibility of replacing district heating systems with STES technologies on a regional scale and to quantify the economic and environmental consequences of such a replacement from an electricity and district heating system perspective.

1.4. Research objectives and research questions

Given the knowledge gaps identified above, this thesis aims to conduct an in-depth analysis and optimization of STES technologies employing solar heat from technical, economic, environmental, and implementation feasibility perspectives to identify their overall attractiveness in the heating market and to assess their benefits in the clean heating transition and renewable power integration. Since heat demand is climate-dependent and building stocks and building traditions differ between nations and regions, such an analysis must

necessarily be regionally specific. The analysis in this thesis focuses on the heat transition in the built environment in China, as China is the world's largest heat consumer with a CO₂ emission intensity 30% higher than the world average [18] and faces significant challenges for a carbon-neutral future. To fulfill the research objective, the following research questions are formulated:

Q1. What is the overall attractiveness of STES technologies compared to other sustainable heating options in terms of techno-economic-environmental performance and implementation feasibility at the local level?

Q2. How do local climate conditions and existing heating infrastructure impact the technical, economic, and environmental performance of STES technologies?

Q3. What are the key technical parameters and their influence on achieving the optimal techno-economic-environmental performance of STES technologies in different climate zones?

Q4. What are the technical feasibility and economic and environmental consequences of replacing the district heating system with STES technologies and its impact on renewable power integration?

Table 1.1 Overview of the chapters and their corresponding research questions.

Chapter	Topic	Research questions			
		Q1	Q2	Q3	Q4
2	Seasonal thermal energy storage: A techno-economic literature review	X			
3	Techno-economic-environmental analysis of seasonal thermal energy storage with solar heating for residential heating in China		X	X	
4	Integrated assessment on the implementation of sustainable heat technologies in the built environment in Harbin, China	X			
5	Seasonal thermal energy storage employing solar heat: A case study of Heilongjiang, China, exploring the transition to clean heating and renewable power integration				X

An overview of the thesis chapters and the research questions they address is given in Table 1.1. We first conduct a comprehensive techno-economic review analysis of STES technologies based on previous research and projects worldwide to provide a general overview of the development status, barriers, and economic competitiveness of STES technologies in the current heating market. Second, we study STES technologies at four locations in China to assess how the local context impacts the optimal configuration planning, techno-economic-environmental performance, and feasibility of STES applications. The key technical parameters for achieving optimal techno-economic-environmental performance and determining the configuration planning of STES technologies in different climate zones are investigated. Third, we zoom in on the most promising regions for STES to compare the

technical, economic, and environmental performance of STES with other sustainable heating technologies and their implementation feasibility at the local level. Finally, we study STES in the context of the regional energy system. We specifically evaluate the impact of replacing (coal-based) district heating systems with STES on the regional power supply and the effects that the introduction of STES has on renewable power integration.

1.5. Thesis outline

Chapter 2 partially answers research question 1 by providing a comprehensive techno-economic review analysis of STES based on 60 projects worldwide covering six STES types, classified according to their storage mechanisms. The development status, barriers, and a representative project of each STES type are introduced. Key operating parameters and their relationships and trends are examined. From an economic perspective, the levelized cost of heat (LCOH), storage volume cost, and storage capacity cost are calculated, and the relationships between economic and technical parameters are identified. Furthermore, a radar plot is drawn to provide a clear understanding of the advantages and disadvantages of each STES type. The LCOHs of different STES types are compared with two current heating options to present the economic competitiveness of STES in the current heating market. Finally, a decision tree considering different STES types is presented to guide potential STES selection, facilitating practical engineering.

Chapter 3 addresses research questions 2 and 3 by quantifying how the local context (climate conditions and existing heating infrastructure) impacts the optimal configuration planning, techno-economic-environmental performance, and feasibility of STES application. This chapter performs a techno-economic-environmental analysis of the application of STES with solar heat at four locations with different climates and heating infrastructures in China, based on the developed TRNSYS model. The key technical parameters to achieve the optimal techno-economic-environmental performance and determine the configuration planning of STES in different climate zones are investigated. An integrated optimization criterion is proposed by including economic and environmental impacts to perform multi-objective optimization on STES system configurations and determine the optimization pathways for different climates. The position of STES compared to other sustainable heating options is identified considering the local context of the four case studies.

Chapter 4 targets research question 1 by investigating the technical, economic, and environmental performance of seven sustainable heating technologies (including STES with solar heat), considering the case of a community in northern China alongside current policies and future renewable energy scenarios. Their implementation feasibility is assessed through semi-quantitative analysis. Since some sustainable heating technologies are dominated by electricity, a power structure for future renewable scenarios is developed based on government policies, reports, and renewable energy potentials. Two perspectives on electricity price forecasting are proposed to deal with the uncertainty of China's electricity

marketization. Uncertainty in economic valuation in future scenarios is addressed by applying the Monte Carlo method.

Chapter 5 addresses research question 4 by evaluating the technical feasibility and the economic and environmental consequences of replacing district heating systems with STES, as well as the impact on renewable power integration. This chapter quantifies the impact of large-scale STES applications on the electricity and district heating sectors of a regional energy system by applying two future scenarios. The extent to which STES with solar heat can replace the traditional fossil fuel-based district heating system in a densely populated area is examined. The economic and environmental consequences of gradually replacing district heating with STES in a regional electricity and district heating system are evaluated until 100% replacement is achieved. The extent to which STES can increase the penetration of renewable energy in the electricity system is quantified.

Chapter 6 summarizes the main findings of chapters 2–5, policy implications, and recommendations for further research.



2

Seasonal thermal energy storage: A techno-economic literature review

Published in: Yang T, Liu W, Kramer GJ, Sun Q. Seasonal thermal energy storage: A techno-economic literature review. Renewable and Sustainable Energy Reviews 2021;139:110732.

Abstract

Seasonal thermal energy storage (STES) holds great promise for storing summer heat for winter use. It allows renewable resources to meet the seasonal heat demand without resorting to fossil-based back up. This paper presents a techno-economic literature review of STES. Six STES technologies are reviewed, and an overview of the representative projects is provided. The key project parameters and operation performances, including the main heat source fraction, storage efficiency, and energy density, are investigated in the technical review. The economic viability is assessed in terms of the levelized cost of heat (LCOH), storage volume cost, and storage capacity cost. The results show that the tank and pit thermal energy storage exhibits relatively balanced and better performances in both technical and economic characteristics. Borehole and aquifer thermal energy storage exhibits better economic performance, while latent and thermochemical heat storage exhibits better technical performance. Compared to the reference heating alternatives, i.e., natural gas and solar heating for decentralized systems, only pit and low-temperature aquifer thermal energy storage is economically competitive. The LCOH of latent heat storage is the highest. To be economically competitive in the heating market, the LCOH of STES needs to be reduced by half to four times less. Meanwhile, a decision tree for STES selection is introduced to facilitate practical engineering. In compiling the data for this review, we find that STES economic studies are limited in number and often lack transparency in their reporting. Going forward, this should be improved to provide a more solid base for policymaking.

Chapter 2

Nomenclature

E_t	annual heat production (MWh _{th})
F	fraction
I	investment cost (€)
N	number
n	lifetime
Q	thermal energy (MWh _{th})
r	real discount rate
t	time

Greek symbols

η	efficiency
--------	------------

Abbreviations

ATES	aquifer thermal energy storage
BTES	borehole thermal energy storage
COP	coefficient of performance
COS	cost of storage
GSHP	ground source heat pump
HP	heat pump
LCOE	levelized cost of energy
LCOH	levelized cost of heat
LHS	latent heat storage
PCM	phase-change material
PTES	pit thermal energy storage
O&M	operation and maintenance

ORC	organic rankine cycle
SC	storage capacity
SCC	storage capacity cost
SHS	sensible heat storage
STES	seasonal thermal energy storage
SV	storage volume
SVC	storage volume cost
THS	thermochemical heat storage
TTES	tank thermal energy storage

Subscripts

cyc	cycle
MHS	main heat source
s	storage
sc	storage capacity
th	thermal power

2.1. Introduction

The built environment accounts for a large proportion of worldwide energy consumption, and consequently, CO₂ emissions. For instance, the building sector accounts for ~40% of the energy consumption and 36%–38% of CO₂ emissions in both Europe and America [53, 54]. Space heating and domestic hot water demands in the built environment contribute to ~40% of energy use in the mid- and high-latitude countries, which is expected to rise by 50% by 2050 [55]. Because of the continued increase in the world population and building stock, the heat demand in the built environment is expected to increase in the coming decades [56]. This growth and dominance of fossil fuels in heat supply systems in countries with a cold climate is the main challenge faced in combating climate change and causes a serious issue of local air pollution.

The applications of seasonal thermal energy storage (STES) facilitate the replacement of fossil fuel-based heat supply by alternative heat sources, such as solar thermal energy, geothermal energy, and waste heat generated from industries. In the STES system, the thermal energy primarily generated from sustainable sources is harvested and stored in summer, to be used in winter. It serves as a supplement and adjustment of the heat supply system and shows the potential to coordinate the seasonal mismatch between the heat supply and demand [57], and further improves the overall efficiency of the heating system [58]. Depending on their storage mechanisms, the STES concepts can be classified into three main types: sensible heat storage (SHS), latent heat storage (LHS), and thermochemical heat storage (THS) (Figure 2.1).

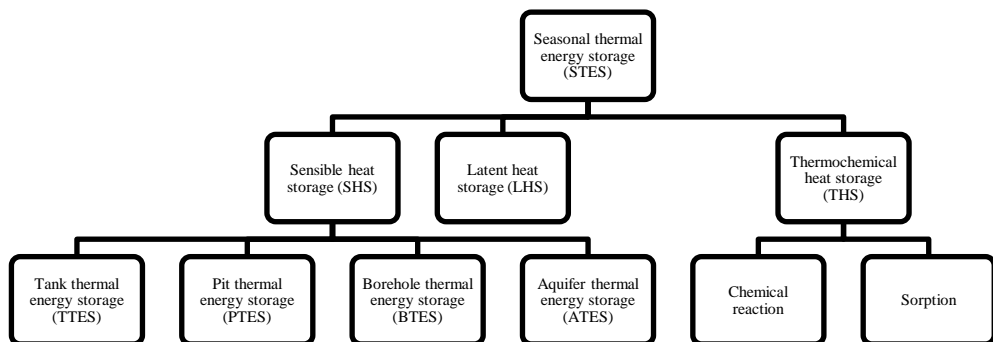


Figure 2.1. Summary of current STES technologies.

The development of various STES technologies has been extensively studied from a technical perspective. Xu et al. [59] presented a fundamental review on SHS, LHS, and THS, focusing on storage materials, existing projects, and future outlook. Guelpa and Verda [60] investigated the implementation of STES incorporated with district heating systems and assessed the technical potential of applying STES to various energy systems. The

technological status, future development, and market prospect of STES in the UK were reviewed and evaluated in [61]. The developments and recent trends of large-scale solar district heating plants in Denmark were reviewed in [62], and the STES projects in Germany were reviewed in [63].

A few studies have focused on one or two specific STES technologies. Schmidt et al. [64] examined the design concepts and tools, implementation criteria, and specific costs of pit thermal energy storage (PTES) and aquifer thermal energy storage (ATES). Shah et al. [65] investigated the technical element of borehole thermal energy storage (BTES), focusing on ground-heat exchangers, solar collectors, and computer simulation tools. Dahesh et al. [66] evaluated the design, modeling, and construction of tank thermal energy storage (TTES) and PTES, while Bott et al. [67] focused on detailed technical elements, including thermal insulation, filling, and waterproofing. The LHS techniques—including phase-change material (PCM) incorporated into a solar collector, storage tank, heat exchanger, as well as PCM slabs and packed bed PCM—were summarized in [68, 69]. The methods of heat-transfer enhancement and design configurations of PCM were evaluated in [70]. Fleuchaus et al. [71] reviewed the historical and technical development, spatial distribution, and market barriers of ATES. The system configurations, suitable materials, and simulation models of THS-incorporating solar energy in buildings were reviewed in [72]. The performance of SHS, combined with heat pumps (HPs) in building projects, was examined in [57], and its energy and exergy performances were evaluated in [73].

Besides the technical viewpoint, a few studies have also documented a brief review of one or two specific STES technologies from an economic viewpoint. For example, Scapino et al. [74] conducted a comparative study on the cost of storage capacity and energy density of liquid and solid sorption storage systems in the application of low-temperature space heating. Böhm and Lindorfer [75] conducted a techno-economic assessment of THS in a district heating system, considering multiple heat sources, e.g., solar thermal energy, geothermal energy, and industrial waste heat. Huang et al. [76] conducted an economic analysis of TTES, combined with solar thermal energy as a heat resource and natural gas boilers as auxiliary heating devices within different technological constraints, e.g., heating terminal units, heating load intensities, and heated areas. They also investigated the feasibility of solar district heating, combined with STES in China, from technical, economic, social, and policy perspectives [34].

Given the above discussion, there is a lack of a comprehensive techno-economic review of STES. A review of the economic competitiveness of STES in the heating market is missing. A better understanding of both technical and economic performances of STES in diverse application contexts can help the decision-making process of selecting and positioning STES in a sustainable heating system. This paper aims to learn the recent developments made in STES by conducting a comprehensive review of both technical and economic parameters and identify the lessons learned from the previous projects to facilitate the future development of

STES in a sustainable heat transition. Considering this objective, a summary of the methodology is first provided, followed by the review results of the technical and economic performances of the examined STES projects, lessons learned, and suggestions for future studies.

2.2. Methodology

To fulfill the research objective, a six-step methodology was proposed and applied in this study (Figure 2.2).

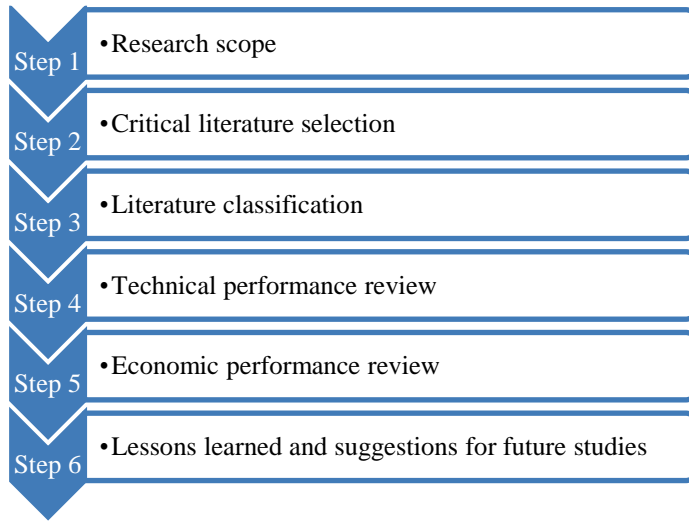


Figure 2.2. Schematic of the methodology used in this study.

2.2.1. Research scope

This study focuses on the technical and economic performances of STES, including SHS, LHS, and THS. The environmental perspective is beyond the scope of this study, and therefore, not included here.

2.2.2. Critical literature selection

Over 140 studies were selected during the initial literature collection, using a keyword-based search of article titles, abstracts, and keywords in Scopus and Google Scholar. The keywords included STES, seasonal heat storage, and interseasonal storage. The studies included peer-reviewed journal articles and project reports, written in English. Because of the large collection, a second selection round was performed under the criterion that the selected study should present economic data and a detailed technical assessment. Research papers and project reports that either assessed the economic feasibility of the technologies or provided detailed cost data were prioritized. Several simulation studies were included because of the

limited transparency in the reports of the established projects. Finally, the number of studies was narrowed down to 60, with ~10 for each STES technology.

2.2.3. Literature classification

The collected studies were classified according to STES types (Figure 2.1). Table 2.1 presents an overview of the examined studies, including the year of initial operation, project scale, main heat source, and back-up heating devices. It indicates that the technical review was based on all collected papers, while the economic review was based on 35 studies because of the availability of economic data. In general, the scale of the STES projects ranged from a house to a community and varied considerably among different STES types. Most of the LHS projects were applied in a greenhouse, while the THS projects were still laboratory prototypes. All projects were located in the mid- and high-latitude countries, and ~80% of them belonged to European countries. The majority used solar thermal energy as the main heat source, followed by waste heat and geothermal energy. In addition, HPs, gas boilers, and electrical heaters were widely used as auxiliary heating devices.

Table 2.1 Overview of the examined studies.

Project location	Year of initial operation	Reference	Project scale	Main heat source	Back-up heating devices	Technical review	Economic review
TTES							
Lisse, NL	1995	[77]	One warehouse	Solar thermal	-	+	
Friedrichshafen, DE	1996	[78]	280 apartments	Solar thermal	Gas boiler	+	
Breda, NL	1996	[77]	One factory	Solar thermal	-	+	
Hannover, DE	2000	[79]	One community	Solar thermal	-	+	+
Munich, DE	2007	[80]	300 houses	Solar thermal	HP	+	+
Gaziantep, TR*	2010	[81]	One house	Solar thermal	HP	+	
Stockholm, SE*	2013	[82]	One house	Solar thermal	HP	+	
Copenhagen, DK*	2017	[83]	One house	Solar thermal	Gas boiler	+	+
Marseille, FR*	2017	[84]	One house	Solar thermal	Gas boiler	+	+
Marseille, FR*	2017	[85]	One house	Solar thermal	Gas boiler	+	+
Jincheon, KR*	2017	[86]	One community	Solar thermal	HP	+	+
Marseille, FR*	2018	[49]	8 houses	Solar thermal	Boiler	+	+
Panningen, NL	2021	[87]	3920 houses	Solar thermal + waste heat	HP	+	+
PTES							
Stuttgart, DE	1986	[88]	One institute building	Solar thermal + waste heat	HP + co-generation plant	+	
Otrupgaard, DK	1996	[89, 90]	22 houses	Solar thermal	Gas boiler	+	
Steinfurt, DE	1999	[63]	42 apartments	Solar thermal	Electrical heaters	+	+
Chemnitz, DE	2000	[79]	One residential complex	Solar thermal	Gas boiler	+	+
Eggenstein, DE	2008	[91]	One school	Solar thermal	HP + gas boiler	+	+
Osijek, HR*	2013	[92]	2000 houses	Biomass	None	+	+
Marstal, DK	2013	[93]	One community	trigeneration system	HP + bio-oil boiler + wood chip boiler with ORC unit	+	+
Dronninglund, DK	2014	[94]	One community	Solar thermal	HP + bio oil boiler + gas engine	+	+

BTES	Neckarsulm, DE	1997	[95]	One community	Solar thermal	Gas boiler	+		
	Anneberg, SE*	2002	[96]	90 houses	Solar thermal	Electrical heaters	+	+	
	Okotoks, CA	2007	[97]	52 houses	Solar thermal	Gas boiler	+	+	
	Harbin, CN	2008	[98]	One house	Solar thermal	GSHP	+		
	Emnaboda, SE	2010	[99]	One factory	Waste heat	External district heating system	+		
	Shanghai, CN	2012	[100]	One greenhouse	Solar thermal	None	+	+	
	Bredstrup, DK	2012	[101]	One community	Solar thermal	HP + gas boiler + electric boiler	+	+	
	Tianjin, CN	2013	[102]	270 houses	Solar thermal	GSHP	+	+	
	Torino, IT	2014	[103]	One laboratory	Solar thermal	-	+		
	Andalusia, ES*	2016	[104]	One community	Solar thermal	Biomass boiler	+	+	
	Ontario, CA*	2017	[105]	One greenhouse	Solar thermal	None	+	+	
	Aberdeen, GB*	2019	[106]	52 houses	Solar thermal	Gas boiler	+	+	
	Camborne, GB*	2019	[106]	52 houses	Solar thermal	Gas boiler	+	+	
	ATES								
	Scarborough, CA	1984	[107]	One community	Waste heat	HP	+		
	Berlin, DE	1999	[108]	One community	Waste heat	HP	+		
	Brasschaat, BE	2000	[109]	One hospital	None	HP	+	+	
	Rostock, DE	2000	[110]	108 houses	Solar thermal	HP + gas boiler	+	+	
	Neubrandenburg, DE	2005	[111]	One community	Waste heat	Boiler	+		
	Adana, TR	2005	[112]	One greenhouse	None	None	+	+	
	Tehran, IR*	2013	[113]	One residential complex	Solar thermal	Boiler	+		
	Groningen, NL*	2020	[114]	11700 houses	Geothermal	-	+	+	
LHS	Biot, FR	1985	[115]	One greenhouse	Solar thermal	Air heater	+		
	Trabzon, TR	1992	[116]	One laboratory	Solar thermal	HP	+		
	Reading, GB	1997	[117]	One greenhouse	Solar thermal	None	+		
	Çukurova, TR	2003	[118]	One greenhouse	Solar thermal	None	+	+	
	Elazığ, TR	2005	[119]	One greenhouse	Solar thermal	-	+	+	
	Lynby, DK	2015	[120]	One house	Solar thermal	Electrical heater	+		

THS									
Stuttgart, DE	2006	[121]	Laboratory prototype	Solar thermal	-	+	+		
Petten, NL	2012	[122]	Laboratory prototype	Solar thermal	None	+	+		
Perpignan, FR	2014	[123]	Laboratory prototype	Solar thermal	-	+	+		
Petten, NL	2014	[124]	Laboratory prototype	Solar thermal	-	+	+		
Wels, AT	2014	[125]	Laboratory prototype	Electrical heater	-	+	+		
Villeurbanne, FR	2015	[126]	One house	Solar thermal	-	+	+		
Eindhoven, NL	2017	[127]	One house	Solar thermal	-	+	+		
Loughborough, GB*	2018	[128]	Laboratory prototype	Solar thermal	-	+	+	+	
Högsölan Dalarna, SE	2005	[121]	Laboratory prototype	Solar thermal	HP	+	+	+	
Rapperswil, CH	2008	[121]	Laboratory prototype	Solar thermal	HP	+	+	+	
Gleisdorf, AT	2008	[121]	One house	Solar thermal	-	+	+	+	
Dübendorf, CH	2008	[121]	Laboratory prototype	Solar thermal	HP	+	+	+	

*simulation case study

2.2.4. Technical performance review

The development status and barriers of different STES types were first summarized to introduce an overview of STES. A representative project of each STES type was presented by showing a schematic layout to introduce an overview and major components of the STES system. The representative projects were selected because they were either the first project implemented in a country or well recognized as a successful case. The key parameters were summed up and calculated to indicate system functions and operation performances. These parameters included annual heat demand, storage volume, storage and heating temperature, heated living area, coefficient of performance (COP) of HP, main heat source fraction (F_{MHS} in Eq. (2.1)), storage efficiency (η_s in Eq. (2.2)), and the number of storage cycles per year (N_{cyc} in Eq. (2.3)). The relations among some key parameters were drawn to help plan a suitable STES system as the technical performances were sensitive to system configuration parameters. Finally, a comparative analysis was conducted between different STES concepts, as well as within the SHS technologies.

$$F_{MHS} = \frac{Q_{MHS}}{Q_{load}} \quad (2.1)$$

$$\eta_s = \frac{Q_{discharged}}{Q_{charged}} \quad (2.2)$$

$$N_{cyc} = \frac{Q_{discharged}}{Q_{sc}} \quad (2.3)$$

where Q_{MHS} is the yearly thermal energy from the main heat source distributed to the total heat demand, Q_{load} is the yearly total heat demand, $Q_{discharged}$ is the yearly thermal energy discharged from the storage, $Q_{charged}$ is the yearly thermal energy charged into the storage, and Q_{sc} is the capacity of the storage medium.

The technical performance review followed the below research steps:

- Introduced the development status, barriers, and one representative project of each STES type.
- Examined key operating parameters of each STES type.
- Identified the characteristics of applications by comparing TTES, PTES, BTES, and ATES.
- Discussed the technical potentials by comparing SHS, LHS, and THS.
- Developed matrices to analyze the trends and relations between different technical parameters.

2.2.5. Economic performance review

A detailed levelized cost of heat (LCOH) was examined using the techno-economic data available in the examined studies. The levelized cost of energy (LCOE) method is well-

Chapter 2

applied in the techno-economic analysis, which is a tool for comparing the costs of different electricity generation technologies within their lifetime. Adapting the LCOE formulation for heat production, LCOH can be expressed as

$$LCOH = \frac{I + \sum_{t=1}^n \frac{O\&M}{(1+r)^t}}{\sum_{t=1}^n \frac{E_t}{(1+r)^t}} \quad (2.4)$$

where I is the initial investment, r is the real discount rate, n is the lifetime, $O\&M$ is the annual cost of operation and maintenance, and E_t is the annual heat production.

For the studies whose detailed economic data were unavailable, the storage volume cost (SVC) and storage capacity cost (SCC) were calculated to present the economic feasibility. They are expressed as

$$SVC = \frac{COS}{SV} \quad (2.5)$$

$$SCC = \frac{COS}{SC} \quad (2.6)$$

where SV and SC are the storage volume and capacity of the storage, and COS is its cost, considering the storage medium, container or reactor, and charging and discharging device.

The economic performance review followed the below research steps:

- Calculated and compared LCOH within predesigned boundaries.
- Assessed the techno-economic parameters, namely the cost of storage volume and storage capacity for the studies lacking detailed economic data.
- Developed matrices to investigate the relations between economic and technical parameters.

2.2.6. Lessons learned and suggestions for future studies

The lessons learned from the examined STES studies were identified by summarizing, integrating, and comparing the technical and economic performance review results. A radar plot was drawn to offer a clear understanding of the advantages and drawbacks of each STES type. Furthermore, the LCOHs of different STES types were compared with two heating options for decentralized heating purposes, namely natural gas boilers and solar heating, to present the economic competitiveness of STES in the current heating market. Finally, a decision tree considering different STES types was used to facilitate practical engineering.

2.3. Technical performance review

2.3.1. SHS

2.3.1.1. TTES

TTES is a mature and mass-market technology applied in small commercial and residential buildings, as well as large-scale or district heating systems [61]. Besides STES, TTES is also utilized as short-term storage or a daily thermal buffer. For example, a 30 m³ hot-water tank was utilized as buffer storage in ATES in Rostock, Germany [110]. One restriction of TTES development is the space constraints, especially for retrofit installations, which usually occurs when fitting very large hot-water tanks into the existing buildings or energy centers without considering TTES integration initially. Besides the space constraints, heat destratification is another barrier that can cause more heat loss in the storage system, especially in very large tanks. Many strategies have been investigated to improve the thermal stratification of TTES [129, 130] including 1) inserting baffles in the tank [131-134], 2) a suitable aspect ratio of the tank [135-138], 3) using multiple tanks [139-142], and 4) a suitable design for the shape [135, 143-146], position [136, 147], and flowrate [135, 143-147] of inlet and outlet ports. Also, much attention has been drawn to the efficient insulation of the tank to prevent heat loss during long storage duration [67, 148]. Generally, there are two arrangements, i.e., thermal insulation attached to the outer wall of the storage and a double-wall vacuum envelope packed with powder particles [148]. Mass-market insulating materials include inorganic fibrous materials (rock wool and glass wool) and organic foamy materials (expanded polystyrene and extruded polystyrene) [149]. Instead of conventional materials, vacuum insulation panels and aerogels are recognized as the most promising superinsulation materials [150, 151].

The first German TTES system connected to a district heating system (Figure 2.3) went into operation in Friedrichshafen in 1996 [78], where a 12,000 m³ hot-water storage was built with reinforced concrete to store heat for 280 apartments and one kindergarten. The heated living area amounted to ~23,000 m², with solar collectors installed in an area of 2700 m². Two gas boilers with capacities of 750 and 900 kW_{th} were integrated as back-up heating devices in case of insufficient solar thermal energy available. A solar fraction between 21% and 30% was obtained during 1997–2004. In 2004, another residential zone with ~110 accommodation units was built. Accordingly, solar collectors with an area of 1350 m² were mounted. Monitoring results of three years' operation after the extension showed that the solar fraction varied between 24% and 33%, failing to meet the design target (43%). One of the reasons for this was that the annual heat demand was 10% higher than expected. Another reason was that the yearly mean net return temperature was ~20 °C higher than the design value (30 °C), causing a higher storage temperature than expected, and accordingly, an increased heat loss of ~200 MWh_{th} per year.

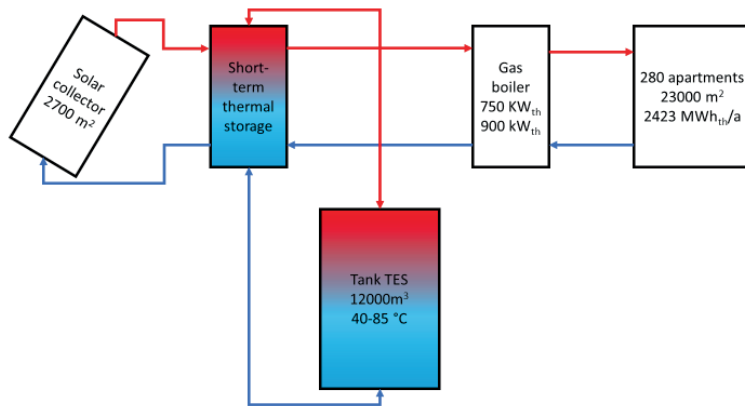


Figure 2.3. Schematic of TTES in Friedrichshafen, Germany (adapted from [152]).

2.3.1.2. PTES

PTES is a mature technology for large-scale SHS with high energy density and system efficiency [92]. The efficient insulation to prevent heat loss is also a key issue for PTES. Typical thermal insulation materials—including glass wool, polyurethane, expanded polystyrene, foam glass, and extruded polystyrene—are normally attached inside or outside the construction material [66]. Also, one of the barriers to PTES applications is the degradation related to vapor condensation, which leads to higher heat loss. Liners made of stainless steel, polymers, and elastomers are introduced in the PTES envelope [153]. However, current materials have drawbacks like the potential of corrosion and lower operating temperature. It requires further research on the cover and lining materials. Other challenges include substantial land and excavation requirements. To address this problem, a novel underground thermal energy storage system using a depleted oil well was proposed in [154].

The first large-scale PTES project was developed at Stuttgart University in 1984 [88]. Figure 2.4 shows a schematic of the system. A hole dug in the ground in the shape of a truncated cone was lined with a 2.5-mm-thick high-density polyethylene foil and filled with a 4-m-high pebble layer, ~3.75 m of which was flooded with water. The entire storage volume was 1050 m³. A solar fraction of 62% and a storage efficiency of 82% were achieved in the heating season between 1986 and 1987. Unglazed collectors were used for saving money but could only achieve temperatures below 35 °C, which was not enough for heating purposes. Based on the experiences in Stuttgart, a much larger rectangular version with a storage volume of 8000 m³ was built in Chemnitz in 1997, and the third generation was built in Steinfurt in 1999 with a geometrical formation of an inverted pyramid frustum having a storage volume of 1600 m³ [155].

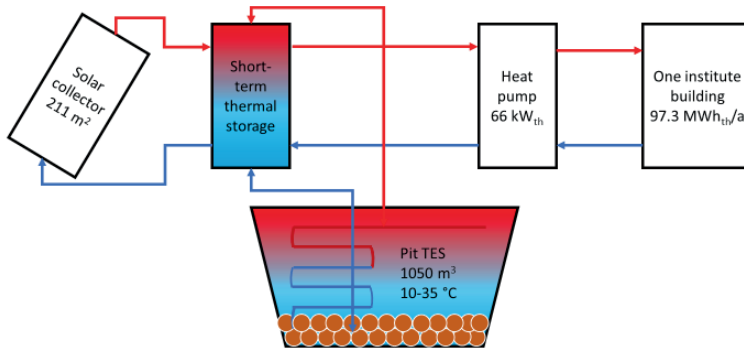


Figure 2.4. Schematic of PTES in Stuttgart, Germany (adapted from [88]).

2.3.1.3. BTES

Recently, a rapid increase in the number of BTES applications has been found in Europe [156] and North America [157]. It is estimated that ~400 BTES projects were in operation in Sweden in 2011, and the number in the Netherlands reached 22,500 in 2007 [158]. However, there are still some barriers limiting BTES development, such as geological conditions. As the installation of BTES systems has higher requirements in terms of hydraulic conductivity and natural groundwater flow, geothermal probes are always required to be installed before borehole drilling [61]. Another barrier is that there is a start-up process (3–4 years) in the system operation—which means that the storage efficiency is very low in the first year of operation and improves over time because heating the ground materials surrounding the boreholes takes time. From a long-term perspective, BTES can cause a gradual increase in average ground temperature, groundwater movement, and soil water content loss [159-161]. Besides, to reduce the thermal interferences between the boreholes, some solutions have been reported, including using a thermal baffle [162], pipe insulation installed on the upward branch pipe [163], and a suitable geometric dimension of the borehole considering spacing, diameter, and depth [164-166].

The Drake Landing Solar Community in Okotoks, Canada, developed the first BTES system, as shown in Figure 2.5, which meets over 90% of residential space-heating needs through solar thermal energy [97]. It uses two water-based buffer storage tanks, 34,000 m³ of borehole storage, and 2293 m² of solar collectors to supply the space heating and hot-water needs of 52 houses with a total heated living area of 7540 m². With a 10-year reliable operation, the solar fraction was calculated as an average of 96% for 2012–2016 and even reached 100% in the 2015–2016 heating season.

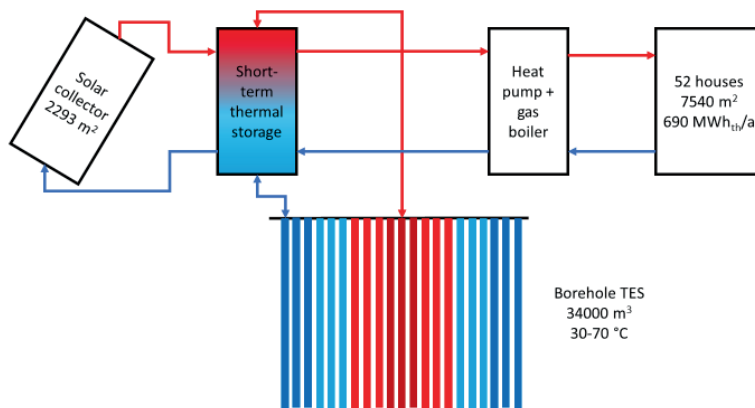


Figure 2.5. Schematic of BTES in Okotoks, Canada (adapted from [167]).

2.3.1.4. ATES

At the end of 2017, 3000 ATES projects were estimated to be in operation in Europe [64]. The successful projects were concentrated in only a few mid- and high-latitude countries: 2500 in the Netherlands, 220 in Sweden, 55 in Denmark, and 30 in Belgium [71]. Before 2000, most ATES systems provided heating and cooling to individual buildings, such as hospitals and offices. The application has recently started turning to district heating systems [168]. An ATES project requires suitable hydrogeological conditions, as they have a strong influence on the system's performance, as well as relatively high thermal loads; moreover, it must meet the regulatory requirements. For example, the Dutch policy currently has two restrictions on ATES: (1) the temperature of the injected water is not allowed to be above 25–30 °C, and (2) thermal imbalance is not allowed between the hot and cold wells [169]. Because of the restriction of the aquifer temperature, 99% of ATES systems worldwide are operating at low temperatures (<25 °C) [71].

The first German ATES central solar heating system went into operation in Rostock in 2000 [110] (Figure 2.6), supplying district heating and domestic hot water to 108 apartments with a total heated living area of 7000 m². The buildings mounted 980 m² solar collectors on the roof, and below the buildings, a doublet of wells was drilled 30 m underground. The target was designed to meet half of the total heat demand every year, which was reached after three years of operation with a solar fraction of 49%.

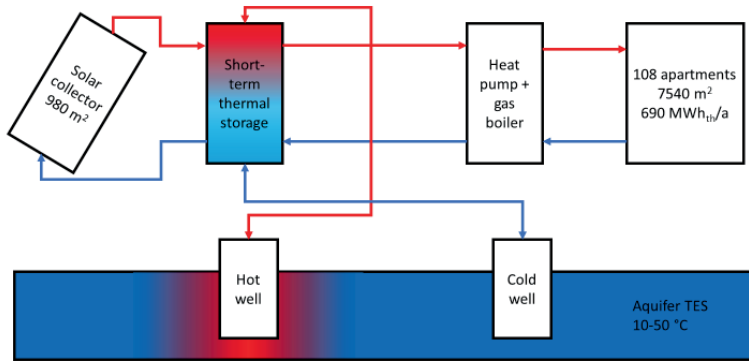


Figure 2.6. Schematic of ATES in Rostock, Germany (adapted from [110]).

2.3.1.5. SHS comparison

Detailed technical data of the examined studies are listed in the Appendix (Table 2.A1). The widely applied technical parameters, including annual heat demand, storage volume, storage and heating temperature, heated living area, COP of HP and system, main heat source fraction, storage efficiency, and the number of storage cycles per year, were investigated to evaluate the performance of TTES, PTES, BTES, and ATES. Most of the examined projects published the specific number of heated living areas, storage and heating temperature, annual heat demand, solar collector area (projects using solar thermal energy as the main heat source), storage volume, and main heat source fraction, or yielded the possibility to calculate these parameters. However, more data, such as storage capacity, COP of HP and system, HP capacity, storage efficiency, and the number of storage cycles per year, should be revealed as well. Besides, it was found that projects in Germany and Denmark provided better data accessibility.

The geographic requirements, advantages, and limitations of SHS technologies learned from the reviewed studies are listed in Table 2.2. Some technical parameters of these projects are further discussed in the following figures. TTES and PTES have relatively high energy density and thermal conductivity. They can be built at nearly any location, owing to their fewer requirements of geographic conditions. Little impact on the natural geology is reported while efforts are needed to prevent leakage. BTES and ATES can be used for both heating and cooling purposes and face fewer leakage problems. However, their energy density and thermal conductivity are relatively low, as ground materials are directly used as the storage medium. Because BTES and ATES require special geological conditions, such as no or low natural groundwater flow, a long initial process is required for an extensive geological investigation. Besides, with a direct touch with natural geology, the storage temperature of BTES and ATES is relatively limited, and a long start-up process (3–4 years) is required to achieve the typical performance.

Table 2.2 Technical comparison of SHS technologies [57, 61, 170, 171].

Storage technology	TTES	PTES	BTES	ATES
Storage medium	Water	Water and gravel	Ground material (soil/rock)	Ground material (sand/gravel...-water)
Geological requirements	<ul style="list-style-type: none"> • Stable ground conditions • Preferably no groundwater • 5–15 m deep 	<ul style="list-style-type: none"> • Stable ground conditions • Preferably no groundwater • 5–15 m deep 	<ul style="list-style-type: none"> • Drillable ground • Groundwater favorable • High heat capacity • High thermal conductivity • Low hydraulic conductivity • Low natural groundwater flow • 30–100 m deep 	<ul style="list-style-type: none"> • Natural aquifer layer with high hydraulic conductivity • Confining layers on top and bottom • Low natural groundwater flow • Suitable water chemistry at high temperatures • Aquifer thickness 20–50 m deep
Advantages	<ul style="list-style-type: none"> • No special geological condition needed • Most mature technology • High stratification • High heat capacity • Easy to install 	<ul style="list-style-type: none"> • No special geological condition needed • Leaving natural aquifer untouched 	<ul style="list-style-type: none"> • Can be used for both heating and cooling • Needs less surface area in case of a vertical borehole • Needs less excavation in case of horizontal duct • Less sensitive to outdoor climate • Feasible for very large and very small applications 	<ul style="list-style-type: none"> • Can be used for both heating and cooling • Ability to produce direct cooling without supporting device • Less maintenance needed • More efficient heat transfer than BTES
Limitations	<ul style="list-style-type: none"> • High heat loss • Potential corrosion • Potential leakage 	<ul style="list-style-type: none"> • Lower stratification than TTES • Potential leakage • Lower energy density than TTES 	<ul style="list-style-type: none"> • Special geological conditions needed • High heat loss • Low energy density • Long initial process for geological investigation • Start-up process needed 	<ul style="list-style-type: none"> • Special geological conditions needed • High heat loss • Low energy density • Clogging effects • Long initial process for geological investigation

The technical performance of STES systems is sensitive to their configuration parameters. For example, the solar collector area impacts the main heat source fraction, while the storage volume influences the level of storage efficiency. Therefore, several key parameters are investigated to facilitate a better understanding of how they relate to each other and the extent to which they influence the technical performances.

The variation in the maximum storage temperature with storage volume in water equivalent is shown in Figure 2.7. It indicates that the storage temperatures of BTES and ATES are

limited to 70 °C as ground materials are used as the storage medium without good insulation. The majority storage volume in water equivalent of SHS ranges from 100 to 50,000 m³. ATES has the advantage of providing the largest storage volume because it uses a natural aquifer as the storage medium.

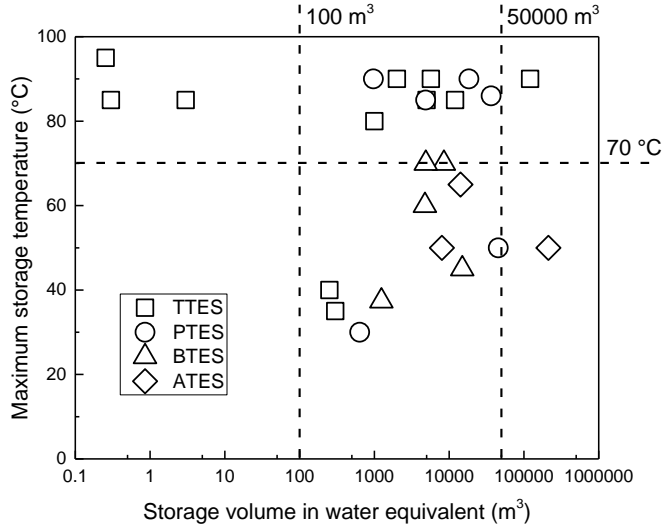


Figure 2.7. Storage temperature and volume in water equivalent.

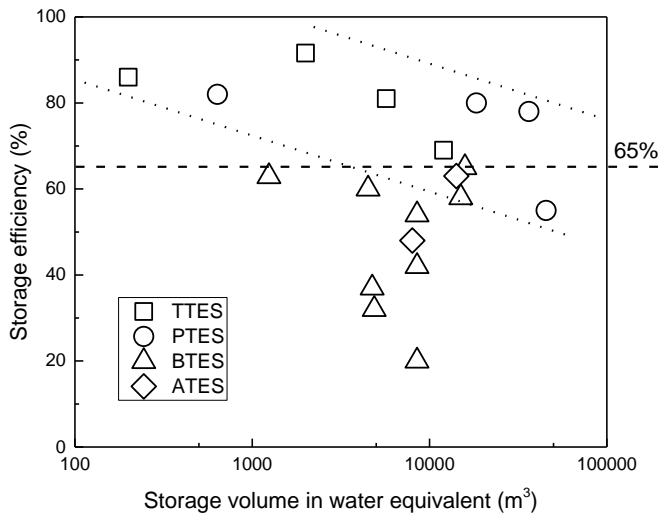


Figure 2.8. Storage efficiency and volume in water equivalent.

The relation between the storage efficiency and storage volume in water equivalent is presented in Figure 2.8. Note that the storage efficiencies of BTES and ATES are limited to

65% because ground materials are used as the storage medium. TTES and PTES, in general, have higher storage efficiencies than BTES and ATES because of their good insulation. Within TTES and PTES, the storage efficiency decreases with an increase in storage volume in water equivalent, which can be explained by more heat loss caused by a higher level of heat destratification.

Figure 2.9 shows the main heat source fraction with the ratio of the solar collector area to annual heat demand in the projects, with solar thermal energy as the main heat source. A higher ratio of the solar collector area to the annual heat demand means that most of the annual heat demand is met by solar thermal energy. In case of BTES and ATES, a higher ratio results in a higher main heat source fraction. In terms of TTES and PTES, the ratio mainly ranges between 1 and 2 because the storage temperature is normally close to 100 °C. Thus, increasing the solar collector area does not lead to more stored thermal energy.

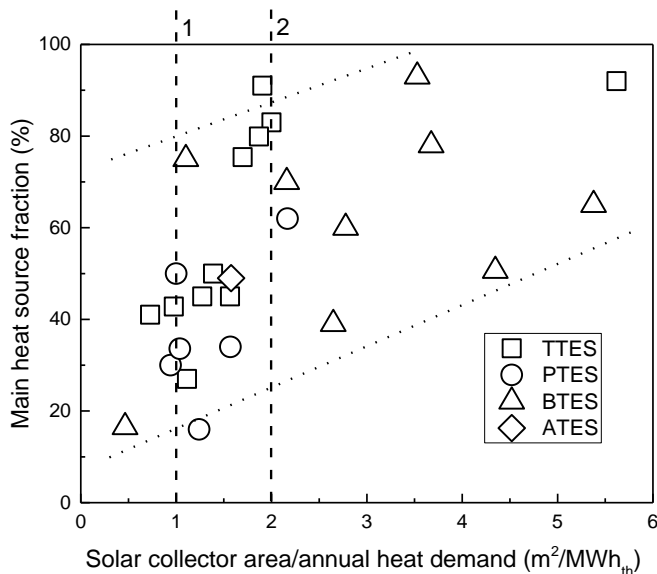


Figure 2.9. Main heat source fraction and solar collector area over annual heat demand.

HPs are widely used as auxiliary heating devices in STES systems. In the projects with solar thermal energy as the main heat source, the ratio of storage volume in water equivalent to the solar collector area indicates the relation between heat demand and heat supply. A higher ratio means a larger heat demand but lesser heat supply from the main heat source. Therefore, the mismatch between the heat supply and demand needs to be compensated by HPs. Figure 2.10 presents the relation between the COP of HP and the ratio of the storage volume in water equivalent to the solar collector area. The COP of HP increases with this ratio and shows that HP, as a supplementary device, performs better with the requirement of compensating more thermal energy.

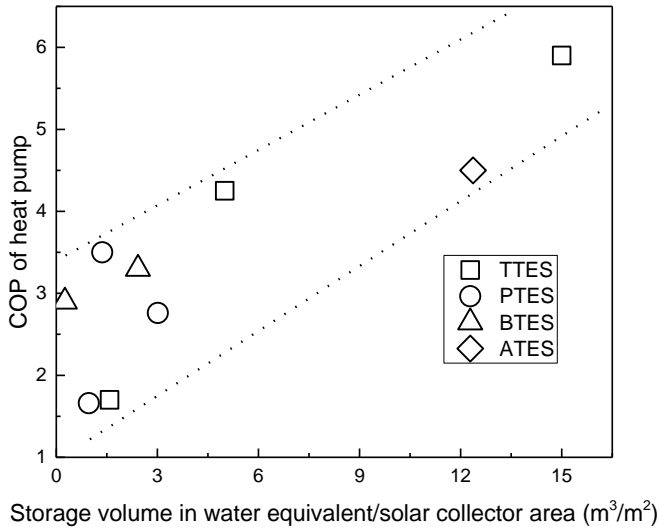


Figure 2.10. COP of HP and storage volume in water equivalent over solar collector area.

2.3.2. LHS

LHS is recognized as a suitable concept of STES due to the high energy density and the fact of being able to maintain a relatively constant temperature during the phase-change process. A summary of the studies conducted on LHS is summarized in the Appendix (Table 2.A2). The implementation of PCMs into building envelopes, e.g., wallboard [172], walls [173], shutters [174], floors [175], and ceilings [176], has been extensively studied for passive heating and cooling purposes. However, the storage ability of most of these applications is relatively low, and their heating and cooling performances are uncontrollable; therefore, they are only suitable for short-term storage. Active LHS, where a main heat source is implemented, plays a significant role in seasonal storage. Since the 1970s, LHS has been applied in greenhouses. The design of LHS systems for greenhouses is dependent on the desired control range of temperature inside the greenhouses and local climates and resources. Some successful implementations have been reported in Turkey [118, 119], Tunisia [177], France [115], UK [117], and China [178]. However, the biggest challenge of implementing LHS as seasonal storage is a lack of fully commercial PCM products, and the potential corrosion, flammability, and toxicity of PCMs significantly reduce their usage.

An LHS system in Çukurova, Turkey, using 6000 kg paraffin wax in a 12 m³ steel tank as PCM was presented in [118]. With a 27 m² solar collector area, it has a melting latent heat of 190 kJ/kg and a melting temperature of 48–60 °C, providing heat to a 180 m² greenhouse (Figure 2.11). During the charging period, the system achieves an average energy efficiency of 74.3% and exergy efficiency of 65.2%.

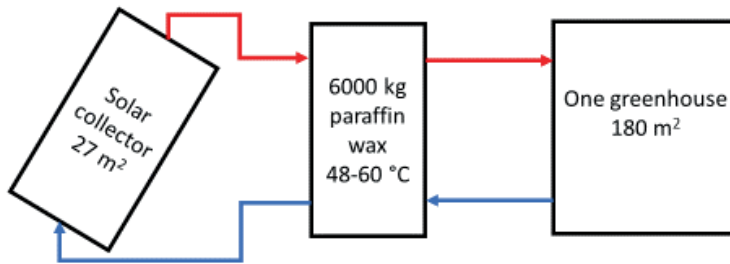


Figure 2.11. Schematic of LHS in Çukurova, Turkey (adapted from [118]).

2.3.3. THS

THS has drawn increasing attention because of its high energy density and negligible heat loss, as the sorbate and substance are placed separately. The examined studies on THS are categorized into two system configurations (open and closed systems). Detailed data regarding this can be found in the Appendix (Table 2.A3). The open system is a simple system operating at atmospheric pressure, while the closed system has more complex operation conditions with a higher discharging temperature and pressure. Currently, THS is still far away from complete market commercialization, and thus, further research on materials and system configuration is required.

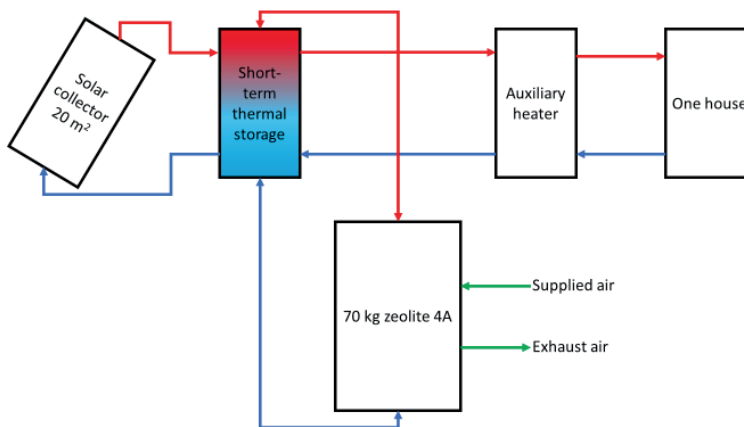


Figure 2.12. Schematic of THS in Stuttgart, German (adapted from [121]).

Long-term open sorption storage (Figure 2.12) for solar thermal space heating with novel zeolite honeycomb structures, instead of ordinarily employed fills, was built in a house at Stuttgart University, Germany, in 2006 [121]. This storage was integrated with a 1 m³ combi-storage, evacuated tube collectors with an area of 20 m², and a 7.85 m³ sorption storage. Humid outlet air was used as the sorbate, and an auxiliary heater was applied in case the sorption system failed to meet the heat demand. The energy density of the prototype storage

was 120 kWh_{th}/m³, and the discharging rate ranged between 1 and 1.5 kW_{th}. Compared to ordinary fills, the newly designed zeolite structures achieved better adsorption properties and a lower pressure loss.

2.3.4. Comparison

To provide comprehensive results for the technical performance review, three main STES concepts, namely SHS, LHS, and THS, were compared to indicate the level of maturity, advantages, and limitations (Table 2.3). SHS is the most stable and mature concept, but some technologies have high requirements for geological conditions. The energy density of SHS is relatively lower than those of LHS and THS; therefore, SHS normally requires a large storage volume. LHS, with a high energy density, can provide heat at an almost constant temperature. However, its storage materials are usually corrosive, poisonous, and lack thermal stability. THS has the highest energy density and negligible heat loss as the storage medium is normally stored separately; however, it requires a more complicated system, and the instability problems of the storage materials need to be addressed.

Table 2.3 Technical comparison of different STES concepts [61, 74].

Storage concept	SHS	LTS	THS
Maturity level	3	2–3	1
Advantages	<ul style="list-style-type: none"> • Unhazardous and low-cost material • Relatively simple system • Reliable • Easy to control 	<ul style="list-style-type: none"> • High energy density • Provide heat at almost constant temperatures 	<ul style="list-style-type: none"> • High energy density • Compact system • Negligible heat loss • Potentially non-toxic materials
Limitations	<ul style="list-style-type: none"> • Low energy density • Large volume required • Heat loss • Geological requirements 	<ul style="list-style-type: none"> • Lack of thermal stability • Potential degradation • Potential corrosion 	<ul style="list-style-type: none"> • Material instability • Cyclability problems • Complex system

(note: maturity levels: 1 = research and development; 2 = demonstration and deployment; 3 = commercialization.)

The project scale and initial operation year of the examined projects are presented in Figure 2.13. Most examined LHS projects started before 2005, and few projects were reported after that. The examined THS projects were initially started after 2005, but they have a very small scale as the technology is still in the stage of laboratory research. Compared to LHS and THS, the project scales of SHS are much larger, from one house to one community, indicating the maturity of these technologies in commercialization. Note that several BTESs were installed in the 2000s, with the project scale ranging between 1 and 1000 household equivalents.

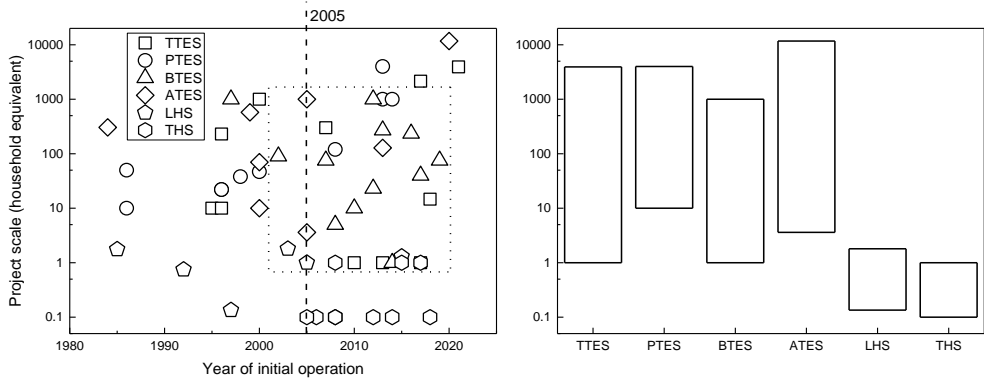


Figure 2.13. Project scale and year of initial operation (the left figure shows the scale and initial operation year of individual projects; the right figure provides the range of application scale of each technology).

2.4. Economic performance review

2.4.1. LCOH

Different LCOH values can be calculated according to the system boundaries. As shown in Figure 2.14, four LCOH values were calculated considering 1) only the renewable energy input part, 2) only the thermal storage part, 3) only the back-up heating device part, and 4) the overall STES system.

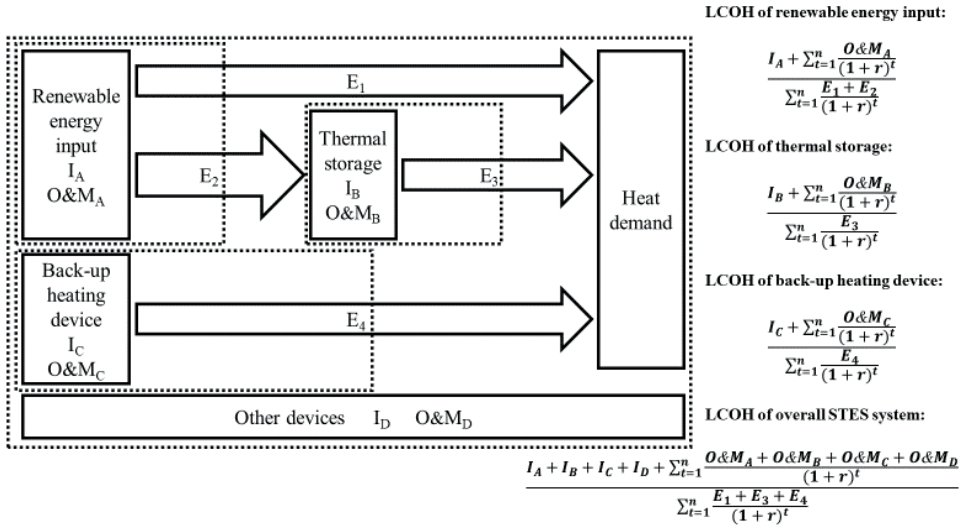


Figure 2.14. Specific system boundaries for LCOH analysis.

The costs of the examined STES projects were converted to 2019 constant prices in euro using the inflation and exchange rate derived from the Organization for Economic Co-operation and Development [179, 180]. In terms of certain missing economic data in several projects, the O&M cost is assumed based on the ratio of that and the investment in projects with available data. The O&M cost of the renewable energy input and thermal storage is assumed as 1% of their initial investments, and that of the overall STES system is assumed as 3.5% of the overall system investment when the data are not available. The real discount rate is considered as a constant (5%) [181, 182].

The LCOH calculation results of the renewable energy input, thermal storage, back-up heating device, and overall STES system of the examined projects are listed in Table 2.4, based on the data provided in the Appendix (Table 2.A4). The LCOH of the thermal storage and overall system varies considerably with different projects among each SHS type. The average LCOH of the thermal storage of BTES is higher than the other storage types because of the high excavation fee. Only one study has recorded the LCOH of the overall system for both LHS and THS. As expected, the LCOH of the overall system of LHS is higher than that of most of the SHS projects; however, THS has a relatively lower LCOH of the overall system, indicating better cost-effectiveness than LHS. Note that these results are based on the limited available studies, and the LCOH of the overall system of THS is calculated from an ideal simulation case study. This may cause uncertainty in LCOH calculation.

Table 2.4 Economic performance review of the examined projects (2019 €).

Project	Reference	LCOH (€/MWh _{th})				SVC (€/m ³)	SCC (€/kWh _{th})
		Renewable energy input	Thermal storage	Back-up heating device	Overall system		
TTES							
Hannover, DE	[79]	-	-	-	-	322.87	5.55
Munich, DE	[80, 183]	-	-	-	-	179.54	2.13
Copenhagen, DK	[83]	60.74		-	241.75	5439.40	-
Marseille, FR	[84]	107.68		-	212.12	3121.24	-
Marseille, FR	[85]	71.5		-	156.5	4855.26	-
Jincheon, KR	[86]	67.19	87.01	413.87	257.95	140.19	-
Marseille, FR	[49]	135.16	142.28	995.28	243.56	108.13	-
Panningen, NL	[87]	-	-	-	130.01	160.2	0.69
PTES							
Steinfurt, DE	[155]	-	-	-	-	456.78	-
Chemnitz, DE	[63, 79]	-	-	-	-	105.05	2.71
Eggenstein, DE	[79]	-	-	-	-	113.02	2.91
Osijek, HR	[92]	46.9	78.75	-	54.77	58.14	-
Marstal, DK	[93, 184]	59.57	55.73	60.92	87.69	36.60	0.46
Dronninglund, DK	[94]	36.26	20.71	28.16	46.74	39.64	0.47

Chapter 2

BTES							
Anneberg, SE	[96]	29.91	20.61	84.69	105.77	2.76	-
Okotoks, CA	[97, 185]	80.92	128.79	-	410.72	15.95	-
Shanghai, CN	[100]	-	-	-	211.87	-	-
Brødstrup, DK	[101, 184]	54.18	177.44	95.46	81.19	16.91	0.8
Tianjin, CN	[102]	-	-	-	110.84	-	-
Andalusia, ES	[104]	34.36	51.61	163.3	130.8	8.6	0.41
Ontario, CA	[105]	63.05	203	-	118.18	16.45	-
Aberdeen, GB	[106]	96.59	286.28	126.53	307.05	14.45	-
Camborne, GB	[106]	78.44	358.49	195.47	434.35	14.45	-
ATES							
Brasschaat, BE	[109]	-	44.88	37.76	86.22	-	-
Rostock, DE	[110]	99.82	155.28	145.13	263.77	12.34	-
Adana, TR	[112]	-	-	-	50.72	-	-
Groningen, NL	[114]	-	13.78	-	-	-	0.054
LHS							
Çukurova, TR	[118, 186]	-	-	-	382.69	-	-
Elazığ, TR	[119]	-	-	-	-	1383.60	148.12
THS							
Stuttgart, DE	[121]	-	-	-	-	3661.85	164.78
Loughborough, GB	[128]	-	-	-	193.18	1233.3	1.49
Högsölan, Dalarna, SE	[121]	-	-	-	-	4310.32	78.82
Rapperswil, CH	[121]	-	-	-	-	2554.6	3065.52
Gleisdorf, AT	[121]	-	-	-	-	5362.69	701.28
Dübendorf, CH	[121]	-	-	-	-	255.46	37.31

Figure 2.15 presents the LCOH of the overall STES system and the share of heat discharged from the storage in the annual heat demand. A general trend can be observed, where a higher share results in a higher LCOH of the overall system, indicating less attraction from an economic perspective. This is because there is always heat loss in the storage device. A higher share of heat discharged from the storage implies a higher heat loss in the overall system, causing a lower LCOH of the overall system.

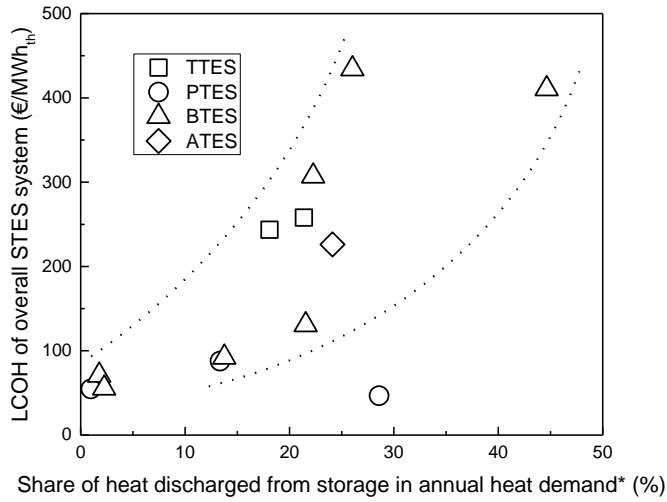


Figure 2.15. LCOH of an STES system and the share of heat discharged from storage in annual heat demand. (Note: the share of heat discharged from storage in annual heat demand is expressed as $E_3/(E_1+E_3+E_4)$ from Figure 2.14)

Figure 2.16 presents the LCOH of thermal storage and storage efficiency. BTES projects have much higher LCOH of thermal storage (over 160 €/MWh_{th}) and lower storage efficiency (up to 60%) than other types. A general trend is that a higher storage efficiency, meaning more heat recovered from storage, leads to a lower LCOH of thermal storage.

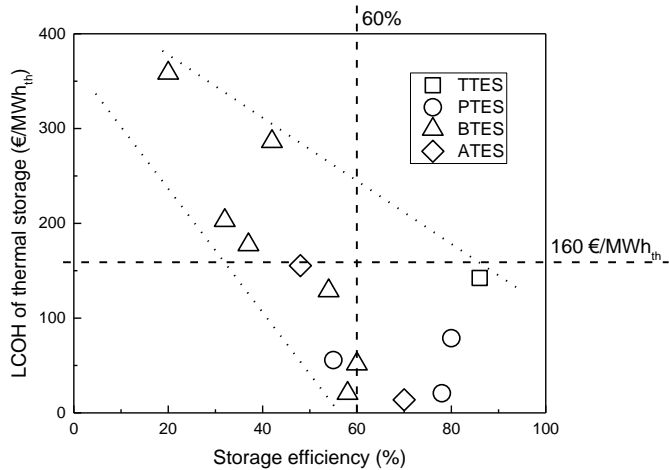


Figure 2.16. LCOH of thermal storage and storage efficiency.

2.4.2. SVC and SCC

Table 2.4 lists the cost of storage volume and storage capacity in the examined studies. For SHS, the storage cost includes the costs of storage materials and relevant storage devices, such as the container and charging and discharging devices. In contrast, for some of the LHS and THS projects, the storage cost only refers to the storage material cost, as most of the projects are at the level of laboratory prototypes. Apparently, the costs of storage volume and storage capacity of LHS and THS are hundreds of times higher than those of SHS. This can be partly explained by the stage of technology development and project scale. The SVC and SCC of TTES and PTES are higher than those of BTES and ATES. Besides, the studies conducted in Copenhagen, Denmark [83], and Marseille, France [84, 85], have indicated that when a TTES is built in a small-scale project, the SVC can be very high.

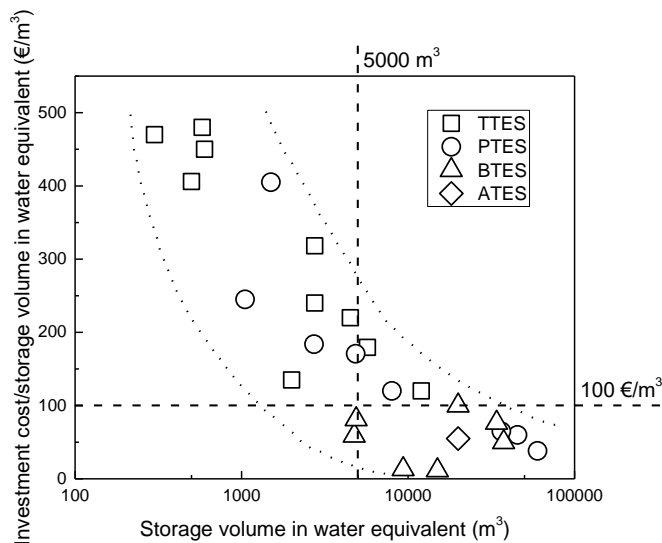


Figure 2.17. Investment cost over storage volume in water equivalent and storage volume in water equivalent.

Figure 2.17 shows the relation between the investment cost of thermal storage over storage volume in water equivalent and that in water equivalent with the data obtained from the projects examined in this study as well as those derived from [63, 88]. It indicates the impact of project scale on the specific investment cost. A clear trend is observed here, where the storage volume in water equivalent is associated with the project scale. The ratio of the investment cost and storage volume in water equivalent decreases with an increase in the storage volume in water equivalent. Besides, BTES and ATES are often applied in large projects with a storage volume in water equivalent over 5000 m³, and the specific investments are very low (up to 100 €/m³). TTES is often applied in projects with a few houses owing to space constraints, and small-scale TTES projects incur very high investment costs.

2.5. Lessons learned and suggestions for future studies

2.5.1. Techno-economic analysis

To offer a clear understanding of the advantages and drawbacks of each STES type, an integrated matrix with six characteristics is drawn in Figure 2.18 to show the overall performances of the STES types. Within the assessment of each characteristic, a higher score refers to better performance. For example, a higher score in energy density and geological requirements refers to higher energy density and fewer requirements under geological conditions, respectively. TTES and PTES are found to exhibit relatively balanced performance in the examined characteristics and cover larger areas in the matrix. The economic performances of BTES and ATES are better than their technical performances, while the opposite feature is observed for LHS and THS. This indicates that LHS and THS are promising alternatives when the cost is reduced using better storage materials or more mature technology.

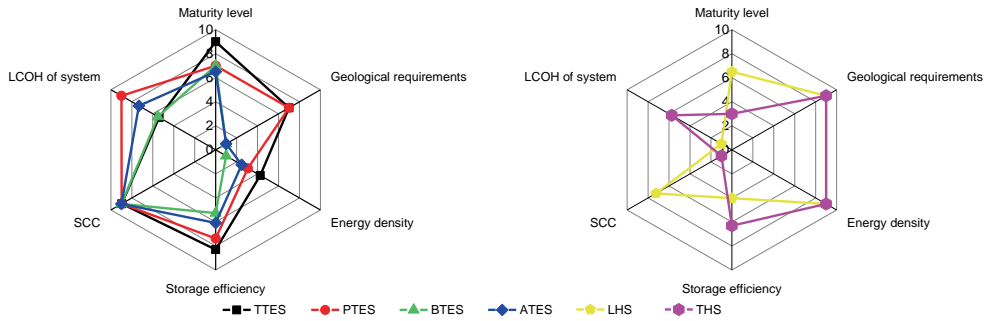


Figure 2.18. Comparison of six STES types with different characteristics (the left figure shows the results of SHS, and the right figure shows those of LHS and THS).

2.5.2. Economic competitiveness

The economic competitiveness of STES types is compared with that of the existing heat supply alternatives, selecting the applications of natural gas boilers and solar heating in decentralized heating as references. The LCOH of the references is calculated based on the techno-economic data derived from [187-192]. The investment costs of the heat supply technologies are converted to constant 2019 prices. During the calculation of the natural gas boiler, the European average price of natural gas in 2019 is applied, which is 17.47 €/GJ for residential purposes [188]. In terms of solar heating, the specific cost of solar collectors is in accordance with the average number of examined projects in this study (380 €/m²).

The results of the LCOH comparison are presented in Figure 2.19 (left). A large range of LCOH exists in some STES as varied economic input data are observed in the reviewed studies. The potential reasons for a very high LCOH include a) an oversized project scale,

which means low heat demand but high heat supply; b) overpriced solar collectors; c) excessive main heat source fraction, which means very low heat production from the back-up heating devices; and d) unsuitable geological conditions. The factors causing a very low LCOH include a) no main heat source (in the case of ATES), b) no back-up heating devices, c) low-priced solar collectors, d) low-priced borehole, and e) a low share of heat discharged from the storage in annual heat demand.

Based on the abovementioned reasons, the LCOH of STES is normalized, and the results are presented in Figure 2.19 (right). The Appendix (Table 2.A5) provides detailed explanations and data for the normalization. As shown in Figure 2.19 (right), only the PTES projects and a part of the ATES projects are economically competitive with the reference systems. The PTES projects selected for the LCOH calculation serve as part of district heating, indicating better economic performance compared to decentralized heating. In terms of ATES, some projects without a main heat source or back-up heating device have very low LCOH, e.g., supplying low-temperature heat (25 °C) to a greenhouse in Adana, Turkey [112]. This indicates that ATES can be economically competitive when used for low-temperature heating purposes. The LCOH of TTES and BTES is over twice that of the reference systems. The LCOH of LHS is the highest (over four times higher than the reference systems). To be made economically attractive, the LCOH of LHS and THS needs to be reduced by 60%–80%. Thus, measures are required to further reduce the STES costs to promote its economic feasibility in the heating market, for example, implementing large-scale STES in existing and new district heating systems, material improvements, and better drilling and insulation methods. The data for calculating LCOH are derived from the limited-access economic studies of STES. Future projects should be more transparent to provide a solid base for policymaking.

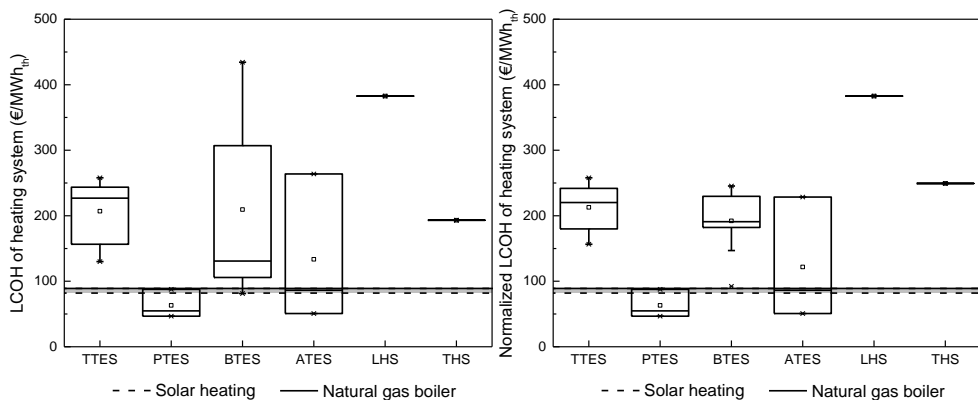


Figure 2.19. LCOH of STES systems in comparison with other heating options (the left figure shows the original results, and the right figure shows the normalized results).

2.5.3. STES selection

Selecting a feasible STES technology depends on various features and parameters, including geological and hydrological conditions, project scale, required cooling demand, and costs. To facilitate practical engineering, a decision tree that may guide potential STES selection is introduced, as shown in Figure 2.20.

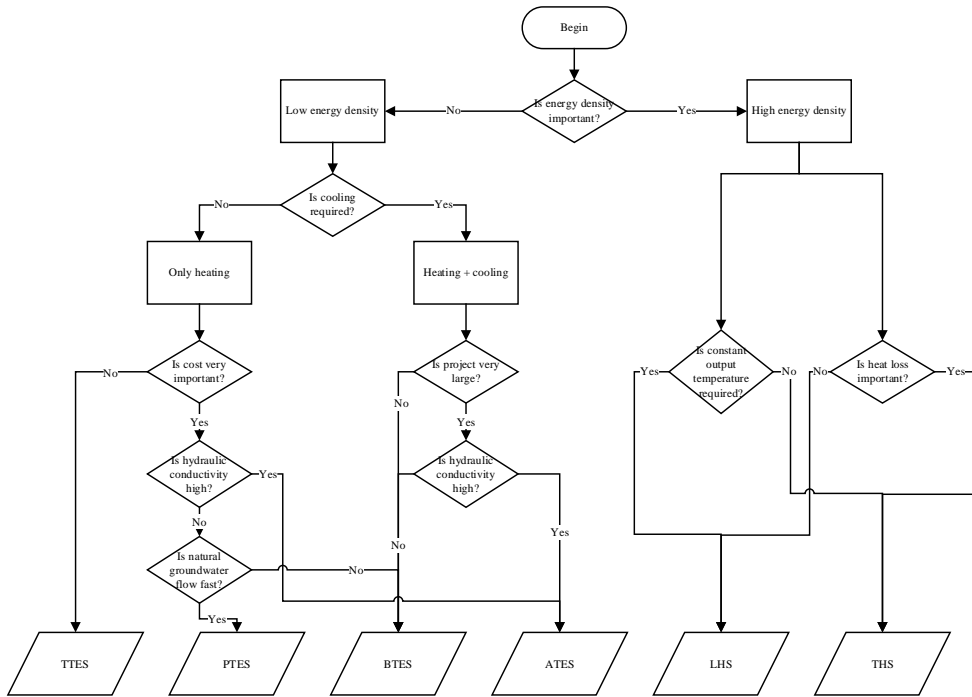


Figure 2.20. Decision tree for selecting STES types.

2.6. Discussion

A limit of this study is the inclusion of representative projects. The objective of this study is to learn the recent developments made in STES by conducting a comprehensive literature review of both technical and economic indicators. It requires detailed technical parameters and economic data to analyze the trends and relations between different technical parameters and to calculate the LCOH. Some representative projects were not included because they were either not reported in English, which is difficult for readers to track or lacking in transparency in techno-economic parameters. The review results are based on the selected and examined studies. For example, this work discussed the storage efficiency of BTES and ATES based on the examined studies. However, the storage efficiency increases as the size of the BTES and ATES systems increases [193–195]. The inclusion of projects with a larger

scale will increase the results of storage efficiency. More transparency is required for future studies to provide a solid base for techno-economic analysis.

Both established projects and simulation studies were included in this study. The latter was included because of their transparent reporting in techno-economic parameters. However, the inclusion of two types of studies brings uncertainty to the comparison of the technical performance. For example, a few key technical indicators (e.g., main heat source fraction and storage efficiency) were reviewed and compared to assess the technical performance of STES. The value of these indicators was either extracted from the selected studies or calculated in this study. The same equations were used to calculate those indicators. In terms of the established projects, the key technical indicators were mainly obtained from the project measurements. For the simulation studies, the technical indicators were obtained from the numerical simulation which often includes some simplifications. The established projects and simulation studies are distinguished in Table 1. The simulation studies often used TRNSYS, MINSUN, or mathematical models in Matlab. These tools are widely used in STES modeling and proved to have a good level of accuracy [57, 65, 196]. The impact of the simplifications on the indicator comparisons was not considered in this study.

In order to pursue a good technical performance like a high main heat source fraction and storage efficiency, STES systems are often oversized, which results in a negative impact on economic performance. For example, Drake Landing Solar Community achieved an average of 96% in the main heat source fraction, but its LCOH was calculated to be 410.72 €/MWh_{th}. Both numbers are much higher than the average level of BTES systems. It is suggested to investigate how to balance the technical and economic performances in future works. Also, solar thermal energy plays a dominant role as the heat supply in current STES systems. Diverse heat supply options (e.g., waste heat, geothermal energy, and power-to-heat) can be implemented in STES systems based on local conditions.

2.7. Conclusions

STES is a key technology for replacing fossil-based heat supply with renewable heat sources, such as solar thermal energy, geothermal energy, or waste heat generated from industries. This paper presents a comprehensive techno-economic literature review of STES technologies and projects. Within the class of SHS technologies, TTES and PTES are mature and mass-market technologies and have an advantage in terms of storage temperature and efficiency because of their good insulation; however, their space requirement and potential of leakage are substantial, limiting their application. Also, their storage efficiency was found to decrease with an increase in storage volume in water equivalent. BTES has developed rapidly in recent years, but it can only be built in locations with suitable underground conditions, and efforts are required to shorten the start-up process. ATES has been increasingly adopted in district heating systems but under the condition of subsurface aquifer availability within a suitable depth. BTES and ATES can be used for both heating and cooling

purposes and provide a large storage volume, but their energy density and thermal conductivity are relatively low. LHS, with a high energy density, can provide heat at an almost constant temperature; however, its current storage materials are usually corrosive, poisonous, and lack thermal stability. THS has the highest energy density and low heat loss as the storage medium is normally stored separately, but it requires a more complicated system, and the instability problems of the storage materials need to be addressed. HPs are widely used as auxiliary heating devices in STES systems, and a higher COP can be obtained by a higher ratio of the storage volume in water equivalent to the solar collector area. Also, solar thermal energy plays a dominant role as the heat supply in current STES systems. The implementation of diverse heat supply options should be investigated in future studies. In general, LHS and THS are advantageous in terms of technical performance, such as high energy density and few geological requirements, while SHS is more mature and largely applied in the current heating market.

The economic study indicates that the configuration parameters and technical performance substantially impact the economic performance; for example, the storage volume and efficiency have a positive impact, while the share of heat discharged from the storage has a negative impact. The average LCOH of the thermal storage of BTES is higher than that of other storage types, while the cost of storage volume and storage capacity of LHS and THS are hundreds of times higher than those of SHS. Compared to the reference heating options, i.e., natural gas boilers and solar heating for decentralized heating systems, none of the STES types is economically competitive, except for PTES and low-temperature ATES. Their LCOH is calculated to be lower than those of the reference systems. The LCOH of LHS is the highest (over four times higher than the reference systems). Thus, to be economically competitive in the heating market, the LCOH of STES must be generally reduced by half to four times less. Continuous efforts are required to explore and improve the technology as well as reduce the costs. In addition, the current economic study in the public domain is limited, and therefore, future projects should be more transparent to provide a solid base for policymaking.

Acknowledgments

The financial support from the China Scholarship Council (No. 201806220072) is gratefully acknowledged.

Appendix

Table 2.A1 Technical review of reference SHS projects.

Project	Year of initial operation	Heated living area (m ²)	Temperature (storage/heating) (°C)	Annual heat demand (MW _{th})	Solar collector area (m ²)	Storage volume (m ³)	Storage capacity (MW _{th})	COP (HP/system)	HP capacity (MW _{th})	No. of storage cycles per year	Main heat source fraction (%)	Storage efficiency (%)	Reference
TTES													
Lisse, NL	1995	-	25-80/-	1583	1200	1000	-	-	-	-	-	-	[77]
Friedrichshafen, DE	1996	23000	40-85/-	2423	2700	12000	-	-	-	-	27	69	[78, 95]
Breda, NL	1996	-	<85/-	1883	2400	5000	-	-	-	-	45	-	[77]
Hannover, DE	2000	-	-	-	1473	2750	160	-	-	-	39	-	[79]
Munich, DE	2007	30000	10-90/55	2300	3600	5700	480	1.7/-	1.4	1-2	40-50	81	[80, 183]
Gaziantep, TR	2010	100	7-35/-	10	20	300	-	5.9/-	-	-	83	-	[81]
Stockholm, SE	2013	-	25-40/30-35	8.9	50	250	-	4.25/-	-	-	92	-	[82]
Copenhagen, DK	2017	-	<95/50	1.7	2.36	0.255	-	-	-	-	50	-	[83]
Marseille, FR	2017	-	<85/50	2.65	4.5	0.3	-	-	-	-	75.4	-	[84]
Marseille, FR	2017	-	<85/60	53.52	100	3	-	-	-	-	79.9	-	[85]
Jincheon, KR	2017	214696	40-90/50	1356	1600	2000	-	-	-	-	42.8	-	[86]
Marseille, FR	2018	1465	-30-60	63	120	200	-	-	-	-	91	86	[49]
Panningen, NL	2021	300000	20-90/55	28333	20600	121100	28268	-/5	2.76	1.23	41	96	[87]
PTES													
Stuttgart, DE	1986	-	0-30/40-50	97.3	211	1050	-	2.76/-	0.066	-	62	82	[88]
Otrupgaard, DK	1996	-	-/50-70	453	562	1500	-	-	-	-	16	-	[89, 90]
Steinfurt, DE	1998	3800	30-90/-	325	510	1600	-	-	-	-	34	-	[63, 155]
Chemnitz, DE	2000	4680	<85/-	573	540	8000	310	-	-	-	30	-	[63, 79]
Eggenstein, DE	2008	12000	-	-	1600	4500	-	-	0.06	-	65	-	[91]
Osijek, HR	2013	400000	85-90/21	64000	0	30350	-	-0.7	-	-	3.7	80	[92]
Marstal, DK	2013	-	25-50/75	33300	33300	75000	6000	3.5/-	1.5	1.26	50	55	[93, 184]

Dronninglund, DK	2014	-	12-86/60-75	36169	37573	60000	5100	1.66/-	2.1	2	33.6	78	[94]
BTES													
Neckarsulm, DE	1997	-	-	1891	5007	63300	-	-	-	-	39	65	[95]
Anneberg, SE	2002	9000	30-45/32-55	1080	3000	60000	-	-	-	-	60	58	[96]
Okotoks, CA	2007	7540	30-70/37-55	650	2293	34000	-	-/30	-	-	93	54	[97, 197]
Harbin, CN	2008	500	3.4-7.7/27.1	-	50	-	-	4.29/6.14	0.0037	-	49.7	76	[98]
Emmaboda, SE	2010	-	40-45/-	8500	0	-	-	-	-	-	18	72	[99]
Shanghai, CN	2012	2304	15-37.4/23.6-50	115	500	4970	-	-/8.7	-	-	50.6	62.9	[100]
Bredstrup, DK	2012	-	12-60/80	40000	18600	19000	400	2.9/-	1.2	1.11	16.5	37	[101, 184]
Tianjin, CN	2013	27000	8-10.3/43.2	2932	1500	-	133	4.22/3.07	-	0.49	-	-	[102]
Torino, IT	2014	-	-	0.26	5	180	-	-	-	-	46	-	[103]
Andalusia, ES	2016	23581	-	1044	1150	18000	375	-	-	0.6	75	60	[104]
Ontario, CA	2017	4000	40-70/50	930	2009	19500	-	3.3/2.9	-	-	70	32	[105]
Aberdeen, GB	2019	7540	-	624	2293	34000	-	-	-	-	78	42	[106]
Camborne, GB	2019	7540	-	426.4	2293	34000	-	-	-	-	65	20	[106]
ATES													
Scarborough, CA	1984	30470	4-50/-	5920	0	530000	-	5-6/-	-	-	46	-	[107]
Berlin, DE	1999	57600	20-70/45	16000	0	-	-	-	-	-	13	77	[108]
Brasschaat, BE	2000	-	8-18/45	-	0	-	-	5.6/-	-	-	46	-	[109]
Rostock, DE	2000	7000	10-50/45-65	622	980	20000	-	4.5/-	-	-	49	48	[110]
Neubrandenburg, DE	2005	-	65-85/-	18125	0	-	-	-	-	-	42.6	46	[111]
Adana, TR	2005	360	35/25	108	0	-	-	-	-	-	78	-	[112]
Tehran, IR	2013	12800	43-65/60	528	-	35387	-	-/19.6	-	-	-	63	[113]
Groningen, NL	2020	-	-/95	50283	0	-	27594	-	-	0.41	95	70	[114]

Table 2.A2 Technical review of reference LHS projects.

Project	Year of initial operation	Heated living area (m ²)	Annual heat demand (MW _{th})	Solar collector area (m ²)	Storage material	Melting temperature (°C)	Heat of fusion (kJ/kg)	Storage volume (kg)	Storage capacity (kW _{th})	Main heat source fraction (%)	Storage efficiency (%)	Reference
Biot, FR	1985	176	-	-	CaCl ₂ ·6H ₂ O	21	150	2105	87.7	-	-	[115]
Trabzon, TR	1992	75	20	30	CaCl ₂ ·6H ₂ O	29.7	187.49	1090	-	60	40	[116]
Reading, UK	1997	13.5	-	-	Salt mixture	8	216	-	-	30	-	[117]
Çukurova, TR	2003	180	-	27	Paraffin wax	48-60	190	6000	317	-	40.4	[118]
Elazig, TR	2005	-	-	11.9	CaCl ₂ ·6H ₂ O	29	187.49	300	15.6	18-23	-	[119]
Lyngby, DK	2015	130	3.63	22.4	Sodium acetate trihydrate	58	265	200	-	80	-	[120]

Table 2.A3 Technical review of reference THS projects.

Project	Year of initial operation	Heated living area (m ²)	Solar collector area (m ²)	Storage material	Sorbate vapor pressure (mbar)	Charging temperature (°C)	Discharging temperature (°C)	Energy density (kWh _{th} /m ³)	Maximum power (kW _{th})	COP (HP/system)	Storage efficiency (%)	Reference
Open system												
Stuttgart, DE	2006	-	20	70 kg zeolite 4A	12	170	20	120	1.5	-	-	[121]
Petten, NL	2012	-	-	17 L MgCl ₂ ·6H ₂ O	12	130	60	138.9	0.15	-/12	-	[122]
Perpignan, FR	2014	-	-	400 kg SrBr ₂	10	80	25	203	0.8	-	-	[123]
Petten, NL	2014	-	-	150 kg zeolite 13X	12	185	25-60	62	0.4	-	>60	[124]
Wels, AT	2014	-	-	53 kg zeolite 4A	10	180	25	148	1.5	-/12	-	[125]
				50 kg zeolite Na-MSX		230		154				
Villeurbanne, FR	2015	100	-	80 kg zeolite 13X	10	180	20	185	2.25	-	53	[126]
Eindhoven, NL	2017	100	-	250 L zeolite 13X	13.5	180	13	216	4.4	-	76.4	[127]
Loughborough, GB	2018	-	8	4426 kg MgSO ₄	-	150	-	828	-	-	-	[128]
Closed system												
Högsölan Dalarna, SE	2005	-	-	54 kg LiCl salt	-	40-85	25	85	8	-	-	[121]
Rapperswil, CH	2008	-	-	7 kg zeolite 13X	23.4	180	22	57.8	0.8	-	-	[121]
Gleisdorf, AT	2008	100	-	200 kg silica gel	-	88	16-38	33.3	1	-	-	[121]
Dübendorf, CH	2008	-	-	160 kg NaOH	-	95	10	5	1	-	-	[121]

Chapter 2

Table 2.A4 Data sources of LCOH and storage volume/capacity cost analysis.

Project	Reference	Initial investment (€)				Annual O&M cost (€)	
		Renewable energy input	Thermal storage	Back-up heating device	Overall system	Renewable energy input	Thermal storage
TTES							
Hannover, DE	[79]	-	887897.49	-	-	-	-
Munich, DE	[80, 183]	-	1038209.01	-	-	-	-
Copenhagen, DK	[83]	688.39	1387.05	-	4109.77	6.88 ^a	-
Marseille, FR	[84]	2392.95	936.37	-	4889.94	23.93 ^a	-
Marseille, FR	[85]	33986.11	14565.77	-	72828.86	339.86 ^a	-
Jincheon, KR	[86]	589821.52	280372.91	87954.02	2178601.32	5898.22 ^a	2803.73 ^a
Marseille, FR	[49]	115338.2	21625.91	48400.85	185364.96	1153.38 ^a	216.26 ^a
Panningen, NL	[87]	767000	19400000	6250000	65155979	15340	60000
PTES							
Steinfurt, DE	[155]	677968.06	730849.57	-	-	-	-
Chemnitz, DE	[63, 79]	-	840368.76	-	-	-	-
Eggenstein, DE	[79]	-	508608.15	-	-	-	-
Osijek, HR	[92]	58138034.84	1764678.43	0	76826847.42	5540494.29	12289.72
Marstal, DK	[93, 184]	10162852.39	2744814.7	7967000.63	24123402.25	40330.48	28151.95
Dronninglund, DK	[94]	6784712.48	2378446.98	3694604.2	14701424.22	67847.12 ^a	23784.47 ^a
BTES							
Anneberg, SE	[96]	443075.43	165414.83	74436.67	1084648.64	4430.75 ^a	1654.15 ^a
Okotoks, CA	[97, 185]	996955.56	542203.9	-	2960258.4	9969.56 ^a	5422.04 ^a
Shanghai, CN	[100]	-	-	0	229857.26	-	-
Brædstrup, DK	[101, 184]	4141983.34	321368.21	818734.05	6495376.42	41419.83 ^a	3213.68 ^a
Tianjin, CN	[102]	186693.68	-	-	1581310.44	1866.94 ^a	-
Andalusia, ES	[104]	461300.52	154826.1	135522.85	1407995.47	4613.01 ^a	1548.26 ^a
Ontario, CA	[105]	716076.91	320791.05	0	1036867.96	7160.77 ^a	3207.91 ^a
Aberdeen, GB	[106]	860932.97	491265.93	44273.63	2156794.51	8609.33 ^a	4912.66 ^a
Camborne, GB	[106]	860932.97	491265.93	44273.63	2156794.51	8609.33 ^a	4912.66 ^a
ATES							
Brasschaat, BE	[109]	0	632723.45	67844.47	1025041.48	0	6327.23
Rostock, DE	[110]	505744.1	246727.25	75874.97	1360139.05	5057.44	2467.27
Adana, TR	[112]	0	-	0	18182.73	0	-
Groningen, NL	[114]	-	1480883	-	-	-	14809 ^a
LHS							
Çukurova, TR	[118, 186]	-	-	0	11348.75	-	-
Elazığ, TR	[119]	-	2310.61 ^b	-	-	-	-
THS							
Stuttgart, DE	[121]	-	1977.40 ^b	-	-	-	-
Loughborough, GB	[128]	494.06	2047.27	0	8237.03	-	-
Högsölan Dalarna, SE	[121]	-	2758.61 ^b	-	-	-	-
Rapperswil, CH	[121]	-	3065.52 ^b	-	-	-	-
Gleisdorf, AT	[121]	-	9116.58 ^b	-	-	-	-
Dübendorf, CH	[121]	-	332.10 ^b	-	-	-	-

Seasonal thermal energy storage: A techno-economic literature review

Annual O&M cost (€)		Annual heat production (MWh _{th})				Lifetime (years)	Cost of storage (€)	Storage volume (m ³)	Storage capacity (MWh _{th})
Back-up heating device	Overall system	Renewable energy input	Thermal storage	Back-up heating device	Overall system				
-	-	-	-	-	-	-	887897.49	2750	160
-	-	-	-	-	-	-	1023370	5700	480
-	143.84 ^a	0.85	-	-	1.7	30	1387.05	0.26	-
-	171.15 ^a	2	-	-	2.65	20	936.37	0.3	-
-	2549.01 ^a	42.78	-	-	53.55	20	14565.77	3	-
166790.73 ^a	175492.67	790	290	420	1356	20	280372.91	2000	-
1830.36 ^a	3295.38	64	11.4	5	63	30	21625.91	200	-
-	100000	-	-	-	28333	50	19400000	121100	28268
-	-	110	-	-	325	-	730849.57	1600	-
-	-	169	-	-	573	-	840368.76	8000	310
-	-	-	-	-	-	-	508608.15	4500	175
0	5708527.58	242100	2397	0	244497	14	1764678.43	30350	-
891032.17	990101.68	14326	4445	25087	33300	20	2744814.7	75000	6000
422918.25 ^a	514549.85 ^a	16840	10338	25518	36169	20	2378446.98	60000	5100
31133.43 ^a	37218.34	1200	650	430	1080	25	165414.83	60000	-
-	103609.04 ^a	998	341	-	764	25	542203.9	34000	-
0	8045 ^a	-	-	0	115	25	-	-	-
182704.66 ^a	227338.17 ^a	6881	163	2600	9200	20	321368.21	19000	400
-	50881.94	-	66	-	1472	25	-	-	133
38875.83 ^a	45037.1	1007	225	292	1044	30	154826.1	18000	375
0	36290.38 ^a	920	128	0	930	25	320791.05	19500	-
24947.24 ^a	38469.23	722	139	222	624	25	491265.93	34000	-
18553.29 ^a	32075.27	889	111	111	426.4	25	491265.93	34000	-
36001.82	42329.05	0	1142	1081	1335	25	632723.45	-	-
40080.15	47604.87	456	143	318	593	20	246727.25	20000	-
0	2969.85	0	-	0	84	25	-	-	-
-	-	47785	11389	-	50283	15	1480883	-	27594
0	397.21	-	-	-	4.3	12	-	11.6	0.32
-	-	-	-	-	-	-	2310.61 ^b	1.67	0.016
-	-	-	-	-	-	-	1977.40 ^b	0.54	0.012
0	288.3	-	-	0	4.26	30	2047.27	1.66	1.37
-	-	-	-	-	-	-	2758.61 ^b	0.64	0.035
-	-	-	-	-	-	-	3065.52 ^b	1.2	0.001
-	-	-	-	-	-	-	9116.58 ^b	1.7	0.013
-	-	-	-	-	-	-	332.10 ^b	1.3	0.0089

a based on the assumption

b cost of the material without container or reactor

Table 2.A5 LCOH after normalization.

Project	LCOH (€/MWh _{th})	Reason	Normalized LCOH (€/MWh _{th})
TTES			
Marseille, FR	243.56	Overpriced solar collectors (961 €/m ² while average: 361 €/m ²)	179.92
Panningen, NL	130.01	Low-priced solar collectors (37 €/m ² while average: 361 €/m ²)	228.15
BTES			
Anneberg, SE	105.77	Low-priced borehole (2.8 €/m ³ while average: 15.6 €/m ³) and low-priced solar collectors (148 €/m ² while average: 361 €/m ²)	182.09
Okotoks, CA	410.72	Pursuit of excessive main heat source fraction (93% while average: 52%)	229.65
Bredstrup, DK	81.19	Low share of heat discharged from storage in annual heat demand (2% while average: 31%)	245.47
Tianjin, CN	110.84	Low share of heat discharged from storage in annual heat demand (2% while average: 31%) and low-priced solar collectors (124 €/m ² while average: 361 €/m ²)	245.47
Andalusia, ES	130.8	Low-priced borehole (8.6 €/m ³ while average: 15.6 €/m ³)	146.93
Aberdeen, GB	307.05	Oversized project scale (ratio of solar collector area to heat production: 3.7 m ² /MWh _{th} while average: 2.3 m ² /MWh _{th})	190.87
Camborne, GB	434.35	Oversized project scale (ratio of solar collector area to heat production: 5.4 m ² /MWh _{th} while average: 2.3 m ² /MWh _{th})	185
ATES			
Rostock, DE	263.77	Overpriced solar collectors (516 €/m ² while average: 331 €/m ²)	228.6
THS			
Loughborough, GB	193.18	Low-priced solar collectors (62 €/m ² while average: 361 €/m ²)	249.32



3

Techno-economic-environmental analysis of seasonal thermal energy storage with solar heating for residential heating in China

Published in: Yang T, Liu W, Sun Q, Hu W, Kramer GJ. Techno-economic-environmental analysis of seasonal thermal energy storage with solar heating for residential heating in China. Energy 2023;283:128389.

Abstract

The application of seasonal thermal energy storage (STES) of solar heat is an option of interest for clean heat transition, as residential heating is often fossil fuel-based. This study 1) proposes an integrated optimization criterion to examine how local context influences the optimal configuration planning, techno-economic-environmental performance, and feasibility of STES application; 2) identifies the position of STES in comparison to other sustainable heating options considering the local context; and 3) provides a comprehensive and transparent showcase highlighting the importance of the local context in determining the feasibility of STES in the clean heating transition. The TRNSYS modeling tool is adopted to analyze the performance of the STES systems, and Pareto optimization is applied to treat the multi-objective optimization. The results indicate that the implementation of STES at the four examined locations is technically feasible. The solar fractions and storage efficiencies of the four case studies range between 58%–67% and 57%–69%, respectively. STES has significant potential to reduce CO₂ emissions (52%–72%) in comparison with the conventional heating systems. However, the heating cost of the STES system (5.4–8.7 €/ct/kWh) is more than twice that of the conventional heating system. The CO₂ avoidance cost of the four case studies ranges between 114–368 €/t. Properly reducing the borehole number in cold climate zones and increasing the solar collector area in warm climate zones help improve the system performance. In northern China, the implementation of STES can increase the renewable energy penetration in fossil fuel-based district heating with a low cost of obtaining environmental benefits. In southern China, where the current heating is based on electricity, decarbonizing the power system rather than STES is a more cost-effective pathway for the clean heat transition.

Chapter 3

Nomenclature

E	energy
G	incident solar irradiance
I	investment cost
m	mass
n	lifetime
Q	thermal energy
r	discount rate
T	temperature
t	time

Greek symbols

ΔCO_2	CO ₂ emission saving
η	efficiency
μ	CO ₂ equivalent emission factor

Abbreviations

ATES	aquifer thermal energy storage
BB	biomass boiler
BTES	borehole thermal energy storage
CCS	carbon capture and storage
CHP	combined heat and power
COP	coefficient of performance
DH	district heating
DHW	domestic hot water
DLSC	Drake Landing Solar Community

GH	geothermal heating
GHI	global horizontal irradiance
GSHP	ground source heat pump
HDD	heating degree day
LCOE	levelized cost of energy
LCOH	levelized cost of heat
NGB	natural gas boiler
O&M	operation and maintenance
PTES	pit thermal energy storage
SF	solar fraction
STES	seasonal thermal energy storage
TRT	thermal response test
TTES	tank thermal energy storage

Superscripts

boreh	borehole
cs	conventional system

Subscripts

amb	ambient
arr	solar collector array
charg	charge
disch	discharge
el	electricity
in	inlet
s	storage

Chapter 3

setp setpoint

sol solar

th thermal

tot total

3.1. Introduction

Energy storage is essential in transitioning from a fossil fuel- to a renewable energy-based energy system, especially in the context of future smart energy systems, since most renewable energy sources are discontinuous [198]. Compared with electricity storage, heat storage provides an option for system balancing and flexibility with lower costs [199]. Heat storage in smart energy systems can facilitate the utilization of multiple renewable energy sources, integrate waste heat and cool, and balance the electrical network [200]. The 5th generation district heating (DH) also highlights the importance of heat storage [201].

Due to the seasonal variations of heating, long-term thermal energy storage in the form of seasonal thermal energy storage (STES) is preferable to coordinate the seasonal mismatch between heat supply and demand. Depending on their storage mechanisms, STES can be classified into three main types: sensible heat storage, latent heat storage, and thermochemical heat storage, of which sensible heat storage (using a water tank, pit, borehole, and aquifer) is mature and mass-market. The main heat sources include solar thermal energy, industrial waste heat, and geothermal energy. Heat pumps, gas boilers, and electrical heaters are widely used as auxiliary heating devices in case STES fails to meet the heat demand [202].

After decades of development, multiple technologies for STES have been implemented [35, 203]. The development of STES has been extensively studied and reviewed from a technical perspective [66, 204]. Xu et al. [100] introduced the technical performance of a demonstrated 2304 m² solar-heated greenhouse with 4970 m³ soil to store the heat collected by 500 m² solar collectors. Guo et al. [203] proposed a large-scale STES integrated with an industrial waste heat heating system and an absorption heat pump and assessed its long-term performance. Kim et al. [86] introduced an STES system for a community comprising 300 energy-plus residential houses in South Korea. The results showed that the STES system reduced by 17% CO₂ emissions with a 6-year payback period compared to the gas boiler system. Salvestroni et al. [205] designed an STES with a 3800 m³ hot water tank and 1000 m² solar collectors, achieving a solar fraction (SF) of 40%.

Table 3.1 Review of STES applications.

Study	Country	Heated area	Main heat source	Inclusion of technical/economic/environmental analysis	Economic and environmental indicator	Inclusion of performance analysis/parametric study/optimization	Objective function of optimization
[206]	China	400,000 m ²	Waste heat + solar energy	+/-/-		+/-/-	
[105]	Canada	A greenhouse	Solar energy	+/-/-	Levelized cost of energy (LCOE) Investment	+/-/-	
[48]	China	19,000 m ²	Solar energy	+/-/-		+/-/+	Renovation cost
[207]	Sweden	A factory	Waste heat	+/-/-		+/-/-	
[208]	China	A university campus	Solar energy	+/-/-		+/-/-	
[209]	Italy	Six houses	Solar energy	+/-/+	Investment, CO ₂ emission saving	+/-/-	
[210]	China	A university campus	Solar energy	+/-/-		+/-/-	
[49]	France	Eight houses	Solar energy	+/-/-	LCOE	+/-/+	SF, solar collector efficiency, LCOE
[205]	China	2304 m ²	Solar energy	+/-/-		+/-/-	
[98]	Italy	20,207 m ²	Solar energy	+/-/-		+/-/-	
[50]	China	500 m ²	Solar energy	+/-/-		+/-/-	
	Switzerland	35 buildings	Solar energy	+/-/+	yearly cost, CO ₂ emissions	+/-/+	Yearly cost
[211]	China	-	Waste heat	+/-/-		+/-/-	
[212]	Denmark	-	Solar energy	+/-/-		+/-/-	
[213]	China	1500 m ²	Solar energy	+/-/-		+/-/-	
[51]	Finland	31,100 m ²	Solar energy	+/-/+	Life cycle cost, LCOE, CO ₂ emissions	+/-/+	Heat production, LCOE

(+ = included; - = not included)

The previous review analysis has concluded that STES economic studies are limited in number and often lack transparency in their reporting [202]. Several STES implementations were reviewed, as listed in Table 3.1. Those studies have concluded that STES positively impacts the clean heat transition. The technical performance of STES projects has been examined through experiments and simulations. However, there is a lack of in-depth insights into economic and environmental performances to provide the facts on the position of STES applications compared with other sustainable heating technologies. There is a need for a comprehensive quantitative method for the techno-economic-environmental performance analysis of STES applications.

The existing studies focus primarily on technical performance assessment and analysis instead of optimization. Within the optimization research, Huang et al. [48] aimed to optimize the system based on minimum renovation cost by testing different water tank sizes. However, the method was a parametric study rather than an optimization. Launay et al. [49] proposed a strategy for multi-criteria optimization using SF, solar collector efficiency, and LCOE as objectives. Fiorentini's optimization aimed to minimize the yearly cost of the energy system [50]. Indicators of environmental performance were missing in these studies. Yuan et al. [51] aimed to find out the optimal solution with high performance and low costs. Shah et al. [52] used minimum life cycle cost and greenhouse gas emissions as objective functions and total solar collector area and borehole length as optimizing variables to optimize the STES systems in six selected cold climate locations. They obtained several optimal solutions for each specific site without a generic conclusion. It failed to identify the key parameters and quantify their influence on the optimization results. There is a need for a better understanding of the optimal economic and environmental performance of STES applications and the conditions to achieve it. It requires an integrated optimization criterion and method to select the optimal solution.

The hypothesis of this study is that the local context plays an important role in the optimal configuration planning, techno-economic-environmental performance, and feasibility of the STES application. The techno-economic-environmental performance and feasibility of STES in cold climates are preferable to those in warm climates. The key influential parameters in determining the optimal performance differ based on climate conditions. With the knowledge gaps discussed above, the main contributions of this study are summarized as two aspects. From the methodological perspective, previous studies on the optimization of STES failed to identify the key parameters and quantify their influence on the optimization results. There is a need for a better understanding of the optimal economic and environmental performance of STES applications and the conditions to achieve it. Therefore, an integrated optimization criterion (CO₂ avoidance cost) is proposed to select the optimal solution and determine the optimization pathways for different climates. By applying this indicator in the optimization, three research questions are answered: 1) How do the local climate condition and existing heating infrastructure influence the CO₂ avoidance cost of STES? 2) What are the key technical parameters in achieving the optimal techno-economic-environmental performance

of STES in different climate zones? 3) What is the position of STES in comparison to other sustainable heating options in terms of CO₂ avoidance cost considering the local context? From the case study perspective, China accounts for 40% of global DH production, with a 30% higher CO₂ emissions intensity than the world average [18]. This study presents four local-specific cases at a community level in representative climate conditions that consider local circumstances and makes an effort to provide an informative and transparent presentation based on regional specificity. It provides a comprehensive and transparent showcase highlighting the importance of context in determining the feasibility of STES in the clean heating transition at the local level.

3.2. Methodology

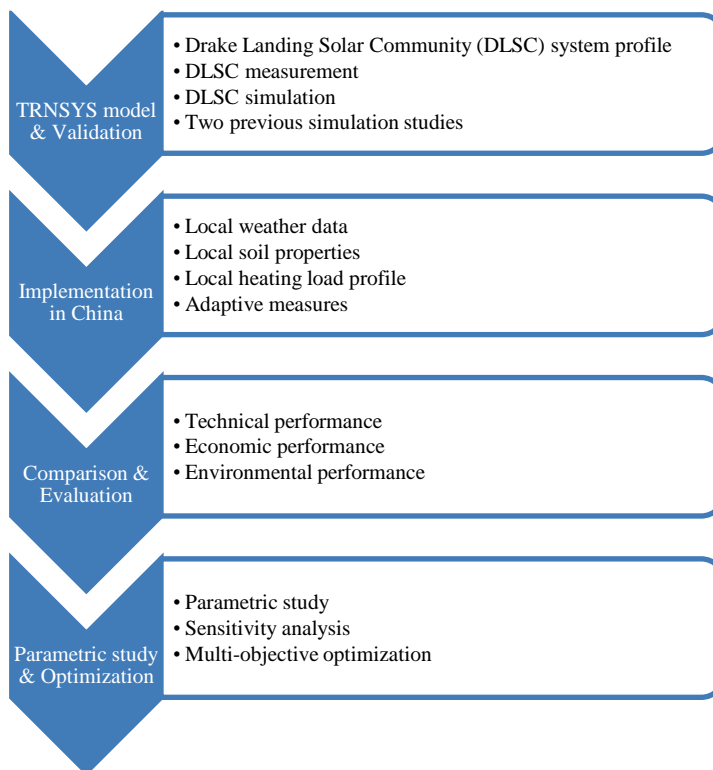


Figure 3.1. Schematic of the methodology employed in this study.

In this study, a four-step methodology was proposed and applied to fulfill the research objective, as shown in Figure 3.1. In this analysis, the technical, economic, and environmental performance of implementing an STES system was investigated in four locations in China: Harbin, Urumqi, Shanghai, and Chengdu. Moreover, a parametric study was conducted to investigate how the system configurations influence the overall performance. Furthermore, multi-objective optimization was performed with the minimum

levelized cost of heat (LCOH) and CO₂ emissions as the objective functions. Based on the optimization, the CO₂ avoidance cost was obtained, and optimal solutions were selected with the minimum CO₂ avoidance cost criteria.

3.2.1. TRNSYS model development

Research and demonstration of STES applications in China have mainly included tank thermal energy storage (TTES) and borehole thermal energy storage (BTES) [214]. The low storage density and high cost of TTES are unsuitable for the high population density of China [202]. Also, the BTES system can substantially improve the system performance in terms of mismatch relieving and CO₂ emission reduction, while tank storage has fewer benefits [215]. Therefore, the BTES was chosen for the analysis in this study. Several pilot BTES projects exist in China; however, their data remain unpublished.

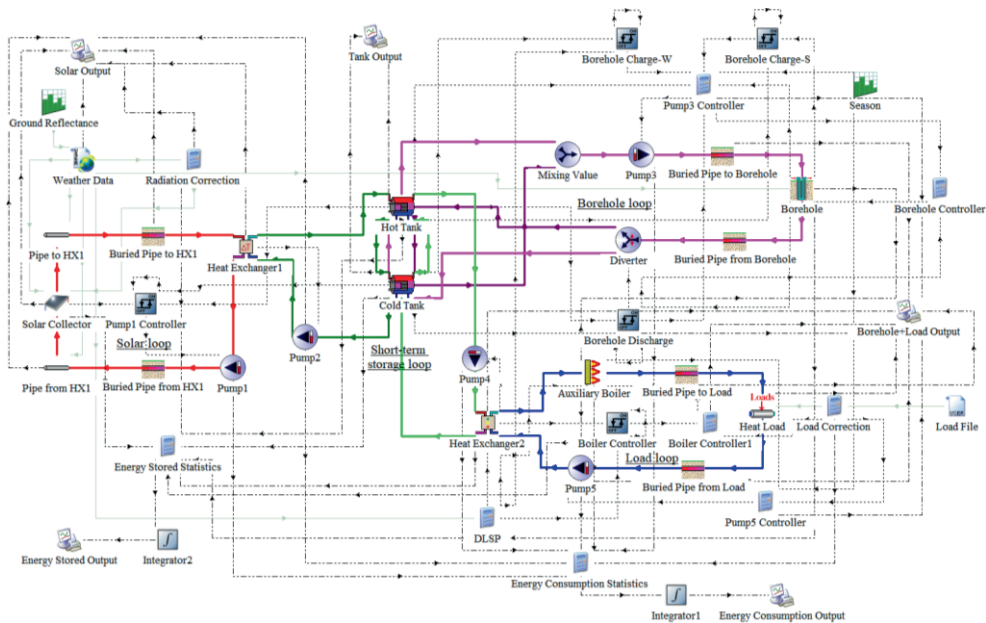


Figure 3.2. TRNSYS model of DLSC.

In this study, a BTES system was modeled using the TRNSYS [216] simulation tool based on the DLSC system schematic design located in Okotoks, Canada (presented in Figure 3.2). The project was well regarded as a successful STES application, and the data are transparent [217, 218]. The system comprises 2293 m² flat-plate glazed collectors, two 120 m³ short-term storage tanks, and 144 boreholes with a diameter of 35 m and a depth of 37 m. The system supplies the space and water heating for 52 houses with a total heated living area of 7540 m². The DLSC system was commissioned in 2007, achieving consistent SFs above 90% since the fifth year of operation. More information about the DLSC system can be found in [40, 167]. The simulation covered five years, from July 1, 2007, to June 30, 2012. The time

step was set as ten minutes since the measurements of the DLSC were on a ten-minute basis [219]. The model comprises four loops: a solar loop, short-term storage loop, borehole loop, and load loop.

3.2.1.1. Weather data

Since a weather station is not present at the DLSC location, the weather data were obtained from Calgary's international airport weather station [220], located 45 km north of the DLSC. The GHI and direct normal irradiance at the DLSC were derived from [221]. Type 99 was used to read the user-defined weather data. The solar irradiance was corrected according to the DLSC measurements at an annual level [97].

3.2.1.2. Solar loop

The flat-plate solar collectors were modeled by Type 1a. The collectors were facing south and tilted at 45°. The efficiency of the solar collector array is defined using the efficiency equation [222]:

$$\eta_{arr} = 0.63 - 3.35\left(\frac{T_{in} - T_{amb}}{G}\right) \quad (3.1)$$

where G denotes the total incident solar irradiance, and T_{in} and T_{amb} represent the solar collector inlet temperature and ambient temperature, respectively.

The working fluid in the solar loop is propylene glycol. The pipe and buried pipe were modeled by Type 31 and Type 952, respectively. The heat exchanger between the solar loop and the short-term storage loop was modeled by Type 761 with cold-side modulation to maintain a temperature difference of 12°C.

3.2.1.3. Short-term storage loop

The two connecting storage tanks, working as short-term buffer storage, were modeled by Type 533 horizontal cylindrical storage tanks. Each tank has a capacity volume of 120 m³ and five nodes to model the stratification observed in the storage tanks. On the one hand, the storage tanks store the heat collected by the solar collectors and charge the borehole. On the other hand, the heat discharged from the borehole is transferred to the load loop through the storage tanks.

3.2.1.4. Borehole loop

The borehole was modeled by Type 557a, a vertical heat exchanger that interacts thermally with the ground. The 144 boreholes were divided into 24 strings of 6 boreholes in series. The charging and discharging processes were performed using a mixer (Type 11h), a diverter (Type 11b), and controllers (Type 2b). The charge and discharge control strategies include

temperature comparisons and seasonal differences (summer or winter) [223]. The borehole was preheated to 25°C before the start of the simulation.

3.2.1.5. Load loop

The heating load was modeled by Type 682, which involved imposing a user-specified load on a flowing stream and calculating the resultant outlet fluid conditions. The hourly heating load was calculated by regression of the ambient temperature [224]:

$$Q_{load} = 1000000 \cdot \text{MAX}(0, (-0.803 \cdot T_{amb,rolling} + 9.31))/24 \quad (3.2)$$

where $T_{amb,rolling}$ denotes the average ambient temperature during the last six-hour period.

Furthermore, the heating load was corrected according to the DLSC measurements at an annual level [97]. The auxiliary gas boiler was modeled by Type 659, supplying heat when the stored heat fails to meet the demand of the load loop. The load loop was set to satisfy the head demand by supplying hot water at the supply setpoint temperature. The setpoint temperature was calculated according to [97]

$$T_{setp} = \begin{cases} 55 \text{ }^{\circ}\text{C}, & T_{amb} \leq -40 \text{ }^{\circ}\text{C} \\ -0.48 \cdot T_{amb} + 35.8, & -40 \text{ }^{\circ}\text{C} < T_{amb} < -2.5 \text{ }^{\circ}\text{C} \\ 37 \text{ }^{\circ}\text{C}, & T_{amb} \geq -2.5 \text{ }^{\circ}\text{C} \end{cases} \quad (3.3)$$

The return temperature is a function of the supply setpoint temperature, which in turn is estimated from the outdoor temperature. The temperature drop varies linearly from 6 to 7 °C for the supply temperatures of 37–55 °C, respectively [222].

3.2.2. Validation

It is necessary to validate the model before implementing it in China. Accordingly, the DLSC measurements, DLSC simulation results, and two previous simulation results of the DLSC system from peer-reviewed articles were used to validate the model developed in this study.

3.2.3. Comparison and evaluation

Implementation was evaluated through several performance indicators from technical, economic, and environmental perspectives.

3.2.3.1. Technical performance

Generally, the technical performance of an STES system is described by its SF and storage efficiency. The SF indicates the percentage of the heating load that can be met by solar thermal energy; it can be expressed as follows:

$$SF = \frac{E_{th,sol}}{E_{th,tot}} = \frac{E_{th,sol}}{E_{th,sol} + E_{th,boil}} \quad (3.4)$$

where $E_{th,sol}$ denotes the heating load met by solar thermal energy, $E_{th,tot}$ represents the total thermal energy supplied to the users, and $E_{th,boil}$ corresponds to the thermal energy provided by the auxiliary natural gas boiler (NGB).

The performance of the borehole was evaluated based on the storage efficiency, illustrating the efficiency of the borehole:

$$\eta_s = \frac{E_{th,disch}^{boreh}}{E_{th,charg}^{boreh}} \quad (3.5)$$

where $E_{th,disch}^{boreh}$ denotes the thermal energy discharged from the borehole, and $E_{th,charg}^{boreh}$ corresponds to the thermal energy charged into the borehole.

3.2.3.2. Economic performance

Economic performance was assessed by calculating the LCOH for the following purposes. First, the relative economic competitiveness of implementing the STES scheme in different climate zones was evaluated. Accordingly, the LCOHs of the STES applications at the four locations were compared. Second, the LCOH of the STES application was compared with the cost of existing heat supply technology to position the STES project in the local heat market. Lastly, an LCOH comparison of the STES system in China, the DLSC system, and the benchmark case in Europe was performed. The LCOH was determined as follows:

$$LCOH = \frac{I + \sum_{t=1}^n \frac{O\&M}{(1+r)^t}}{\sum_{t=1}^n \frac{E_{th}}{(1+r)^t}} \quad (3.6)$$

where I denotes the initial investment, r represents the discount rate, n is the lifetime, $O\&M$ symbolizes the annual operation and maintenance cost, and E_{th} corresponds to the annual heat production.

The heating costs of the conventional systems were calculated as [225]:

$$Heating\ cost = \frac{Depreciation + O\&M}{Heat\ production} \quad (3.7)$$

Table 3.2 Investment costs of the main equipment.

Equipment	Unit	Cost range	Mean cost	Reference
Solar collector	€/m ²	52–73	63	[226]
Short-term storage tank	€/m ³	61–123	94	[226]
Borehole	€/m	16–34	24	[48, 227–230]
Natural gas boiler	€/unit	8359–11060	9568	[226]
Pump	€/unit	405–673	512	[226]
Pipeline	€/m	86–120	108	[226]

In this study, the lifetime used in the LCOH calculation was 25 years. The discount rate was 5% [231], which is approximately equivalent to the long-term interest rate of Chinese central banks for housing mortgage loans [232]. The investment costs of the system's leading equipment are listed in Table 3.2. The unit price of system components was based on China's market price, and the values were sourced from China's leading platform for wholesale trade [226] and several Chinese studies [48, 227-230].

Considering the inclusive labor cost of design, mounting, and commissioning of the STES system construction in Europe (100 €/m² solar collector area) [233] and the average hourly labor cost in Europe (26 €/h) [234], the working hour was calculated as 3.8 h/m² solar collector area. The working hours were applied to the four locations in China, combined with the local hourly labor cost [235, 236] to calculate the labor cost of the STES systems at the four chosen locations; the values are listed in Table 3.3.

The annual fixed O&M cost was set at 0.75% of the total investment cost of the equipment [233]. The annual variable O&M cost was calculated based on the annual electricity consumption of the pumps and the natural gas consumption of the auxiliary natural gas boiler. The electricity and natural gas prices at the four locations are listed in Table 3.3.

Table 3.3 The labor costs and electricity and natural gas prices of the STES system at the four locations.

	Unit	Harbin	Urumqi	Shanghai	Chengdu	Reference
Hourly labor cost	€/h	4.4	5.1	9.6	5.3	[235]
Labor cost of STES system	€/m ² solar collector area	16.9	19.6	36.8	20.6	
Electricity price	€-ct/kWh	9.3	5.3	9.1	7.9	[237]
Natural gas price	€-ct/kWh	4.4	3.2	5.0	4.1	[238-241]

3.2.3.3. Environmental performance

The environmental performance of the STES system was evaluated by CO₂ emission savings. The mass of CO₂ emitted while consuming energy was calculated as

$$m_{CO_2} = \mu_{CO_2}^E \cdot E \quad (3.8)$$

where $\mu_{CO_2}^E$ denotes the CO₂ equivalent emission factor, and E represents the energy consumption.

The CO₂ emission saving was determined by comparing the CO₂ emissions of the conventional system with that of the proposed STES system:

$$\Delta CO_2 = m_{CO_2}^{CS} - m_{CO_2}^{STES} \quad (3.9)$$

Chapter 3

where $m_{CO_2}^{CS}$ and $m_{CO_2}^{STES}$ represent the CO₂ emissions of the conventional system and the STES system, respectively, which can be calculated as

$$m_{CO_2}^{CS} = \mu_{CO_2}^{th} \cdot E_{th} \quad (3.10)$$

$$m_{CO_2}^{STES} = \mu_{CO_2}^{el} \cdot E_{el} + \mu_{CO_2}^{th} \cdot E_{th} \quad (3.11)$$

where $\mu_{CO_2}^{th}$ and $\mu_{CO_2}^{el}$, respectively, denote the CO₂ equivalent emission factors of heating and electricity production, and E_{th} and E_{el} indicate the heating and electricity consumption, respectively. The CO₂ equivalent emission factors used for the four locations are presented in Table 3.4.

Table 3.4 CO₂ equivalent emission factors for the four locations.

	Unit	Harbin	Urumqi	Shanghai	Chengdu	Reference
CO ₂ equivalent emission factor for electricity production	kg/kWh	1.08	0.89	0.79	0.86	[242]
CO ₂ equivalent emission factor for natural gas consumption	kg/kWh	0.20	0.20	0.20	0.20	[243]
CO ₂ equivalent emission factor for conventional systems	kg/kWh	0.40	0.21	0.26	0.29	[242, 244]

3.2.4. Parametric study and optimization

A parametric study was conducted to investigate the impact of system configurations on the technical, economic, and environmental performance of the STES system and provide evidence for optimization. The tested system configurations included the solar collector area, short-term storage tank volume, and the borehole number. The indicators used in the parametric study included SF, LCOH, and CO₂ emission savings. Besides, a sensitivity analysis was conducted to investigate the influence of the equipment unit prices, discount rate, and electricity and natural gas prices on the LCOH calculation.

The minimum LCOH and the minimum CO₂ emissions of the STES system were chosen as the multi-objective functions for optimization, with economic feasibility and environmental impact considered as two crucial factors. The solar collector area and borehole number were selected as the main variables in the optimization. The optimal solutions for the STES system were obtained through Pareto optimization. One Pareto front was obtained for each case by changing relevant parameters, running simulations, and calculating LCOH and CO₂ emissions. Moreover, the CO₂ avoidance cost was determined based on the Pareto front, which describes the cost of CO₂ emission reduction of the proposed system compared with the conventional system, providing a useful way of comparing the costs of various methods of reducing emissions. The optimal solution was selected from the Pareto front by minimum CO₂ avoidance cost criteria. CO₂ avoidance cost can be calculated as follows:

$$CO_2 \text{ avoidance cost} = \frac{\text{Heating cost of STES system} - \text{Heating cost of conventional system}}{CO_2 \text{ emission saving}} \quad (3.12)$$

3.3. Case study

In China, 80% of the demand for heating of urban buildings in northern areas is supplied by DH systems [245]. The total heated area increased by 112%, and the total heat supply amount increased by 35% from 2010 to 2019 [19]. The Chinese government issued the *Winter Clean Heating Plan for Northern China (2017–2021)* in 2017 and the *14th Five-year Plan and Vision 2035* in 2021. These planning policies aim to support renewable energy heating and promote a clean heat transition in northern areas, where STES systems may play a role in facilitating the decarbonization of heat supply systems. In southern China, it has been reported that promoting DH in suitable areas can improve residential welfare and potentially bring economic and environmental benefits [246].

Generally, solar radiation is abundant in China; over two-thirds of the territory receives an irradiance of more than 5000 MJ/m² and more than 2200 hours of sunshine annually [33]. Figure 3.3 illustrates the solar resource distribution. Regarding solar heat applications, 70% of the global solar collector installations are in China [247], which further highlights the potential of STES applications in DH in China.

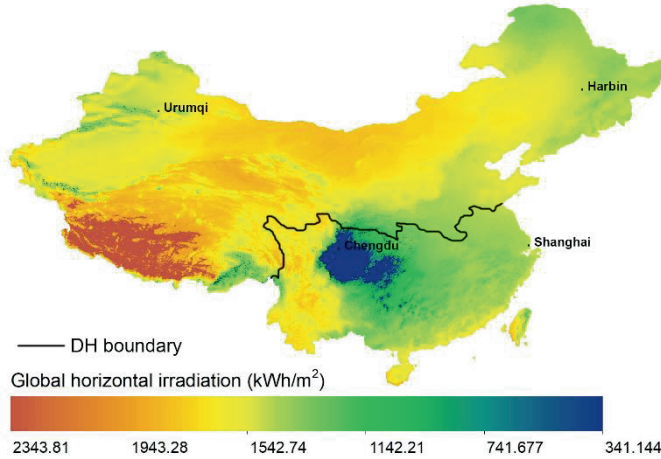


Figure 3.3. Solar resources in China [32].

3.3.1. Local properties

The DH and non-DH areas in China were set according to the “Qin Mountains-Huai River” boundary, named the north-south heating line [246]. As shown in Figure 3.3, Harbin and Urumqi are located in northern China with a DH system, while Shanghai and Chengdu do not have a DH system in southern China. The climatic conditions of the four locations are listed in Table 3.5. The four locations have different heating loads and solar resources. Figure

Chapter 3

3.4 illustrates the monthly average temperature and average global horizontal irradiance (GHI) at the four locations.

Table 3.5 Climatic conditions of the four locations.

	Unit	Harbin	Urumqi	Shanghai	Chengdu
Climate		Temperate monsoon climate	Temperate continental climate	Subtropical monsoon climate	Monsoon-influenced humid subtropical climate
Latitude	°	45	43	31	30
HDD18	°C·day	5032	4329	1540	1344
Average temperature	°C	5.5	8.0	17.5	17.4
Average GHI	W/m ²	151	164	145	113

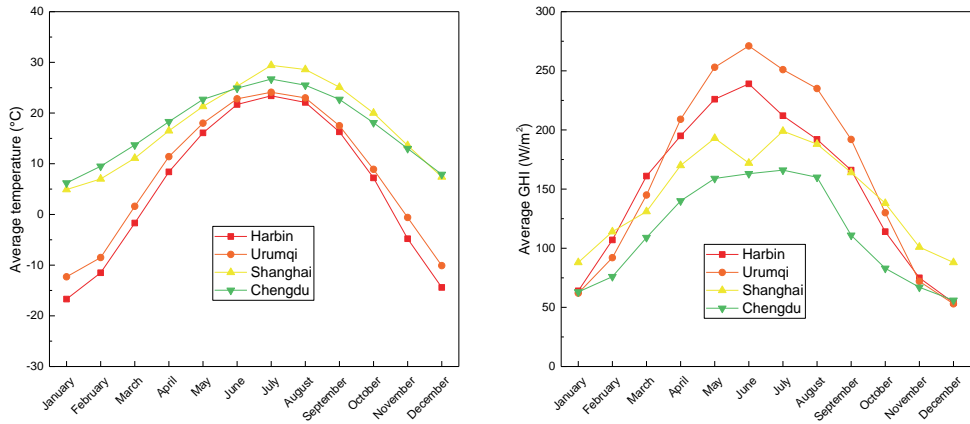


Figure 3.4. Monthly average temperature and GHI at the four locations.

3.3.2. Implementation in China

Table 3.6 Soil properties at the four locations.

Location	Specific heat capacity	Thermal conductivity	Density	Thermal diffusivity	Reference
Unit	kJ/(kg·K)	kJ/(h·m·K)	kg/m ³	×10 ⁻⁷ m ² /s	
Harbin	1.50	8.64	2000	8.0	[248]
Urumqi	0.91	3.26	2120	4.7	[249, 250]
Shanghai	1.31	6.30	1840	7.3	[100, 251]
Chengdu	0.81	4.64	2016	7.9	[251]

The validated model was implemented in four locations in China using local profiles. The weather data, soil properties, and heating load profile were modified to make the model suitable for application in China. Typical meteorological year data generated from

Meteonorm [252] were used as the yearly weather data for the four locations. The soil properties at the four locations are listed in Table 3.6.

A five-floor residential building with 12 family apartments on each floor was analyzed based on a typical local residential building. The selected building was developed in Sketchup [253], as shown in Figure 3.5. The thermal characteristics of the building envelopes, personnel occupancy rate, lighting utilization rate, and equipment utilization rate were assumed according to the *Chinese Design Standard for Residential Buildings* [254, 255]. Table 3.7 summarizes the building design characteristics at the four locations. A community comprising eight typical residential buildings with a total heated area of 33,600 m² was simulated to quantify the hourly heating in each location. The heating load profile at each location was acquired by simulating the building model in TRNSYS using local weather data with an indoor cut-off temperature of 18°C [254, 255]. The hourly and cumulative heating loads at the four locations are presented in Figure 3.6. Note that only space heating was considered. Domestic hot water (DHW) was excluded because there is hardly a central supply system for it in the built environment in China.

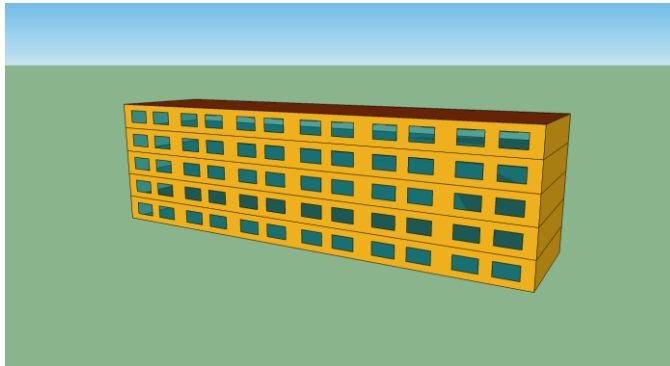


Figure 3.5. Modeled residential building.

Table 3.7 Building design characteristics at the four locations [254-257].

		Unit	Harbin	Urumqi	Shanghai	Chengdu
External wall	U-value	W/(m ² ·K)	0.246	0.246	0.228	0.228
Roof	U-value	W/(m ² ·K)	0.124	0.124	0.228	0.228
Floor	U-value	W/(m ² ·K)	0.159	0.159	0.441	0.441
Window	U-value	W/(m ² ·K)	1.1	1.1	1.1	1.1
	G-value		0.62	0.62	0.62	0.62
Air change of infiltration		1/h	0.5	0.5	1	1
Personnel density		m ⁻²	0.04	0.04	0.04	0.04
Lighting power density		W/m ²	5	5	5	5
Equipment power density		W/m ²	3.8	3.8	3.8	3.8

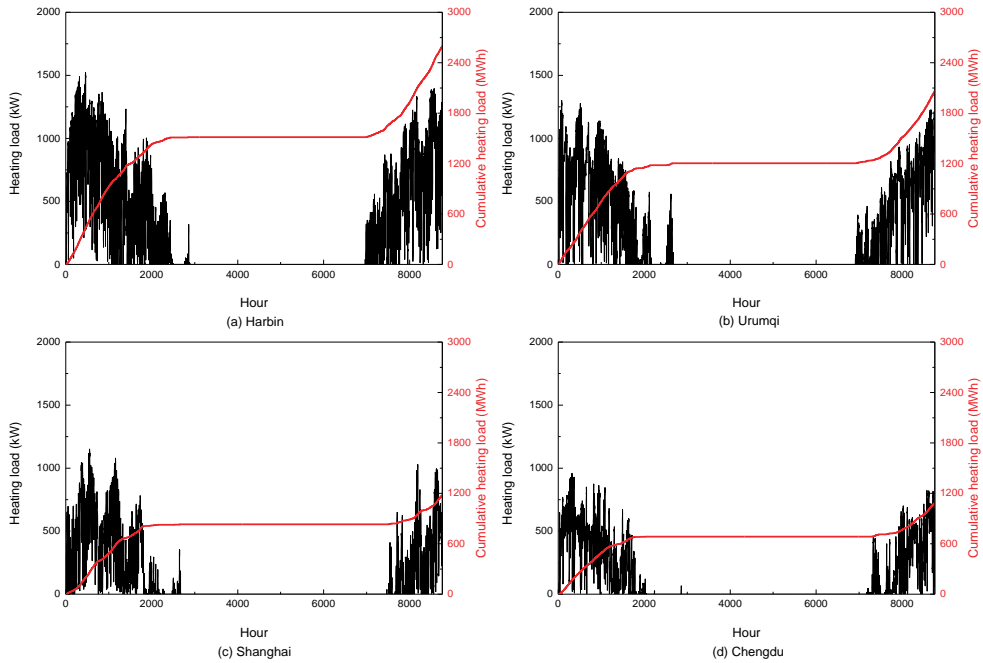


Figure 3.6. Heating load profiles at the four locations.

3.3.3. Adaptive measures

Adaptive measures were introduced to the system design to meet the local climate and heating load profiles at the four locations, including the solar collector tilt angle, solar collector area, short-term storage tank volume, and borehole number. In accordance with the technical standard for solar water heating systems for civil buildings, the solar collector tilt angle should be within plus or minus 10° of latitude [258]. Accordingly, 45° (solar collector tilt angle of the DLSC), latitude -10° , latitude, and latitude $+10^\circ$ were examined. The SF in the fifth year was chosen as the indicator to select a suitable tilt angle. As illustrated in Figure 3.7, the most favorable solar collector tilt angle (45° for Harbin, 53° for Urumqi, 31° for Shanghai, and 20° for Chengdu) was utilized.

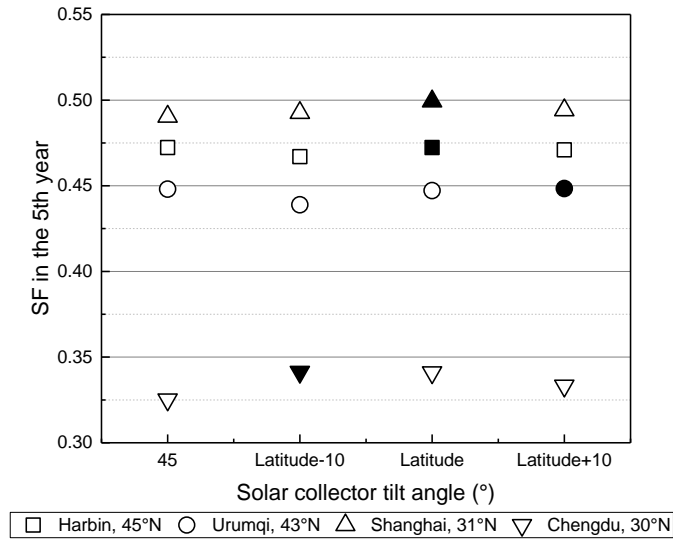


Figure 3.7. SFs in the fifth year of different solar collector tilt angles at the four locations.

Furthermore, the solar collector area was determined by considering an oversizing of 20% of the heating load to cover peak demands [104]. Additionally, the borehole number for each location was revised based on the heating load relative to the DLSC system. The short-term storage tank volume was calculated based on the solar collector area and solar intensity according to [258]. Table 3.8 summarizes the adaptive system configurations for the four locations.

Table 3.8 Adaptive system configurations for the four locations.

Location	Unit	Harbin	Urumqi	Shanghai	Chengdu
Solar collector area	m ²	4870	4460	3230	4400
Short-term storage tank volume	m ³	180	200	120	140
Borehole number		534	426	240	222

3.4. Results

This section summarizes the findings from model validation, techno-economic-environmental analysis, parametric study, and optimization.

3.4.1. Model validation

The annual energy flows and the SFs of the TRNSYS model developed in this study were compared with those of the DLSC measurements, DLSC simulation results, and two previous simulation results of the DLSC system (Renaldi's [106] and Flynn's [222]), as shown in Figure 3.8. The energy flows and SFs of the developed TRNSYS model, DLSC

measurements, Renaldi's, and Flynn's were performed from July 1, 2007, to June 30, 2012, while those of the DLSC simulation were performed from January 1, 2007, to December 30, 2012.

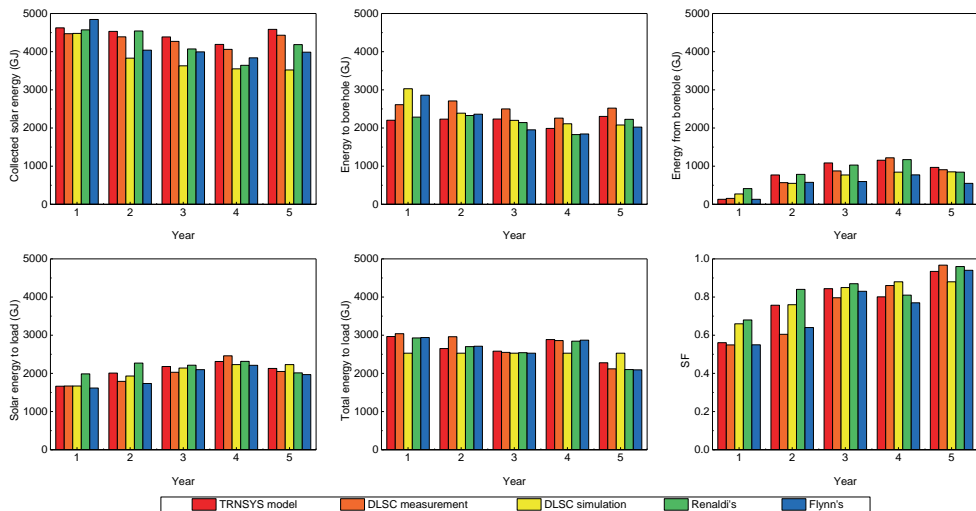


Figure 3.8. Energy flows and SFs during the first five years of operation from different sources.

Generally, the developed TRNSYS model agrees with the trend of DLSC measurements. The different solar irradiation sources can explain the differences in the annual solar energy collected. The solar irradiation adopted in the TRNSYS model was satellite-based data, whereas the DLSC measurements were based on ground-measured data. Although the solar irradiation used in the developed TRNSYS model was corrected according to the DLSC measurement, the correction was based on a year-level while the simulation ran in a timestep of ten minutes. The differences in energy flow charging to and discharging from the borehole are attributable to the modifications made throughout the years. As described by Sibbitt et al. [259], the implementation of system modifications and controls allowed the system to operate in accordance with the design. The modifications in the district loop temperature control settings can also explain the differences in solar energy to load and total energy to load. Moreover, the limitation of the load correction can also partially explain the differences.

Table 3.9 summarizes the differences compared with the DLSC measurements among the different simulation results. The mean difference of the developed TRNSYS model is lower than that of the other sources, which indicates that the developed TRNSYS model has sufficient accuracy for implementation in the examined locations.

Table 3.9 Differences between different simulation results and DLSC measurements.

Source	Collected solar energy	Energy to borehole	Energy from borehole	Solar energy to load	Total energy to load	SF	Mean difference
TRNSYS model	3.2%	12.9%	17.2%	6.0%	4.5%	8.7%	8.8%
DLSC simulation [97]	12.2%	12.8%	25.3%	6.3%	12.6%	12.8%	13.7%
Renaldi's [106]	5.2%	14.3%	46.2%	12.5%	2.9%	15.7%	16.1%
Flynn's [222]	7.7%	16.5%	25.1%	4.8%	2.9%	4.7%	10.3%

3.4.2. Performance evaluation

This section presents the technical, economic, and environmental performances of implementing STES at the four examined locations.

3.4.2.1. Technical performance

The representative energy flows at the four locations are shown in Figure 3.9. A decreasing trend is observed in the figure of solar energy collected, which can be explained by the fact that more thermal energy is needed to charge the borehole during the first few years. More heat is charged into the borehole, and less heat is discharged to reach a thermal balance in the early years. Therefore, a decreased energy flow to the borehole and an increased energy flow from the borehole were observed. Since the borehole stores more heat during operation, the solar energy to the load increases over time, and the energy flow from the boiler to the load decreases accordingly. The total energy to load is stable because the same heating load profile is used yearly. Besides, since the Harbin case comprises the highest heating load, the energy flows are the largest compared with the other cases. It should be noted that more heat is charged into the borehole in the Harbin case; however, less heat is discharged from the borehole than in the Urumqi case, which can be explained by the higher heat loss of the borehole in the Harbin case because of the larger borehole volume, higher soil thermal diffusivity, and cold climate. The energy flows of the Chengdu case were the lowest because the Chengdu case has the lowest heating load. However, the energy flow from the boiler to the load is higher in the Chengdu case than in the Shanghai case, primarily owing to the low solar irradiation in the Chengdu case; therefore, more heat from the boiler is required to meet the heat demand.

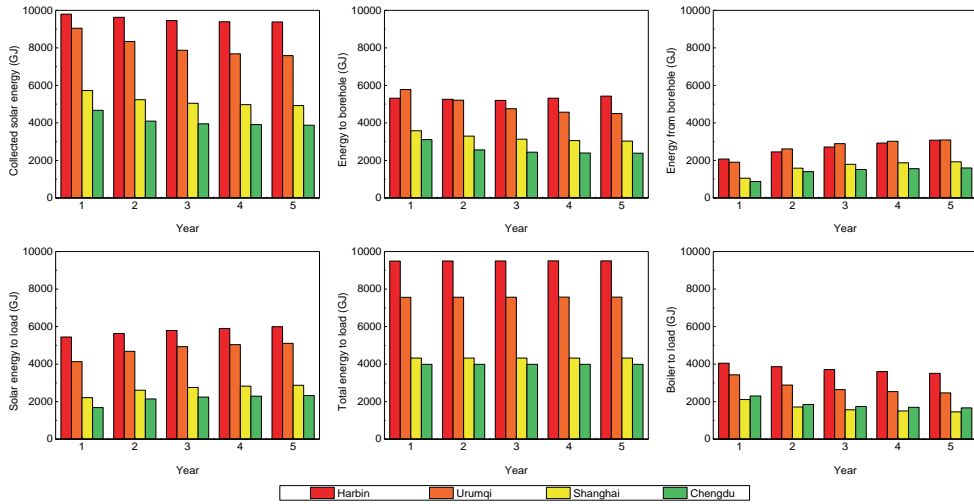


Figure 3.9. Energy flows of the STES systems at the four locations.

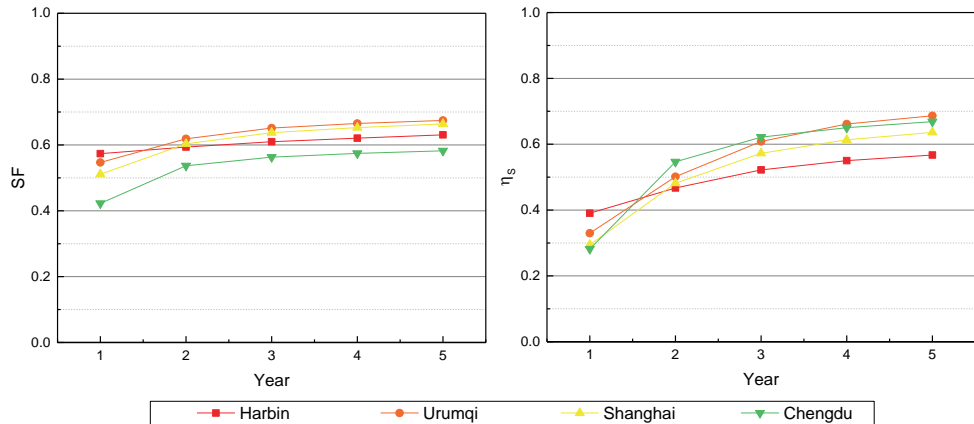


Figure 3.10. SFs and storage efficiencies of the STES systems at the four locations.

Figure 3.10 illustrates the SFs and storage efficiencies at the four locations. The SFs and storage efficiencies have a faded growth trend because the borehole gradually reaches a thermal balance during operation. Since the Urumqi case has richer solar resources than other locations, it has the highest SF and storage efficiency. The SF in the Chengdu case is the lowest owing to the low solar irradiation in the area. Notably, in the Harbin case, both the SF and storage efficiency are the highest in the first year of operation; however, the other cases gradually exceed the figure. It is because the borehole is preheated to 25°C, and the Harbin case has the largest borehole volume; therefore, initially, the Harbin case stores the most

thermal energy. However, the high heat loss of the borehole caused by the cold climate and high soil thermal diffusivity slows the growth trend.

3.4.2.2. Economic performance

Economic performance was evaluated through LCOH analysis and comparison. Figure 3.11 shows the LCOH of the proposed STES systems at the four locations. Identical equipment unit prices were used for different cases, and the electricity and natural gas prices were location-based. It was found that the Urumqi case achieves the lowest heating cost owing to its cheaper electricity and natural gas prices than the other locations. The Chengdu case has the highest heating cost owing to its low solar irradiation. There was no significant difference in LCOH in a similar climate zone. In summary, the STES system is more attractive in the northern area, with a higher heating load and better solar irradiation than in the southern region.

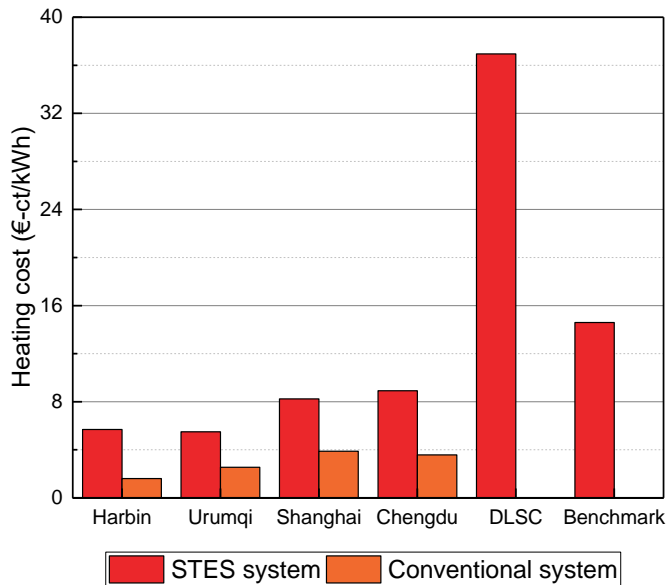


Figure 3.11. Heating costs of the STES and conventional systems at the four locations, the DLSC system, and the benchmark case in Europe (Calculation process presented in the Appendix (Tables 3.A1-A3)).

The heating costs of the conventional systems were also calculated to position the STES project in the local heat energy market. The calculations were based on a coal-fired combined heat and power (CHP) system for the Harbin case and a natural gas-fired CHP for the Urumqi case. For the Shanghai and Chengdu cases, it was assumed that air conditioning systems supplied heat to the proposed community because air conditioning systems account for the highest share of the most common household heating devices in southern China [17]. Figure

3.11 compares the heating costs of the STES and conventional systems at the four locations. It was found that the heating cost of the STES system in Harbin was more than three times that of the coal-fired CHP. The heating cost of the STES system in Urumqi is more than twice that of the natural gas-fired CHP. The heating costs of the STES systems in Shanghai and Chengdu were more than twice those of air conditioning systems. It is evident that STES cannot compete with existing fossil fuel-dominated heating supply technologies. Currently, individual heating in the southern area is more expensive than DH in the north.

Furthermore, the heating costs of the STES systems at the four locations were also compared with those of the DLSC system and the benchmark case in Europe, as shown in Figure 3.11. The benchmark case in Europe was based on the STES with solar heating presented by the International Energy Agency Solar Heating and Cooling program, indicating the average heating cost of 14 practice examples in operation in Europe [233]. The costs of the examined STES projects were converted to 2021 constant prices in Euros using the inflation and exchange rates derived from the Organization for Economic Co-operation and Development [179, 180]. It was found that the implementation of the STES system in China has a lower LCOH, primarily because of the low-priced equipment and labor. Meanwhile, the LCOH of the DLSC system is much higher than that of the other cases because it was designed to achieve over 90% SF; namely, the system is oversized.

3.4.2.3. Environmental performance

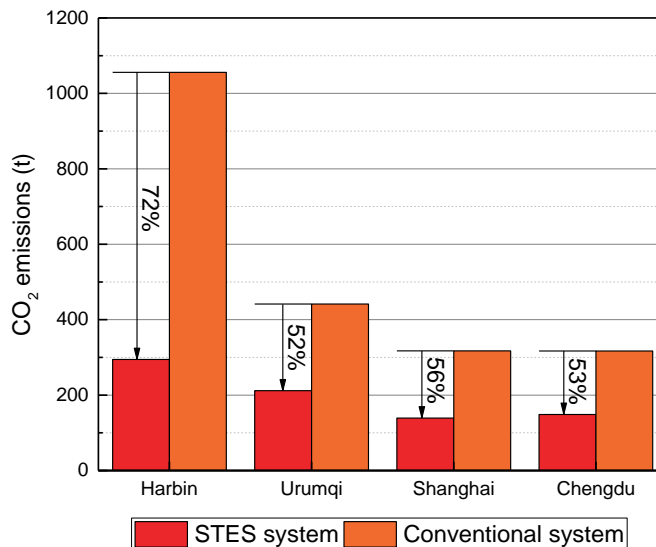


Figure 3.12. CO₂ emission saving of the STES systems at the four locations. (Calculation process presented in the Appendix (Table 3.A4)).

The CO₂ emission saving of the STES systems at the four locations is illustrated in Figure 3.12. Compared with the existing heating system, the implementation of the STES has the potential to reduce CO₂ emissions at all the examined locations. The Harbin case has the highest reduction potential since 95.8% of the existing DH system is based on coal combustion [260]. The Urumqi case reduces the least CO₂ emissions, primarily because natural gas dominates the existing DH system [261].

3.4.3. Parametric study and optimization

This section summarizes the findings from a parametric study investigating how the system configurations influence the overall performance, a sensitivity analysis on the LCOH calculation, and a multi-objective optimization considering economic feasibility and environmental impact.

3.4.3.1. Parametric study

Several system configurations were further investigated to determine the impact on the technical, economic, and environmental performance and provide a solid base for the following optimization, including solar collector area, short-term storage tank volume, and borehole number. Accordingly, SF, LCOH, and CO₂ emission savings were utilized as indicators, and the Harbin case was used to perform the parametric study.

The SFs, LCOHs, and CO₂ emission savings for various solar collector areas are shown in Figure 3.13. The SF increases as the solar collector area increases. However, the increased extent decreases because more solar energy collected through the larger solar collector area can cause a higher temperature of the borehole, leading to greater heat loss. In addition, the SF trends of different solar collector areas are similar; however, a higher solar collector area leads to a more rapid increment in the early years. It is primarily because more heat collected owing to a larger solar collector area helps speed up the warm-up process of the borehole. As the solar collector area increased, the LCOH decreased when the solar collector area was lower than 4870 m² but increased subsequently. The decreasing trend is because more solar energy is harvested to supply the load, which corresponds to less natural gas usage. However, as the solar collector area increases, the benefits of more solar energy collected cannot offset the impact of increased investment in the LCOH; therefore, the LCOH starts to increase. It highlights the significance of choosing an appropriate solar collector area to achieve the lowest LCOH. The blind pursuit of a high SF has a negative impact on economic performance. In addition, the STES system reduces more CO₂ emissions as the solar collector area increases. The increased rate of CO₂ emission savings was found to decrease. The trend also agrees with the previous analysis of SF.

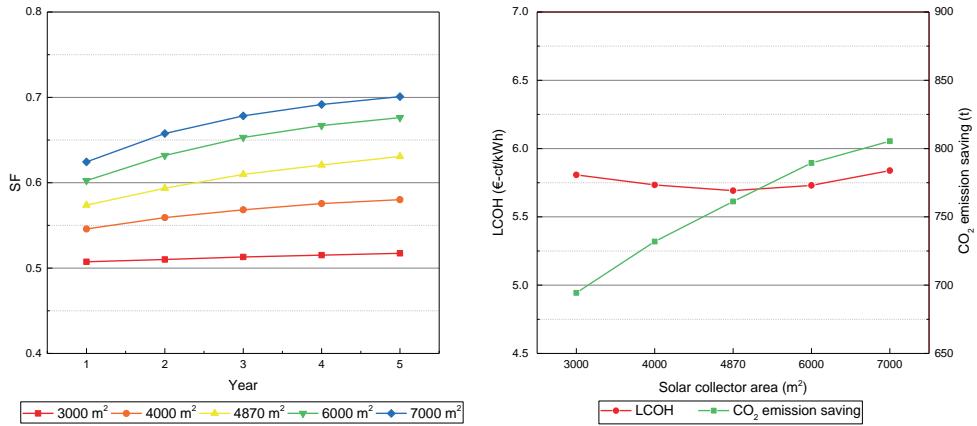


Figure 3.13. SFs, LCOHs, and CO₂ emission savings for various solar collector areas.

The SFs, LCOHs, and CO₂ emission savings for various short-term storage tank volumes are presented in Figure 3.14. It was found that the short-term storage tank volume had less influence on the system performance than the solar collector area. A larger short-term storage tank volume helps increase SF slightly and reduce more CO₂ emissions. Since enlarging the short-term storage tank allows to store more heat in the buffer, additional solar thermal energy will be transferred to the load directly, leading to less heat loss caused by long-term storage. In addition, with an increment in the short-term storage tank volume, the influence on the performance gradually decreases, similar to the tendency of the solar collector area. A turning point of the LCOH was found for the same reason as the solar collector area.

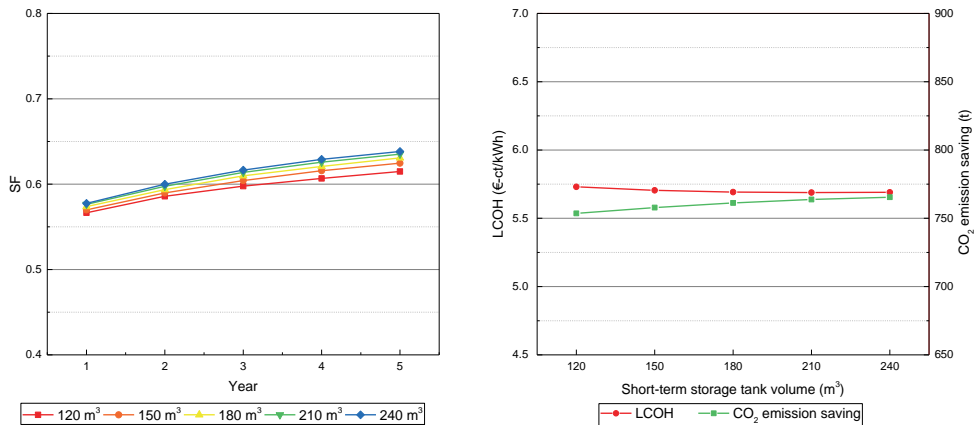


Figure 3.14. SFs, LCOHs, and CO₂ emission savings for various short-term storage tank volumes.

Figure 3.15 illustrates the SFs, LCOHs, and CO₂ emission savings for various borehole numbers. As the borehole number increases, the SF increases until the borehole number is less than 420 and decreases afterward because increasing the borehole number helps store more thermal energy. However, an oversized borehole can cause more heat loss. Additionally, borehole investment accounts for the highest proportion of the total investment; therefore, increasing the borehole number can rapidly increase the LCOH. Since the borehole number is less influential on the SF but has a larger impact on the LCOH, it is possible to reduce it to achieve a lower LCOH. Moreover, increasing the borehole number helps reduce more CO₂ emissions because more heat can be stored owing to the larger storage size. However, unduly increasing the borehole number negatively affects the reduction of CO₂ emissions because a higher borehole volume can reduce the borehole storage temperature. Consequently, the boiler needs to consume more natural gas to increase the temperature to meet the supply setpoint temperature.

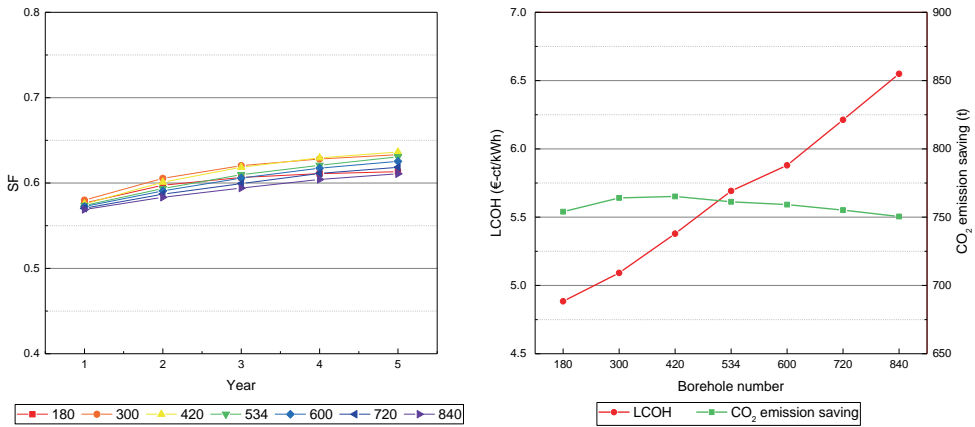


Figure 3.15. SFs, LCOHs, and CO₂ emission savings for various borehole numbers.

3.4.3.2. Sensitivity analysis

A sensitivity analysis based on the Harbin case was conducted to investigate the influence of the equipment unit prices, discount rate, and electricity and natural gas prices on the LCOH calculation. The fifth-year results were used in the calculation because the BTES system develops its maximum capacity for energy contribution from the fifth year of operation [104]. Figure 3.16 presents the effect of 5% and 10% increases or decreases in investment cost, fuel cost, and discount rate value on the LCOH of the STES system. Note that the unit price of the borehole, solar collector, and pipeline are influential factors in the LCOH of the STES system among the investment costs. The LCOH is more sensitive to the natural gas price than electricity. The discount rate also has a significant impact on the LCOH calculation. Considering that the natural gas price and discount rate are locally based, cheaper solar

collectors and pipelines and more efficient borehole construction can reduce the LCOH of the STES system.

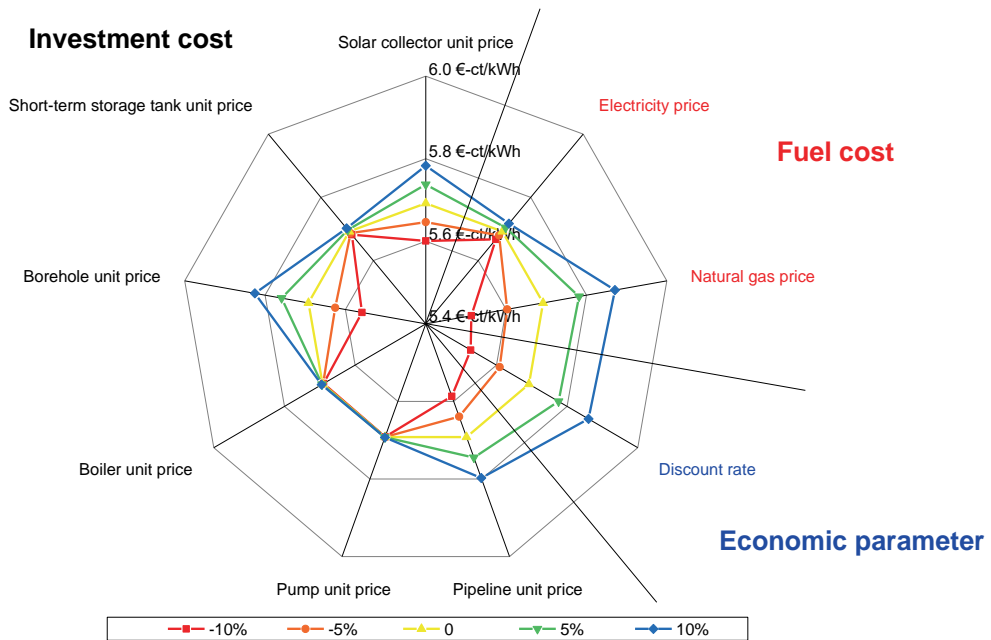


Figure 3.16. Sensitivity analysis of the LCOH calculation with 5% and 10% increases or decreases in investment cost, fuel cost, and discount rate.

3.4.3.3. Multi-objective optimization

The parametric study found that the solar collector area and borehole number are the most influential variables in the system configurations; therefore, they were selected as the main variables in the optimization. Figure 3.17 (left) presents the Pareto fronts of the four cases through multi-objective optimization. These curves demonstrate the non-dominated solutions where minimum LCOH and CO₂ emissions occur. The LCOH increased when CO₂ emissions decreased, and the opposite trend was observed. The CO₂ emission increased when the LCOH was reduced. For comparison, the conventional heating options at the four locations are presented in Figure 3.17 (left). The proposed STES systems at the four locations fail to compete with conventional heating options in terms of cost. However, they certainly have a positive influence on the environment.

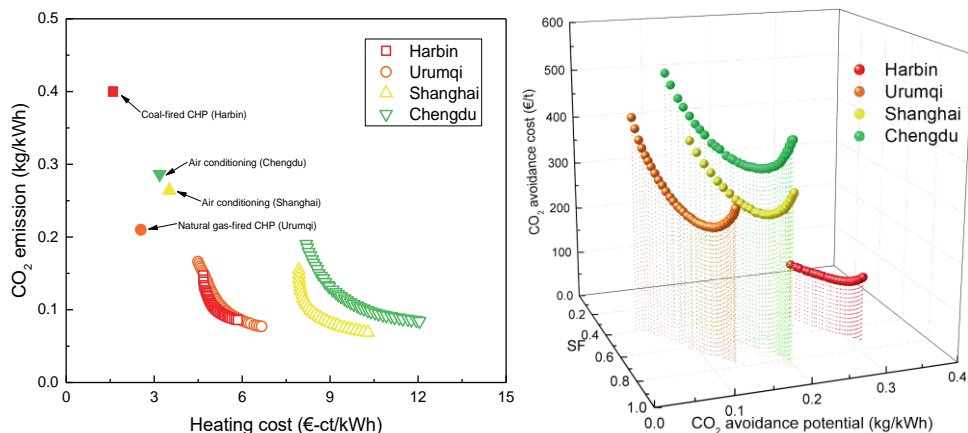


Figure 3.17. Pareto fronts (left) and CO₂ avoidance costs (right) of the four cases.

Upon identifying the Pareto front, it is critical to select a solution from the Pareto front by following the wills and needs of the stakeholders [262]. Therefore, the CO₂ avoidance costs of the four cases were calculated based on the set of non-dominated solutions on the Pareto fronts, as shown in Figure 3.17 (right). Accordingly, the Harbin achieved the lowest CO₂ avoidance cost at the same SF value. It also has the highest CO₂ avoidance potential because the conventional heating option is coal-fired CHP. Besides, Chengdu's highest CO₂ avoidance cost at the same SF value is due to its weak solar resources. A larger system size is needed to achieve the same level of SF as in the other cases, namely, higher costs. The Urumqi case has the lowest CO₂ avoidance potential since its conventional heating option is a natural gas-fired CHP with a lower CO₂ equivalent emission factor.

The optimal solutions for the four cases were selected with the minimum CO₂ avoidance cost criteria. Table 3.10 lists the system configurations and techno-economic-environmental performances of the optimal solutions for the four cases. Compared with the original design, it was found that the pathway of optimization in the cold climate zone (Harbin and Urumqi) involves reducing the borehole number to reach a higher storage efficiency and lower LCOH while reducing less CO₂ emissions. The optimization pathway for the warm climate zone (Shanghai and Chengdu) involves increasing the solar collector area to increase the SF and reduce more CO₂ emissions, although the LCOH slightly increases. Moreover, the soil properties should be considered when designing the borehole number. For instance, in the two cases in the cold climate zone, the borehole number of the Urumqi case is more than twice that of the Harbin case because the soil thermal diffusivity of the Harbin case is higher than that of the Urumqi case. Significant heat loss can occur in the cold climate zone if the thermal diffusivity of the soil is high. Thus, reducing the borehole number for cases with high soil thermal diffusivity can help increase the storage efficiency of the borehole. Besides, the specific heat capacity of the Urumqi case was also lower than that of the Harbin case. Notably, increasing the borehole number for cases with a low specific heat capacity can help decrease

the borehole temperature and reduce the heat loss accordingly. Within the two cases in the warm climate zone, the borehole number of the Chengdu case is higher than that of the Shanghai case because the specific heat capacity of the Chengdu case is lower than that of the Shanghai case.

Table 3.10 System configurations and techno-economic-environmental performances of the optimal solutions for the four cases (compared with the original design).

	Unit	Harbin	Urumqi	Shanghai	Chengdu
Solar collector area	m ²	5000 (3%)	5000 (12%)	4500 (39%)	5000 (14%)
Borehole number		150 (-72%)	330 (-23%)	240 (0%)	270 (22%)
SF	%	60.8 (-4%)	66.7 (-1%)	75.8 (14%)	64.3 (10%)
Storage efficiency	%	69.2 (22%)	70.5 (3%)	60.5 (-5%)	66.6 (0%)
LCOH	€-ct/kWh	4.9 (-15%)	5.4 (-2%)	8.5 (3%)	9.3 (4%)
CO ₂ emission saving	t/a	752.5 (-1%)	228.5 (-1%)	205.0 (15%)	183.2 (9%)
CO ₂ emission saving per heat	kg/MWh	285.1 (-1%)	108.7 (-1%)	170.6 (15%)	165.4 (9%)
CO ₂ avoidance cost	€/t	114.4 (-19%)	260.8 (-3%)	291.4 (-9%)	368.3 (-2%)

3.5. Discussion

This study performed a techno-economic-environmental analysis of applying STES with solar heating in different climate zones of China based on the developed TRNSYS model. There are underlying assumptions in the TRNSYS model that influence model accuracy. For instance, the borehole component (type 557a) assumes that boreholes are uniformly placed within a cylindrical storage volume of the ground. In addition, it only considers the conductive heat transfer between the pipes and soil, ignoring the groundwater flow. The storage efficiency decreases with the presence of groundwater flow [263]. A lower storage efficiency leads to a lower SF and more gas consumption from the gas boiler, negatively impacting the technical, economic, and environmental performance of STES. Some studies have used detailed modeling software for boreholes (for example, Ground Heat Exchanger Analysis, Design and Simulation) to provide flexibility in the borehole layout design and produce more favorable results in borehole simulations [264, 265]. Nevertheless, TRNSYS has been widely used in STES modeling and has been proven to exhibit a good level of accuracy [57, 130].

More accurate weather data, heating load profiles, and more suitable model components were used in this study to obtain a better validation result. Consequently, the difference between the simulation results of this study and the DLSC measurements remained within 10%. It indicates that the model is sufficiently accurate for predicting the performance of subsequent implementations. Moreover, the soil properties of the examined locations chosen in this study were derived from peer-reviewed journal articles, indicating their potential values in these locations. Since soil properties affect the technical performance of the STES system, especially the storage efficiency [106, 266], in situ thermal response tests (TRT) from

practical engineering are required to improve the accuracy of the performance prediction [166, 267].

This study developed an STES model based on the DLSC schematic design. The model was validated with the DLSC measurements and previous simulation results, and the system size was adapted to be allocated in different climates. The limitation of the solar thermal collector and borehole installation was not considered. Applying a uniform system structure in the four case studies enabled quantifying the impact of local context (climate conditions and existing heating infrastructure) on the optimal configuration planning, techno-economic-environmental performance, and feasibility of the STES application. Conclusions on the key technical parameters in achieving the optimal techno-economic-environmental performance and determining the configuration planning of STES in different climate zones were drawn by comparing the optimal configuration and the original design. DHW was excluded in this study since there is no central DHW supply in the conventional system. However, adding DHW has a positive impact on solar energy integration. It is suggested to be included in future sustainable heating systems.

STES with solar heat can reduce fossil fuel consumption and CO₂ emissions, facilitating the clean heating transition. It can also be beneficial to other low-cost sources, including industrial waste heat and waste heat from CHP-based power generation outside the heating season. Besides working as the heat supply unit, STES can be integrated with heat pumps, taking advantage of low-temperature heat sources during the summer and leading to a high coefficient of performance (COP) of heat pumps. Coupling with power-to-heat technologies can increase the utilization of renewable power sources and provide electrical network balancing [200].

In northern China, DH systems primarily use fossil-based boilers and CHP plants (in which coal-based heat supply units accounted for 92% of the total [17]). A series of national development plans have encouraged clean fossil-based DH, and carbon capture and storage (CCS) is regarded as a potential method. According to the Intergovernmental Panel on Climate Change [268], the total costs for CO₂ capture, transport, and geological storage are approximately 30–71 \$/t and will cause a 20%–30% loss in plant efficiency; the corresponding cost will increase by 40%–80%. Carbon capture costs will be higher in the upfront installation costs of CCS equipment because CCS-related devices are not installed in traditional coal-based plants in China [269]. Therefore, the heating cost of the STES application may be slightly higher than that of the coal-based heating options combined with CCS. However, it can help increase the share of renewable energy in DH systems.

Electricity-based heating solutions are commonly used in southern China, among which air conditioning and electric heaters are prevalent [17]. According to *China's National Economic and Social Development Statistics Bulletin* in 2020, China's installed power generation capacity is 2200 GW with 56.6% thermal power, 16.8% hydropower, 24.3%

renewable power, and 2.3% nuclear power [270]. The ratio of thermal power is expected to decrease to 46.8% by 2025 [271]. The development of renewable power may reduce the advantage of STES in terms of CO₂ emission reductions compared to conventional heating systems in the south. The carbon intensity of the electricity generation sectors needs to be reduced by 66% and 62%, respectively, to make the CO₂ emission level of conventional heating in Shanghai and Chengdu comparable with the STES system. The cost of decarbonizing China's power sector through wind and solar power is between 19–31€/t [272], which is cheaper than STES (291–368 €/t). Therefore, for clean heat transition in southern China, decarbonizing the power sector is more economically attractive than STES.

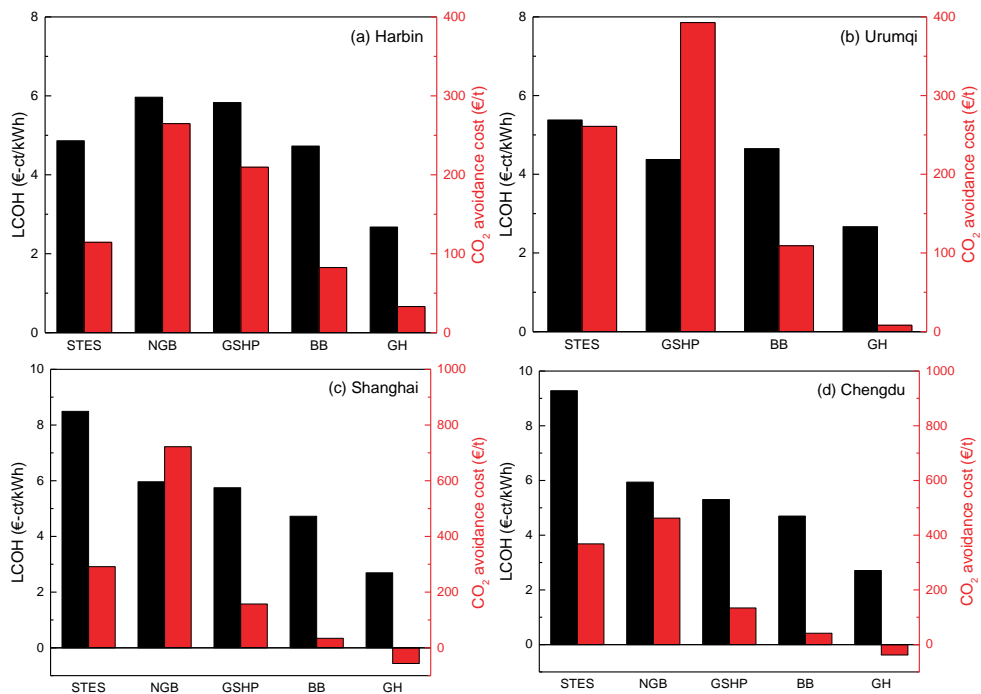


Figure 3.18. LCOHs and CO₂ avoidance costs of the sustainable heating options in the four locations.

Some studies have investigated the economic and environmental performance of sustainable heating options replacing coal-based heating in the Chinese context, including NGBs [22], ground source heat pumps (GSHPs) [273], biomass boilers (BBs) [22], and geothermal heating (GH) [274]. Figure 3.18 compares the LCOHs and CO₂ avoidance costs of the STES and the sustainable heating options. The cost and emission data were derived from the previous studies and adopted based on the local context in the four locations. It is evident that GH has the lowest LCOH and CO₂ avoidance cost, especially in Shanghai and Chengdu, where it has a lower LCOH than the conventional system and emits less CO₂; however, the application partially depends on the suitability of local geological conditions. BB also has a

relatively low LCOH and CO₂ avoidance cost. Still, the limited availability of biomass resources should be aware, and biomass is also needed in other sectors to support decarbonization transitions. STES has lower CO₂ avoidance costs than GSHP in the two northern locations. In comparison, it has higher CO₂ avoidance costs than GSHP in the two southern locations, indicating STES is attractive in northern areas, and GSHP is attractive in southern regions.

3.6. Conclusions

STES combined with DH positively impacts clean heat transition. Literature study shows a lack of in-depth insights into economic and environmental performances to provide the facts on the position of STES applications compared with other sustainable heating technologies. An optimization approach is needed to obtain insights into the optimal economic and environmental performance and the conditions to achieve it. It requires an integrated optimization criterion and method to select the optimal solution. This study develops a comprehensive quantitative method for the techno-economic-environmental performance analysis and proposes an integrated optimization criterion by including economic and environmental impacts to perform a multi-objective optimization on STES system configurations. The impact of local context on the optimal configuration planning, techno-economic-environmental performance, and feasibility of the STES application is examined. The key technical parameters in achieving the optimal techno-economic-environmental performance and determining the configuration planning of STES in different climate zones are investigated. The position of STES compared to other sustainable heating options considering the local context is identified. The TRNSYS modeling tool is adopted to analyze the performance of the STES systems, and Pareto optimization is applied to treat the multi-objective optimization. This study provides a comprehensive and transparent showcase highlighting the importance of the local context in determining the feasibility of STES in the clean heating transition.

From a technical perspective, the four examined locations can potentially implement the STES system. During the operation, the energy flows of solar energy collected, energy to the borehole, and boiler to load decreased, while energy from the borehole and solar energy to load increased. The SFs and storage efficiencies had a faded growth trend. The Urumqi achieved the highest SF and storage efficiency. The SFs and storage efficiencies of the four case studies ranged between 58%–67% and 57%–69%, respectively, which are fairly similar in very different climates. It was found that implementation in locations with higher solar irradiation and heat retention of soil can achieve higher SF and storage efficiency. From an economic point of view, the Urumqi case achieved the lowest heating cost among the four case studies (5.4–8.7 €/ct/kWh). However, the heating costs of the STES systems in all examined locations were more than twice those of the conventional system (fossil fuel-based CHP for Harbin and Urumqi and air conditioning for Shanghai and Chengdu). Compared with the DLSC project and the benchmark case in Europe, the LCOH of STES applications

in China is one to three times lower. From an environmental perspective, the STES system is the most attractive in Harbin to replace the conventional coal-based DH system (72% CO₂ emission saving). Implementing the STES system in the other three locations also has a large potential to reduce CO₂ emissions (52%–56%). The CO₂ avoidance cost of the four case studies ranges between 114–368 €/t. Harbin achieved the lowest CO₂ avoidance cost because the conventional heating option is coal-fired CHP. Chengdu's highest CO₂ avoidance cost is due to its weak solar resources. In summary, implementing the STES system in China is technically feasible. It is attractive in locations with rich solar resources, high heating loads, and currently coal-based heating systems.

The parametric study shows that a larger solar collector area and short-term storage tank volume help increase SF and reduce more CO₂ emissions. A turning point was found in the LCOH trend, indicating the significance of choosing an appropriate size to achieve the lowest LCOH. A larger borehole number can cause an increase in the LCOH, while a turning point was found in the SF and CO₂ emissions trends. Since the borehole number is less influential on the SF but has a larger impact on the LCOH, it is possible to reduce it to achieve a lower LCOH. The parametric study highlights that the solar collector area has a more significant impact on the SF and CO₂ emission reduction, and the borehole number has a greater influence on the LCOH, while the short-term storage tank is less influential than those two parameters. Besides, the sensitivity analysis on the LCOH calculation shows that the unit price of the borehole, solar collector, and pipeline are influential factors in the LCOH of the STES system among the investment costs. The LCOH is more sensitive to the natural gas price than electricity. The discount rate also has a significant impact on the LCOH calculation. Moreover, the multi-objective optimization for minimizing LCOH and CO₂ emissions proposes that appropriately reducing the borehole number for the STES system in cold climate zones can help achieve a higher storage efficiency and a lower LCOH. Increasing the solar collector area in warm climate zones is conducive to achieving higher SF and greater CO₂ emission reduction. The soil properties should be considered when designing the borehole number.

For sustainable heat transition in China, STES helps increase the share of renewable energy in fossil fuel-based DH in the northern area. In southern China, where electric heating is the dominant heat supply, decarbonizing the power sector is more economically attractive than applying the STES system. Compared to other sustainable heating options, STES fails to compete with GH and BB, but their applications are limited by geological conditions and availability. STES has a lower expense for obtaining environmental benefits than NGB and GSHP in the northern area, while GSHP is more attractive than STES in the southern region. The focus of this study is STES. For future research, it is suggested to carry out an integrated assessment of the technical, economic, and environmental performances of various sustainable heating technologies and their implementation feasibility at the local level. This way, STES with solar heating will be assessed in a broad context in which locally available sustainable heat options are included.

Acknowledgments

The financial support from the China Scholarship Council (No. 201806220072) is gratefully acknowledged. The authors would like to thank Renaldi Renaldi (University of Oxford, UK) for his help in this work.

Appendix

Table 3.A1 LCOH calculation of the STES systems at the four locations.

	Unit	Harbin	Urumqi	Shanghai	Chengdu
Investment					
Solar collector	k€	306.8	281.0	203.5	277.2
Short-term storage tank	k€	33.8	37.6	22.6	26.3
Borehole	k€	448.6	357.8	201.6	186.5
Natural gas boiler	k€	9.6	9.6	9.6	9.6
Pump	k€	2.6	2.6	2.6	2.6
Pipeline	k€	354.7	354.7	354.7	354.7
Labor cost	k€	82.1	87.3	119.0	90.4
Total investment	M€	1.2	1.1	0.9	0.9
O&M					
Maintenance	k€/a	8.7	7.8	6.0	6.4
Electricity	k€/a	6.6	3.5	5.6	4.1
Natural gas	k€/a	47.2	24.1	22.5	21.0
Total O&M	k€/a	62.4	35.4	34.1	31.6
Production					
Heat production	GWh/a	2.6	2.1	1.2	1.1
Parameter					
Discount rate	%	5	5	5	5
Lifetime	year	25	25	25	25
Result					
LCOH	€-ct/kWh	5.7	5.5	8.2	8.9

Table 3.A2 Heating cost calculation of the conventional systems at the four locations.

CHP	Unit	Harbin- coal-fired	Urumqi- natural gas- fired	Air conditioning	Unit	Shanghai	Chengdu
Depreciation	M€/a	5.2	11.1	Investment	B€	131.9	131.9
O&M	M€/a	18.9	59.6	O&M	B€/a	31.7	24.7
Heat production	TWh/a	1.5	2.8	Heat production	TWh/a	1.2	1.1
				Discount rate	%	5	5
				Lifetime	year	12	12
Heating cost	€- ct/kWh	1.6	2.5	Heating cost	€- ct/kWh	3.9	3.6

Table 3.A3 Heating cost comparison of the STES systems at the four locations, DLSC system, and benchmark case in Europe.

	Unit	Harbin	Urumqi	Shanghai	Chengdu	DLSC [40]	Benchmark case [233]
Investment							
Specific equipment cost	k€/m ²	254.2	253.5	282.8	215.3	1217.2	571.4
Specific labor cost	k€/m ²	16.9	19.6	36.8	20.6	107.8	109.6
Specific investment cost	k€/m ²	271.1	273.1	319.6	235.8	1325.0	681.1
O&M							
Maintenance	k€/a	8.7	7.8	6.0	6.4	20.9	21.4
Electricity	k€/a	6.6	3.5	5.6	4.1	2.0	1.8
Natural gas	k€/a	47.2	24.1	22.5	21.0	0.2	0
Total O&M	k€/a	62.4	35.4	34.1	31.6	23.1	23.3
Production							
Heat production	GWh/a	2.6	2.1	1.2	1.1	0.6	1.5
Parameter							
Discount rate	%	5	5	5	5	4 [275]	3
Lifetime	year	25	25	25	25	25	25
Result							
LCOH	€- ct/kWh	5.7	5.5	8.2	8.9	36.9	14.6

Table 3.A4 CO₂ emission saving calculation of the STES systems at the four locations.

	Unit	Harbin	Urumqi	Shanghai	Chengdu
STES					
CO ₂ emissions for electricity production	kg/kWh	76.1	58.2	48.6	44.9
CO ₂ emissions for natural gas consumption	kg/kWh	218.6	153.6	90.7	103.8
Conventional system					
CO ₂ emissions	kg/kWh	1055.9	441.6	317.2	317.0
Result					
CO ₂ emission saving	t/a	761.2	229.8	178.0	168.3
CO ₂ emission saving	%	72.1	52.0	56.1	53.1
CO ₂ emission saving per heat	kg/MWh	288.4	109.3	148.1	151.9



4

Integrated assessment on the implementation of sustainable heat technologies in the built environment in Harbin, China

Published in: Yang T, Liu W, Kramer GJ. Integrated assessment on the implementation of sustainable heat technologies in the built environment in Harbin, China. *Energy Conversion and Management* 2023;279:116764.

Abstract

Heating in built environments is an essential factor regarding energy consumption and CO₂ emissions. Thus, the application of sustainable heating technologies is vital for reducing CO₂ emissions. The literature indicates the requirement for a comprehensive assessment of the technical, economic, and environmental performances of various sustainable heating technologies and their implementation feasibility at the local level. Accordingly, this study presents a quantitative assessment relative to Harbin, a typical northern city with a coal-dominated heating system. Seven sustainable heating technologies were examined using current policy and future renewable scenarios. The results indicate that the examined heating technologies are technically feasible. Biomass heating saves costs and emissions (CO₂ avoidance costs of 24–47 €/t), although fuel availability and storage management limit its implementation. Solar heating is a promising technology with reduced costs and low CO₂ emissions (CO₂ avoidance costs can decline by 50% from 2020 to 2050). However, its current resident acceptance is relatively low as lengthy investigations and periods for underground construction are required. Electric heating is preferable in terms of implementation feasibility; however, its economic competitiveness and environmental impact depend heavily on electricity prices and grid cleanliness (CO₂ avoidance costs of 120–463 €/t). This study contributes to the existing literature on sustainable heat transition in China by providing informative local circumstances in Harbin and presenting assumption-making methods in detail when local data is not transparent. The integrated assessment provides solid evidence to facilitate decision-making in the clean heating transition in northern cities of China. The methods are applicable to other countries with similar heat-supply structures and climate conditions.

Chapter 4

Nomenclature

Symbols

E	energy (kWh)
I	investment cost (€)
m	mass (kg)
n	lifetime (year)
r	discount rate
t	time (year)

Greek symbols

ΔCO_2	CO ₂ emission reduction (kg)
η	efficiency
μ	CO ₂ emission factor (kg/kWh)

Abbreviations

ASHP	air source heat pump
BB	biomass boiler
CAC	CO ₂ avoidance cost
COP	coefficient of performance
EB	electric boiler
GSHP	ground source heat pump
HP	heat pump
LCOH	levelized cost of heat
MCM	Monte Carlo method
NGB	natural gas boiler
O&M	operation and maintenance

SAGSHP	solar-assisted ground source heat pump
SF	solar fraction
SHT	sustainable heating technology
STES	seasonal thermal energy storage
TMY	typical meteorological year

Subscripts

bore	borehole
CS	conventional system
el	electricity
sys	system
th	thermal

4.1. Introduction

As the world's largest energy consumer, contributing approximately 30% of global CO₂ emissions, China has promised a peak in CO₂ emissions by 2030 and to achieve carbon neutrality before 2060 [9]. Heating is an important factor in energy consumption and is a significant CO₂ emitter in China's building sector [276]. In 2020, urban heating in the northern area consumed 214 million tons of coal equivalent and emitted 550 million tons of CO₂, accounting for 26% and 33% of national energy consumption and CO₂ emissions in the built environment, respectively [277]. Therefore, decarbonizing residential heating is essential to achieving China's carbon neutrality target.

To alleviate environmental pollution and carbon emissions caused by coal-dominated heating, China issued the *Clean Winter Heating Plan in Northern China (2017–2021)*, clarifying the definition of clean heating for the first time [21]. Clean heating, in the plan, refers to using natural gas, electricity, geothermal, biomass, solar energy, industrial waste heat, clean coal (ultra-low emission), and nuclear energy to achieve low-emission and low-energy-consumption heating methods through highly efficient heating systems. These technologies largely align with the focus of alternative heating methods emerging in developed countries and regions [278]. The implementation of this plan requires local authorities to comprehensively evaluate and select suitable sustainable heating technologies (SHTs) based on local conditions.

The clean heating transition is essential to an effective response to climate change. Itten et al. [279] discussed the transition to sustainable heating systems (e.g., district heating systems, heat pumps, and solar thermal systems, in combination with thermal insulation) with a focus on developing, implementing, and testing incentives that target home/building owners to make investments. Yuan et al. [280] analyzed the trade-off problem between excess industrial heat and heat pumps in district heating systems under a 100% renewable energy scenario for 2050 for Aalborg. López-Bernabé et al. [281] introduced energy-efficiency policies for decarbonizing residential heating in Spain, analyzing the role of perceptions from different stakeholders in the heating transition process. Molar-Cruz et al. [282] proposed the cost-optimal coordinated deployment of geothermal heating plants with heat transport and distribution networks to simultaneously supply geothermal heat to multiple urban areas. Those studies either focused on one solution or discussed the transition from policies and public participation perspectives.

Previous studies have focused on decarbonizing China's heating systems. Xiong et al. [283] formulated a development strategy for district heating in China, indicating reductions of 60% and 15% in the energy consumption for residential heating and heating costs, respectively. Zhang et al. [284] proposed four district heating pathways combining renovations of heating sources and buildings in the Inner Mongolia autonomous region, reducing coal consumption by 41%. However, these studies ignored the fluctuations in fuel and electricity prices

influenced by the improvement of the power structure. Zhang et al. [285] analyzed how Beijing could develop a low-carbon heating sector in 2030 by deploying natural gas boilers (NGBs) and heat pumps (HPs) in the EnergyPLAN model. They found that gas heating fails to continuously reduce direct CO₂ emissions; however, HPs can be advantageous in terms of carbon emissions and benefits to the power grid. Zhang et al. [286] discussed three heating system scenarios in Beijing dominated by gas heating, HPs, and solar-thermal power plants. Yuan et al. [287] found that integrating large-scale HPs in the Beijing–Tianjin–Hebei region could result in 10% energy savings and 9% CO₂ emission reduction.

The primary focus of existing studies has been the strategical development of an energy system on a country, province, or city scale. Several SHTs were integrated into the heating strategies; however, the overall performance of such technologies and their implementation feasibility at the local level remains unknown. Moreover, the influence of fuel and electricity price dynamics on economic performance has not been examined extensively. Thus, there is a requirement for a comprehensive quantitative assessment of the technical, economic, and environmental performances of SHTs and their feasibility at the local level.

Harbin, the northernmost capital city in China, endures severely cold winters with a half-year heating season. District heating supplies 95% of the heat demand in the built environment in Harbin, of which 96% is supplied by coal-fired cogeneration plants and boilers [260]. The annual heat supply for residential heating is 189.7 PJ, which equals 20.2 GJ per capita and 576.4 MJ/m² [288]. Following the national plan, Harbin published the *Clean Winter Heating Implementation Plan in Harbin (2019–2021)*, which promotes natural gas, biomass, electricity, ground source heat pumps (GSHPs), and industrial waste heat usage in district heating systems [260]. Harbin is a representative city with a high demand for heating, a coal-dominant district heating system, and an ambition to implement a clean heating transition. Therefore, it was selected as a case study to implement the proposed methodological steps and gain insight into the performance of SHTs. It also serves as a showcase for investigating the feasibility of implementing multiple technologies.

Previous experimental and numerical studies have investigated the performance of some SHTs in Harbin and primarily focused on technical performance; economic competitiveness and environmental impact have hardly been evaluated. In addition, the feasibility of implementing certain technologies at the local level has not yet been examined. The assessment in this study was based on a local residential community in Harbin. Several SHTs are evaluated regarding technical, economic, environmental, and implementation feasibility involving current policy and future renewable scenarios. As Harbin City is adopted for representation, the results can facilitate a policymaker's decision-making in the clean heating transition field.

This study aimed to answer the following research question: What are the technical, economic, and environmental performances of various SHTs and their implementation

feasibility at the local level regarding the current policy and future renewable scenarios? The main contributions of this study are summarized as follows: 1) The knowledge gap in the existing literature is filled through analyses of the techno-economic-environmental performance of the seven SHTs and their implementation feasibility in a community where coal is predominantly used as the heat supply. 2) The methods embody electricity price forecasting in future sustainable heating system scenarios. Electricity price can significantly impact the economic comparativeness of electricity-dominated heating technologies; however, it has rarely been examined in previous studies. 3) The research can assist in the formulation of clean heating transition policies, and the methods are generic and applicable to other northern cities in China and countries with similar climatic conditions. The rest of the paper is organized as follows. Section 4.2 comprehensively details the methods, including heating system modeling and simulation, scenario development, assessment indicators, and uncertainty analysis. Section 4.3 provides the results of the techno-economic-environmental, implementation feasibility, and uncertainty analyses. The discussion and conclusions are presented in Sections 4.4 and 4.5, respectively.

4.2. Methods

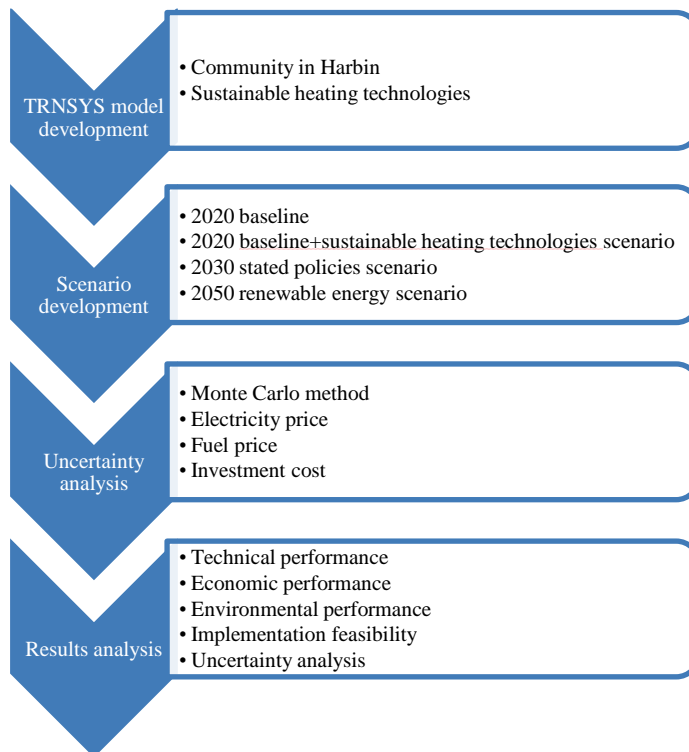


Figure 4.1. Flowchart of the methods employed in this study.

A four-step method was proposed to fulfill the research objectives of this study (Figure 4.1). The technical, economic, and environmental performances as well as implementation feasibility of different SHTs were investigated considering the case of a community in Harbin besides the current policy and future renewable scenarios. Because some SHTs are electricity-dominant, a power structure for future renewable scenarios based on government policies, reports, and renewable energy potentials was developed. Two perspectives on electricity price prediction have been proposed to address the uncertainty of China's electricity marketization. In addition, the Monte Carlo method (MCM) was applied to address the uncertainty of economic performance in future scenarios.

4.2.1. Hourly dynamic heating load simulation

The selected community, located in the northwest area of Harbin City, consists of eight eleven-floor residential buildings, with eight family apartments on each floor. Each apartment includes one kitchen, dining room, living room, restroom, balcony, and two bedrooms, with a total area of 75 m² and housing three or four residents. A three-dimensional model of the building was developed in Sketchup [253] and then imported into TRNBuild for further parameter settings. The layout of two adjacent apartments and the developed building model are illustrated in Figure 4.2. The thermal characteristics of the building envelopes were set according to architectural design instructions, and personnel occupancy, lighting, and equipment utilization rates were set according to the Chinese design standard for residential buildings [254], as summarized in Table 4.1. The heating load profile of the community was acquired by simulating the building model in TRNSYS using local typical meteorological year (TMY) weather data with the indoor cut-off temperature of 18 °C [254]. The hourly and cumulative heating loads are presented in Figure 4.3. Note that only space heating was considered, and domestic hot water was excluded because these two systems are typically separate in China.

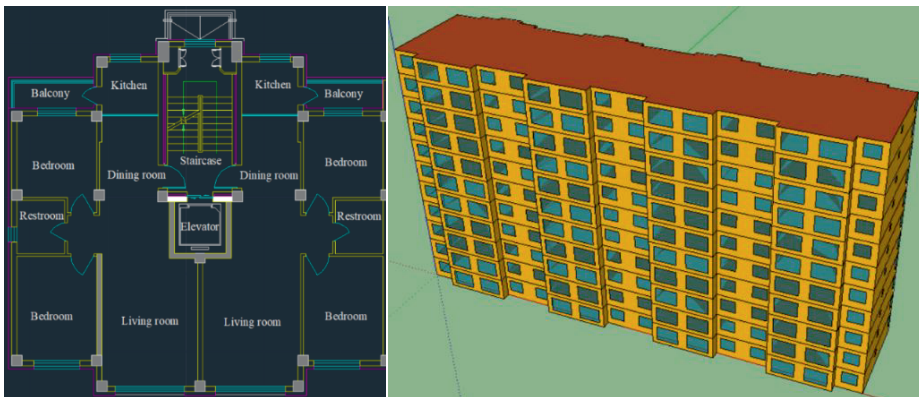
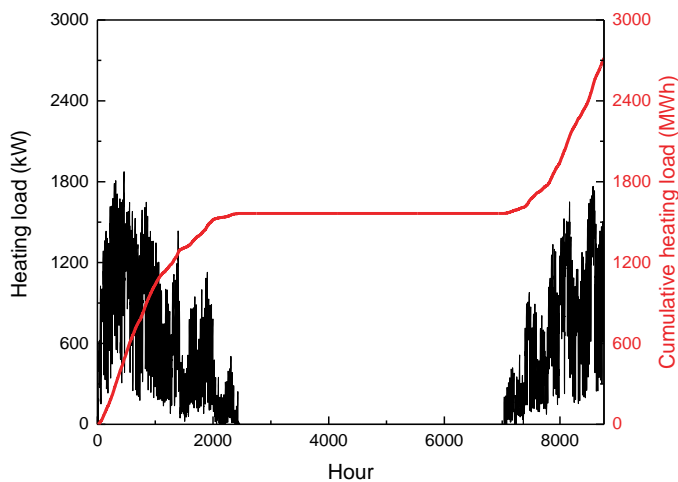


Figure 4.2. Layout of two adjacent apartments and the building model created in Sketchup.

Table 4.1 Building design characteristics of the selected community in Harbin.

	Unit	Value
$U_{\text{exterior wall}}$	$\text{W}/(\text{m}^2 \cdot \text{K})$	0.244
$U_{\text{adjacent wall}}$	$\text{W}/(\text{m}^2 \cdot \text{K})$	0.358
U_{roof}	$\text{W}/(\text{m}^2 \cdot \text{K})$	0.124
U_{floor}	$\text{W}/(\text{m}^2 \cdot \text{K})$	0.184
U_{window}	$\text{W}/(\text{m}^2 \cdot \text{K})$	1.1
g_{glazing}		0.62
Air change of infiltration	1/h	0.5
Personnel density	m^{-2}	0.05
Lighting power density	W/m^2	5
Equipment power density	W/m^2	3.8

**Figure 4.3.** Heating load profiles considering the selected community.

4.2.2. Simulation details for sustainable heating technologies

Previous studies have investigated the performance of SHTs in Harbin. Zhang et al. [289] experimentally tested the heating temperature, coefficient of performance (COP), and frost characteristics of an air-source heat pump (ASHP) on cold days. Low COPs were observed owing to the large difference between indoor and outdoor air temperatures. Other experimental and simulation studies have also indicated that ASHP applications in Harbin are limited by their relatively poor performance [17, 290]. Similarly, GSHP applications in Harbin can cause a soil thermal imbalance with severe cold accumulation, leading to a decline in heating performance and heating deficiency [291, 292]. Thus, the hybrid GSHP system should be integrated with other technologies to maintain an effective long-term operation. Solar-assisted ground source heat pumps (SAGSHPs) can decrease cold accumulation in soil and ensure the COP stability of the HP unit by storing solar energy in the soil [98]. In addition

to HP systems, seasonal thermal energy storage (STES) has been recognized as an effective method for clean heating in northern China owing to its low energy consumption and emissions [202]. Several numerical studies have tested the performance of STES applications in Harbin and demonstrated a positive application prospect [256, 293].

Heilongjiang province has the largest forest region and the highest crop yield per capita in China, promoting biomass heating applications in Harbin [294]. Wang et al. [295] integrated biomass gasification into the cooling, heating, and power systems of a hotel in Harbin and effectively reduced CO₂ emissions. Many studies in Harbin have focused on improving the performance of biomass boilers (BBs) to facilitate their applications [296, 297]. Additionally, benefitting from the abundant renewable electricity resources and “coal-to-gas” policy, electric and gas heating has become a substitute for coal-based heating in Harbin [298]. Several studies have further discussed the possibility of integrating electric boilers (EBs) and NGBs for heating purposes [299, 300].

According to Harbin’s local renewable energy resources and national and local clean heating plans, seven SHTs were selected for analysis in this study, including:

- Natural gas boiler (NGB)
- Biomass boiler (BB)
- Electric boiler (EB)
- STES with an NGB as the auxiliary heating device (STES+NGB)
- STES with a BB as the auxiliary heating device (STES+BB)
- STES with an EB as the auxiliary heating device (STES+EB)
- Solar-assisted ground source heat pump (SAGSHP).

These technologies are further categorized into boiler, STES, and SAGSHP systems. A schematic of the boiler system is presented in Figure 4.4. The boiler is set as open when there is a heating load during the heating season. A variable-speed pump is used to maintain the difference between the supply and return temperatures.

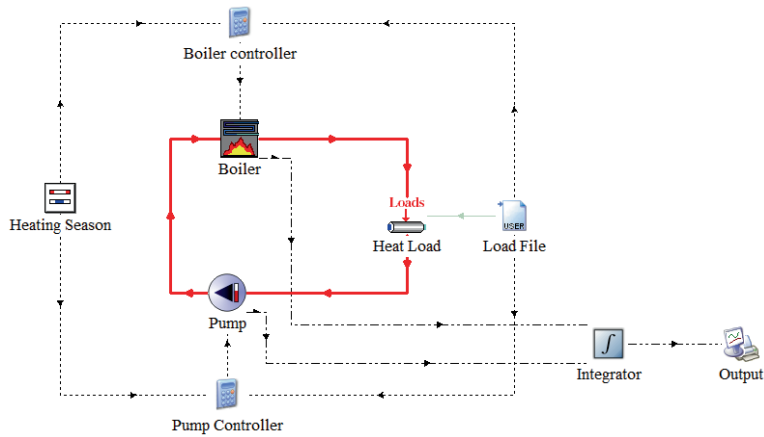


Figure 4.4. Boiler system diagram.

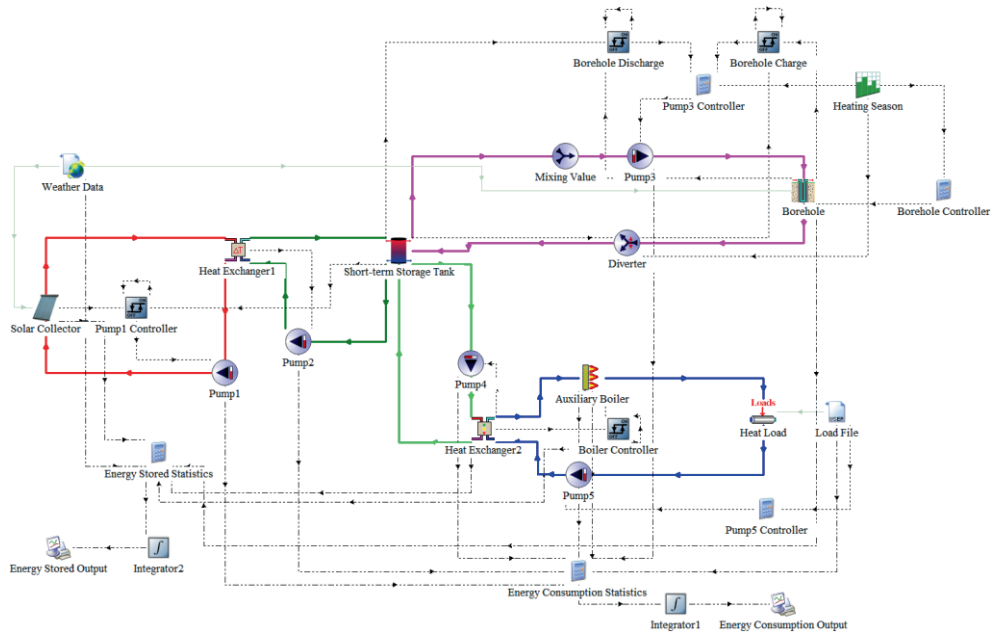


Figure 4.5. Diagram of the STES system.

The STES system constitutes a solar loop, short-term storage loop, borehole storage loop, and load loop, as shown in Figure 4.5. The system comprises evacuated tube solar collectors totaling 5,000 m² and 98 boreholes with a spacing of 4 m and a depth of 100 m. The area of solar collectors depends on the maximum installation area in the community, with the aim of increasing the solar thermal energy penetration. The borehole number was set according to multi-optimization, considering the economic and environmental impacts. The borehole depth was determined according to Harbin's groundwater level (110–150 m) [301]. The tilt

angle and azimuth of the solar collectors were set to 54° and 4° , respectively, optimized using GenOpt [302], with maximum solar thermal energy penetration as the objective. The ground was preheated to 25°C before the operation to expedite the startup process [202]. The thermal energy collected by the solar collectors is first transferred to the short-term storage tank and then charged into the borehole. When a heating load occurs, the stored thermal energy is discharged from the borehole to users through the tank. An auxiliary boiler was used to heat the supply water when it failed to meet the setpoint supply temperature.

The SAGSHP system comprises a solar loop, borehole storage loop, and load loop, as illustrated in Figure 4.6. The solar collector and borehole configurations are similar to those of the STES system. Two HPs were utilized to provide heating services to users, among which GSHP 2 only worked when GSHP 1 reached 90% capacity. A water tank was employed as the heat source in the HPs when the temperature in the water tank was 10°C higher than that in the borehole. Otherwise, the ground was used as the heat source.

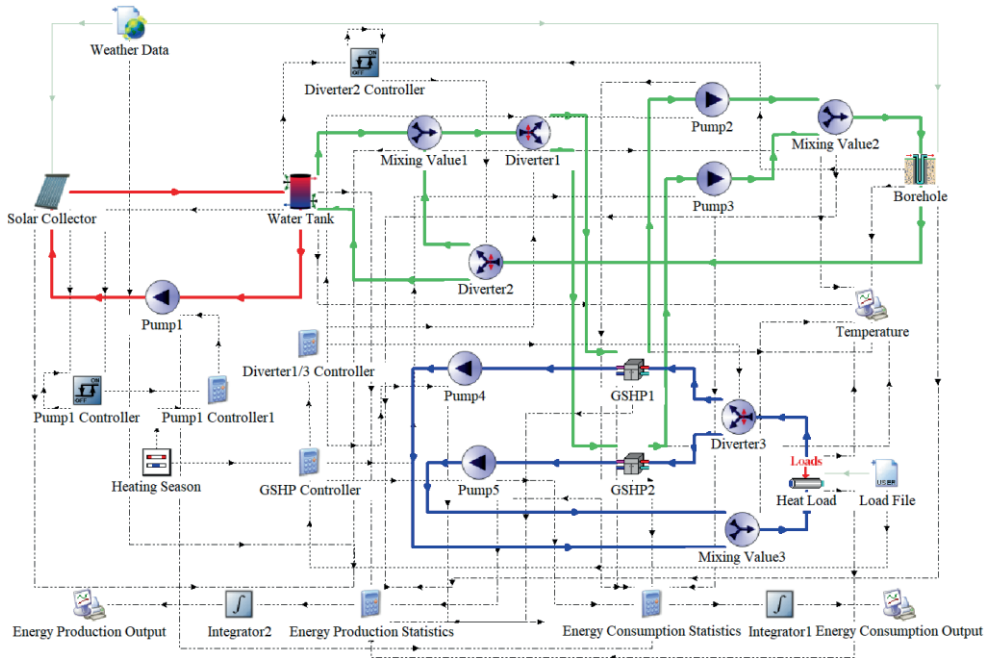


Figure 4.6. Diagram of the SAGSHP system.

A five-year simulation of the systems was conducted from July 1 to June 30, with a timestep of 0.125 h. The heating season was set from October 20 to April 20, according to *Harbin City Heating Measures* [303]. The supply and return temperatures for heating were set to 40°C and 35°C , respectively, in accordance with the radiant heating system in the *Design Code for Heating Ventilation and Air Conditioning of Civil Buildings* [304]. The 4th Generation of district heating also suggests that lower distribution temperatures can decrease grid losses

Chapter 4

and increase efficiencies [305]. The TMY weather profile in Harbin and the heating load profile generated from the building simulation were applied to these models. The TRNSYS types, functions of these components, and a summary of the main equipment parameters are provided in Table 4.2 and Table 4.3.

Table 4.2 TRNSYS types and functions.

No.	TRNSYS type	Function
1	Type 2b	On/off differential controller
2	Type 4c	Storage tank
3	Type 9e	Data reader for heating load
4	Type 11f	Controlled flow diverter
5	Type 11h	Tee piece
6	Type 14h	Time-dependent forcing function
7	Type 15-6	Weather data processor
8	Type 24	Quantity integrator
9	Type 65a	Online graphical plotter with an output file
10	Type 71	Evacuated tube solar collector
11	Type 110	Variable speed pump
12	Type 114	Single speed pump
13	Type 122	Boiler
14	Type 225	Water-to-water heat pump
15	Type 512	Heat exchanger with hot-side modulation to keep cold-side outlet above its setpoint
16	Type 515	Heating season scheduler
17	Type 534	Cylindrical storage tank
18	Type 557a	Vertical u-tube ground heat exchanger
19	Type 659	Auxiliary heater
20	Type 682	Heating loads imposed on a flowing stream
21	Type 761	Heat exchanger with cold-side modulation to maintain a temperature difference
22	Equation	Calculation or controller

Table 4.3 Parameters of system components.

	Unit	Value
Evacuated tube solar collector		
Tilted angle	°	54
Azimuth	°	4
Collector area	m ²	5000
Fluid specific heat	kJ/(kg·K)	3.64
Flowrate at test conditions	kg/(h·m ²)	36
Intercept efficiency		0.739
Negative of first-order efficiency coefficient	kJ/(h·m ² ·K)	3.888
Negative of second-order efficiency coefficient	kJ/(h·m ² ·K ²)	0.02016
Tank		
Tank volume	m ³	250
Tank loss coefficient	kJ/(h·m ² ·K)	1.44
Borehole		
Number of boreholes		98
Borehole depth	m	100

Borehole spacing	m	4
Borehole radius	m	0.06
Pipe radius	m	0.016
Number of boreholes in series		8
Number of U-tubes per borehole		2
Storage thermal conductivity	$\text{kJ}/(\text{h} \cdot \text{m} \cdot \text{K})$	8.64
Storage heat capacity	$\text{kJ}/(\text{m}^3 \cdot \text{K})$	3000
Initial ground temperature	$^{\circ}\text{C}$	5.5
Heat pump		
Number of units		2
Rated heating capacity	kW	1100
Rated heating power	kW	250
Rated condenser flowrate	m^3/h	180
Rated evaporator flowrate	m^3/h	220

4.2.3. Heating supply scenario

The year 2020 was selected as the base year because it was the latest year with complete data. The heating system in Harbin in 2020 was regarded as the reference case for comparison with various SHTs under different scenarios.

Three scenarios were developed to analyze the economic feasibility and environmental impacts of the current policy and future renewable scenarios. As some SHTs are electricity-dominant, a higher renewable energy portion of the power generation system may significantly influence the economic performance of these heating options through the electricity cost and the environmental performance via the power grid CO_2 emission factor. China's power grid was grouped into six relatively independent regional power grids, and Harbin was affiliated with the northeast power grid (Liaoning, Jilin, Heilongjiang, and East Inner Mongolia). However, owing to statistical data availability, Inner Mongolia is considered to be a single sub-region of the northern power grid [306]. In this study, the power grid boundary was set for the other three provinces.

2020 baseline+ (2020 B+) scenario: The 2020 baseline+ scenario was designed based on the 2020 baseline, and the original heating system was replaced with the examined SHTs. The power generation mix was obtained from [307].

2030 stated policy (2030 SP) scenario: The current energy strategy involves increasing the proportion of renewable energy in the energy system, and renewable power plants are expected to develop rapidly. Since 2020, provincial governments have gradually released the *14th Five-year Plan and the 2035 Long-range Objectives*. The power generation mix of the 2030 SP scenario was based on the projected power generation or installed capacity in 2030. The utilization hours of recent years were used to predict the power generation accompanied by the projected installed capacity.

2050 renewable energy (2050 RE) scenario: The 2050 RE scenario was promoted to eliminate dependence on fossil fuels to evaluate the selected SHTs in a 100% renewable energy system. The power generation mix was simulated using EnergyPLAN [308] according to the renewable energy potential and projected electricity demand (illustrated in the Appendix). Notably, among the seven SHTs, two related to NGBs were not applicable to this scenario. The power generation mixes for the three scenarios are depicted in Figure 4.7.

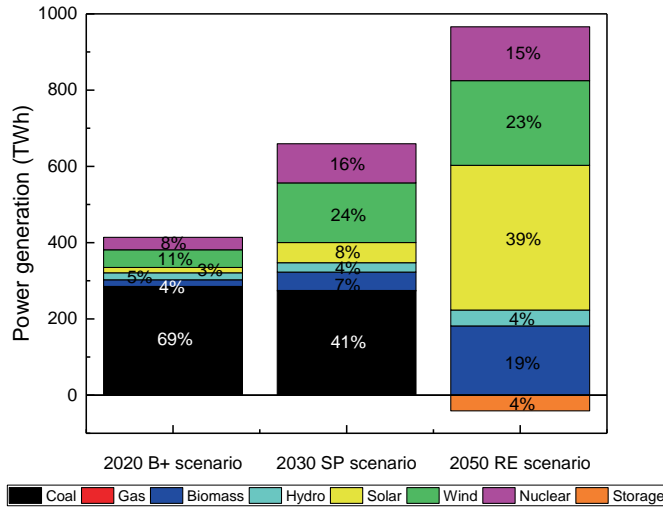


Figure 4.7. Power generation mixes in the three scenarios.

4.2.4. Techno-economic-environmental assessment

The performance of SHTs in different scenarios was evaluated using several technical, economic, and environmental indicators.

4.2.4.1. Technical performance

Indicators considered in the technical performance analysis include the solar fraction (SF), storage efficiency (η_{bore}), COP, and system efficiency (η_{sys}). SF indicates the proportion of the heating load met by solar thermal energy and can be expressed as:

$$\text{SF} = \frac{\text{solar heat to load}}{\text{total heat to load}} \quad (4.1)$$

The performance of a borehole in the STES systems was evaluated based on the storage efficiency, indicating the efficiency of the borehole given by:

$$\eta_{\text{bore}} = \frac{\text{heat discharged from borehole}}{\text{heat charged into borehole}} \quad (4.2)$$

The performance of an HP is usually evaluated by the COP, which expresses the ratio of the amount of heat produced to the electricity consumed by the compressor. The COP of the HP unit and system can be calculated using:

$$\text{COP}_{\text{HP}} = \frac{\text{heat production of heat pump}}{\text{electricity consumption of heat pump}} \quad (4.3)$$

$$\text{COP}_{\text{sys}} = \frac{\text{heat production of system}}{\text{electricity consumption of system}} \quad (4.4)$$

The system efficiency is expressed as the ratio of the heat output to the energy input of the system:

$$\eta_{\text{sys}} = \frac{\text{total heat production}}{\text{total energy consumption}} \quad (4.5)$$

4.2.4.2. Economic performance

The levelized cost of heat (LCOH) was calculated to assess the economic performance and can be determined using:

$$\text{LCOH} = \frac{I + \sum_{t=1}^n \frac{\text{O\&M}}{(1+r)^t}}{\sum_{t=1}^n \frac{E_{th}}{(1+r)^t}} \quad (4.6)$$

where I is the initial investment, n denotes the lifetime, t represents time, O&M indicates the annual operation and maintenance cost, r is the discount rate, and E_{th} is the annual heat production.

In this study, the lifetime of the heating system was set to 25 years. The discount rate is 5%, which is approximately equivalent to the long-term housing loan interest rate [231]. The main equipment unit prices of a system in the 2020 B+ scenario were sourced from China's leading wholesale trade platform [226] and several studies performed in China [48, 227-230]. The solar collector and borehole storage costs were expected to reduce by 8% and 10% in the 2030 SP scenario and by 18% and 17% in the 2050 RE scenario, respectively, while other equipment costs were relatively constant [309, 310].

Table 4.4 Investment costs of the main equipment in the three scenarios.

Equipment	Unit	2020 B+	2030 SP	2050 RE
Solar collector	€/m ²	122	112	100
Short-term storage tank	€/m ³	94	94	94
Borehole	€/unit	2400	2160	1992
NGB	€/unit	18429	18429	18429
BB	€/unit	21734	21734	21734
EB	€/unit	27350	27350	27350
HP	€/unit	58974	58974	58974
Pump	€/unit	512	512	512
Pipeline	€/m	108	108	108

Table 4.4 summarizes the investment costs of the main equipment in the three scenarios. The cost of the conventional heating system at the baseline was acquired from a heating supplier in Harbin. The annual fixed O&M cost was set at 0.75% of the total investment costs [233], while the variable O&M cost was calculated based on the annual electricity and fuel consumption of the heating system. The electricity price in 2020 B+ was taken from [237], and those in the 2030 SP and 2050 RE scenarios were calculated based on the projected power generation mix from the policy and technical innovation perspectives (presented in the Appendix). The fuel prices in the 2020 B+ scenario were sourced from [226, 238], and those in the 2030 SP and 2050 RE scenarios were derived from [311-314]. The electricity and fuel prices for the three scenarios are presented in Table 4.5.

Table 4.5 Electricity and fuel prices in the three scenarios.

	Unit	2020 B+	2030 SP	2050 RE
Electricity	€-ct/kWh	9.3	10.5 (from a policy perspective) 9.7 (from a technical innovation perspective)	8.5
Natural gas	€-ct/kWh	4.5	5.0	-
Biomass	€-ct/kWh	3.0	3.3	3.9

4.2.4.3. Environmental performance

The environmental performances of the SHTs were evaluated based on the corresponding CO₂ emission reduction and CO₂ equivalent emission factor of the overall system. The mass of CO₂ emitted while consuming energy was calculated as follows:

$$m_{CO_2} = \mu_{CO_2}^E \cdot E \quad (4.7)$$

where $\mu_{CO_2}^E$ denotes the CO₂ emission factor, and E represents the energy consumption.

The CO₂ emission reduction was determined by comparing the CO₂ emissions of an SHT system with that of the conventional system:

$$\Delta CO_2 = m_{CO_2}^{CS} - m_{CO_2}^{SHT} \quad (4.8)$$

where $m_{CO_2}^{CS}$ and $m_{CO_2}^{SHT}$ represent the CO₂ emissions of the conventional heating system of the baseline and SHT, respectively, which can be calculated from:

$$m_{CO_2}^{CS} = \mu_{CO_2}^{th} \cdot E_{th} \quad (4.9)$$

$$m_{CO_2}^{SHT} = \mu_{CO_2}^{el} \cdot E_{el} + \mu_{CO_2}^{th} \cdot E_{th} \quad (4.10)$$

where $\mu_{CO_2}^{th}$ and $\mu_{CO_2}^{el}$ denote the CO₂ emission factors of heating and electricity production, respectively, and E_{th} and E_{el} indicate heat production and electricity consumption, respectively. The total heat production and fuel consumption in the 2020 baseline were obtained from [28]. Accordingly, the CO₂ emission factor of a heating system was calculated

using the CO₂ emission factors of various fuels (presented in the Appendix). The grid CO₂ emission factors in the 2020 B+ and 2030 SP scenarios were 0.56 and 0.32 kg/kWh, respectively (details in the Appendix). The CO₂ emission factor for natural gas heating was 0.20 kg/kWh [243].

The CO₂ equivalent emission factor indicates the emission level of an overall system during the heat-producing process, expressed as:

$$\mu_{\text{CO}_2} = \frac{m_{\text{CO}_2}}{E_{\text{th}}} \quad (4.11)$$

The CO₂ avoidance cost (CAC) was employed to evaluate the marginal costs of CO₂ emission reduction for SHTs compared with the conventional system and is given by:

$$\text{CAC} = \frac{\text{LCOH}_{\text{SHT}} - \text{LCOH}_{\text{CS}}}{\Delta \text{CO}_2} \quad (4.12)$$

4.2.5. Implementation feasibility assessment

In addition to the techno-economic-environmental evaluation, the feasibility of implementing the SHTs was assessed. The perspectives considered in the assessment included interaction with the rest of the energy system, infrastructure requirements, investigation and construction period, fuel availability, affordability, application prospects, public acceptance, and government support. Based on the literature and government document reviews, a half-quantitative assessment was conducted to identify the positive or negative impact of these factors on technology implementation at the local level.

4.2.6. Uncertainty analysis

The MCM was adopted for analysis of the economic uncertainty in future scenarios. This method involves a mathematical model to propagate probability distributions and applies it to cases where the output result relies on different input variables [315, 316]. MCM simulations were performed using @RISK [317], generating arbitrary values for selected variables and deriving the results using the designed mathematical model, including LCOH and CAC, in the 2030 SP and 2050 RE scenarios. The selected variables included the costs of electricity, fuel, and investment. The electricity prices in the 2030 SP and 2050 RE scenarios were projected based on the power generation mixes and the LCOE of power generation technologies. A triangular distribution was applied to the LCOE of the power generation technologies derived from different sources. Normal distribution was used to address the uncertainties in transmission and distribution prices and government funds and supplements. For fuel prices, the historical prices of natural gas and wood fuel from 2001 to 2021 were collected [318, 319]. The trends in the data points were combined with knowledge of the underlying quantities to determine the distribution type [320]. The coefficient of variation of the historical data was applied to the distribution of selected variables. The

Chapter 4

uncertainty of the investment cost was addressed using a normal distribution within a certain range.

Table 4.6 summarizes the ranges and probability distribution parameters of the input variables. For normal and lognormal distributions, A and B represent the mean and standard deviation, respectively. For the ExtValueMin distribution, A is the location parameter, and B is the shape parameter. For a triangular distribution, A is the minimum value, B is the most likely value, and C is the maximum value. The MCM simulation was performed 100,000 times.

Table 4.6 Ranges and probability distribution parameters of the input variables.

	Unit	Distribution	5% level	95% level	A	B	C
2030 SP scenario							
LCOE of coal power generation	€-ct/kWh	Triangular	5.70	6.56	5.50	6.13	6.76
LCOE of gas power generation	€-ct/kWh	Triangular	7.89	9.72	7.47	8.80	10.14
LCOE of biomass power generation	€-ct/kWh	Triangular	5.70	8.73	5.07	6.84	9.50
LCOE of hydropower generation	€-ct/kWh	Triangular	2.94	3.20	2.88	3.07	3.27
LCOE of solar power generation	€-ct/kWh	Triangular	1.82	2.36	1.69	2.09	2.49
LCOE of wind power generation	€-ct/kWh	Triangular	3.30	3.71	3.21	3.51	3.80
LCOE of nuclear power generation	€-ct/kWh	Triangular	4.94	5.40	4.83	5.22	5.49
Transmission and distribution price	€-ct/kWh	Normal	3.68	4.34	4.01	0.20	
Government funds and supplements	€-ct/kWh	Normal	0.29	0.35	0.32	0.02	
Gas price	€-ct/kWh	Lognormal	3.51	11.69	6.59	2.69	
Biomass price	€-ct/kWh	ExtValueMin	2.09	3.68	3.48	0.39	
Solar collector price	€/m ²	Normal	103.01	121.47	112.24	5.61	
Borehole price	€/unit	Normal	1982	2338	2160	108	
2050 RE scenario							
LCOE of biomass power generation	€-ct/kWh	Triangular	5.70	8.73	5.07	6.84	9.50
LCOE of hydropower generation	€-ct/kWh	Triangular	2.94	3.20	2.88	3.07	3.27
LCOE of solar power generation	€-ct/kWh	Triangular	1.25	1.26	1.24	1.26	1.27
LCOE of wind power generation	€-ct/kWh	Triangular	2.52	3.22	2.36	2.87	3.38
LCOE of nuclear power generation	€-ct/kWh	Triangular	4.91	5.25	4.83	5.08	5.33
Transmission and distribution price	€-ct/kWh	Normal	3.68	4.34	4.01	0.20	
Government funds and supplements	€-ct/kWh	Normal	0.29	0.35	0.32	0.02	
Biomass price	€-ct/kWh	ExtValueMin	2.50	4.41	4.17	0.47	
Solar collector price	€/m ²	Normal	91.81	108.27	100.04	5.00	
Borehole price	€/unit	Normal	1828.2	2155.8	1992	99.6	

4.3. Results

This section summarizes the findings from techno-economic-environmental performance analysis, implementation feasibility assessment, and uncertainty analysis.

4.3.1. Technical performance

The representative energy flows, SFs, and storage efficiencies of the STES system are displayed in Figure 4.8. In the first year of operation, little heat was discharged from the borehole because the borehole was under the startup process. The collected solar energy was directly transferred to the load through a short-term storage tank. The collected solar energy decreased over time because more thermal energy was required in the early years to heat the borehole. Decreasing and increasing trends were observed in the energy flows charged into the borehole and discharged from the borehole, respectively, indicating that the ground gradually reached a thermal balance during the operation. As more thermal energy is stored in the borehole, the portion of the load met by solar thermal energy increases, and that met by the boiler decreases accordingly. The total energy to load was constant because the same load profile was applied annually. The SF and storage efficiency increased over time from 47% to 77% and from 0 to 44%, respectively, and the growth trend gradually plateaued. As the borehole gradually reached a thermal balance, the indicators gradually stabilized.

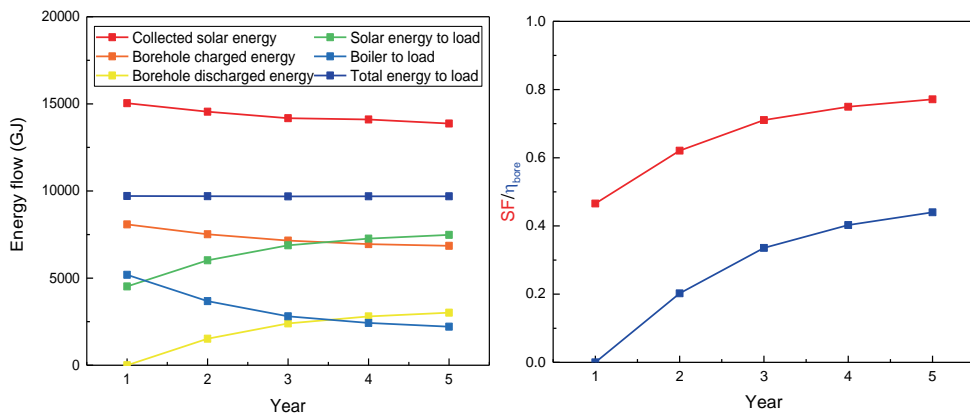


Figure 4.8. Energy flow, SF, and storage efficiency results for the STES systems.

Figure 4.9 (left) exhibits the unit and system COPs of the SAGSHP system. The unit and system COPs increased by 11% and 7%, respectively, during the five years of operation. Unlike a normal GSHP applied in cold regions whose COP would gradually decrease over the years [291, 321], the average borehole temperature of the SAGSHP system rises slightly during operation with the collected solar heat, leading to a higher COP. The results are similar to those of previous studies on SAGSHP applications in cold regions [322, 323]. The heat sources of the SAGSHP system are presented in Figure 4.9 (right). Stored solar heat in the tank and heat in the ground account for 62% of total heat demand, which helps reduce

electricity usage. During the operation, the share of electricity usage in the heat sources slightly decreases because the solar input helps slowly increase the ground temperature.

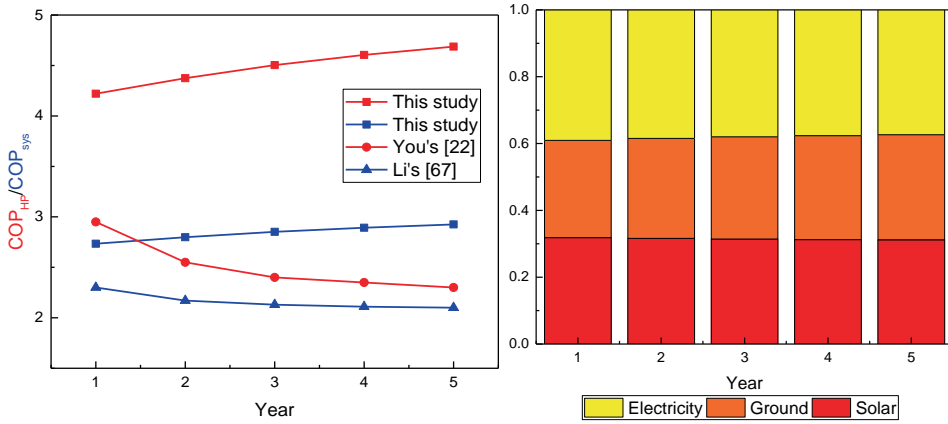


Figure 4.9. Unit and system COPs (left) and heat sources of the SAGSHP system (right).

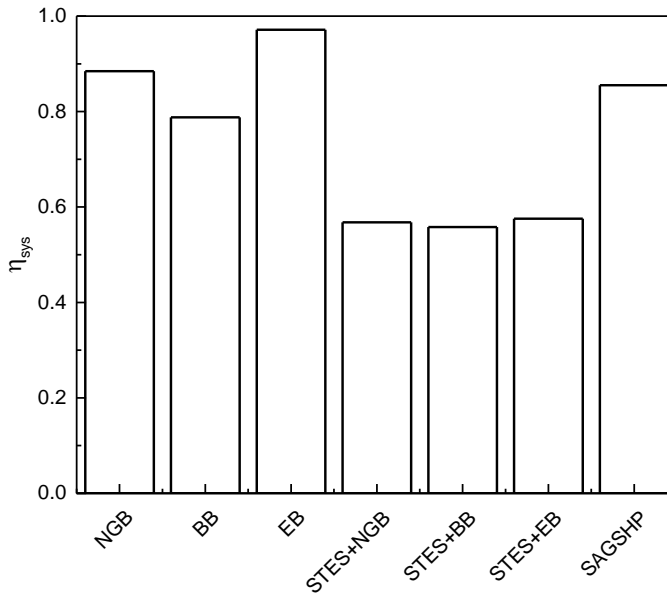


Figure 4.10. Efficiencies of the boiler, STES, and SAGSHP systems.

The system efficiencies of the boiler, STES, and SAGSHP systems are compared in Figure 4.10. The efficiencies of the boiler systems illustrate the heat production associated with the fuel and electricity consumption. In contrast, the efficiencies of the STES and SAGSHP systems present heat production related to fuel and electricity consumption and the collected solar thermal energy. The efficiencies of the STES systems are relatively low because of the seasonal storage of solar heat. In the SAGSHP system, the collected solar energy is directly

used as the heat source for the heat pump, leading to a higher system efficiency than that of the STES system.

4.3.2. Economic performance

Figure 4.11 (left) shows the LCOHs of the various SHTs in the designed scenarios and the heating system at the 2020 baseline. The LCOH configurations of the various SHTs in the 2020 B+ scenario are depicted in Figure 4.11 (right). All SHTs in each scenario exhibit higher LCOHs than the baseline. The EB system presents the highest LCOH because the cost of electricity consumption was much higher than that of gas and biomass. Similarly, the STES+EB system produced the highest LCOH among the three STES systems. The LCOHs of the STES and SAGSHP systems decrease from the 2020 B+ scenario to the 2050 RE scenario because their investment costs, accounting for 50%–60% of the LCOH calculation, are projected to decrease. Unlike the other options, the LCOH of the BB system in the 2050 RE scenario is higher than those in the 2020 B+ and 2030 SP scenarios because the biomass price is predicted to increase, accounting for the highest proportion of its LCOH calculation. The LCOHs of the EB, STES+EB, and SAGSHP systems indicate more significant differences (3%–7%) than the other options (less than 1%) between the policy and technical innovation perspectives in the 2030 SP scenario because the electricity price is a larger influential factor in their LCOH calculation. The BB system indicated the lowest LCOH in the 2020 B+ scenario, while that of the STES+BB system was the lowest in the other scenarios.

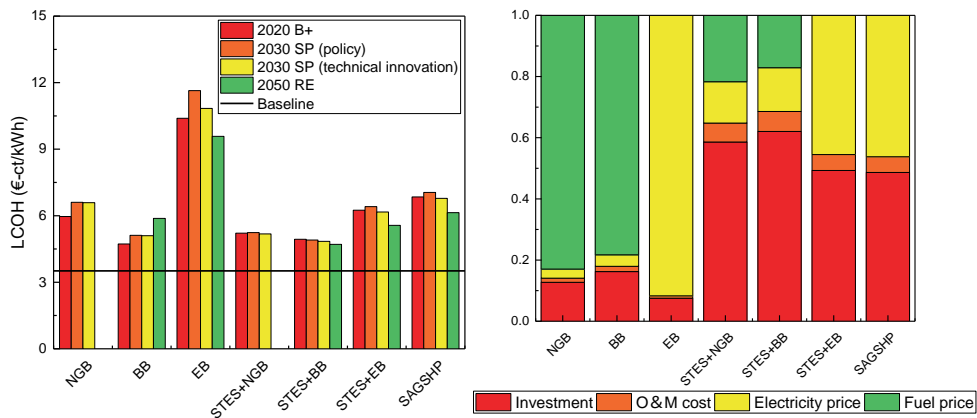


Figure 4.11. LCOHs (left) and LCOH configurations (right) of the SHTs in the designed scenarios.

4.3.3. Environmental performance

The CO₂ equivalent emission factors of the various SHTs in the designed scenarios and the heating system in the 2020 baseline are displayed in Figure 4.12. Evidently, the SHTs

demonstrate significant potential to reduce CO₂ emissions, except for the EB system in the 2020 B+ scenario. This indicates that replacing the current heating system with the EB system fails to reduce CO₂ emissions when considering the power generation mix. A similar finding was reported in [324] that the environmental benefits of electric heating primarily depend on the power structure, and the application scale of electric heating should be coordinated with the power structure. In addition, with a gradually cleaner power generation mix, the CO₂ equivalent emission factors of the SHTs showed a decreasing trend from the 2020 B+ scenario to the 2030 SP scenario and reached zero in the 2050 scenario. The extent of the decline between the 2020 B+ and 2030 SP scenarios of different heating options depends on their electricity-dominant level. The BB system exhibited the most significant potential for reducing CO₂ emissions in the designed scenarios.

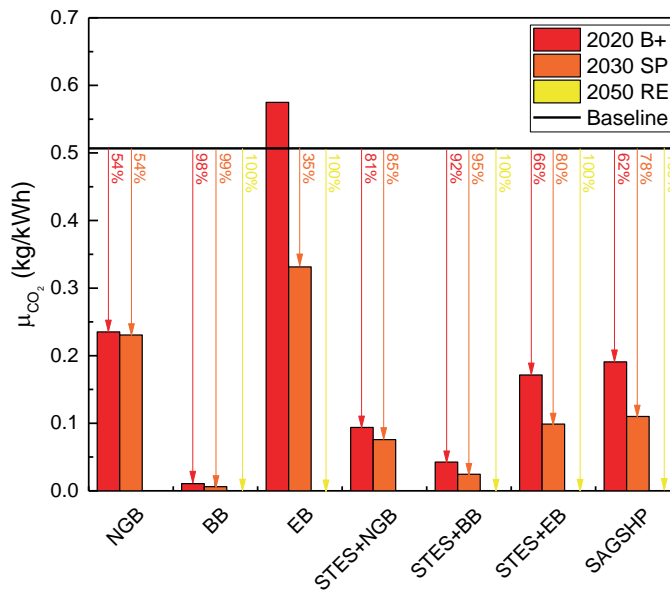


Figure 4.12. CO₂ equivalent emission factors of the SHTs in the designed scenarios.

Figure 4.13 presents the CACs of the SHTs in the designed scenarios. Owing to higher LCOH and lower CO₂ emission reduction, the EB system exhibits the highest CAC among the examined heating technologies and fails to reduce CO₂ emissions in the 2020 B+ scenario. Although the EB system demonstrates the potential to reduce CO₂ emissions with a cleaner power generation mix in the 2030 SP and 2050 RE scenarios, it is still limited by the high cost. Meanwhile, the NGB and BB systems exhibit no significant differences in their LCOHs; however, the BB system benefits from higher CO₂ emission reduction; therefore, it has a lower CAC. The CACs of the STES and SAGSHP systems exhibit a declining tendency from the 2020 B+ scenario to the 2050 RE scenario because their investment costs are projected to reduce, and they can greatly reduce CO₂ emissions. Generally, the BB system has the

lowest CAC in the 2020 B+ scenario, while the STES+BB system has the lowest CAC in the other scenarios.

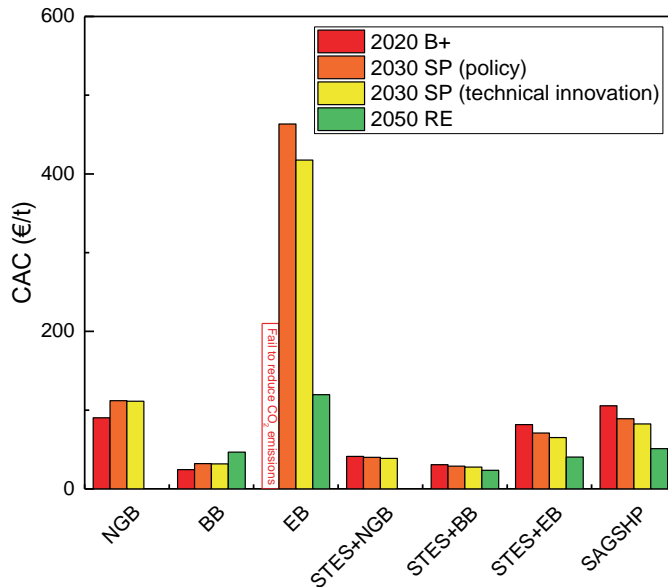


Figure 4.13. CAC results for the SHTs in the designed scenarios.

4.3.4. Implementation feasibility

The results of the feasibility assessment are summarized in Table 4.7. From a policy incentive perspective, Harbin has announced that it provides subsidies of 15.7, 5.2, and 47.2 k€/t based on the tonnage of newly built boilers for those who use NGBs, BBs, and EBs to replace coal-fired boilers, and the subsidy of 4.7 €/m² for those who use solar heating and HPs [325]. In addition, the subsidy of 1.3 €/ct/m³ is provided for natural gas usage, while the “coal-to-electricity” electricity price policy was formulated to extend the valley period time and reduce the valley period electricity price. In terms of the case community, these policies can bring a reduction of approximately 17%–19% in the LCOHs of the EB, STES+EB, and SAGSHP applications. The LCOHs of STES+NGB and STES+BB systems decreased by 13%, while those of NGBs and BBs decreased by less than 4%.

NGBs are highly accepted by the public and the most widely used heat-producing mode in urban areas to replace low-efficiency coal burning in China. The NGB system is relatively mature, and has strong industrial support and marketing possibilities [326]. However, in the long term, gas heating might be phased out by a fully renewable society. Large-scale STES systems with solar heating remain in an emerging stage. China’s solar thermal industry (mainly domestic hot water systems) has a long history and has developed rapidly, accounting for 70% of global solar collector installations [214]. It is expected that STES with solar

heating will have broad applications in Harbin, with abundant solar resources and favorable policies [34]. Electric heating is also a promoting option as grid cleanliness increases.

Table 4.7 Implementation feasibility of the SHTs.

	NGB	BB	EB	STES+NB	STES+BB	STES+EB	SAGSHP
Policy support	+	+	+++	++	++	+++	+++
Resident acceptance	+++	+	++	---	---	---	+
Application prospect	-	++	+++	+	+++	+++	+++
Infrastructure requirement	-	--	N	---	---	---	---
Investigation and construction	N	N	N	---	---	---	---
Fuel availability	--	--	N	-	-	N	N
Affordability	--	-	---	-	-	--	--
Impact on the power grid	N	N	---	-	-	--	--

(Note: + and – symbolize positive and negative impacts on implementation feasibility, respectively; N represents ignorable impact).

As for infrastructure requirement issues, a storage tank or pipeline needs to be built for NGB applications, and BB applications require a large storage space with a concern for fire hazards [327]. This also raises ash handling and management issues, requiring extra equipment [328]. Meanwhile, STES and SAGSHP require a relatively long investigation and construction period for underground construction compared with boiler applications.

Considering fuel availability, the natural gas production in Heilongjiang province in 2020 was 4.7 billion m³, 40% of which was used for industry [28]. The rest could only meet 48% of the heat demand in Harbin. China has become the world’s largest natural gas importer since 2018, with a much faster growth in gas consumption than production [329]. The extensive implementation of gas heating will increase China’s import dependence as well as harm national energy security. Regarding biomass applications, Heilongjiang province has abundant biomass resources (129.2 TWh), of which 17.4% are located in Harbin [330]. The demand for heating in Harbin is 52.7 TWh, accounting for 41.8% of the total provincial district heating consumption [331]. Therefore, the local biomass resource can potentially sustain only 34% of the district heating demand in Harbin, which is insufficient. Biomass is also needed in the power and transport sectors to support low-carbon transitions.

From an affordability perspective, EBs have the highest LCOH, primarily because of their high electricity price. Electricity-dominant heating technologies, including EB, STES+EB, and SAGSHP, may negatively influence the power grid operation [332]. If EBs dominate the heat supply in the built environment in Harbin, electricity demand will increase by 54.2 TWh, which is more than twice the total electricity consumption in 2020. The increased load can pose a burden for constructing new electricity production units and extending the existing capacity of the electric grids.

In general, gas heating is an easy-to-implement option benefitting from the public acceptance and “coal-to-gas” policy. However, it poses a threat to national energy security and is not

preferable for a fully renewable society in the long term. Biomass heating has significant potential to reduce CO₂ emissions; however, fuel availability and raw material management limit its wide implementation. Electric heating is becoming increasingly attractive as grid cleanliness increases, with significant support from the government. However, its LCOH is higher than that of other technologies owing to the high electricity prices. STES and SAGSHP are promising technologies with decreasing LCOH and increasing CO₂ emission reduction ability. The current resident acceptance in the local area is relatively low, but it holds a prospective future in large-scale applications with sufficient local resources and strong support from governments.

4.3.5. Uncertainty analysis

Considering that the analyses in the 2030 SP and 2050 RE scenarios were based on the projected costs of electricity, fuel, and investment, the MCM was employed to address uncertainties in the economic performance. Figure 4.14 presents the MCM simulation results of the LCOHs of the SHTs in the designed scenarios. The LCOH for the NGB system has an extensive range because it is mainly determined by the gas price, and the lognormal distribution with a long tail on the right-hand side was applied to the gas price. Similarly, the LCOH of the BB system exhibits a long tail on the left-hand side because biomass price is a dominant factor, and it is associated with the ExtValueMin distribution. Within the two figures in the 2030 SP scenario, the SHTs present similar relative positions of the LCOH, while the LCOHs from the technical innovation perspective are lower because of lower electricity prices. However, in the 2050 RE scenario, the LCOHs of the STES and SAGSHP systems are more significantly reduced than those of the boiler systems because the solar and storage costs decrease, and the declining electricity price has a greater influence on the LCOH.

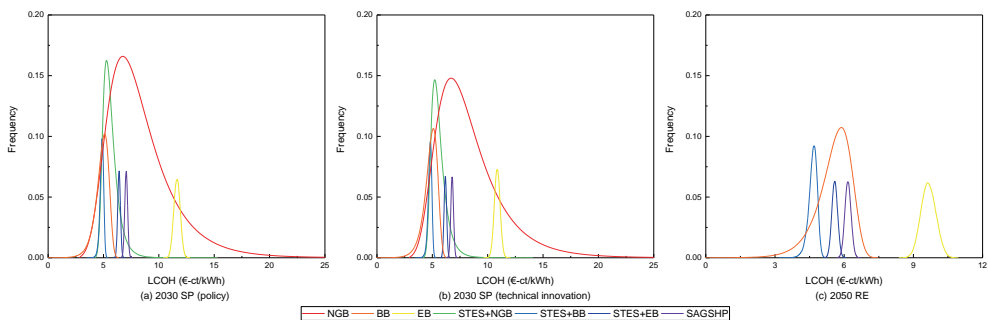


Figure 4.14. MCM simulation results for the LCOHs of the SHTs in the designed scenarios.

The MCM simulation results for the CACs of the SHTs in the designed scenarios are presented in Figure 4.15. The relative positions are similar to those of the LCOHs. Note that the CACs of the NGB and BB systems might have negative values because they may be able to simultaneously reduce CO₂ emissions and have a lower LCOH than the baseline. In

addition, considering the uncertainties of the electricity price, fuel price, and investment cost, the NGB, BB, STES+NGB, and STES+BB systems provide favorable options in the 2030 SP scenario. Whereas, the BB and STES+BB systems may be favorable options for the 2050 RE scenario.

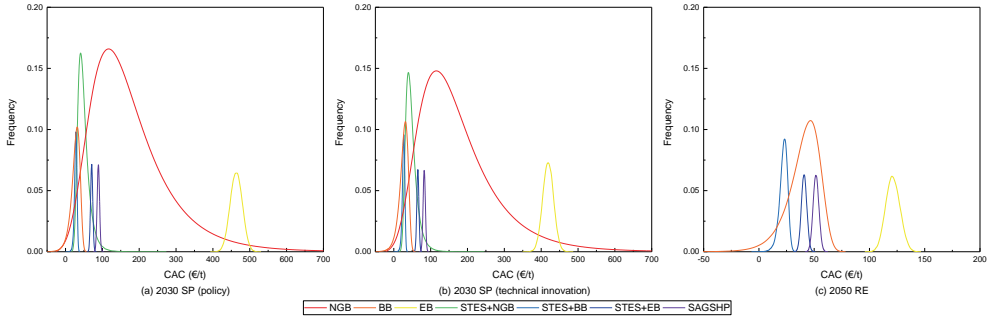


Figure 4.15. MCM simulation results of the CACs of the SHTs in the designed scenarios.

4.4. Discussion

This study performed techno-economic-environmental analyses of seven SHTs and evaluated their implementation feasibility at the local level regarding the current policy and future renewable scenarios. The assessment was based on a case study community in a coal-dominated location. The results indicate that BB and STES+BB are attractive in terms of cost and CO₂ emission reduction. However, fuel availability is an issue in large-scale implementation. In addition, biomass heating faces storage and ash handling and management issues. Solar heating is a promising technology with decreasing LCOH and increasing CO₂ emission reduction ability. However, its current resident acceptance in China is relatively low and usually requires a longer investigation and period for underground construction. Electric heating is preferable in terms of implementation feasibility; however, its economic competitiveness and environmental impact depend heavily on electricity prices and grid cleanliness. It can also pose a burden for constructing new electricity production units and extending the existing capacity of electric grids for large-scale implementations. In addition, replacing the current heating system with electric heating failed to reduce CO₂ emissions. Based on the released policies and reports, it can reduce CO₂ emissions in the 2030 and 2050 scenarios; however, its LCOH is still much higher than those of the other SHTs owing to high electricity prices. Recent research has suggested that the synergistic development of electric heating and idle renewable energy generation could help reduce wind or solar power curtailment as well as increase the flexibility of the energy system [333]. Electric heating using renewable energy curtailment can significantly improve its economic competitiveness and emission-reduction ability.

For a long time, northern China has lacked the overall planning of heating supply in various energy forms, leading to an insufficient heat supply and demand balance and an unscientific

heating layout. The clean heating transition is a systematic project. Local governments are required to coordinate the heat supply and demand balance and comprehensively adopt various clean heating methods to reduce emissions in the heating field. Based on the local resource endowment and infrastructure, local governments should formulate appropriate clean heating strategies with scientific evaluation and full consideration of residents' consumption capacity. In addition, heat, natural gas, and electricity prices are all subject to the unified pricing of local governments, which lack market-oriented adjustment ability. Local governments should adopt supporting policies to reduce the cost of electric heating, including improving the peak-valley time-of-use price system, optimizing the tiered price policy for residential electricity consumption, and expanding market-based transactions. Moreover, natural gas heating costs can be reduced by improving the tiered price system, implementing seasonal price differential policies, and using market-based trading mechanisms. The price of clean heating should be reasonably set within the range of residents' affordability, considering clean heating renovation and operating costs [21].

The Chinese government has implemented electricity market reforms twice since 2002; however, the pricing and operating mechanisms of the power sector remain under government control [334]. Previous studies on sustainable heating transition ignored electricity price fluctuations in future scenarios. As some SHTs are electricity-dominant, electricity prices can significantly influence the economic competitiveness of SHT applications. Appropriate methods are required to estimate the future electricity price when the pricing mechanism becomes market-oriented [335]. This study proposed two methods for predicting electricity prices in future scenarios: one follows current policies, whereas the other involves facing a competitive pricing mechanism, which can provide a reference for future research.

This study was a local-specific case that comprehensively considered local circumstances in Harbin and made an effort to provide an informative and transparent presentation based on regional specificity. A case community in Harbin was selected and modeled to obtain a representative heating profile. The examined SHTs were based on a review of local clean heating plans and previous studies for Harbin. Three scenarios (current situation, stated policies, and future renewable scenarios) were developed. Local policies on energy system planning and local renewable energy potential were comprehensively considered. The feasibility assessment was carried out by thoroughly considering the current energy system situation, fuel availability, and incentives for promoting clean energy use issued by the local government. This study provided a comprehensive and transparent showcase of the clean heating transition at the local level. The integrated assessment method developed in this study comprehensively considered the technical, economic, environmental, and implementation feasibility perspectives regarding the current policy and future renewable scenarios. It can be used for case studies in other countries with similar climate conditions and an objective of clean heat transition. In the application, local-based SHTs, renewable energy potential, energy system planning, and implementation feasibility are suggested to be considered.

This study used EnergyPLAN to predict the power generation structure in 2050 to guarantee the grid supply and demand balance at an hourly level. The forecast is based on the local renewable energy potential and the projected electricity demand. Although the predicted power generation mix might not be unique, the results of this study are representative because the prediction was aimed at the maximum solar and wind energy penetration, as they were expected to be the cheapest power generation technologies in the next few decades [336].

For the environmental assessment, only the CO₂ emissions from fuel combustion were considered, ignoring fuel production and transportation processes. Biomass-related heating alternatives show great potential for CO₂ emission reduction because biomass is derived from renewable resources and is basically carbon-neutral in terms of growth and combustion [337]. However, the biogenic carbon neutrality principle is not applicable to life cycle analysis [338]. The results of this study were based on the assumption that biomass is carbon-neutral.

Moreover, this study only evaluated the techno-economic-environmental performances and implementation feasibility of the seven SHTs according to Harbin's local renewable energy resources, as well as national and local clean heating plans. Other options, including geothermal heating and industrial waste heat heating, can be assessed within the framework in future studies to provide comprehensive evidence to facilitate a policymaker's decision-making regarding clean heating transition.

4.5. Conclusions

The transition to clean heating plays an important role in realizing a peak in CO₂ emissions before 2030 and carbon neutrality before 2060 in China. A literature review demonstrates the requirement for a comprehensive and quantitative assessment of the performance of SHTs and their implementation feasibility at the local level. Accordingly, this study evaluated seven SHTs from technical, economic, and environmental perspectives and their implementation feasibility regarding the current policy and future renewable scenarios. The assessment was based on a community in Harbin, a typical city where fossil fuels dominate heating systems.

Consequently, the seven SHTs are applicable from a technical perspective, considering Harbin's climatic conditions and heat demand. Concerning economic and environmental performances, the BB system is a favorable option in the 2020 B+ scenario, with a CAC of 24 €/t. However, with the prediction of rising biomass prices, the STES+BB system is advantageous in the 2030 SP and 2050 RE scenarios, with CACs of 28 and 24 €/t, respectively. Replacing the current heating system with electric heating failed to reduce CO₂ emissions. Based on the released policies and reports, CO₂ emissions can be reduced accordingly in the 2030 and 2050 scenarios. However, the corresponding CACs (over 400 €/t in 2030 and 120 €/t in 2050) remain much higher than those of other SHTs owing to high electricity prices. Considering the uncertainties in future scenarios, the MCM results indicate that the NGB, BB, STES+NGB, and STES+BB systems can all provide favorable options in the 2030 SP scenario. The BB and STES+BB systems may be favorable alternatives for the

2050 RE scenario. In addition, power structure is an important issue that should be considered when implementing electricity-dominant heating technologies.

Considering the feasibility of implementation, gas heating has the highest public acceptance. However, it may threaten national energy security and is not preferable for a fully renewable society in the long term. Although Harbin could benefit from abundant forest and crop resources in Heilongjiang Province, fuel availability remains an issue for biomass heating. Electric heating is also a promoting option with a relatively high public acceptance and increased grid cleanliness. However, it exhibits a high LCOH and requires additional power supply units as well as expansion of electric grids. Solar heating currently has relatively low residential acceptance but broad application prospects with abundant solar resources and favorable policies.

This study contributes to the existing literature on sustainable heat transition in China by providing informative local circumstances in Harbin and presenting methods of assumption-making in detail when local data is not transparent. Formulating appropriate clean heating strategies requires local governments to comprehensively adopt various SHTs based on local resource endowments and infrastructure, with scientific evaluation and full consideration of residents' consumption capacity. This study conducted an integrated assessment of SHTs considering the technical, economic, and environmental performances, besides implementation feasibility, providing solid evidence to facilitate the decision-making process in the clean heating transition in northern cities of China. Furthermore, these methods are applicable in other countries with similar energy mixes and climate conditions.

Acknowledgments

The financial support from the China Scholarship Council (No. 201806220072) is gratefully acknowledged.

Appendix

Power generation mix in the 2050 RE scenario

The power generation mix was simulated using EnergyPLAN according to the renewable energy potential and projected electricity demand, aiming at maximum solar and wind energy penetration. The renewable energy potential of the northeast power grid is detailed in Table 4.A1. According to previous studies, each province's annual electricity consumption per capita is proportional to its GDP per capita [339, 340]. The relationship between electricity consumption and GDP per capita for each province was fitted with their population, electricity consumption, and GDP in 2011–2020, taken from the National Bureau of Statistics of China [19]. The GDP in 2050 for each province was based on the OECD's long-term GDP forecast [341] and adjusted with their projected GDP growth in 2020–2025 [342–344]; accordingly, the electricity demand in 2050 was determined. These results are comparable to those of previous studies [345]. The hourly electricity demand profile was determined based on the annual, weekly, and daily patterns, as shown in Figure 4.A1. The annual distribution was based on the monthly electricity consumption in 2020, and the weekly distribution was based on [346]. The daily distributions of agricultural, industrial, commercial, and residential electricity usage were obtained from [347], and the portions of these types of electricity consumption were derived from [307].

Table 4.A1 Renewable energy potentials of the northeastern power grid.

	Unit	Renewable energy potential	Reference
Biomass	TWh	912.4	[27]
Hydropower	GW	15.1	[348]
Solar power	GW	774.2	[349]
Wind power	GW	311.6	[349]

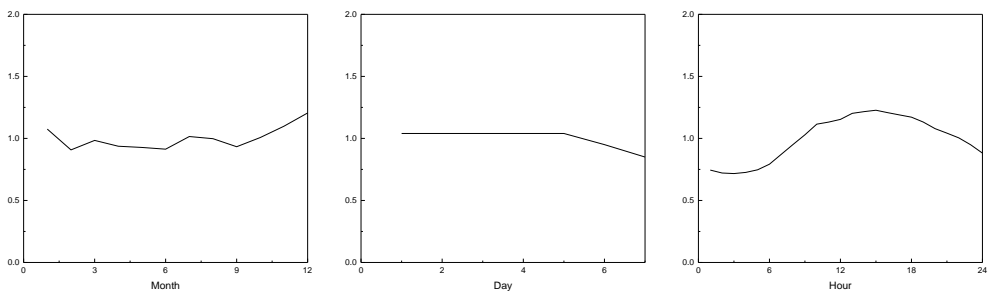


Figure 4.A1. Illustration of the load formulation: a) annual, b) weekly, and c) daily distributions.

The hourly distributions of renewable energy availability are also essential inputs for the EnergyPLAN. The hourly distributions of solar and wind power generation were based on

Chapter 4

23 and 17 weather stations, respectively, according to the current installation locations of the solar and wind power plants. Additionally, the solar power output considers the impact of global solar radiation, wind speed, ambient temperature, optimum tilt, and azimuth angle at each location [349, 350]. The wind power output was based on the turbine power curve considering the regional dependence of wind turbine suitability [349].

Electricity price in the 2030 SP and 2050 RE scenarios

The price of electricity in China includes on-grid tariffs, transmission and distribution prices, and government funds and supplements. The on-grid tariff is a weighted average of various power generation technologies within the regional power grid, and the provincial government determines the other two elements. The 2020 electricity prices in Heilongjiang, Jilin, and Liaoning were used to validate the calculation method, as presented in Table 4.A2. The on-grid tariffs, transmission and distribution prices, and government funds and supplements for each province were derived from the Provincial Development and Reform Commission. The differences within 4% suggest that the method is sufficiently accurate for predicting the electricity prices in the 2030 SP and 2050 RE scenarios.

Table 4.A2 Validation of calculation method with 2020 electricity price.

		Heilongjiang	Jilin	Liaoning
Electricity price				
On-grid tariff (€-ct/kWh)	Coal	4.90	4.89	4.91
	Gas	8.65	8.65	8.65
	Biomass	9.17	9.17	9.17
	Hydro	4.91	5.04	4.32
	Solar	4.90	4.89	4.91
	Wind	4.90	4.89	4.91
	Nuclear	-	-	5.01
	Weighted average	5.09		
Transmission and distribution price (€-ct/kWh)		4.01	3.79	3.12
Government funds and supplements (€-ct/kWh)		0.32	0.59	0.35
Validation				
Calculated electricity price (€-ct/kWh)		9.44	9.48	8.58
Actual electricity price (€-ct/kWh)		9.26	9.27	8.20
Difference		2%	2%	4%

According to the current electricity price policy, the on-grid tariffs for solar and wind power generation are determined by the coal-fired generation on-grid tariff [351]. China is gradually advancing market-oriented reforms in the power sector and improving market-pricing mechanisms for electricity [335]. Therefore, the electricity price in the 2030 SP scenario was predicted from technical innovation and policy perspectives. Regarding technical innovation, the on-grid tariffs for all power generation types were adjusted according to their costs. From the policy perspective, the on-grid tariffs for coal and gas power generation were equal to their costs; the on-grid tariffs for solar and wind power generation were equal to those of coal-fired generation; and the on-grid electricity tariffs for biomass, hydro, and nuclear power remained constant. The electricity price in the 2050 RE scenario was projected from a technical innovation perspective. The levelized cost of energy (LCOE) of different power generation types was taken from various sources in the Chinese context [336, 352-355], as shown in Figure 4.A2. The transmission and distribution prices and government funds and

Chapter 4

supplements are assumed to be constant. Table 4.A3 illustrates the electricity price calculation in the 2030 SP scenario from technical innovation and policy perspectives and the 2050 RE scenario.

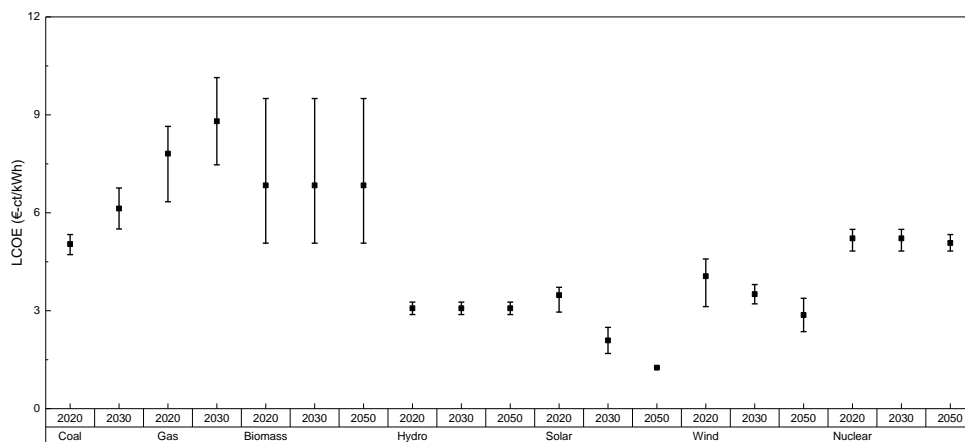


Figure 4.A2. LCOE of various power generation technologies.

Table 4.A3 Electricity prices in the 2030 SP and 2050 RE scenarios.

		2030 SP scenario (technical innovation)			2030 SP scenario (policy)			2050 RE scenario
		Heilongjiang	Jilin	Liaoning	Heilongjiang	Jilin	Liaoning	
On-grid tariff (€-ct/kWh)	Coal	5.96	5.95	5.98	6.13	6.13	6.13	-
	Gas	9.75	9.75	9.75	8.80	8.80	8.80	-
	Biomass	9.17	9.17	9.17	9.17	9.17	9.17	9.17
	Hydro	4.91	5.04	4.32	4.91	5.04	4.32	4.76
	Solar	2.95	2.94	2.95	6.13	6.13	6.13	1.77
	Wind	4.23	4.22	4.25	6.13	6.13	6.13	3.47
	Nuclear	-	-	5.01	-	-	5.01	4.87
	Weighted average		5.36			6.14		4.13
Transmission and distribution price (€-ct/kWh)		4.01			4.01			4.01
Government funds and supplements (€-ct/kWh)		0.32			0.32			0.32
Electricity price (€-ct/kWh)		9.69			10.47			8.47

Heating CO₂ emission factor in the 2020 baseline

The CO₂ emission factor of the heating system at the baseline was calculated using the total heat production, fuel consumption, and CO₂ emission factors of the various fuels. The total heat production and fuel consumption were obtained from [28], and the CO₂ emission factors of various fuels were derived from [243, 314], as listed in Table 4.A4. The CO₂ emission factor of the heating system was determined as 0.51 kg/kWh with the total heat production of 492.2 PJ.

Table 4.A4 Fuel consumption and CO₂ emission factors of heating system in the 2020 baseline.

Fuel	Consumption (tce)	Emission factor (tCO ₂ /tce)
Raw coal	23,292.8	2.69
Other washed coal	349.6	2.62
Coal products	65.1	2.95
Coal gangue	423.2	2.71
Coke oven gas	9.5	1.49
Blast furnace gas	79.8	1.28
Diesel oil	1.7	2.13
Fuel oil	107.7	2.22
Refinery dry gas	1238.1	1.92
Natural gas	573.5	1.63
Other energy	569.3	1.28

Grid CO₂ emission factor in the 2020 B+ and 2030 SP scenarios

The CO₂ emission factor of the regional power grid should be used when calculating CO₂ emissions from electricity usage [243]. The latest released CO₂ emission factors for China's regional power grids were in 2011 and 2012 [356]. However, these numbers have reduced with more renewable energy integration in the power system in recent years, with the national average of 0.581 kg/kWh [357]. Therefore, the CO₂ emission factors of the power system in the 2020 B+ and 2030 SP scenarios were calculated using [243]:

CO₂ emission factor

$$\begin{aligned}
 &= \frac{\text{fuel consumption} \times \text{carbon content} \times \text{carbon oxidation rate}}{\text{power generation}} \\
 &\times 44/12 \\
 &= \text{coal equivalent consumption rate of power generation} \\
 &\times \text{calorific value} \times \text{carbon content} \times \text{carbon oxidation rate} \times 44/12
 \end{aligned}$$

The coal equivalent consumption rate of power generation was obtained from [307]. The calorific value of the coal equivalent is 29.29 MJ/kg. The carbon contents and carbon oxidation rates of coal and natural gas were determined as 25.41 and 15.32 t/TJ, and 98% and 99%, respectively. Before implementing the method in the 2020 B+ and 2030 SP scenarios, the CO₂ emission factors of the northeast power grid in 2011 and 2012 were considered to validate the calculation method, as presented in Table 4.A5. The power generation mix and coal equivalent consumption rates were derived from the *China Electricity Statistical Yearbook*. The difference of 1% suggests that the method is sufficiently accurate to predict the grid CO₂ emission factor in the 2020 B+ and 2030 SP scenarios. Table 4.A6 details the grid CO₂ emission factor calculation results for the 2020 B+ and 2030 SP scenarios. The coal equivalent consumption rate of power generation was obtained from the *China Electricity Statistical Yearbook* and the National Development and Reform Commission.

Table 4.A5 Validation of calculation method using grid CO₂ emission factors in 2011 and 2012.

	2011	2012
Coal equivalent consumption rate of power generation (g/kWh)		
Heilongjiang-coal	348.5	344.0
Liaoning-coal	331.0	326.0
Jilin-coal	329.5	324.0
CO₂ emission factor of power generation (g/kWh)		
Heilongjiang-coal	932.3	920.3
Liaoning-coal	885.5	872.1
Jilin-coal	881.5	866.8
Power generation (TWh)		
Heilongjiang-coal	77.5	77.2
Liaoning-coal	131.6	134.5
Jilin-coal	59.2	59.1
Validation		
Calculated grid CO ₂ emission factor (g/kWh)	813.6	787.0
Released grid CO ₂ emission factor (g/kWh)	818.9	776.9
Difference	1%	1%

Table 4.A6 Grid CO₂ emission factors in the 2020 B+ and 2030 SP scenarios.

	2020 B+	2030 SP
Coal equivalent consumption rate of power generation (g/kWh)		
Heilongjiang-coal	310.8	295.8
Liaoning-coal	302.1	295.5
Jilin-coal	297.2	295.2
Natural gas	224.5	224.5
CO₂ emission factor of power generation (g/kWh)		
Heilongjiang-coal	831.5	791.3
Liaoning-coal	808.2	790.4
Jilin-coal	795.1	789.9
Natural gas	365.9	365.9
Power generation (TWh)		
Heilongjiang-coal	81.1	74.3
Liaoning-coal	138.2	130.9
Jilin-coal	65.2	58.9
Natural gas	0.6	1.3
Result		
Grid CO ₂ emission factor (g/kWh)	558.5	321.9



5

Seasonal thermal energy storage employing solar heat: A case study of Heilongjiang, China, exploring the transition to clean heating and renewable power integration

Submitted to: Yang T, Liu W, Kramer GJ. Seasonal thermal energy storage employing solar heat: A case study of Heilongjiang, China exploring the transition to clean heating and renewable power integration. *Renewable Energy* 2023; under review.

Abstract

Decarbonizing heating in built environments is essential for reducing energy consumption and CO₂ emissions. Seasonal thermal energy storage (STES) offers an attractive option for realizing a sustainable heating transition. A literature review revealed knowledge gaps in the technical feasibility of replacing the district heating (DH) system with STES and the economic and environmental consequences and impact on renewable power integration. The effects of large-scale STES applications on the power and DH sectors in a regional energy system were quantified by applying the 2030 and 2050 scenarios. The results indicated that STES reduces fossil fuel consumption and CO₂ emissions at an affordable cost. It facilitates the integration of wind and solar power into power grids. With 100% replacement of DH by STES, fossil fuel consumption and CO₂ emissions can be reduced by approximately 45% and 40% in 2030 and 2050, respectively, with an annual cost increase of 20%. The CO₂ avoidance costs were predicted to be approximately 60 €/t in 2030 and well below 50 €/t in 2050. STES will reduce renewable power curtailment by 10% in 2030 and 18% in 2050. In this study, STES was investigated from an energy-system perspective, and the results support the formulation of clean heating transition policies.

Chapter 5

Nomenclature

Abbreviations

CAC	CO ₂ avoidance cost
CHP	combined heat and power
DH	district heating
GDP	gross domestic product
HP	heat pump
O&M	operation and maintenance
RE	renewable energy
SP	stated policy
STES	seasonal thermal energy storage

Subscripts

e	electricity
REF	reference
th	thermal

5.1. Introduction

The building sector is a significant contributor to global energy consumption and CO₂ emissions. It accounts for >30% of energy consumption and CO₂ emissions in Europe and China [53, 358]. The burning of fossil fuels meets approximately 85% of the global residential heat demand [55]. Many countries and regions have promised to achieve carbon-neutral targets. For instance, the European Union is committing to achieve carbon neutrality by 2050 [359]. China aims to have a CO₂ emissions peak before 2030 and achieve carbon neutrality before 2060 [9]. Decarbonizing the heat demand in the built environment is essential for meeting these carbon-neutral targets.

A challenge in decarbonizing heating systems is the seasonal mismatch between heat demand and generation from sustainable sources. Many sustainable heat supply systems are characterized by large initial investments and low operational costs [22]. Therefore, an installed capacity tailored to peak demand is not cost-effective. Extending the operation period to an annual level can help meet energy requirements, reduce costs, and achieve decarbonization. The optimal usage of sustainable heat requires long-term storage to account for seasonal fluctuations in supply and demand.

Seasonal thermal energy storage (STES) harvests and stores solar thermal energy in summer and uses it in winter for heating purposes, facilitating the replacement of fossil fuel-based heat supply and coordinating the seasonal mismatch between heat supply and demand [35]. The technical feasibility of the STES has been widely studied. Mesquita et al. [97] introduced an STES system with gas boilers in the Drake Landing Solar Community with 52 detached houses; the average solar fraction reached 96%. Terziotti et al. [360] evaluated an STES system for a five-story student housing complex and demonstrated that solar thermal energy could satisfy 90% of the building heating load. Ma et al. [38] analyzed the heat-transfer performance of a ground source heat pump (HP) with STES for a 30-floor building under different climatic conditions but did not address the percentage of total heat demand met by solar thermal energy. Studies investigating the technical feasibility of STES application in densely populated areas (including low- and high-rise communities) and its implementation limitations (solar collectors and borehole installations) are lacking. Additionally, the feasibility of the large-scale implementation of STES in densely populated areas remains unknown.

Researchers have evaluated the economic and environmental performance of STES. Semple et al. [105] investigated an STES system for greenhouse applications, reporting a levelized cost of energy of 32.9 \$/GJ and a payback period of seven years. The system was able to reduce annual CO₂ emissions by 64%. Durga et al. [361] studied the technical and economic feasibility of heating a university hall using STES with HP, which also reduced CO₂ emissions by 64%. The levelized cost of energy of the system was calculated as 17.6 \$/GJ, and a payback period of 10–11 years is expected. Li et al. [215] applied STES to a campus

district heating (DH) system, achieving a 6% reduction in the annual energy bill and an 8% reduction in CO₂ emissions. The scope of these studies was limited to individual projects, whereas the effects of STES applications on power and DH systems remain unknown. There is a need to assess the feasibility of replacing DH systems with STES at a regional level and to quantify the economic and environmental consequences of such replacements from the perspectives of power and DH systems.

In recent years, renewable power generation penetration—particularly that of wind and solar energy—has increased substantially owing to policies, incentives, and declining technology costs, resulting in increased curtailment in many regions [362]. In this context, technologies that allow flexible coupling of the power and heat sectors can contribute to renewable power integration and decarbonization [363]. In contrast to the case of electric boilers and HPs [364, 365], knowledge on the ability of STES to facilitate renewable power integration is limited.

The objective of this study was to partially fill these knowledge gaps by evaluating the technical feasibility and economic and environmental consequences of replacing DH systems with STES, along with the impact on renewable power integration. The Heilongjiang province of northeast China, where STES has exhibited promising results considering the local context (cold climate and coal-dominant DH) [22], was selected for a case study. The main contributions of this research are as follows: 1) we investigated the extent to which STES with solar heat can replace the traditional fossil fuel-based DH system in a densely populated area, 2) we evaluated the economic and environmental consequences of gradually replacing DH with STES in a regional power and DH system until 100% replacement is achieved, and 3) we quantified the extent to which STES can increase renewable energy penetration in the power system.

The remainder of this paper is organized as follows. Section 5.2 presents the research background and information regarding the case study. Section 5.3 comprehensively details the methodology, including the modeling tool, scenario development, model validation, evaluation indicator, and data collection. Section 5.4 presents the results for different scenarios. Discussions and conclusions are presented in Sections 5.5 and 5.6, respectively.

5.2. Case study

5.2.1. Heilongjiang

Heilongjiang is a northeastern province of China (Figure 5.1). It has a total area of 473,000 km² and a population density of 6.7 thousand people/km². The gross domestic product (GDP) per capita in 2020 was 5700 €. The energy structure of Heilongjiang is shown in Figure 5.2. The total primary energy supply was 994.4 TWh, of which coal accounted for 77.2% of the total. The installed capacities for thermal, hydro, wind, and solar power were 24.2, 1.1, 6.9, and 3.2 GW, respectively. Power generation was coal-dominated, accounting for 81.0% of

Exploring the transition to clean heating and renewable power integration

total power generation. Industry was the most significant energy consumer, followed by the residential and transportation sectors.



Figure 5.1. Location of Heilongjiang province (orange) within China.

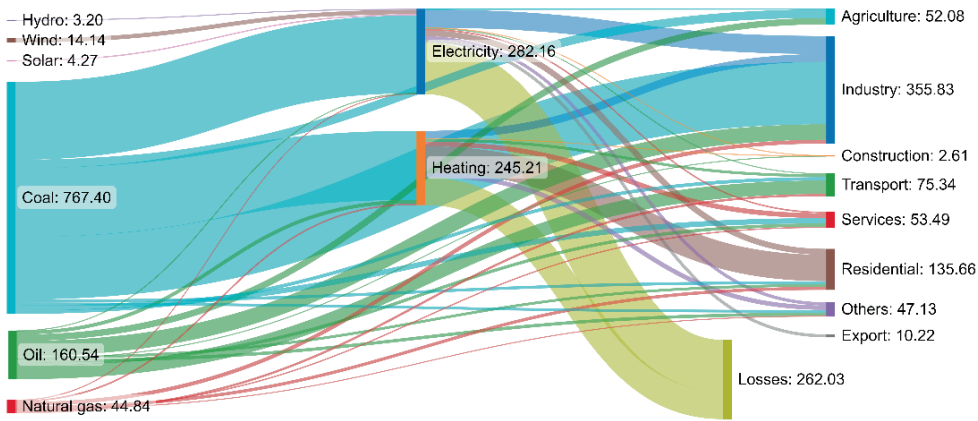


Figure 5.2. Heilongjiang energy balance in 2020 (unit: TWh) [28].

Heilongjiang has a frigid, temperate continental monsoon climate. It is characterized by severely cold winters with a mean temperature between -15 and -35 °C, resulting in a half-year heating season. In 2020, DH met 87% of the heat demand in the built environment, of which 93% was supplied by coal-fired combined heat and power (CHP) plants and boilers [331]. The demand for DH in different cities in Heilongjiang province is shown in Figure 5.3. Harbin—the capital city—accounted for nearly half of the total heat demand. The heat demand per capita in Heilongjiang province in 2020 was 4.8 MWh.

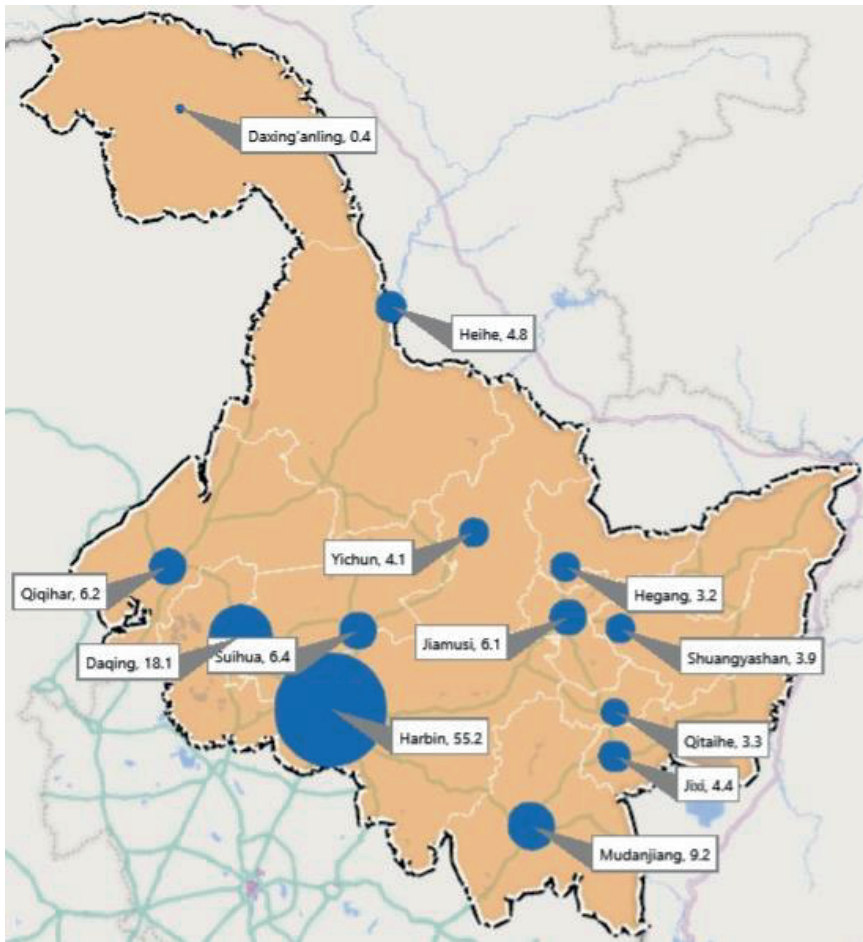


Figure 5.3. DH demands in different cities in Heilongjiang province in 2020 (unit: TWh) [331].

5.2.2. Heat supply in built environment in Heilongjiang

Before 2000, residential communities in Heilongjiang were mainly low-rise buildings (fewer than seven floors) without elevators. After 2000, high-rise buildings were rapidly built in urban areas owing to land shortages for urban construction. The proportions of low- and high-rise buildings in Heilongjiang in 2020 were 74.9% and 25.1%, accounting for 40.5% and 59.5% of the total heat demand, respectively [366]. District boilers were the main heating supply technology prior to CHP development. In 2000, the National Development and Reform Commission issued regulations that encouraged CHP plants to replace coal-fired boilers. After 2000, CHP plants were newly built or converted from thermal power units. CHP plants supplied 92.9 TWh of heat in 2020, mainly for high-rise buildings, whereas boilers supplied 60.8 TWh, mainly for low-rise buildings.

5.3. Methodology

5.3.1. Heat-demand simulation

A low-rise residential community and a high-rise community (Figure 5.4) were selected as examples to simulate heat demand and investigate the feasibility of implementing STES. As shown in Table 5.1, the selected low-rise community consisted of 14 four-to-six-floor buildings with a space-heating area of 43,200 m² and an annual heat demand of 1.5 GWh. The high-rise community comprised 13 18-to-31-floor buildings with a space-heating area of 181,600 m² and an annual heat demand of 6.3 GWh. The area for solar collector installation was calculated according to the total roof area and the criterion that the spacing of the solar collectors should be equal to their height. Public areas available for borehole installation include those with open spaces and greenery.

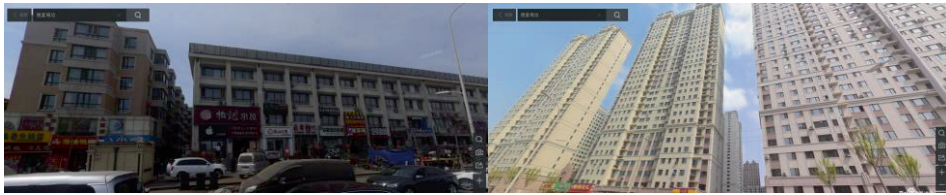


Figure 5.4. Examples of low-rise (left) and high-rise (right) residential communities considered in this study.

Table 5.1 Information on the example communities considered.

	Number of buildings	Number of floors	Annual heat demand	Roof area	Area for solar-collector installation	Public area available for borehole installation
Unit			GWh	m ²	m ²	m ²
Low-rise community	14	4–6	1.5	8,600	6,120	4,000
High-rise community	13	18–31	6.3	8,900	6,400	30,000

The STES systems in the two example communities were modeled using TRNSYS (Figure 5.5) to simulate the heat demand in a manner similar to that in our previous work [22, 367]. The solar-collector area was set according to the maximum installation area. The borehole number was determined using a multi-optimization procedure considering the economic and environmental impacts. The results indicated that the STES could meet 100% and 50% of the heat demand for low- and high-rise residential communities, respectively. An auxiliary heating device is needed to satisfy the remaining heat demand of high-rise communities. In this study, HPs were selected as the auxiliary heating device because 1) HPs are commonly used as auxiliary heating devices for STES with solar heat [202], 2) STES coupled with HPs

exhibits good performance in Heilongjiang province [22], and 3) HPs use power for heating, potentially increasing the extent to which renewable energy can be integrated into the power system [368]. The HP capacity was set to cover the peak demand for heating.

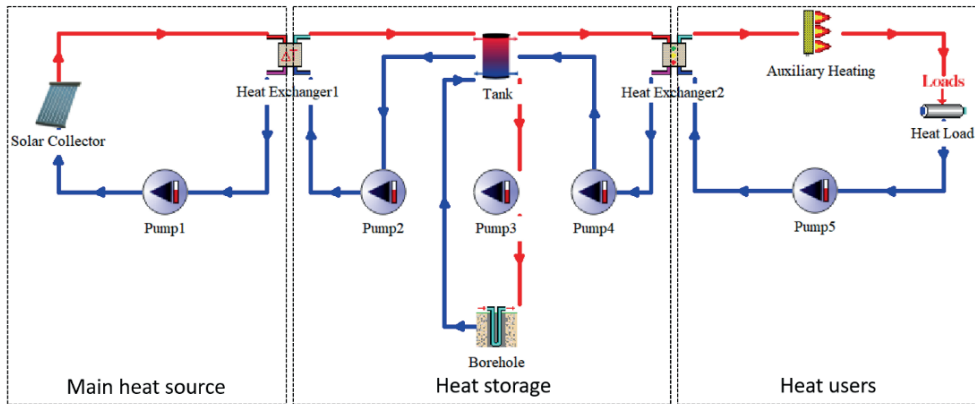


Figure 5.5. Simplified diagram of the STES system.

5.3.2. Scenario development

Two reference scenarios for evaluating future DH and power systems were developed on the basis of the circumstances prior to the replacement of CHP systems and boilers with STES. The subsequent energy demand in the power and DH sectors of Heilongjiang province is forecasted to 2050.

5.3.2.1. 2030 SP scenario

A 2030 stated policy (SP) scenario was developed according to local policies. The energy generation structure of the 2030 SP scenario was predicted using the power generation or installed capacity combined with the utilization hours of recent years in 2030, according to policy documents released by the Heilongjiang local government [344].

5.3.2.2. 2050 RE scenario

A 2050 renewable energy (RE) scenario was developed to investigate the consequences of replacing DH with STES along with an optimal future power system. The installed capacities of wind and solar power generation in the 2050 RE scenario were determined using a multi-objective optimization procedure considering economic and environmental consequences. Different wind and solar power capacity combinations were tested, with the minimum total annual cost and CO₂ emissions as the optimization objectives. The optimal solution was obtained via Pareto optimization and was selected from the Pareto front by considering a marginal CO₂ avoidance cost (CAC) equal to the CO₂ price. When the marginal CAC corresponding to the given reduction target is collected as the CO₂ price, the reduction target

is achieved because of the emitter's rational action of cost minimization [369]. Table 5.2 presents the estimated installed capacities of wind and solar power generation at different penetration levels.

Table 5.2 Estimated installed capacities of wind and solar power generation for meeting fixed penetration levels.

Penetration	10%	20%	30%	40%	50%	60%	70%	80%	90%	100%
Wind (GW)	9.45	18.90	28.36	37.81	47.26	56.71	66.16	75.62	85.07	94.52
Solar (GW)	14.52	29.03	43.55	58.07	72.59	87.10	101.62	116.14	130.65	145.17

5.3.2.3. Energy-demand forecasting

The energy consumption in the power and DH sectors from 2003 to 2020 was derived from the *China Energy Statistical Yearbooks*. The trends in the energy consumption in these sectors were analyzed, together with the changes in population, GDP, and GDP per capita from 2003 to 2020, to provide a basis for energy-demand forecasting to 2050. Linear relationships were observed among the power consumption, DH consumption, and GDP per capita. These relationships were fitted and used for forecasting (see Appendix (Figure 5.A1 and Tables 5.A2-A3)). The GDP until 2050 was based on the long-term GDP forecast for China published by the Organization for Economic Co-operation and Development [341] and was adjusted to the projected GDP growth in Heilongjiang in 2020–2025 [344]. The population was based on World Bank data [370]. The resulting energy-demand forecast for the power and DH sectors in Heilongjiang province until 2050 is shown in Figure 5.6. The technically exploitable renewable energy generation capacities of Heilongjiang province are presented in Table 5.3.

Table 5.3 Technically exploitable renewable energy generation capacity in Heilongjiang province.

	Unit	Technically exploitable amount	Reference
Solar power	GW	284.58	[349]
Wind power	GW	138.70	[349]
Hydropower	GW	8.16	[348]

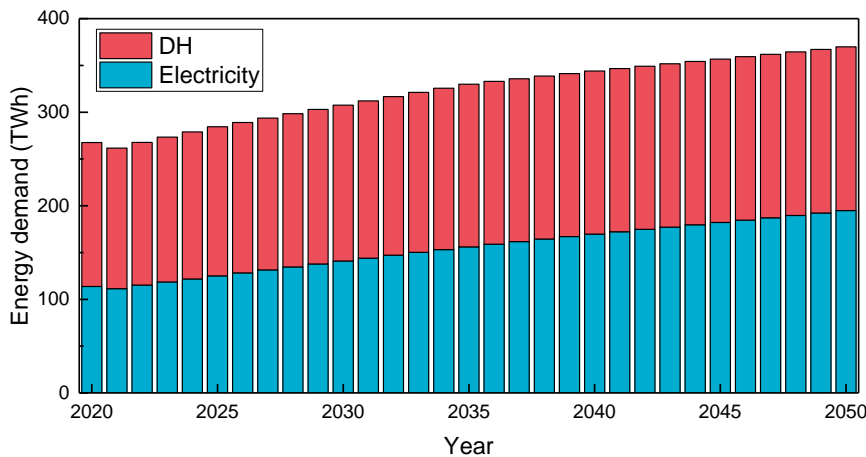


Figure 5.6. Energy-demand forecasting results for the DH and power sectors in Heilongjiang province until 2050.

5.3.3. Power and DH system modeling

EnergyPLAN is a comprehensive hourly simulation model tool that simulates the energy system, including the power, heating, cooling, industrial, and transport sectors [308]. It is widely adopted for simulating and optimizing 1) the integration of various renewable energy sources [371, 372], 2) the feasibility and synergy of multiple technologies [280, 373], and 3) the development of energy strategies [374, 375]. The structure of the EnergyPLAN tool and its specific applications in this study are presented in Figure 5.7.

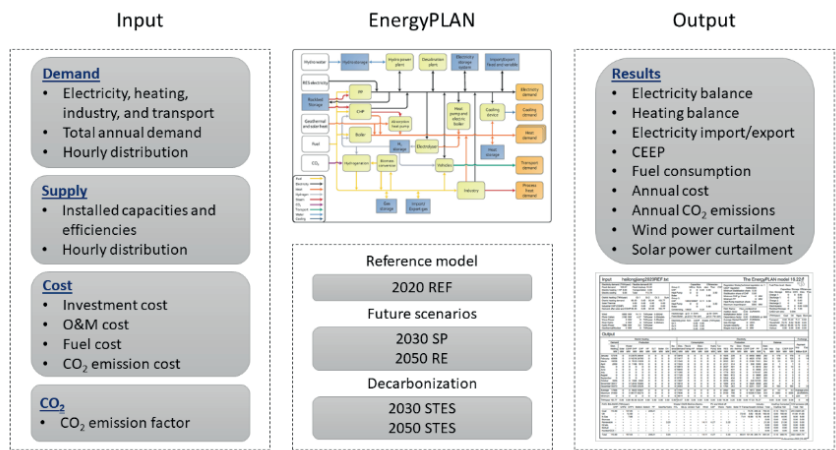


Figure 5.7. Structure of the EnergyPLAN tool and its specific application in this study.

The following fundamental assumptions were considered to secure grid stabilization. 1) CHP plants primarily guarantee heat production during the heating period, and 2) at least 30% of the electricity must be generated by the generation plants able to stabilize the grid, for example, thermal power and hydropower plants in the 2020 reference system and 2030 SP scenario. This setting was removed in the 2050 RE scenario for maximum renewable power integration without regulation limitations. 3) Wind and solar power plants can not provide load regulation service, and 4) wind power generation should be curtailed first, followed by solar, according to the policy of the National Energy Administration.

5.3.4. Model validation

A reference model of the power and DH system in Heilongjiang province in 2020 was built to describe the current power and DH structures. The capacities and power generation of different power generation technologies were obtained from the *China Electricity Statistical Yearbook* [307]. The fossil fuel consumption in the thermal power and DH sectors was derived from the *China Energy Statistical Yearbook* [28].

The hourly distributions of the power and DH demands and renewable energy availability are essential inputs for EnergyPLAN. The hourly electricity demand profile was determined according to annual, weekly, and daily patterns, as shown in Figure 5.8. The annual distribution was based on monthly electricity consumption in 2020, and the weekly distribution was based on [346]. The daily distributions of agricultural, industrial, commercial, and residential electricity usage were obtained from [347], and the proportions of these types of electricity consumption were derived from [307]. The hourly DH demand profile was obtained by simulating a case community by applying weather profiles for different cities in Heilongjiang province using TRNSYS.

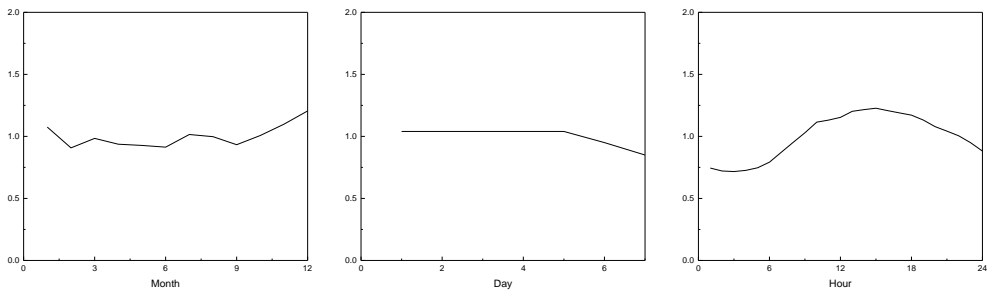


Figure 5.8. Illustration of the load formulation: a) annual, b) weekly, and c) daily distributions.

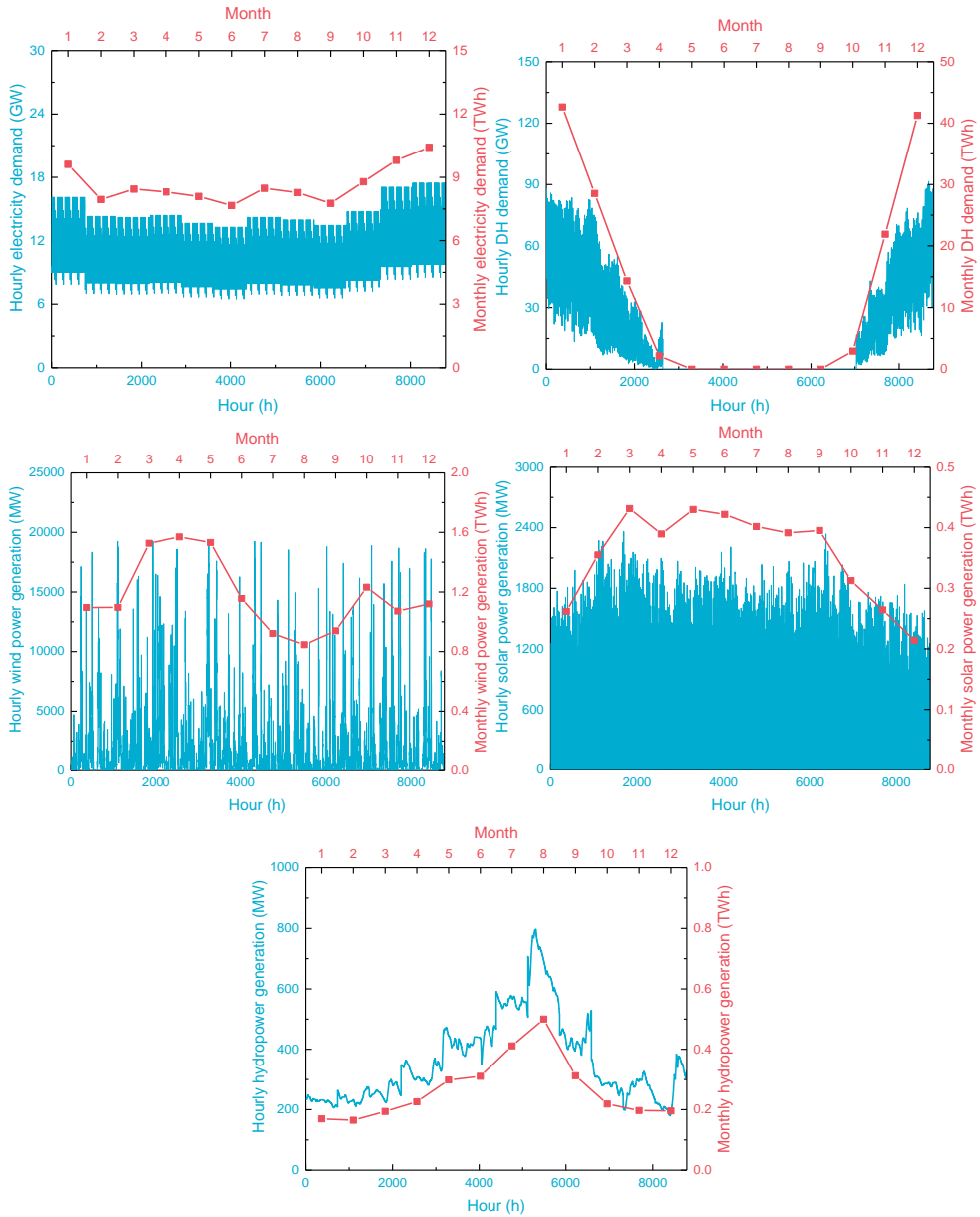


Figure 5.9. Hourly distribution data for electricity and heat demands and renewable power generation.

The hourly distributions of the solar and wind power generation were based on 17 and 20 weather stations, respectively, according to the current installation locations of the solar and wind power plants. In addition, the solar power output considers the impact of global solar radiation, wind speed, ambient temperature, and optimal tilt and azimuth angles at each

location [349, 350]. The wind power output was based on the turbine power curve, considering the regional dependence on wind turbine suitability [349]. The hourly distribution of the hydropower generation was defined as described in a previous study [283]. Figure 5.9 presents the hourly distribution data for electricity and DH demands and renewable power generation.

The simulation outputs of the reference model were compared with actual data to confirm the consistency and reliability of the model (see Appendix (Table 5.A1)). The simulation results exhibited a minor discrepancy compared with the actual values (<1.6%), which indicates that the model performs well in simulating the current power and DH system; therefore, it was used to develop the designed future scenarios.

5.3.5. Evaluation indicator and data collection

Table 5.4 Costs of different technologies and energy system infrastructures [283, 287, 311, 376].

Unit		Investment costs (M€/unit)			Fixed O&M costs (% of investment cost)	Lifetime (years)
		2020	2030	2050		
Heat and electricity						
Power plant	MW _e	0.54	0.53	0.51	3	40
CHP	MW _e	0.60	0.58	0.56	4	30
DH boiler	MW _{th}	0.08	0.08	0.08	3	25
HP	MW _e	0.48	0.39	0.38	1	25
Transmission line	MW	0.24	0.24	0.24	2	40
Renewable energy						
Wind power	MW _e	0.95	0.82	0.67	2	25
Solar power	MW _e	1.82	1.10	0.66	1	30
Hydropower	MW _e	0.85	0.85	0.85	1.5	50
Solar thermal	TWh/year	131.03	120.55	107.44	0.75	30
Heat storage solar	GWh	0.50	0.45	0.42	0.7	20
Hydro pump	MW _e	0.66	0.52	0.46	1.5	50
Hydro storage	GWh	1.05	0.92	0.89	1	50

The economic and environmental performance of the designed system was assessed by considering the fossil fuel consumption, total annual cost, CO₂ emissions, and average and marginal CACs. The total system cost includes the investment, operation and maintenance (O&M), fuel, and electricity exchange costs. Table 5.4 presents the costs of different technologies and energy system infrastructures. The fuel prices, handling costs, and CO₂ emission factors for Heilongjiang province are summarized in Table 5.5. The electricity exchange and CO₂ emission costs are 77.3 €/MWh and 5.8 €/t, respectively. The average and marginal CAC values can be calculated as follows:

$$CAC_{average} = \frac{Cost_{i\% STES} - Cost_{REF}}{CO_2 \text{ emissions}_{REF} - CO_2 \text{ emissions}_{i\% STES}} \quad (5.1)$$

$$CAC_{marginal} = \frac{Cost_{i\% STES} - Cost_{(i-10)\% STES}}{CO_2 \text{ emissions}_{(i-10)\% STES} - CO_2 \text{ emissions}_{i\% STES}} \quad (5.2)$$

where $i\%$ STES denotes the STES share in DH.

Table 5.5 Fuel prices, handling costs, and CO₂ emission factors for Heilongjiang province in 2020, 2030, and 2050 [243, 311-314, 377].

	Unit	Coal	Fuel oil	Natural gas
Fuel price				
2020	€/GJ	5.12	7.17	12.37
2030	€/GJ	5.46	9.00	13.91
2050	€/GJ	5.67	12.30	15.54
Fuel handling cost				
Power stations (central)	€/GJ	0.075	0.280	0.472
Distributed CHP, DH, and industry	€/GJ	0.075	1.914	1.857
Emission factor				
CO ₂ emission factor	kg/GJ	91.31	72.15	55.61

5.4. Results

5.4.1. STES replacement in 2030 SP scenario

Figure 5.10 shows the fossil fuel consumption, total annual cost, and CO₂ emissions of the power and DH system for the 2030 SP scenario, where the share of STES in the DH varies from 10% to 100%. With increased STES implementation, the fossil fuel consumption of the DH decreased, whereas that of the power sector increased. This is because the additional electricity demand caused by HP implementation required more power generation. A 5.1% reduction in fossil fuel consumption was observed for every 10% increase in the STES share in the DH. In addition, as STES replaced the conventional DH system to a greater extent, the annual investment and O&M costs increased, and the fuel cost decreased. The cost of electricity exchange decreased because of the increased demand for electricity caused by the HP implementation. A 2.3% increase in the total annual cost was observed for every 10% increase in the STES share in the DH. In addition, as the share of STES in the DH system increased, the CO₂ emissions of the DH decreased, whereas those of the power sector increased. The CO₂ emissions of the system decreased by 4.8% per 10% STES implementation.

Exploring the transition to clean heating and renewable power integration

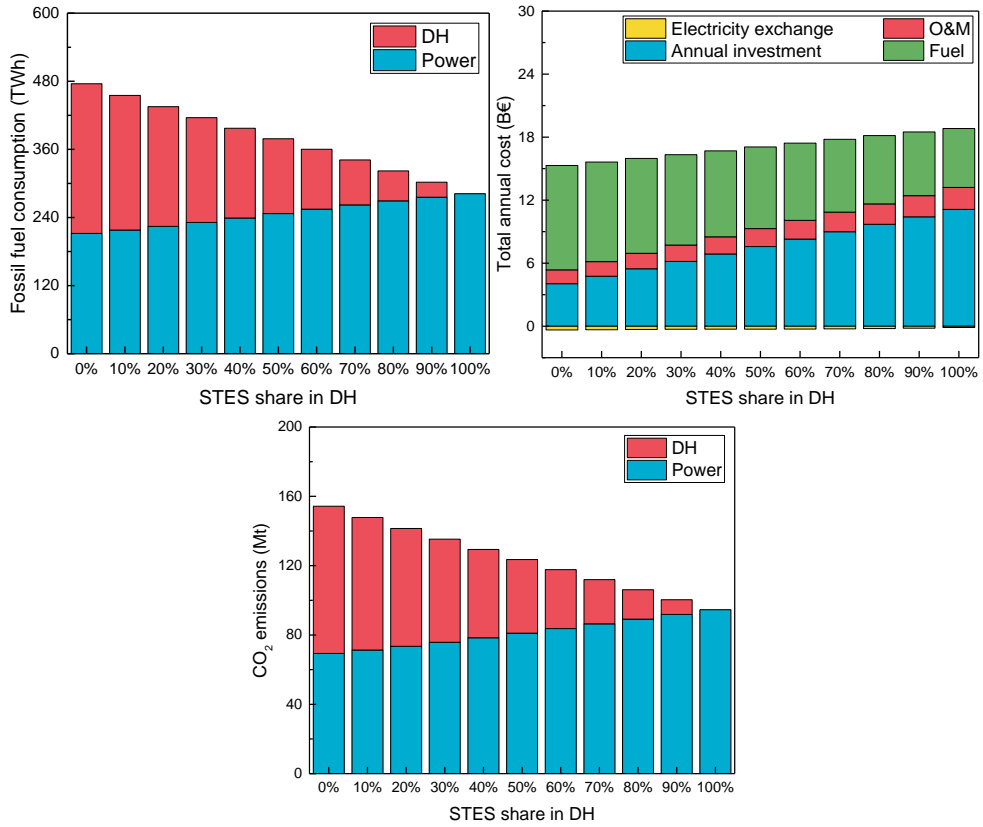


Figure 5.10. Fossil fuel consumption, total annual cost, and CO₂ emissions of the designed system in the 2030 SP scenario.

The average and marginal CACs of the designed system in the 2030 SP scenario are shown in Figure 5.11. As the share of STES in DH increased, the CACs increased because the benefit of renewable power integration decreased. The marginal CO₂ emission reduction decreased. Compared with the estimates of the marginal CAC for China in previous studies (250 \$/t on average) [378], STES exhibited a reasonable cost for heating decarbonization.

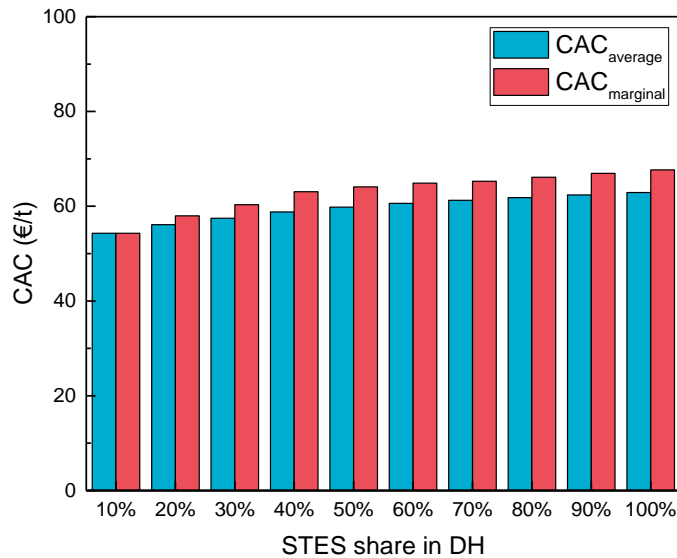


Figure 5.11. Average and marginal CACs of the designed system in the 2030 SP scenario.

The wind and solar power curtailments of the designed system in the 2030 SP scenario are shown in Figure 5.12. Curtailments occurred because of the supply-and-demand balancing issues of the local network and transmission congestion. The curtailment of wind power exceeded that of solar power because a higher installed wind power capacity was deployed, and wind power generation was curtailed first, followed by solar. With further STES implementation, the wind and solar power curtailments decreased. One reason for this was that the application of STES reduced the thermal load of CHP plants, resulting in less power generation by thermal power plants because CHP plants primarily guarantee heat production during the heating period. Another reason was that the implementation of the HP increased the electricity demand, helping to integrate more wind and solar power into the system. The wind and solar power curtailments were reduced by 10.4% and 50.0%, respectively, with 100% replacement of the DH system by STES.

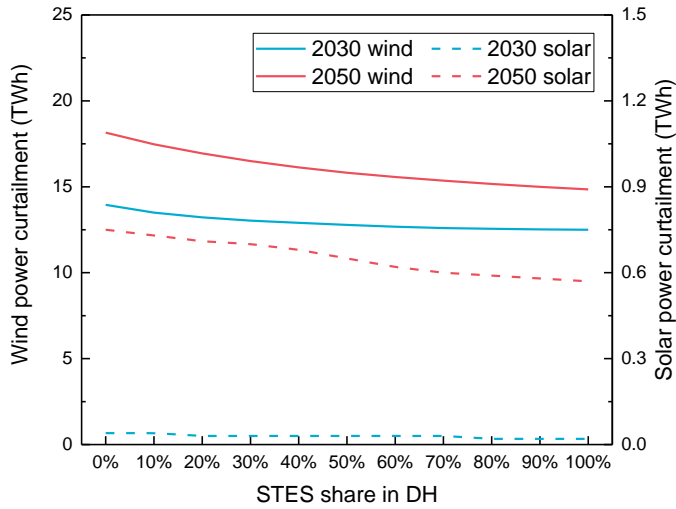


Figure 5.12. Wind and solar power curtailments of the designed system in the 2030 SP and 2050 RE scenarios.

Figure 5.13 presents a comparison of the wind power generation in the 2030 SP and 2030 100% STES scenarios. Owing to the ability of the STES to reduce wind power curtailment, the 2030 100% STES scenario allowed more wind power integration. Additional wind power integration mainly occurred in winter, and the wind speed in Heilongjiang was relatively high from late autumn to early spring [379]. Therefore, STES in DH has considerable potential for increasing the integration of wind power generation.

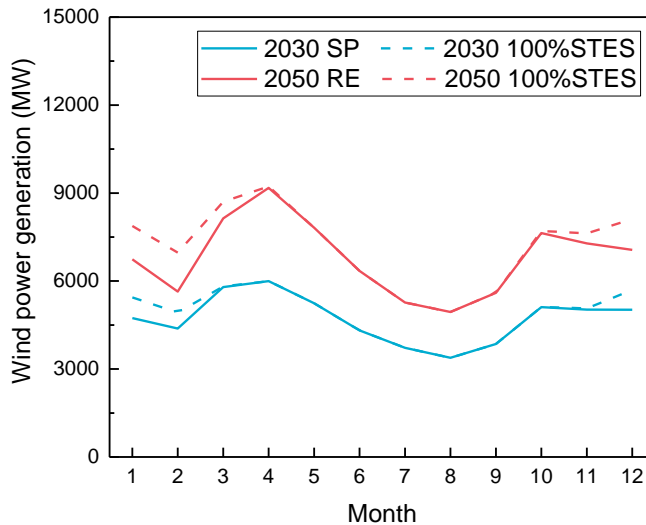


Figure 5.13. Wind power generation in the 2030 SP, 2030 100% STES, 2050 RE, and 2050 100% STES scenarios.

5.4.2. STES replacement in 2050 RE scenario

As the basis for building the power structure in the 2050 RE scenario, the Pareto front of different wind and solar power combinations were obtained with the minimum total annual cost and CO₂ emissions as the optimization objectives, as shown in Figure 5.14. Increasing wind and solar power penetration can reduce CO₂ emissions. However, the trend of the total annual cost indicates that excessively high and excessively low penetration can have negative economic consequences, which highlights the importance of setting a suitable combination of wind and solar capacities. The optimal solution was selected by considering a marginal CAC equal to the CO₂ price (5.8 €/t) to ensure that the reduction target was achieved as a result of the rational action of cost minimization. The wind and solar power generation penetration levels were identified as 40% and 30%, respectively, resulting in a total annual cost of 16.4 billion € and CO₂ emissions of 154.1 Mt for the power and DH system.

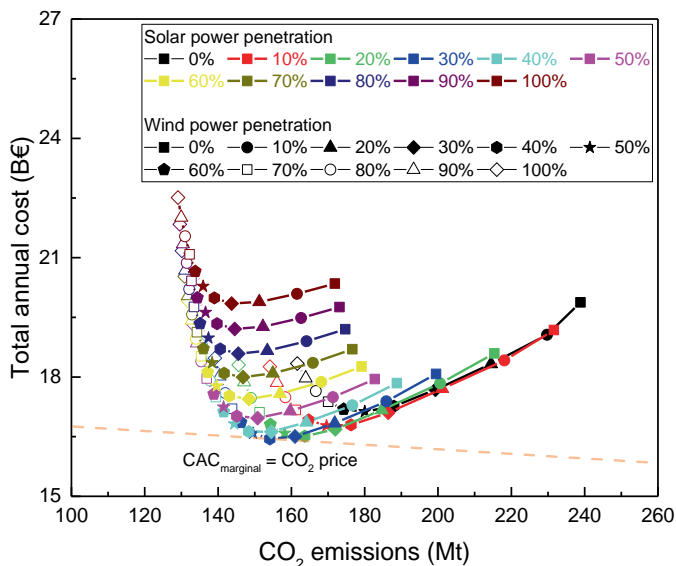


Figure 5.14. Pareto front of different wind and solar power combinations (CO₂ price is 5.8 €/t).

Figure 5.15 shows the fossil fuel consumption, total annual cost, and CO₂ emissions of the designed system, where STES replaced DH from 10% to 100% for the 2050 RE scenario. Trends similar to those in the 2030 SP scenario were observed in the 2050 RE scenario. A 6.7% reduction in fossil fuel consumption, 1.6% increase in the total annual cost, and 5.2% reduction in the CO₂ emissions of the system were observed for every 10% increase in the STES share in DH.

Exploring the transition to clean heating and renewable power integration

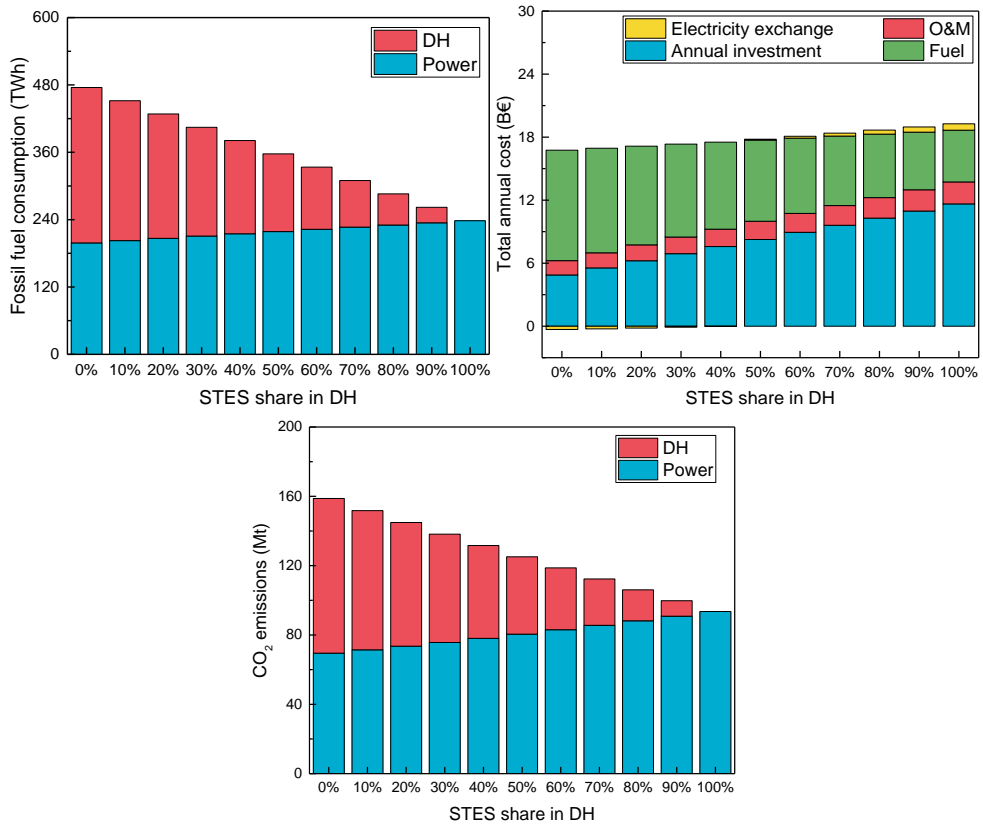


Figure 5.15. Fossil fuel consumption, total annual cost, and CO₂ emissions of the designed system in the 2050 RE scenario.

The average and marginal CACs of the designed system in the 2050 RE scenario are presented in Figure 5.16. The CACs in the 2050 RE scenario were lower than those in the 2030 SP scenario because the cost of STES was expected to decrease, and the CO₂ emissions continued to decrease because the optimal combination of wind and solar power generation allowed more renewable power integration.

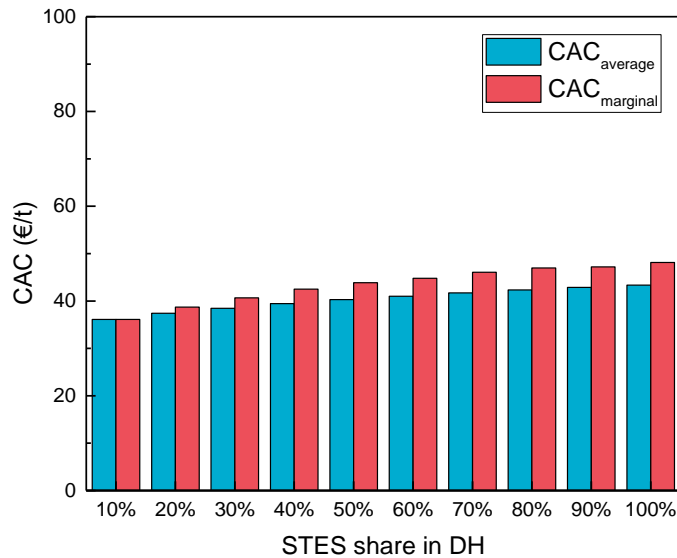


Figure 5.16. Average and marginal CACs of the designed system in the 2050 RE scenario.

In the 2050 RE scenario, increased STES implementation led to a gradual reduction in wind and solar power curtailment (Figure 5.12). These reductions were larger than those in the 2030 SP scenario because of the higher installed capacity of renewable power and the more flexible power system. The wind and solar power curtailments were reduced by 18.2% and 24.0%, respectively, with 100% replacement of the DH system by STES. The wind power generation in the 2050 RE and 2050 100% STES scenarios is compared in Figure 5.13, indicating that STES implementation allowed more wind power integration in winter. Although the minimum grid stabilization share was removed in the 2050 RE scenario, wind and solar power curtailment occurred. Efforts to utilize storage technologies and improve the transmission capacity and grid infrastructure can facilitate renewable power integration.

5.5. Discussion

We analyzed the feasibility and quantified the impact of replacing the conventional DH system in Heilongjiang province with STES. The results indicated considerable potential to reduce fossil fuel consumption and CO₂ emissions and reduce the curtailments of wind and solar power generation, although at an increased total annual cost. The increased cost is mainly due to the investment cost of STES and solar heat systems and the additional electricity demand. To completely replace conventional DH systems, STES systems were designed to cover the peak demand of the DH network, which increases costs. Biomass boilers or direct electric heaters are the preferred options for meeting the peak demand and reducing DH supply costs [380]. In addition, from a policy incentive perspective, the local government announced a subsidy of 4.7 €/m² for those who use solar heating and HPs, which

may reduce the cost of STES by up to 13% [22]. Therefore, with sufficient local resources and strong government support, the STES is promising for large-scale applications.

The results for the 2030 SP and 2050 RE scenarios indicated that replacing the conventional DH system with STES in 2050 can reduce fossil fuel consumption and CO₂ emissions and allow wind and solar power integration to a greater extent compared with 2030, with a smaller increase in the total annual cost. In addition, the average and marginal CACs are expected to decrease by 2050. One reason for this is that the cost of STES is expected to decrease, and another is that the optimal combination of wind and solar power generation allows more renewable power integration. This indicates that with a higher degree of renewable power integration in the power structure, more benefits can be obtained by replacing DH with STES.

The minimum grid stabilization share indicates the share of total electricity production every hour that must be supplied by a grid-stabilizing unit, for example, thermal power and hydropower. The share was set to 30% in the 2030 SP scenario and removed from the 2050 RE scenario for maximum renewable power integration without regulation limitations. A reduction in the minimum grid stabilization share increases the flexibility of the electricity system and therefore allows a higher degree of penetration of intermittent renewable power generation [381]. Nevertheless, grid-stabilizing units are essential because they can adjust power generation according to the requirements of the grid to adapt to power market changes in current and future energy systems. Heilongjiang province announced that new coal-fired CHP units would no longer be installed after 2025. Compared with traditional energy sources, the volatility and intermittency of renewable power generation have introduced new operational challenges to power systems [382]. Considering the decommissioning rate of coal-fired CHP units and the ambition for rapid wind and solar power generation development, power systems require more flexible resources to stabilize the power grid and match supply and demand. Solutions include thermal power unit flexibility retrofitting [383], the construction and optimization of inter-regional transmission lines [384], the use of gas-fired power generation plants with better peak regulation ability, and electricity storage methods such as batteries, hydro storage, and vehicle-to-grid [385, 386].

The power structure for the 2050 RE scenario was developed using an optimal combination of wind and solar power capacities. The optimal solution was selected from the Pareto front by considering a marginal CAC equal to the CO₂ price. The CO₂ price in China (5.8 €/t) is lower than that in Europe, which reached 100 €/t by 2023 [387]. A roadmap for rapid decarbonization proposed that the CO₂ price should be increased to >400 \$/t by 2050 to achieve net zero CO₂ emissions [388]. A higher CO₂ price can encourage more wind and solar power to penetrate the power structure, promoting the application of STES. In this context, replacing the DH system with STES can reduce fossil fuel consumption and CO₂ emissions and allow more renewable power integration with a smaller cost increase. STES applications can become more attractive with the expectation of reducing the CAC.

In this study, we used low- and high-rise residential communities as examples to investigate the feasibility of implementing STES as a replacement for conventional DH systems. These two types of buildings are good representatives but are unable to cover the full diversity of buildings. According to the *Planning and Design Standards for Urban Residential Areas* [389], the building density of residential communities should be maintained below 30%. A sufficient public area was available for borehole installation. Evaluating the feasibility of implementing commercial buildings requires an in-depth geographic information system-based analysis. In addition, typical meteorological year data were used to predict the heat demand, ignoring the influence of extreme weather, which may impact the performance of the STES. In future studies, diverse application scenarios and the impact of extreme weather should be analyzed.

STES is promising for the realization of a clean heating transition and renewable power integration. However, its current rate of resident acceptance in China is relatively low, and underground construction usually requires a long investigation period [22]. In addition, STES with HPs serving as auxiliary heating devices can impose a burden on the power grid. The additional electricity demand for 100% replacement in the 2030 SP and 2050 RE scenarios is 16.8 and 17.6 TWh, accounting for 11% and 8% of the total electricity demand, respectively. Such routes require substantial investment in the construction of the power infrastructure.

5.6. Conclusions

The introduction of STES as part of the clean heating transition can facilitate the decarbonization of domestic heat and enhance renewable power integration, significantly helping to achieve carbon neutrality targets. In this study, we quantified the technical feasibility of replacing the DH system with STES in the densely populated areas of Heilongjiang, China and considered the economic and environmental consequences for the power and DH sectors.

In the 2030 SP scenario, a 41% reduction in fossil fuel consumption, 25% increase in total annual cost, and 39% reduction in CO₂ emissions were observed with 100% replacement of the DH system by STES. The CAC was calculated as approximately 60 €/t and was linearly correlated with the STES share in the DH. The wind and solar power curtailments were reduced by 10% and 50%, respectively. Additional wind power integration occurred mainly in winter, which was the high-wind speed period, indicating that STES in the DH has considerable potential for increasing the degree of wind power generation integration.

The 2050 RE scenario was determined via the Pareto optimization of different wind and solar power combinations with the minimum total annual cost and CO₂ emissions as the optimization objectives. The optimal penetration levels were found to be 40% and 30% for wind and solar power generation penetration, respectively. A 100% share of STES led to a 50% reduction in fossil fuel consumption, 17% increase in total annual cost, and 41%

reduction in CO₂ emissions. A CAC of well below 50 €/t was obtained. The wind and solar power curtailments were reduced by 18% and 24%, respectively. With more renewable power generation in the power structure, more benefits can be obtained by replacing DH with STES.

STES can reduce fossil fuel consumption and CO₂ emissions and promote the integration of wind and solar power generation into the power sector at an affordable cost. With sufficient local resources and strong government support, STES is promising for large-scale applications. However, it can also impose a burden on the power grid owing to an increase in power demand. Additional renewable power generation, energy storage, and other units that promote the flexibility of the regional energy system are needed to stabilize the power grid and match power supply and demand.

Acknowledgments

The financial support from the China Scholarship Council (No. 201806220072) is gratefully acknowledged. The authors would like to thank Chris Spiersb (Utrecht University, the Netherlands) for his valuable and constructive feedback.

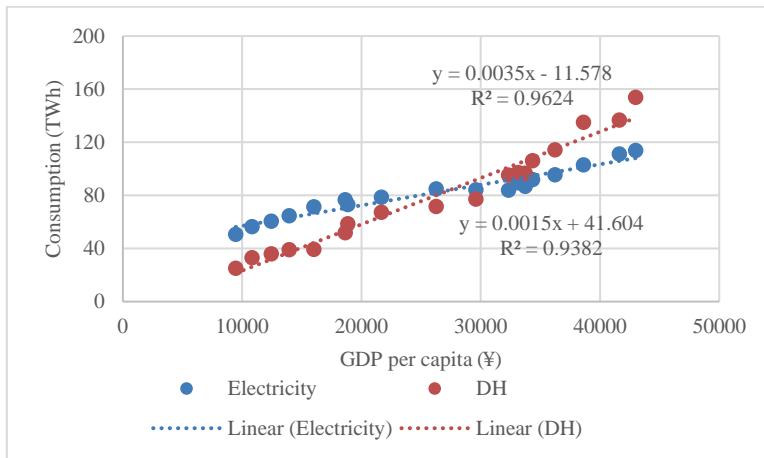


Figure 5.A1 Relations between electricity and district heating consumption and GDP per capita.

Table 5.A1 Comparison between the simulation results of the reference model and actual data in 2020.

	Actual data (TWh)	EnergyPLAN (TWh)	Difference (TWh)	Difference (%)
Electricity				
Thermal power	92.18	92.20	0.02	0.02
Wind power	14.14	14.14	0	0
Solar power	4.27	4.27	0	0
Hydropower	3.20	3.20	0	0
Import/export	10.22	10.25	0.03	0.29
DH				
CHP	92.94	92.94	0	0
Boiler	60.83	60.83	0	0
Fuel				
Coal	485.33	482.85	-2.48	-0.51
Oil	12.66	12.6	-0.06	-0.47
Natural gas	7.76	7.88	0.12	1.55
Renewable	21.61	21.58	-0.03	-0.14
Total	527.36	524.91	-2.45	-0.46

Table 5.A2 Historical population, GDP, and electricity and district heating consumptions in Heilongjiang province.

Year	2003	2004	2005	2006	2007	2008	2009	2010	2011
Population (Million)	38.15	38.17	38.20	38.23	38.24	38.25	38.26	38.33	37.82
GDP (B¥)	360.97	413.47	475.64	532.98	612.63	713.42	721.89	830.83	993.50
Electricity consumption (TWh)	50.66	56.39	60.41	64.61	71.33	76.67	73.16	78.57	84.94
DH consumption (TWh)	25.17	32.96	35.95	38.98	39.26	51.81	58.51	67.30	71.49
Year	2012	2013	2014	2015	2016	2017	2018	2019	2020
Population (Million)	37.24	36.66	36.08	35.29	34.63	33.99	33.27	32.55	31.71
GDP (B¥)	1101.58	1184.91	1217.08	1169.00	1189.50	1231.30	1284.65	1354.44	1363.34
Electricity consumption (TWh)	84.17	83.93	86.74	89.50	91.93	95.43	102.93	111.03	113.79
DH consumption (TWh)	77.07	95.20	96.67	97.08	106.05	114.19	135.11	136.73	153.77

Table 5.A3 Forecasting population, GDP, and electricity and district heating consumptions in Heilongjiang province.

Year	2021	2022	2023	2024	2025	2026	2027	2028	2029	2030
Population (Million)	31.74	31.82	31.90	31.97	32.02	32.06	32.10	32.12	32.13	32.14
GDP (B¥)	1477.67	1561.95	1637.66	1709.85	1780.91	1851.44	1921.63	1991.39	2060.36	2128.30
Electricity consumption (TWh)	111.44	115.22	118.61	121.84	125.03	128.22	131.41	134.60	137.78	140.94
DH consumption (TWh)	150.23	152.52	154.82	157.12	159.41	160.86	162.30	163.75	165.19	166.63
Year	2031	2032	2033	2034	2035	2036	2037	2038	2039	2040
Population (Million)	32.14	32.12	32.10	32.07	32.04	31.99	31.94	31.88	31.81	31.74
GDP (B¥)	2194.98	2260.25	2323.90	2385.70	2445.45	2503.03	2558.38	2611.54	2662.57	2711.58
Electricity consumption (TWh)	144.06	147.15	150.19	153.18	156.11	158.97	161.77	164.49	167.15	169.74
DH consumption (TWh)	168.08	169.52	170.96	172.41	173.85	173.93	174.00	174.08	174.16	174.23
Year	2041	2042	2043	2044	2045	2046	2047	2048	2049	2050
Population (Million)	31.67	31.58	31.49	31.40	31.29	31.18	31.06	30.93	30.79	30.64
GDP (B¥)	2758.70	2804.09	2847.93	2890.43	2931.80	2972.30	3012.22	3051.87	3091.52	3131.41
Electricity consumption (TWh)	172.28	174.78	177.25	179.70	182.15	184.60	187.09	189.62	192.20	194.88
DH consumption (TWh)	174.31	174.39	174.46	174.54	174.62	174.69	174.77	174.85	174.92	175.00



6

Conclusions

In this thesis, we set out to conduct an in-depth analysis and optimization of STES technologies employing solar heat from technical, economic, environmental, and implementation feasibility perspectives to identify their overall attractiveness in the heating market and to assess their benefits in the clean heating transition and renewable power integration. The analysis focuses on the heat transition in the built environment in China. Four research questions are raised within this work, and the answers are summarized in the following paragraphs.

6.1. The overall attractiveness of STES

The technical feasibility of STES technologies employing solar heat has been widely demonstrated. There is a need to understand their attractiveness from economic, environmental, and implementation feasibility perspectives.

Q1. What is the overall attractiveness of STES technologies compared to other sustainable heating options in terms of techno-economic-environmental performance and implementation feasibility at the local level?

This research question is addressed in Chapters 2 and 4. Chapter 2 provides a comprehensive techno-economic review analysis of STES based on 60 projects worldwide covering six STES types classified according to their storage mechanisms. Their levelized costs of heat (LCOHs) are calculated to compare the costs of different heat production technologies over their lifetime.

In addition to evaluating the global economic competitiveness by reviewing the data from existing projects in Chapter 2, Chapter 4 investigates the technical, economic, and environmental performance of seven sustainable heating technologies (including borehole storage with solar heat) and their implementation feasibility at the local level in China, under the current policy and future renewable energy scenarios. A community in Harbin, northern China, is selected as a case study to implement the proposed methodological steps and gain insight into the performance of sustainable heating technologies, as it is a representative city with a high heating demand, a coal-dominated district heating system, and an ambition to implement a clean heating transition.

From a global perspective, the LCOHs of the four sensible heat storage technologies (tank, pit, borehole, and aquifer storage) are in the range of 50–250 €/MWh, and those of the latent and thermochemical heat storage are well above 250 €/MWh. Compared to decentralized natural gas boilers and solar heating, only pit storage projects used for district heating and aquifer storage projects used for low-temperature heating are economically competitive. The LCOH of tank and borehole storage is over twice that of the references. The LCOH of latent heat storage is the highest (over four times higher than the reference). Thus, measures are required to further reduce the STES costs to promote its economic feasibility, for example,

implementing large-scale STES in existing and new district heating systems, material improvements, and better drilling and insulation methods.

In China, the research and demonstration of STES applications have mainly included tank and borehole storage, of which borehole storage is more suitable for the high population density of China. The LCOHs of borehole storage with natural gas, biomass, and electric boilers as auxiliary heating devices are in the range of 49–62 €/MWh, lower than the global level. They are expected to decrease by 2% and 7% in 2030 and 2050, respectively. Although its current acceptance by residents in China is relatively low, and it usually requires a longer investigation and period for underground construction, solar heating is a promising technology with decreasing LCOH and increasing ability to reduce CO₂ emissions (CO₂ avoidance cost (CAC) can decrease by 50% from 2020 to 2050). Biomass heating is attractive regarding cost and CO₂ emission reduction (CACs of 24–47 €/t). However, fuel availability is an issue for large-scale implementation. In addition, biomass heating faces storage and ash handling and management issues. Electric heating is preferable in terms of implementation feasibility; however, its economic competitiveness and environmental impact depend heavily on electricity prices and grid cleanliness (CACs of 120–463 €/t). It can also be a burden for constructing new power generation units and expanding existing power grid capacity for large-scale implementation.

Based on these findings, we conclude that from a global review perspective, pit and aquifer storage applications are economically competitive with decentralized natural gas boilers and solar heating. In China, borehole storage is attractive with competitive LCOH and CAC compared to other sustainable heating technologies. Its residential acceptance in China is relatively low. Still, it is a promising technology to contribute to the clean heat transition in China, with the expectation that its LCOH and CAC will decrease in the future.

6.2. STES in different climate zones

As STES of solar heat is a niche technology, it is important to investigate the specific conditions under which its application is attractive.

Q2. How do local climate conditions and existing heating infrastructure impact the technical, economic, and environmental performance of STES technologies?

Chapter 3 addresses this question by developing a comprehensive quantitative method for techno-economic-environmental performance analysis of applying STES technologies with solar heat in two northern cities (Harbin and Urumqi) and two southern locations (Shanghai and Chengdu) in China. These four cases are located in different climates and have different heating infrastructures.

From a technical perspective, the solar fraction and storage efficiency of the four case studies range between 58%–67% and 57%–69%, respectively, which are fairly similar in very

different climates. Urumqi has better solar resource potential than other locations; therefore, the STES system in Urumqi has the highest solar fraction and storage efficiency. The solar fraction in the Chengdu case is the lowest owing to the low solar irradiation in the area. In the Harbin case, both the solar fraction and the storage efficiency are the highest in the first year of operation; however, those of the other cases gradually exceed the Harbin's. It is because the borehole is preheated to 25°C, and the Harbin case has the largest borehole volume; therefore, initially, the Harbin case stores the most thermal energy. However, the high heat loss of the borehole caused by the cold climate and the high soil thermal diffusivity slows down the growth trend.

The energy flows in the Harbin case are the largest compared to the other cases since Harbin comprises the highest heating load, namely, the coldest climate. More heat is charged into the borehole in the Harbin case; however, less heat is discharged from the borehole than in the Urumqi case, which can be explained by the higher heat loss of the borehole in the Harbin case because of the larger borehole volume, higher soil thermal diffusivity, and cold climate. The energy flows of the Chengdu case are the lowest because the Chengdu case has the lowest heating load. However, the energy flow from the boiler to the load is higher in the Chengdu case than in the Shanghai case, primarily owing to the low solar irradiation in the Chengdu case; therefore, more heat from the boiler is required to meet the heat demand. Implementation in locations with higher solar irradiation and heat retention of soil can achieve higher solar fraction and storage efficiency.

From an economic point of view, the LCOHs of the four case studies are calculated with identical equipment unit prices and location-based electricity and natural gas prices. The Urumqi case achieves the lowest heating cost among the four case studies (5.4–8.7 €/ct/kWh) owing to its cheaper electricity and natural gas price than the other locations. The Chengdu case has the highest heating cost owing to its low solar irradiation. There is no significant difference in LCOH in a similar climate zone. The LCOHs of the STES systems in the four case studies are compared with their conventional heating systems. The heating cost of the STES system in Harbin is more than three times that of the coal-fired CHP. The heating cost of the STES system in Urumqi is more than twice that of the natural gas-fired CHP. The heating costs of the STES systems in Shanghai and Chengdu are more than twice those of air conditioning systems.

From an environmental perspective, the STES system is the most attractive in Harbin to replace the conventional coal-based district heating system (72% CO₂ emission reduction). The implementation of the STES system in the other three locations also has a large potential to reduce CO₂ emissions (52%–56%), among which the Urumqi case reduces the least CO₂ emissions, primarily because natural gas dominates the existing district heating system. The CAC of the four case studies ranges between 114–368 €/t. Harbin achieves the lowest CAC because the conventional heating option is coal-fired CHP. Chengdu has the highest CAC due to its weak solar resources.

So, we conclude that the prospects for STES of solar heat vary across China. In northern China, the implementation of STES technologies can increase the renewable energy penetration in fossil fuel-based district heating at a low CAC. In southern China, where electric heating dominates, electricity system decarbonization is a more cost-effective route to heat decarbonization than STES technologies. STES implementation is attractive in locations with rich solar resources, high heating loads, and current coal-based heating systems.

6.3. Techno-economic optimization of STES

In terms of methods for STES system optimization, there is a need for a better understanding of the optimal economic and environmental performance of STES applications and the conditions to achieve it in different climate zones.

Q3. What are the key technical parameters and their influence on achieving the optimal techno-economic-environmental performance of STES technologies in different climate zones?

In Chapter 3, we consider this question by identifying the key technical parameters for achieving optimal techno-economic-environmental performance and determining the configuration planning of STES in different climate zones.

A parametric study is conducted to investigate the impact of system configurations on the technical, economic, and environmental performance of the STES system and to provide evidence for optimization. A larger solar collector area and short-term storage tank volume help increase the solar fraction and reduce CO₂ emissions to a greater extent. A turning point is found in the LCOH trend, indicating the importance of selecting an appropriate size to achieve the lowest LCOH. A larger borehole number can cause an increase in LCOH, while a turning point is found in the solar fraction and CO₂ emissions trends. Since the borehole number is less influential on the solar fraction but has a larger impact on the LCOH, it is possible to reduce it to achieve a lower LCOH. The parametric study highlights that the solar collector area has a more significant impact on the solar fraction and CO₂ emission reduction, and the borehole number has a greater influence on the LCOH, while the short-term storage tank is less influential than these two parameters.

A multi-objective optimization is performed using minimum LCOH and minimum CO₂ emissions as objective functions, with economic feasibility and environmental impact considered as two crucial factors. The solar collector area and borehole number are selected as optimization variables. An integrated optimization criterion (CAC) is proposed by including economic and environmental impacts to select the optimal solution from the Pareto front. The key technical parameters for achieving optimal techno-economic-environmental performance and determining the configuration planning of STES in different climate zones are identified by comparing the optimal configuration with the original design. The borehole

number for the STES system in cold climate zones should be reduced to achieve higher storage efficiency and lower LCOH, and the solar collector area in warm climate zones should be increased to achieve higher solar fraction and greater CO₂ emission reduction.

Therefore, we conclude that solar collector area and borehole number are the most influential variables in system configurations. By tuning the borehole number and the solar collector area of the STES system to local climates, low carbon abatement costs can be achieved for a wide range of conditions.

6.4. Energy system impact of STES

Extending the scope of individual projects to the energy system level, we would like to understand the economic and environmental consequences of replacing district heating systems with STES technologies on a regional scale and its impact on renewable power integration.

Q4. What are the technical feasibility and economic and environmental consequences of replacing the district heating system with STES technologies and its impact on renewable power integration?

Chapter 5 looks into this by evaluating the technical feasibility and economic and environmental consequences of replacing district heating systems with STES technologies with solar heat, as well as the impact on renewable power integration. This chapter quantifies the impact of large-scale STES applications on the power and district heating sectors of a regional energy system by applying two future scenarios. Low-rise and high-rise communities are selected as examples to simulate heat demand and investigate the feasibility of implementing STES as a replacement for conventional district heating systems. STES of solar heat can meet 100% and 50% of the heat demand for low- and high-rise residential communities, respectively. An auxiliary heating device (heat pump) is needed to meet the remaining heat demand of high-rise communities.

The economic and environmental consequences of gradually replacing district heating with STES technologies in a regional power and district heating system in 2030 and 2050 scenarios are evaluated until 100% replacement is achieved. The extent to which STES technologies can increase renewable energy penetration in the power system is quantified. The replacement reduces the fossil fuel consumption of the district heating system, whereas it increases that of the power sector. As the share of STES in district heating increases, the CACs increase because the benefit of renewable power integration decreases. The marginal CO₂ emission reduction decreases.

In the 2030 scenario, a 41% reduction in fossil fuel consumption, a 25% increase in total annual cost, and a 39% reduction in CO₂ emissions are observed with a 100% replacement of the district heating system by STES. The CAC is calculated as approximately 60 €/t and

is linearly correlated with the STES share in the district heating. The wind and solar power curtailments are reduced by 10% and 50%, respectively. Additional wind power integration occurs mainly in winter, which is the high-wind speed period, indicating that STES in district heating has considerable potential to increase the degree of wind power generation integration.

In 2050, a 100% share of STES leads to a 50% reduction in fossil fuel consumption, a 17% increase in total annual cost, and a 41% reduction in CO₂ emissions. A CAC of well below 50 €/t is obtained. The wind and solar power curtailments are reduced by 18% and 24%, respectively. With more renewable power generation in the power structure, more benefits can be obtained by replacing district heating with STES.

Based on the above findings, we conclude that replacing fossil fuel-based district heating systems with STES technologies can reduce fossil fuel consumption and CO₂ emissions across the combined heat and power systems at an affordable cost. It facilitates the integration of wind and solar power into power grids by reducing curtailment. As more solar and wind power is added to the grid, the benefits of such substitution increase.

6.5. General conclusions and policy implications

The generation conclusions and policy recommendations are drawn from the previous chapters.

STES of solar heat offers an attractive option for realizing a sustainable heating transition when specific conditions are met. It should be evaluated in the context of their intended use, which requires a comprehensive assessment of the technical, economic, and environmental performance and their implementation feasibility at the local level.

Chapter 3 examines the STES implementation in four locations in China with different climate conditions and existing heating infrastructure and shows that the local context significantly impacts the optimal configuration planning, techno-economic-environmental performance, and feasibility of the STES application. STES of solar heat is preferred for northern China, which has abundant solar resources, high heat loads, and fossil fuel-based district heating systems. Chapter 4 evaluates the implementation of STES of solar heat with respect to current policies and future renewable energy scenarios and shows that local energy system planning policies influence the selection of sustainable heating technologies. Therefore, local energy system planning policies and local renewable energy potentials should be fully considered when planning the implementation of sustainable heating technologies. The feasibility assessment should be conducted by thoroughly considering the current energy system situation, resource availability, and local government incentives to promote the use of clean energy.

STES technologies employing solar heat are attractive in line with the carbon-neutral target. With China's ambition to rapidly develop wind and solar power generation, the

benefits of replacing fossil fuel-based district heating systems with STES of solar heat are increasing. Chapter 5 shows that with 100% replacement of district heating by STES, fossil fuel consumption and CO₂ emissions can be reduced by approximately 45% and 40% in 2030 and 2050, respectively, with a 20% increase in the total annual cost. The CAC is predicted to be approximately 60 €/t in 2030 and well below 50 €/t in 2050. Replacing district heating with STES in the 2050 scenario with a higher renewable power generation penetration in the power sector can deliver 6% more benefits in reducing fossil fuel consumption and CO₂ emissions than in 2030, with an 8% lower cost increase. China has shown ambition to rapidly develop wind and solar power generation after committing to peak CO₂ emissions before 2030 and achieve carbon neutrality before 2060. In this context, replacing the district heating system with STES can reduce fossil fuel consumption and CO₂ emissions to a greater extent and allow more renewable power integration at a lower cost increase. In addition, renewable power generation penetration (especially wind and solar) has increased substantially, increasing curtailment in many regions. Replacing fossil fuel-based district heating systems with STES employing solar heat with heat pumps as auxiliary heating devices STES can reduce renewable power curtailment by 10%–20%. The current CO₂ price in China is more than ten times lower than that in developed countries. A higher CO₂ price can encourage more wind and solar power to penetrate the power structure. STES applications can become more attractive with the expectation of reducing the CAC.

To formulate appropriate clean heating strategies, local governments need to comprehensively adopt various sustainable heating technologies based on local resource endowments and infrastructure, with scientific evaluation and full consideration of residents' consumption levels. For a long time, northern China has lacked comprehensive planning of heating supply in different energy forms, resulting in insufficient heat supply and demand balance and unscientific heating design. Chapter 4 conducts an integrated assessment of seven sustainable heating technologies, considering the technical, economic, and environmental performance, as well as the feasibility of implementation, using a community in northern China as a case study under the current policy and future renewable energy scenarios. It provides solid evidence to facilitate the decision-making process in the clean heating transition in northern cities of China. The clean heating transition is a systematic project. Local governments are required to coordinate the heat supply and demand balance and comprehensively adopt various clean heating methods to reduce emissions in the heating field.

The prices of heat, natural gas, and electricity should allow for market-based adjustment rather than all being subject to uniform pricing by local governments. District heating is part of the social welfare system in China. It is priced based on room area and does not compete with other space heating services in the heating market, which hinders the adoption of sustainable heating technologies. Customers have to pay two to three times more for STES technologies than for district heating. From the policy incentive perspective, although the government has announced a subsidy to promote the use of sustainable heating

technologies, which can reduce the cost by more than 10%–20%, market reforms of heat prices should be implemented, and more aggressive incentive policies for sustainable heating technologies can be proposed. Local governments should adopt supportive policies to reduce the cost of electricity-dominated heating methods, including improving the peak-valley time-of-use pricing system, optimizing the tiered pricing policy for residential electricity consumption, and expanding market-based transactions. In addition, natural gas heating costs can be reduced by improving the tiered pricing system, implementing seasonal price differentiation policies, and using market-based trading mechanisms. The price of clean heating should be reasonably set within the affordability range for residents, taking into account the renovation and operating costs of clean heating.

6.6. Recommendations for further research

The work presented in this thesis can be improved and extended in numerous ways. Methodological limitations and follow-up topics are discussed in the following paragraphs.

Regarding the methodological limitations of this work, the review analysis in Chapter 2 is based on the selected and examined studies. Some representative projects are not included because they lack transparency in techno-economic parameters, which may lead to incomplete review results. The development of STES technologies has been extensively studied and reviewed from a technical perspective. However, economic studies of STES technologies are limited in number and often lack transparency in their reporting. More transparency is needed for future studies to provide a solid basis for techno-economic analysis and to accurately position STES technologies in the heating market.

Typical meteorological year data is used to predict heat demand, ignoring the influence of extreme weather that may affect the performance of STES technologies. Nonetheless, the unprecedented meteorological events due to climate change, such as extreme temperature and precipitation, may reduce the performance of the STES system and lead to infrastructure damage. In future studies, the impact of climate change and extreme weather should be analyzed.

There are underlying assumptions in numerical simulation that affect the accuracy of the model. For example, numerical simulation does not accurately describe tank stratification and groundwater flow, which negatively affects the technical, economic, and environmental performance of STES technologies. The heat transfer mechanism and temperature field distribution in the storage tank and borehole need to be determined experimentally. Several questions remain to be answered, including how groundwater flow affects heat transfer between boreholes and the surrounding soil and how the temperature rise of the soil affects the groundwater.

Domestic hot water is excluded from this study because there is no central hot water supply in the conventional system in China. Residents usually use an electric water heater to provide

hot water. However, adding domestic hot water can have a positive impact on solar energy integration and cost reduction. It is suggested to be included in future sustainable heating systems. The combination of space heating and domestic hot water is worth promoting in China.

In Chapter 5, we examine the feasibility of implementing STES of solar heat as a replacement for conventional district heating systems using low-rise and high-rise residential communities as examples. These two building types are good representatives but cannot cover the full diversity of buildings. Evaluating the feasibility of implementing STES in commercial buildings requires in-depth geographic information system-based analysis. In addition to urban district heating, STES of solar heat can be an option to replace individual heating in rural areas. Different application scenarios can be analyzed in future studies.

This work also raises several interesting topics that can be pursued as a follow-up. Chapter 4 develops a framework to evaluate the techno-economic-environmental performance and implementation feasibility of several sustainable heating technologies according to local renewable energy resources and clean heating plans. The integrated assessment method developed in this study comprehensively considers the technical, economic, environmental, and implementation feasibility perspectives with respect to current policies and future renewable energy scenarios. It can be used for case studies in other countries with similar climate conditions and an objective of clean heat transition. Other sustainable heating technologies, including the use of geothermal and industrial waste heat for heating, can be assessed within this framework in future studies to provide comprehensive evidence to facilitate policymaker's decision-making on the clean heating transition.

Solar thermal energy plays a dominant role as a heat source in current STES systems. Depending on local conditions, diverse heat supply options (e.g., industrial waste heat, geothermal energy, and waste heat from cogeneration units outside the heating season) can be implemented in STES systems. As for the selection of auxiliary heat sources, gas boilers, heat pumps, and electric heaters can be applied, considering local availability and prices. In addition to its function as a heat supply unit, STES technologies can be integrated with heat pumps, taking advantage of low-temperature heat sources in summer and resulting in a high coefficient of performance of heat pumps. Coupling with power-to-heat technologies can increase the use of renewable power sources and provide electrical network balancing.

BIBLIOGRAPHY

- [1] IPCC. Climate Change 2023: Synthesis Report Summary for Policymakers. 2023.
- [2] IPCC. Climate Change 2021: The Physical Science Basis: Working Group I Contribution to the Sixth Assessment Report of the Intergovernmental Panel on Climate Change. Cambridge: Cambridge University Press; 2023.
- [3] IEA. Greenhouse Gas Emissions from Energy Data Explorer, <https://www.iea.org/data-and-statistics/data-tools/greenhouse-gas-emissions-from-energy-data-explorer>; 2021 [accessed 20 July 2023].
- [4] UNFCCC. Paris Agreement. 2015. https://unfccc.int/sites/default/files/english_paris_agreement.pdf.
- [5] IEA. Energy Statistics Data Browser, <https://www.iea.org/data-and-statistics/data-tools/energy-statistics-data-browser>; 2022 [accessed 20 July 2023].
- [6] IEA. Heating, <https://www.iea.org/energy-system/buildings/heating>; 2023 [accessed 20 July 2023].
- [7] Statista. Primary energy consumption worldwide in 2021, by country, <https://www.statista.com/statistics/263455/primary-energy-consumption-of-selected-countries/>; 2022 [accessed 20 July 2023].
- [8] Statista. Distribution of carbon dioxide emissions worldwide in 2021, by select country, <https://www.statista.com/statistics/271748/the-largest-emitters-of-co2-in-the-world/>; 2022 [accessed 20 July 2023].
- [9] IEA. An energy sector roadmap to carbon neutrality in China. 2021. <https://www.iea.org/reports/an-energy-sector-roadmap-to-carbon-neutrality-in-china>.
- [10] Zhang S, Chen W. Assessing the energy transition in China towards carbon neutrality with a probabilistic framework. Nat Commun 2022;13(1):87. <https://doi.org/10.1038/s41467-021-27671-0>.
- [11] Our World in Data. Carbon intensity of energy production, <https://ourworldindata.org/grapher/co2-per-unit-energy?facet=entity>; 2023 [accessed 20 July 2023].
- [12] National Energy Administration. 14th Five-Year Plans on Renewable Energy Development. 2022.
- [13] National Development and Reform Commission. Energy Production and Consumption Revolution Strategy (2016–2030). 2019. https://www.ndrc.gov.cn/xxgk/zcfb/tz/201704/t20170425_962953.html.
- [14] Ministry of Housing and Urban-Rural Development of the People's Republic of China. Thermal design code for civil building (GB 50176-2016). Beijing: China Architecture & Building Press; 2016.
- [15] Ministry of Housing and Urban-Rural Development of the People's Republic of China. China urban-rural construction statistical yearbook. Beijing: China Statistics Press; 2022.
- [16] Wang J, Zhou Z, Zhao J, Zheng J, Guan Z. Towards a cleaner domestic heating sector in China: Current situations, implementation strategies, and supporting measures. Appl Therm Eng 2019;152:515-31. <https://doi.org/10.1016/j.applthermaleng.2019.02.117>.
- [17] Su C, Madani H, Palm B. Heating solutions for residential buildings in China: Current status and future outlook. Energy Convers Manag 2018;177:493-510. <https://doi.org/10.1016/j.enconman.2018.10.005>.
- [18] IEA. District Heating, <https://www.iea.org/reports/district-heating>; 2022 [accessed 19 March 2023].

BIBLIOGRAPHY

- [19] National Bureau of Statistics of China. National data, <https://data.stats.gov.cn/>; 2021 [accessed 8 April 2021].
- [20] Lin B, Lin J. Evaluating energy conservation in China's heating industry. *J Clean Prod* 2017;142:501-12. <https://doi.org/10.1016/j.jclepro.2016.06.195>.
- [21] National Development and Reform Commission. Clean winter heating plan in northern China (2017-2021), https://www.ndrc.gov.cn/xxgk/zcfb/tz/201712/t20171220_962623.html; 2017 [accessed 18 February 2022].
- [22] Yang T, Liu W, Kramer GJ. Integrated assessment on the implementation of sustainable heat technologies in the built environment in Harbin, China. *Energy Convers Manag* 2023;279:116764. <https://doi.org/10.1016/j.enconman.2023.116764>.
- [23] Zhao X-g, Wan G. Current situation and prospect of China's geothermal resources. *Renew Sustain Energy Rev* 2014;32:651-61. <https://doi.org/10.1016/j.rser.2014.01.057>.
- [24] Wang S, Yan J, Li F, Hu J, Li K. Exploitation and utilization of oilfield geothermal resources in China. *Energies* 2016;9(10):798.
- [25] Lin Y, Chong CH, Ma L, Li Z, Ni W. Quantification of waste heat potential in China: A top-down Societal Waste Heat Accounting Model. *Energy* 2022;261:125194. <https://doi.org/10.1016/j.energy.2022.125194>.
- [26] Fu L, Li Y, Wu Y, Wang X, Jiang Y. Low carbon district heating in China in 2025- a district heating mode with low grade waste heat as heat source. *Energy* 2021;230:120765. <https://doi.org/10.1016/j.energy.2021.120765>.
- [27] Kang Y, Yang Q, Bartocci P, Wei H, Liu SS, Wu Z, et al. Bioenergy in China: Evaluation of domestic biomass resources and the associated greenhouse gas mitigation potentials. *Renew Sustain Energy Rev* 2020;127:109842. <https://doi.org/10.1016/j.rser.2020.109842>.
- [28] National Bureau of Statistics of China. China energy statistical yearbook 2021. Beijing, China: China Statistics Press; 2022.
- [29] Østergaard PA, Jantzen J, Marczinkowski HM, Kristensen M. Business and socioeconomic assessment of introducing heat pumps with heat storage in small-scale district heating systems. *Renew Energy* 2019;139:904-14. <https://doi.org/10.1016/j.renene.2019.02.140>.
- [30] Mathiesen BV, Lund H, Connolly D. Limiting biomass consumption for heating in 100% renewable energy systems. *Energy* 2012;48(1):160-8. <https://doi.org/10.1016/j.energy.2012.07.063>.
- [31] Kwon PS, Østergaard PA. Priority order in using biomass resources – Energy systems analyses of future scenarios for Denmark. *Energy* 2013;63:86-94. <https://doi.org/10.1016/j.energy.2013.10.005>.
- [32] Solargis. Solar resource maps of China, <https://solargis.com/maps-and-gis-data/download/china>; 2019 [accessed 8 April 2021].
- [33] Liu W, Lund H, Mathiesen BV, Zhang X. Potential of renewable energy systems in China. *Appl Energy* 2011;88(2):518-25. <https://doi.org/10.1016/j.apenergy.2010.07.014>.
- [34] Huang J, Fan J, Furbo S. Feasibility study on solar district heating in China. *Renew Sustain Energy Rev* 2019;108:53-64. <https://doi.org/10.1016/j.rser.2019.03.014>.
- [35] Yang T, Liu W, Kramer GJ, Sun Q. State of the art review of seasonal sensible heat storage. *Energy Proc* 2019;5:4255. <https://doi.org/10.46855/energy-proceedings-4255>.
- [36] Narula K, De Oliveira Filho F, Chambers J, Romano E, Hollmuller P, Patel MK. Assessment of techno-economic feasibility of centralised seasonal thermal energy storage for decarbonising the Swiss residential heating sector. *Renew Energy* 2020;161:1209-25. <https://doi.org/10.1016/j.renene.2020.06.099>.

- [37] Maragna C, Rey C, Perreux M. A novel and versatile solar Borehole Thermal Energy Storage assisted by a Heat Pump. Part 1: System description. *Renew Energy* 2023;208:709-25. <https://doi.org/10.1016/j.renene.2023.03.105>.
- [38] Ma Q, Fan J, Liu H. Energy pile-based ground source heat pump system with seasonal solar energy storage. *Renew Energy* 2023;206:1132-46. <https://doi.org/10.1016/j.renene.2023.02.116>.
- [39] Ushamah HM, Ahmed N, Elfeky KE, Mahmood M, Qaisrani MA, Waqas A, et al. Techno-economic analysis of a hybrid district heating with borehole thermal storage for various solar collectors and climate zones in Pakistan. *Renew Energy* 2022;199:1639-56. <https://doi.org/10.1016/j.renene.2022.09.059>.
- [40] Wong B, Mesquita L. Drake landing solar community: Financial summary and lessons learned. *Proceedings of the ISES Solar World Congress 2019*; 2019 Nov 4-7; Santiago, Chile; 2019. p. 482-93.
- [41] Reed AL, Novelli AP, Doran KL, Ge S, Lu N, McCartney JS. Solar district heating with underground thermal energy storage: Pathways to commercial viability in North America. *Renew Energy* 2018;126:1-13. <https://doi.org/10.1016/j.renene.2018.03.019>.
- [42] Chu S, Sethuvenkatraman S, Goldsworthy M, Yuan G. Techno-economic assessment of solar assisted precinct level heating systems with seasonal heat storage for Australian cities. *Renew Energy* 2022;201:841-53. <https://doi.org/10.1016/j.renene.2022.11.011>.
- [43] Shah SK, Aye L, Rismanchi B. Validations of a double U-tube borehole model and a seasonal solar thermal energy storage system model. *Renew Energy* 2022;201:462-85. <https://doi.org/10.1016/j.renene.2022.10.109>.
- [44] Antoniadis CN, Martinopoulos G. Optimization of a building integrated solar thermal system with seasonal storage using TRNSYS. *Renew Energy* 2019;56-66. <https://doi.org/10.1016/j.renene.2018.03.074>.
- [45] Zhang L, Xu P, Mao J, Tang X, Li Z, Shi J. A low cost seasonal solar soil heat storage system for greenhouse heating: Design and pilot study. *Appl Energy* 2015;156:213-22. <https://doi.org/10.1016/j.apenergy.2015.07.036>.
- [46] Bahlawan H, Losi E, Manservigi L, Morini M, Pinelli M, Spina PR, et al. Optimization of a renewable energy plant with seasonal energy storage for the transition towards 100% renewable energy supply. *Renew Energy* 2022;198:1296-306. <https://doi.org/10.1016/j.renene.2022.08.126>.
- [47] Xu L, Torrens JI, Guo F, Yang X, Hensen JLM. Application of large underground seasonal thermal energy storage in district heating system: A model-based energy performance assessment of a pilot system in Chifeng, China. *Appl Therm Eng* 2018;137:319-28. <https://doi.org/10.1016/j.applthermaleng.2018.03.047>.
- [48] Huang J, Fan J, Furbo S. Demonstration and optimization of a solar district heating system with ground source heat pumps. *Sol Energy* 2020;202:171-89. <https://doi.org/10.1016/j.solener.2020.03.097>.
- [49] Launay S, Kadoch B, Le Métayer O, Parrado C. Analysis strategy for multi-criteria optimization: Application to inter-seasonal solar heat storage for residential building needs. *Energy* 2019;171:419-34. <https://doi.org/10.1016/j.energy.2018.12.181>.
- [50] Fiorentini M, Heer P, Baldini L. Design optimization of a district heating and cooling system with a borehole seasonal thermal energy storage. *Energy* 2023;262:125464. <https://doi.org/10.1016/j.energy.2022.125464>.
- [51] Yuan X, Heikari L, Hirvonen J, Liang Y, Virtanen M, Kosonen R, et al. System modelling and optimization of a low temperature local hybrid energy system based on solar energy for a residential district. *Energy Convers Manag* 2022;267:115918. <https://doi.org/10.1016/j.enconman.2022.115918>.

BIBLIOGRAPHY

- [52] Shah SK, Aye L, Rismanchi B. Multi-objective optimisation of a seasonal solar thermal energy storage system for space heating in cold climate. *Appl Energy* 2020;268. <https://doi.org/10.1016/j.apenergy.2020.115047>.
- [53] EU. Directive 2010/31/EU of the European Parliament and of the Council of 19 May 2010 on the energy performance of buildings (recast). *Off J Eur Union* 2010;153:13-35.
- [54] Amasyali K, El-Gohary NM. A review of data-driven building energy consumption prediction studies. *Renew Sustain Energy Rev* 2018;81:1192-205. <https://doi.org/10.1016/j.rser.2017.04.095>.
- [55] IEA. Transition to Sustainable Buildings: Strategies and Opportunities to 2050. Paris: CORLET; 2013.
- [56] IEA. World Energy Outlook 2019. 2019. <https://www.iea.org/reports/world-energy-outlook-2019>.
- [57] Hesaraki A, Holmberg S, Haghighat F. Seasonal thermal energy storage with heat pumps and low temperatures in building projects—A comparative review. *Renew Sustain Energy Rev* 2015;43:1199-213. <https://doi.org/10.1016/j.rser.2014.12.002>.
- [58] de Gracia A, Cabeza LF. Phase change materials and thermal energy storage for buildings. *Energy Build* 2015;103:414-9. <https://doi.org/10.1016/j.enbuild.2015.06.007>.
- [59] Xu J, Wang RZ, Li Y. A review of available technologies for seasonal thermal energy storage. *Sol Energy* 2014;103:610-38. <https://doi.org/10.1016/j.solener.2013.06.006>.
- [60] Guelpa E, Verda V. Thermal energy storage in district heating and cooling systems: A review. *Appl Energy* 2019;252:113474. <https://doi.org/10.1016/j.apenergy.2019.113474>.
- [61] Department for Business, Energy & Industrial Strategy. Evidence gathering: thermal energy storage (TES) technologies. 2016. https://assets.publishing.service.gov.uk/government/uploads/system/uploads/attachment_data/file/545249/DELTA_EE_DECC_TES_Final_1_.pdf [accessed 14 May 2019].
- [62] Tian Z, Zhang S, Deng J, Fan J, Huang J, Kong W, et al. Large-scale solar district heating plants in Danish smart thermal grid: Developments and recent trends. *Energy Convers Manag* 2019;189:67-80. <https://doi.org/10.1016/j.enconman.2019.03.071>.
- [63] Schmidt T, Mangold D, Müller-Steinhagen H. Central solar heating plants with seasonal storage in Germany. *Sol Energy* 2004;76(1):165-74. <https://doi.org/10.1016/j.solener.2003.07.025>.
- [64] Schmidt T, Pauschinger T, Sørensen PA, Snijders A, Djebbar R, Boulter R, et al. Design Aspects for Large-scale Pit and Aquifer Thermal Energy Storage for District Heating and Cooling. *Energy Procedia* 2018;149:585-94. <https://doi.org/10.1016/j.egypro.2018.08.223>.
- [65] Shah SK, Aye L, Rismanchi B. Seasonal thermal energy storage system for cold climate zones: A review of recent developments. *Renew Sustain Energy Rev* 2018;97:38-49. <https://doi.org/10.1016/j.rser.2018.08.025>.
- [66] Dahash A, Ochs F, Janetti MB, Streicher W. Advances in seasonal thermal energy storage for solar district heating applications: A critical review on large-scale hot-water tank and pit thermal energy storage systems. *Appl Energy* 2019;239:296-315. <https://doi.org/10.1016/j.apenergy.2019.01.189>.
- [67] Bott C, Dressel I, Bayer P. State-of-technology review of water-based closed seasonal thermal energy storage systems. *Renew Sustain Energy Rev* 2019;113:109241. [10.1016/j.rser.2019.06.048](https://doi.org/10.1016/j.rser.2019.06.048).
- [68] Sharif MKA, Al-Abidi AA, Mat S, Sopian K, Ruslan MH, Sulaiman MY, et al. Review of the application of phase change material for heating and domestic hot water systems. *Renew Sustain Energy Rev* 2015;42:557-68. <https://doi.org/10.1016/j.rser.2014.09.034>.

- [69] Zhou D, Zhao CY, Tian Y. Review on thermal energy storage with phase change materials (PCMs) in building applications. *Appl Energy* 2012;92:593-605. <https://doi.org/10.1016/j.apenergy.2011.08.025>.
- [70] Kenisarin M, Mahkamov K. Solar energy storage using phase change materials. *Renew Sustain Energy Rev* 2007;11(9):1913-65. <https://doi.org/10.1016/j.rser.2006.05.005>.
- [71] Fleuchaus P, Godschalk B, Stober I, Blum P. Worldwide application of aquifer thermal energy storage – A review. *Renew Sustain Energy Rev* 2018;94:861-76. <https://doi.org/10.1016/j.rser.2018.06.057>.
- [72] Krese G, Koželj R, Butala V, Stritih U. Thermochemical seasonal solar energy storage for heating and cooling of buildings. *Energy Build* 2018;164:239-53. <https://doi.org/10.1016/j.enbuild.2017.12.057>.
- [73] Li G. Sensible heat thermal storage energy and exergy performance evaluations. *Renew Sustain Energy Rev* 2016;53:897-923. <https://doi.org/10.1016/j.rser.2015.09.006>.
- [74] Scapino L, Zondag HA, Van Bael J, Diriken J, Rindt CCM. Energy density and storage capacity cost comparison of conceptual solid and liquid sorption seasonal heat storage systems for low-temperature space heating. *Renew Sustain Energy Rev* 2017;76:1314-31. <https://doi.org/10.1016/j.rser.2017.03.101>.
- [75] Böhm H, Lindorfer J. Techno-economic assessment of seasonal heat storage in district heating with thermochemical materials. *Energy* 2019;179:1246-64. <https://doi.org/10.1016/j.energy.2019.04.177>.
- [76] Huang J, Fan J, Furbo S, Chen D, Dai Y, Kong W. Economic analysis and optimization of combined solar district heating technologies and systems. *Energy* 2019;186:1-16. <https://doi.org/10.1016/j.energy.2019.115886>.
- [77] Bokhoven TP, Van Dam J, Kratz P. Recent experience with large solar thermal systems in the Netherlands. *Sol Energy* 2001;71(5):347-52. [https://doi.org/10.1016/S0038-092X\(00\)00124-9](https://doi.org/10.1016/S0038-092X(00)00124-9).
- [78] Bauer D, Marx R, Nußbicker-Lux J, Ochs F, Heidemann W, Müller-Steinhagen H. German central solar heating plants with seasonal heat storage. *Sol Energy* 2010;84(4):612-23. <https://doi.org/10.1016/j.solener.2009.05.013>.
- [79] Mangold D, Schmidt T, Dohna A. Das Wissensportal für die saisonale Wärmespeicherung, <http://www.saisonalspeicher.de/Projekte/ProjekteinDeutschland/tabid/91/Default.aspx>; 2014 [accessed 14 May 2019].
- [80] Keil C, Plura S, Radspieler M, Schweigler C. Application of customized absorption heat pumps for utilization of low-grade heat sources. *Appl Therm Eng* 2008;28(16):2070-6. <https://doi.org/10.1016/j.applthermaleng.2008.04.012>.
- [81] Yumrutaş R, Ünsal M. Energy analysis and modeling of a solar assisted house heating system with a heat pump and an underground energy storage tank. *Sol Energy* 2012;86(3):983-93. <https://doi.org/10.1016/j.solener.2012.01.008>.
- [82] Hesarakı A, Halilovic A, Holmberg S. Low-temperature heat emission combined with seasonal thermal storage and heat pump. *Sol Energy* 2015;119:122-33. <https://doi.org/10.1016/j.solener.2015.06.046>.
- [83] Furbo S, Dragsted J. Reference system, Denmark solar domestic hot water system for single-family house. 2017. <http://task54.iea-shc.org/Data/Sites/1/publications/A12-Info-Sheet--Ref-SF-SDHW-System--Denmark.pdf> [accessed 14 May 2019].
- [84] Mugnier D. Reference single family solar domestic hot water system for France. 2017. <http://task54.iea-shc.org/Data/Sites/1/publications/A17-Info-Sheet--Ref-SF-SDHW--France.pdf> [accessed 14 May 2019].

BIBLIOGRAPHY

- [85] Mugnier D. Reference system, France drain-back multi-family solar domestic hot water system. 2017. <http://task54.iea-shc.org/Data/Sites/1/publications/A16-Info-Sheet--Ref-MF-Drainback-SDHW--France.pdf> [accessed 14 May 2019].
- [86] Kim M-H, Kim D, Heo J, Lee D-W. Techno-economic analysis of hybrid renewable energy system with solar district heating for net zero energy community. *Energy* 2019;187:1-19. <https://doi.org/10.1016/j.energy.2019.115916>.
- [87] Ecovat. Ecovat Seasonal Thermal Energy Storage, <https://www.ecovat.eu/>; 2020 [accessed 10 April 2020].
- [88] Hahne E. The ITW solar heating system: an oldtimer fully in action. *Sol Energy* 2000;69(6):469-93. [https://doi.org/10.1016/S0038-092X\(00\)00115-8](https://doi.org/10.1016/S0038-092X(00)00115-8).
- [89] Ellehaug K, Pedersen T. Solar heat storages in district heating networks. 2007. http://www.buildvision.dk/pdf/nordby_maarup_varmevaerk.pdf [accessed 14 May 2019].
- [90] Heller A. 15 Years of R&D in central solar heating in Denmark. *Sol Energy* 2000;69(6):437-47. [https://doi.org/10.1016/S0038-092X\(00\)00118-3](https://doi.org/10.1016/S0038-092X(00)00118-3).
- [91] Ochs F, Nußbicker-Lux J, Marx R, Koch H, Heidemann W, Müller-Steinhagen H. Solar assisted district heating system with seasonal thermal energy storage in Eggenstein-Leopoldshafen. Proceedings of the EuroSun 2008; 2008 Oct 8-10; Lisboa, Portugal; 2008.
- [92] Dominković DF, Čosić B, Bačelić Medić Z, Duić N. A hybrid optimization model of biomass trigeneration system combined with pit thermal energy storage. *Energy Convers Manag* 2015;104:90-9. <https://doi.org/10.1016/j.enconman.2015.03.056>.
- [93] Kjaergaard L, Jensen NA, Fjernvarme M. Innovative, multi-applicable-cost efficient hybrid solar (55%) and biomass energy (45%) large scale (district) heating system with long term heat storage and organic Rankine cycle electricity production. 2014. https://www.euroheat.org/wp-content/uploads/2016/04/SUNSTORE4_Report.pdf [accessed 14 May 2019].
- [94] PlanEnergi. SUNSTORE 3, Phase 2 and SUNSTORE 3, Additional application. 2015. https://energiteknologi.dk/sites/energiteknologi.dk/files/slutrappporter/sunstore_3_-_final_report_id_480800.pdf [accessed 14 May 2019].
- [95] Schmidt T, Nußbicker J, Raab S. Monitoring results from German central solar heating plants with seasonal storage. Proceedings of the ISES Solar World Congress 2005; 2005 Aug 6-12; Orlando, USA; 2005. p. 1555-60.
- [96] Nordell B, Hellström G. High temperature solar heated seasonal storage system for low temperature heating of buildings. *Sol Energy* 2000;69(6):511-23. [https://doi.org/10.1016/S0038-092X\(00\)00120-1](https://doi.org/10.1016/S0038-092X(00)00120-1).
- [97] Mesquita L, McClenahan D, Thornton J, Carriere J, Wong B. Drake landing solar community: 10 years of operation. Proceedings of the ISES Solar World Congress 2017; 2017 Oct 29-Nov 2; Abu Dhabi, UAE; 2017. p. 333-44.
- [98] Wang X, Zheng M, Zhang W, Zhang S, Yang T. Experimental study of a solar-assisted ground-coupled heat pump system with solar seasonal thermal storage in severe cold areas. *Energy Build* 2010;42(11):2104-10. <https://doi.org/10.1016/j.enbuild.2010.06.022>.
- [99] Nordell B, Andersson O, Rydell L, Scorpo AL. Long-term performance of the HT-BTES in Emmaboda, Sweden. Proceedings of the Greenstock 2015: International Conference on Underground Thermal Energy Storage; 2015.
- [100] Xu J, Li Y, Wang RZ, Liu W. Performance investigation of a solar heating system with underground seasonal energy storage for greenhouse application. *Energy* 2014;67:63-73. <https://doi.org/10.1016/j.energy.2014.01.049>.
- [101] PlanEnergi. Boreholes in Brødstrup. 2013. <http://planenergi.dk/wp-content/uploads/2018/05/15-10496-Slutrapport-Boreholes-in-Br%C3%A6dstrup.pdf> [accessed 14 May 2019].

- [102] Zhu N, Wang J, Liu L. Performance evaluation before and after solar seasonal storage coupled with ground source heat pump. *Energy Convers Manag* 2015;103:924-33. <https://doi.org/10.1016/j.enconman.2015.07.037>.
- [103] Giordano N, Comina C, Mandrone G, Cagni A. Borehole thermal energy storage (BTES). First results from the injection phase of a living lab in Torino (NW Italy). *Renew Energy* 2016;86:993-1008. <https://doi.org/10.1016/j.renene.2015.08.052>.
- [104] Lizana J, Ortiz C, Soltero VM, Chacartegui R. District heating systems based on low-carbon energy technologies in Mediterranean areas. *Energy* 2017;120:397-416. <https://doi.org/10.1016/j.energy.2016.11.096>.
- [105] Semple L, Cariveau R, Ting DSK. A techno-economic analysis of seasonal thermal energy storage for greenhouse applications. *Energy Build* 2017;154:175-87. <https://doi.org/10.1016/j.enbuild.2017.08.065>.
- [106] Renaldi R, Friedrich D. Techno-economic analysis of a solar district heating system with seasonal thermal storage in the UK. *Appl Energy* 2019;236:388-400. <https://doi.org/10.1016/j.apenergy.2018.11.030>.
- [107] Morofsky E, Chant V, Hickling JF, LeFeuvre T. Seasonal storage of building waste heat in an aquifer. *Proceedings of the 1st EC Conference on Solar Heating*; Brussels and Luxembourg; 1984. p. 881-5.
- [108] Seibt P, Kabus F. Aquifer thermal energy storage–projects implemented in Germany. *Proceedings of the ECOSTOCK 2006: Conference on Energy Storage Technology*; Pomona, USA; 2006.
- [109] Vanhoudt D, Desmedt J, Van Bael J, Robeyn N, Hoes H. An aquifer thermal storage system in a Belgian hospital: Long-term experimental evaluation of energy and cost savings. *Energy Build* 2011;43(12):3657-65. <https://doi.org/10.1016/j.enbuild.2011.09.040>.
- [110] Schmidt T, Müller-Steinhagen H. The central solar heating plant with aquifer thermal energy store in Rostock-results after four years of operation. *Proceedings of the 5th ISES Europe Solar Conference*; 2004 Jun 20-23; Freiburg, Germany; 2004.
- [111] Kabus F, Wolfgramm M, Seibt A, Richlak U, Beuster H. Aquifer thermal energy storage in Neubrandenburg–monitoring throughout three years of regular operation. *Proceedings of the 11th International Conference on Energy Storage–EffStock*; Stockholm, Sweden; 2009.
- [112] Turgut B, Paksoy H, Bozdog S, Evliya H, Abak K, Dasgan H. Aquifer thermal energy storage application in greenhouse climatization. *Proceedings of the 10th International Conference on Thermal Energy Storage*; Stockton, USA; 2006.
- [113] Ghaebi H, Bahadori MN, Saidi MH. Performance analysis and parametric study of thermal energy storage in an aquifer coupled with a heat pump and solar collectors, for a residential complex in Tehran, Iran. *Appl Therm Eng* 2014;62(1):156-70. <https://doi.org/10.1016/j.applthermaleng.2013.09.037>.
- [114] Wesselink M, Liu W, Koornneef J, van den Broek M. Conceptual market potential framework of high temperature aquifer thermal energy storage - A case study in the Netherlands. *Energy* 2018;147:477-89. <https://doi.org/10.1016/j.energy.2018.01.072>.
- [115] Boulard T, Razafinjohany E, Baille A, Jaffrin A, Fabre B. Performance of a greenhouse heating system with a phase change material. *Agric For Meteorol* 1990;52(3):303-18. [https://doi.org/10.1016/0168-1923\(90\)90088-N](https://doi.org/10.1016/0168-1923(90)90088-N).
- [116] Esen M. Thermal performance of a solar-aided latent heat store used for space heating by heat pump. *Renew Sustain Energy Rev* 2000;69(1):15-25. [https://doi.org/10.1016/S0038-092X\(00\)00015-3](https://doi.org/10.1016/S0038-092X(00)00015-3).
- [117] Kürklü A, Wheldon AE, Hadley P. Use of phase change material (PCM) for frost prevention in a model greenhouse. *J Eng Sci Univ Pamukkale* 1997;3(2):359-63.

BIBLIOGRAPHY

- [118] Öztürk HH. Experimental evaluation of energy and exergy efficiency of a seasonal latent heat storage system for greenhouse heating. *Energy Convers Manag* 2005;46(9):1523-42. <https://doi.org/10.1016/j.enconman.2004.07.001>.
- [119] Benli H, Durmuş A. Performance analysis of a latent heat storage system with phase change material for new designed solar collectors in greenhouse heating. *Sol Energy* 2009;83(12):2109-19. <https://doi.org/10.1016/j.solener.2009.07.005>.
- [120] Johansen JB, Englmair G, Dannemand M, Kong W, Fan J, Dragsted J, et al. Laboratory Testing of Solar Combi System with Compact Long Term PCM Heat Storage. *Energy Procedia* 2016;91:330-7. <https://doi.org/10.1016/j.egypro.2016.06.230>.
- [121] Bales C, Gantenbein P, Jaenig D, Kerskes H, Summer K, Van essen M, et al. Laboratory tests of chemical reactions and prototype sorption storage units. 2008. https://pdfs.semanticscholar.org/0469/b9aff44c6b624a27c138a6f0bed56170ccf3.pdf?_ga=2.16604342.1692541323.1588188390-1010737723.1588188390 [accessed 14 May 2019].
- [122] Zondag H, Kikkert B, Smeding S, de Boer R, Bakker M. Prototype thermochemical heat storage with open reactor system. *Appl Energy* 2013;109:360-5. <https://doi.org/10.1016/j.apenergy.2013.01.082>.
- [123] Michel B, Mazet N, Neveu P. Experimental investigation of an innovative thermochemical process operating with a hydrate salt and moist air for thermal storage of solar energy: Global performance. *Appl Energy* 2014;129:177-86. <https://doi.org/10.1016/j.apenergy.2014.04.073>.
- [124] de Boer R, Smeding S, Zondag H, Krol G. Development of a prototype system for seasonal solar heat storage using an open sorption process. *Proceedings of the Eurotherm Seminar# 99, Advances in Thermal Energy Storage*; 2014.
- [125] Zettl B, Englmair G, Steinmaurer G. Development of a revolving drum reactor for open-sorption heat storage processes. *Appl Therm Eng* 2014;70(1):42-9. <https://doi.org/10.1016/j.applthermaleng.2014.04.069>.
- [126] Johannes K, Kuznik F, Hubert JL, Durier F, Obrecht C. Design and characterisation of a high powered energy dense zeolite thermal energy storage system for buildings. *Appl Energy* 2015;159:80-6. <https://doi.org/10.1016/j.apenergy.2015.08.109>.
- [127] van Alebeek R, Scapino L, Beving MAJM, Gaeini M, Rindt CCM, Zondag HA. Investigation of a household-scale open sorption energy storage system based on the zeolite 13X/water reacting pair. *Appl Therm Eng* 2018;139:325-33. <https://doi.org/10.1016/j.applthermaleng.2018.04.092>.
- [128] Mahon D, Henshall P, Claudio G, Eames PC. Feasibility study of MgSO_4 + zeolite based composite thermochemical energy stores charged by vacuum flat plate solar thermal collectors for seasonal thermal energy storage. *Renew Energy* 2020;145:1799-807. 10.1016/j.renene.2019.05.135.
- [129] Han YM, Wang RZ, Dai YJ. Thermal stratification within the water tank. *Renew Sustain Energy Rev* 2009;13(5):1014-26. <https://doi.org/10.1016/j.rser.2008.03.001>.
- [130] Pinel P, Cruickshank CA, Beausoleil-Morrison I, Wills A. A review of available methods for seasonal storage of solar thermal energy in residential applications. *Renew Sustain Energy Rev* 2011;15(7):3341-59. <https://doi.org/10.1016/j.rser.2011.04.013>.
- [131] Altuntop N, Arslan M, Ozceyhan V, Kanoglu M. Effect of obstacles on thermal stratification in hot water storage tanks. *Appl Therm Eng* 2005;25(14):2285-98. <https://doi.org/10.1016/j.applthermaleng.2004.12.013>.
- [132] Samet A, Ben Souf MA, Fakhfakh T, Haddar M. Numerical investigation of the baffle plates effect on the solar water storage tank efficiency. *Energy Sources, Part A Recover Util Environ Eff* 2020;42(16):2034-48. 10.1080/15567036.2019.1607925.

- [133] Lou W, Fan Y, Luo L. Single-tank thermal energy storage systems for concentrated solar power: Flow distribution optimization for thermocline evolution management. *J Energy Storage* 2020;32:101749. <https://doi.org/10.1016/j.est.2020.101749>.
- [134] Zhang Z, Song P, Fan Y. Experimental investigation on the geometric structure with perforated baffle for thermal stratification of the water tank. *Sol Energy* 2020;203:197-209. <https://doi.org/10.1016/j.solener.2020.04.040>.
- [135] Hegazy AA. Effect of inlet design on the performance of storage-type domestic electrical water heaters. *Appl Energy* 2007;84(12):1338-55. <https://doi.org/10.1016/j.apenergy.2006.09.014>.
- [136] Farmahini-Farahani M. Investigation of four geometrical parameters on thermal stratification of cold water tanks by exergy analysis. *Int J Exergy* 2012;10(3):332-45. 10.1504/ijex.2012.046814.
- [137] Kurşun B, Ökten K. Effect of rectangular hot water tank position and aspect ratio on thermal stratification enhancement. *Renew Energy* 2018;116:639-46. <https://doi.org/10.1016/j.renene.2017.10.013>.
- [138] Bai Y, Yang M, Wang Z, Li X, Chen L. Thermal stratification in a cylindrical tank due to heat losses while in standby mode. *Sol Energy* 2019;185:222-34. <https://doi.org/10.1016/j.solener.2018.12.063>.
- [139] Ragoonanan V, Davidson JH, Homan KO, Mantell SC. The benefit of dividing an indirect thermal storage into two compartments: Discharge experiments. *Sol Energy* 2006;80(1):18-31. <https://doi.org/10.1016/j.solener.2005.09.003>.
- [140] Mather DW, Hollands KGT, Wright JL. Single- and multi-tank energy storage for solar heating systems: fundamentals. *Sol Energy* 2002;73(1):3-13. [https://doi.org/10.1016/S0038-092X\(02\)00034-8](https://doi.org/10.1016/S0038-092X(02)00034-8).
- [141] Dickinson RM, Cruickshank CA, Harrison SJ. Charge and discharge strategies for a multi-tank thermal energy storage. *Appl Energy* 2013;109:366-73. <https://doi.org/10.1016/j.apenergy.2012.11.032>.
- [142] Dickinson RM, Cruickshank CA, Harrison SJ. Thermal behaviour of a modular storage system when subjected to variable charge and discharge sequences. *Sol Energy* 2014;104:29-41. <https://doi.org/10.1016/j.solener.2013.09.038>.
- [143] Moncho-Esteve IJ, Gasque M, González-Altozano P, Palau-Salvador G. Simple inlet devices and their influence on thermal stratification in a hot water storage tank. *Energy Build* 2017;150:625-38. <https://doi.org/10.1016/j.enbuild.2017.06.012>.
- [144] Rendall JD, Gluesenkamp KR, Worek W, Abu-Heiba A, Nawaz K, Gehl T. Empirical characterization of vertical-tube inlets in hot-water storage tanks. *Int Commun Heat Mass Transf* 2020;119:104838. <https://doi.org/10.1016/j.icheatmasstransfer.2020.104838>.
- [145] Chandra YP, Matuska T. Numerical prediction of the stratification performance in domestic hot water storage tanks. *Renew Energy* 2020;154:1165-79. <https://doi.org/10.1016/j.renene.2020.03.090>.
- [146] Jordan U, Furbo S. Thermal stratification in small solar domestic storage tanks caused by draw-offs. *Sol Energy* 2005;78(2):291-300. <https://doi.org/10.1016/j.solener.2004.09.011>.
- [147] Shah LJ, Furbo S. Entrance effects in solar storage tanks. *Sol Energy* 2003;75(4):337-48. <https://doi.org/10.1016/j.solener.2003.04.002>.
- [148] Villasmil W, Fischer LJ, Worlitschek J. A review and evaluation of thermal insulation materials and methods for thermal energy storage systems. *Renew Sustain Energy Rev* 2019;103:71-84. <https://doi.org/10.1016/j.rser.2018.12.040>.

BIBLIOGRAPHY

- [149] Omer SA, Riffat SB, Qiu G. Technical note: Thermal insulations for hot water cylinders: a review and a conceptual evaluation. *Build Serv Eng Res Technol* 2007;28(3):275-93. [10.1177/0143624406075269](https://doi.org/10.1177/0143624406075269).
- [150] Baetens R, Jelle BP, Thue JV, Tenpierik MJ, Grynning S, Uvsløkk S, et al. Vacuum insulation panels for building applications: A review and beyond. *Energy Build* 2010;42(2):147-72. <https://doi.org/10.1016/j.enbuild.2009.09.005>.
- [151] Cuce E, Cuce PM, Wood CJ, Riffat SB. Toward aerogel based thermal superinsulation in buildings: A comprehensive review. *Renew Sustain Energy Rev* 2014;34:273-99. <https://doi.org/10.1016/j.rser.2014.03.017>.
- [152] Raab S, Mangold D, Heidemann W, Müller-Steinhagen H. Solar assisted district heating system with seasonal hot water heat store in Friedrichshafen (Germany). *Proceedings of the EuroSun 2004*; 2004. p. 20-3.
- [153] Ochs F, Dahash A, Tosatto A, Bianchi Janetti M. Techno-economic planning and construction of cost-effective large-scale hot water thermal energy storage for Renewable District heating systems. *Renew Energy* 2020;150:1165-77. [10.1016/j.renene.2019.11.017](https://doi.org/10.1016/j.renene.2019.11.017).
- [154] Xie K, Nian Y-L, Cheng W-L. Analysis and optimization of underground thermal energy storage using depleted oil wells. *Energy* 2018;163:1006-16. <https://doi.org/10.1016/j.energy.2018.08.189>.
- [155] Pfeil M, Koch H. High performance–low cost seasonal gravel/water storage pit. *Sol Energy* 2000;69(6):461-7. [https://doi.org/10.1016/S0038-092X\(00\)00123-7](https://doi.org/10.1016/S0038-092X(00)00123-7).
- [156] Sanner B, Karytsas C, Mendrinos D, Rybach L. Current status of ground source heat pumps and underground thermal energy storage in Europe. *Geothermics* 2003;32(4):579-88. [https://doi.org/10.1016/S0375-6505\(03\)00060-9](https://doi.org/10.1016/S0375-6505(03)00060-9).
- [157] Gao Q, Li M, Yu M, Spitler JD, Yan YY. Review of development from GSHP to UTES in China and other countries. *Renew Sustain Energy Rev* 2009;13(6):1383-94. <https://doi.org/10.1016/j.rser.2008.09.012>.
- [158] Gao L, Zhao J, Tang Z. A Review on Borehole Seasonal Solar Thermal Energy Storage. *Energy Procedia* 2015;70:209-18. <https://doi.org/10.1016/j.egypro.2015.02.117>.
- [159] Li M, Lai ACK. Review of analytical models for heat transfer by vertical ground heat exchangers (GHEs): A perspective of time and space scales. *Appl Energy* 2015;151:178-91. <https://doi.org/10.1016/j.apenergy.2015.04.070>.
- [160] Rad FM, Fung AS. Solar community heating and cooling system with borehole thermal energy storage – Review of systems. *Renew Sustain Energy Rev* 2016;60:1550-61. <https://doi.org/10.1016/j.rser.2016.03.025>.
- [161] Reuss M, Beck M, Müller JP. Design of a seasonal thermal energy storage in the ground. *Sol Energy* 1997;59(4):247-57. [https://doi.org/10.1016/S0038-092X\(97\)00011-X](https://doi.org/10.1016/S0038-092X(97)00011-X).
- [162] Chen S, Mao J, Hou P, Li C. Numerical investigation of a thermal baffle design for single ground heat exchanger. *Appl Therm Eng* 2016;103:391-8. <https://doi.org/10.1016/j.applthermaleng.2016.04.106>.
- [163] Li X-Y, Li T-Y, Qu D-Q, Yu J-W. A new solution for thermal interference of vertical U-tube ground heat exchanger for cold area in China. *Geothermics* 2017;65:72-80. <https://doi.org/10.1016/j.geothermics.2016.08.002>.
- [164] Li Y, An Q, Liu L, Zhao J. Thermal Performance Investigation of Borehole Heat Exchanger with Different U-tube Diameter and Borehole Parameters. *Energy Procedia* 2014;61:2690-4. <https://doi.org/10.1016/j.egypro.2014.12.278>.
- [165] Walch A, Mohajeri N, Gudmundsson A, Scartezzini J-L. Quantifying the technical geothermal potential from shallow borehole heat exchangers at regional scale. *Renew Energy* 2021;165:369-80. <https://doi.org/10.1016/j.renene.2020.11.019>.

- [166] Javadi H, Mousavi Ajarostaghi SS, Rosen MA, Pourfallah M. Performance of ground heat exchangers: A comprehensive review of recent advances. *Energy* 2019;178:207-33. <https://doi.org/10.1016/j.energy.2019.04.094>.
- [167] DLSC. Drake landing solar community, <https://dlsc.ca/>; 2021 [accessed 8 April 2021].
- [168] Hendriks M, Snijders A, Boid N. Underground thermal energy storage for efficient heating and cooling of buildings. *Proceedings of the 1st International Conference on Industrialised, Integrated, Intelligent Construction*; Loughborough, UK; 2008. p. 315-24.
- [169] Hartog N, Drijver B, Dinkla I, Bonte M. Field assessment of the impacts of Aquifer Thermal Energy Storage (ATES) systems on chemical and microbial groundwater composition. *Proceedings of the European Geothermal Conference*; Pisa, Italy; 2013.
- [170] Schmidt T, Mangold D, Müller-Steinhagen H. Seasonal thermal energy storage in Germany. *Proceedings of the ISES Solar World Congress 2003*; 2003 Jun 14-19; Goteborg, Sweden; 2003.
- [171] Pavlov GK, Olesen BW. Thermal energy storage—A review of concepts and systems for heating and cooling applications in buildings: Part 1—Seasonal storage in the ground. *HVAC&R Res* 2012;18(3):515-38. 10.1080/10789669.2012.667039.
- [172] Kuznik F, Virgone J, Roux J-J. Energetic efficiency of room wall containing PCM wallboard: A full-scale experimental investigation. *Energy Build* 2008;40(2):148-56. <https://doi.org/10.1016/j.enbuild.2007.01.022>.
- [173] Cabeza LF, Castellón C, Nogués M, Medrano M, Leppers R, Zubillaga O. Use of microencapsulated PCM in concrete walls for energy savings. *Energy Build* 2007;39(2):113-9. <https://doi.org/10.1016/j.enbuild.2006.03.030>.
- [174] Mehling H. Strategic project ‘Innovative PCM-Technology—Results and future perspectives’. *Proceedings of the 8th Eptert Meting and Wrkshop*; Kizkalesi, Turkey; 2004.
- [175] Huang K, Feng G, Zhang J. Experimental and numerical study on phase change material floor in solar water heating system with a new design. *Sol Energy* 2014;105:126-38. <https://doi.org/10.1016/j.solener.2014.03.009>.
- [176] Pasupathy A, Velraj R. Effect of double layer phase change material in building roof for year round thermal management. *Energy Build* 2008;40(3):193-203. <https://doi.org/10.1016/j.enbuild.2007.02.016>.
- [177] Lazaar M, Bouadila S, Kooli S, Farhat A. Conditioning of the tunnel greenhouse in the north of Tunisia using a calcium chloride hexahydrate integrated in polypropylene heat exchanger. *Appl Therm Eng* 2014;68(1):62-8. <https://doi.org/10.1016/j.applthermaleng.2014.04.014>.
- [178] Chen S, Zhu Y, Chen Y, Liu W. Usage strategy of phase change materials in plastic greenhouses, in hot summer and cold winter climate. *Appl Energy* 2020;277:115416. <https://doi.org/10.1016/j.apenergy.2020.115416>.
- [179] OECD. Exchange rates, <https://doi.org/10.1787/037ed317-en>; 2021 [accessed 8 April 2021].
- [180] OECD. Inflation (CPI), <https://doi.org/10.1787/eee82e6e-en>; 2021 [accessed 8 April 2021].
- [181] García-Gusano D, Espegren K, Lind A, Kirkengen M. The role of the discount rates in energy systems optimisation models. *Renew Sustain Energy Rev* 2016;59:56-72. <https://doi.org/10.1016/j.rser.2015.12.359>.
- [182] Steinbach J, Staniaszek D. Discount rates in energy system analysis. 2015. http://bpie.eu/wp-content/uploads/2015/10/Discount_rates_in_energy_system-discussion_paper_2015_ISI_BPIE.pdf [accessed 14 May 2019].
- [183] Gibb D, Seitz A, Johnson M, Romaní J, Gasia J, Cabeza LF, et al. Applications of thermal energy storage in the energy transition. 2018. <https://www.eces-a30.org/wp->

BIBLIOGRAPHY

- [content/uploads/Applications-of-Thermal-Energy-Storage-in-the-Energy-Transition-Annex-30-Report.pdf](#) [accessed 14 May 2019].
- [184] Sørensen PA, Schmidt T. Design and construction of large scale heat storages for district heating in Denmark. Proceedings of the 14th International Conference on Energy Storage; 2018 Apr 25-28; Adana, Turkey; 2018.
- [185] Sibbitt B, McClenahan D, Djebbar R, Thornton J, Wong B, Carriere J, et al. Measured and simulated performance of a high solar fraction district heating system with seasonal storage. Proceedings of the 30th ISES Solar World Congress; 2011 Aug 28-Sept 2; Kassel, Germany; 2011. p. 3037-48.
- [186] Demirel Y, Öztürk HH. Thermoeconomics of seasonal latent heat storage system. *Int J Energy Res* 2006;30(12):1001-12. 10.1002/er.1206.
- [187] Hansen K. Decision-making based on energy costs: Comparing levelized cost of energy and energy system costs. *Energy Strategy Rev* 2019;24:68-82. <https://doi.org/10.1016/j.esr.2019.02.003>.
- [188] Eurostat [Internet]. Gas prices by type of user. 'c'2020 [cited 10 April 2020]. Available from: <https://ec.europa.eu/eurostat/databrowser/view/ten00118/default/table?lang=en>.
- [189] Markets Insider [Internet]. CO₂ European Emission Allowances. 'c'2020 [cited 10 April 2020]. Available from: <https://markets.businessinsider.com/commodities/co2-european-emission-allowances>.
- [190] Zijlema PJ. The Netherlands: list of fuels and standard CO₂ emission factors. 2019. <https://english.rvo.nl/sites/default/files/2019/05/The%20Netherlands%20list%20of%20fuel%20version%20January%202019.pdf> [accessed 10 April 2020].
- [191] Bruckner T, Chum H, Jäger-Waldau A, Killingtveit Å, Gutiérrez-Negrín L, Nyboer J, et al. Recent Renewable Energy Cost and Performance Parameters. 2011. <https://www.ipcc.ch/site/assets/uploads/2018/03/Annex-III-Recent-Renewable-Energy-Cost-and-Performance-Parameters-1.pdf> [accessed 10 April 2020].
- [192] IEA SHC. Levelised Cost of Heat and the Calculations behind it, <https://www.solarthermalworld.org/news/iea-shc-levelised-cost-heat-and-calculations-behind-it>; 2016 [accessed 10 April 2020].
- [193] Skarphagen H, Banks D, Frengstad BS, Gether H. Design Considerations for Borehole Thermal Energy Storage (BTES): A Review with Emphasis on Convective Heat Transfer. *Geofluids* 2019;2019:4961781. 10.1155/2019/4961781.
- [194] Bloemendal M, Hartog N. Analysis of the impact of storage conditions on the thermal recovery efficiency of low-temperature ATES systems. *Geothermics* 2018;71:306-19. <https://doi.org/10.1016/j.geothermics.2017.10.009>.
- [195] Beernink S, Hartog N, Bloemendal M, van der Meer M. ATES systems performance in practice: analysis of operational data from ATES systems in the province of Utrecht, The Netherlands. Proceedings of the European Geothermal Congress 2019; 2019 Jun 11-14; Den Haag, The Netherlands; 2019.
- [196] Allegrini J, Orehounig K, Mavromatidis G, Ruesch F, Dorer V, Evins R. A review of modelling approaches and tools for the simulation of district-scale energy systems. *Renew Sustain Energy Rev* 2015;52:1391-404. <https://doi.org/10.1016/j.rser.2015.07.123>.
- [197] Sibbitt B, McClenahan D, Djebbar R, Thornton J, Wong B, Carriere J, et al. The Performance of a High Solar Fraction Seasonal Storage District Heating System – Five Years of Operation. *Energy Procedia* 2012;30:856-65. <https://doi.org/10.1016/j.egypro.2012.11.097>.
- [198] Lund H, Østergaard PA, Connolly D, Mathiesen BV. Smart energy and smart energy systems. *Energy* 2017;137:556-65. <https://doi.org/10.1016/j.energy.2017.05.123>.

- [199] Lund H, Østergaard PA, Connolly D, Ridjan I, Mathiesen BV, Hvelplund F, et al. Energy storage and smart energy systems. *Int J Sustain Energy Plan Manag* 2016;11(0):3-14. <https://doi.org/10.5278/ijsepm.2016.11.2>.
- [200] Lyden A, Brown CS, Kolo I, Falcone G, Friedrich D. Seasonal thermal energy storage in smart energy systems: District-level applications and modelling approaches. *Renew Sustain Energy Rev* 2022;167:112760. <https://doi.org/10.1016/j.rser.2022.112760>.
- [201] Lund H, Østergaard PA, Nielsen TB, Werner S, Thorsen JE, Gudmundsson O, et al. Perspectives on fourth and fifth generation district heating. *Energy* 2021;227:120520. <https://doi.org/10.1016/j.energy.2021.120520>.
- [202] Yang T, Liu W, Kramer GJ, Sun Q. Seasonal thermal energy storage: A techno-economic literature review. *Renew Sustain Energy Rev* 2021;139:110732. <https://doi.org/10.1016/j.rser.2021.110732>.
- [203] Guo F, Zhu X, Li P, Yang X. Low-grade industrial waste heat utilization in urban district heating: Simulation-based performance assessment of a seasonal thermal energy storage system. *Energy* 2022;239:122345. <https://doi.org/10.1016/j.energy.2021.122345>.
- [204] Mahon H, O'Connor D, Friedrich D, Hughes B. A review of thermal energy storage technologies for seasonal loops. *Energy* 2022;239:122207. <https://doi.org/10.1016/j.energy.2021.122207>.
- [205] Salvestroni M, Pierucci G, Pourreza A, Fagioli F, Taddei F, Messeri M, et al. Design of a solar district heating system with seasonal storage in Italy. *Appl Therm Eng* 2021;197:117438. <https://doi.org/10.1016/j.applthermaleng.2021.117438>.
- [206] Guo F, Zhu X, Zhang J, Yang X. Large-scale living laboratory of seasonal borehole thermal energy storage system for urban district heating. *Appl Energy* 2020;264:114763. <https://doi.org/10.1016/j.apenergy.2020.114763>.
- [207] Nilsson E, Rohdin P. Performance evaluation of an industrial borehole thermal energy storage (BTES) project – Experiences from the first seven years of operation. *Renew Energy* 2019;143:1022-34. [10.1016/j.renene.2019.05.020](https://doi.org/10.1016/j.renene.2019.05.020).
- [208] Liu L, Zhu N, Zhao J. Thermal equilibrium research of solar seasonal storage system coupling with ground-source heat pump. *Energy* 2016;99:83-90. <https://doi.org/10.1016/j.energy.2016.01.053>.
- [209] Ciampi G, Rosato A, Sibilio S. Thermo-economic sensitivity analysis by dynamic simulations of a small Italian solar district heating system with a seasonal borehole thermal energy storage. *Energy* 2018;143:757-71. <https://doi.org/10.1016/j.energy.2017.11.029>.
- [210] Tao T, Zhang F, Zhang W, Wan P, Shen X, Li H. Low cost and marketable operational experiences for a solar heating system with seasonal thermal energy storage (SHSSTES) in Hebei (China). *Energy Procedia* 2015;70:267-74. <https://doi.org/10.1016/j.egypro.2015.02.123>.
- [211] Xiao X, Jiang Z, Owen D, Schrank C. Numerical simulation of a high-temperature aquifer thermal energy storage system coupled with heating and cooling of a thermal plant in a cold region, China. *Energy* 2016;112:443-56. <https://doi.org/10.1016/j.energy.2016.06.124>.
- [212] Kubiński K, Szablowski Ł. Dynamic model of solar heating plant with seasonal thermal energy storage. *Renew Energy* 2020;145:2025-33. [10.1016/j.renene.2019.07.120](https://doi.org/10.1016/j.renene.2019.07.120).
- [213] Jiao Q, Liu W, Liu G, Zhang Y, Cai J, Qin H. Data measurement and analysis of a solar heating system with seasonal storage. *Energy Procedia* 2015;70:241-8. <https://doi.org/10.1016/j.egypro.2015.02.120>.
- [214] Zhou X, Xu Y, Zhang X, Xu D, Linghu Y, Guo H, et al. Large scale underground seasonal thermal energy storage in China. *J Energy Storage* 2021;33:102026. <https://doi.org/10.1016/j.est.2020.102026>.

BIBLIOGRAPHY

- [215] Li H, Hou J, Hong T, Ding Y, Nord N. Energy, economic, and environmental analysis of integration of thermal energy storage into district heating systems using waste heat from data centres. *Energy* 2021;219:119582. <https://doi.org/10.1016/j.energy.2020.119582>.
- [216] TRNSYS. Transient system simulation tool, <http://www.trnsys.com/>; 2021 [accessed 8 April 2021].
- [217] Hyrzyński R, Ziółkowski P, Gotzman S, Kraszewski B, Ochrymiuk T, Badur J. Comprehensive thermodynamic analysis of the CAES system coupled with the underground thermal energy storage taking into account global, central and local level of energy conversion. *Renew Energy* 2021;169:379-403. <https://doi.org/10.1016/j.renene.2020.12.123>.
- [218] Karasu H, Dincer I. Life cycle assessment of integrated thermal energy storage systems in buildings: A case study in Canada. *Energy Build* 2020;217:109940. <https://doi.org/10.1016/j.enbuild.2020.109940>.
- [219] McDowell TP, Thornton JW. Simulation and model calibration of a large-scale solar seasonal storage system. *Proceedings of the 3rd National Conference of IBPSA-USA*; 2008 Jul 30-Aug 1; Berkeley, USA; 2008. p. 174-81.
- [220] Government of Canada. Historical climate data, <https://climate.weather.gc.ca/>; 2020 [accessed 24 November 2020].
- [221] National Resources Canada. Drake landing satellite solar resource data, https://ftp.nrcan.gc.ca/energy/SOLAR/DrakeLanding_SatteliteSolarResourceData/; 2020 [accessed 24 November 2020].
- [222] Flynn C, Sirén K. Influence of location and design on the performance of a solar district heating system equipped with borehole seasonal storage. *Renew Energy* 2015;81:377-88. <https://doi.org/10.1016/j.renene.2015.03.036>.
- [223] Yang L, Entchev E, Rosato A, Sibilio S. Smart thermal grid with integration of distributed and centralized solar energy systems. *Energy* 2017;122:471-81. <https://doi.org/10.1016/j.energy.2017.01.114>.
- [224] Quintana H. A practical approach to model predictive control (MPC) for solar communities [dissertation]. Montréal: École Polytechnique de Montréal; 2013.
- [225] National Development and Reform Commission. Supervision and examination method for pricing cost of urban district heating, <https://www.ndrc.gov.cn/yjzxDownload/gg3czjzgrjghsfgl.pdf>; 2020 [accessed 6 October 2021].
- [226] Alibaba Group. Alibaba.com, <https://www.alibaba.com/>; 2021 [accessed 8 April 2021].
- [227] Yang L, Qiao B, Xu W, Zhou Q. Analysis of the influence of borehole depth on energy efficiency and cost of ground source heat pump system. *Proceedings of the 12th IEA Heat Pump Conference*; 2017 May 15-18; Rotterdam, the Netherlands; 2017.
- [228] Chi H. Economic evaluation of ground source heat pump in a residential building. *Energy Conserv* 2014;33(04):33-7. (In Chinese).
- [229] Yu L, Cheng J. Study on engineering design and cost performance of borehole heat exchangers. *Math Probl Eng* 2015;2015:870380. <https://doi.org/10.1155/2015/870380>.
- [230] Luo J, Zhang Y, Rohn J. Analysis of thermal performance and drilling costs of borehole heat exchanger (BHE) in a river deposited area. *Renew Energy* 2020;151:392-402. <https://doi.org/10.1016/j.renene.2019.11.019>.
- [231] The People's Bank of China. Benchmark interest rate for RMB loans of financial institutions, <http://www.pbc.gov.cn/>; 2021 [accessed 8 April 2021].
- [232] Li J, Colombier M, Giraud P-N. Decision on optimal building energy efficiency standard in China—The case for Tianjin. *Energy Policy* 2009;37(7):2546-59. <https://doi.org/10.1016/j.enpol.2009.01.014>.

- [233] Mauthner F, Herkel S. Technology and demonstrators. Technical report subtask C - Part C1, <http://task3.iea-shc.org/data/sites/1/publications/IEA-SHC-Task52-STC1-Classification-and-benchmarking-Report-2016-03-31.pdf>; 2016 [accessed 8 April 2021].
- [234] Eurostat. Labour costs annual data, <https://ec.europa.eu/eurostat/databrowser/view/tps00173/default/table?lang=en>; 2021 [accessed 8 April 2021].
- [235] National Bureau of Statistics of China. China labor statistical yearbook. Beijing: China Statistics Press; 2020.
- [236] Ministry of Human Resources and Social Security of the People's Republic of China. Notice on the annual average monthly working hours and wage conversion of employees, http://www.mohrss.gov.cn/SYrlzyhshbzb/laodongguanxi/_zwcwj/gzzfbz/202002/t20200210_359074.html; 2008 [accessed 8 April 2021].
- [237] China Electricity Council. China electricity price system, <http://cep.cec.org.cn/api/index.html>; 2021 [accessed 8 April 2021].
- [238] Harbin Development and Reform Commission. Notice on adjusting the sales price of pipeline natural gas for non-residential use, http://fgw.harbin.gov.cn/art/2020/3/15/art_24909_951074.html; 2020 [accessed 8 April 2021].
- [239] Urumqi Development and Reform Commission. Notice on the phased reduction of the natural gas sales price for non-residential use, <http://www.wlmq.gov.cn/fjbm/fgw/zcfg/441244.htm>; 2020 [accessed 8 April 2021].
- [240] Shanghai Municipal Development and Reform Commission. Notice on adjusting the price of natural gas for non-resident use, <https://fgw.sh.gov.cn/jgl/20210401/973b7fdda318496095a31ca4d634ae8c.html>; 2021 [accessed 8 April 2021].
- [241] Chengdu Gas Group Corporation Ltd. Natural gas tariff, <http://www.cdgas.com/serviceGuid/guide-3/index.html>; 2021 [accessed 8 April 2021].
- [242] Takahashi K, Louhisuo M. IGES list of grid emission factors, <https://www.iges.or.jp/en/pub/list-grid-emission-factor/en>; 2021 [accessed 8 April 2021].
- [243] National Center for Climate Change Strategy and International Cooperation (NCSC). Guidelines for compiling provincial greenhouse gas inventories, http://www.ncsc.org.cn/SY/tjkhybg/202003/t20200319_769763.shtml; 2011 [accessed 8 April 2021].
- [244] Zheng W, Hennessy JJ, Li H. Reducing renewable power curtailment and CO2 emissions in China through district heating storage. Wiley Interdiscip Rev Energy Environ 2020;9(1):e361. <https://doi.org/10.1002/wene.361>.
- [245] Zhang L, Li Y, Zhang H, Xu X, Yang Z, Xu W. A review of the potential of district heating system in Northern China. Appl Therm Eng 2021;188:116605. <https://doi.org/10.1016/j.applthermaleng.2021.116605>.
- [246] Guo J, Huang Y, Wei C. North-South debate on district heating: Evidence from a household survey. Energy Policy 2015;86:295-302. <https://doi.org/10.1016/j.enpol.2015.07.017>.
- [247] Weiss W, Spörk-Dür M. Solar heat worldwide, <https://www.iea-shc.org/Data/Sites/1/publications/Solar-Heat-Worldwide-2020.pdf>; 2020 [accessed 8 April 2021].
- [248] Zhang H, Han Z, Li X, Ji M, Zhang X, Li G, et al. Study on the influence of borehole spacing considering groundwater flow and freezing factors on the annual performance of the ground source heat pump. Appl Therm Eng 2021;182:116042. <https://doi.org/10.1016/j.applthermaleng.2020.116042>.

BIBLIOGRAPHY

- [249] Li B, You T, Wang B, Li X, Shi W. Analysis of the application effect of the ground source heat pump system with compound heat supplement in the north area. *Build Sci* 2012;28(S2):178-83. <https://doi.org/10.13614/j.cnki.11-1962/tu.2012.s2.039>. (In Chinese).
- [250] Kan-ji R, Lin M, Li W, Li W, Han Y. Design and operation effect of solar-ground source heat pump heating system in Xinjiang. *Sol Energy* 2016(05):30-5. (In Chinese).
- [251] Wang G, Wang W, Luo J, Zhang Y. Assessment of three types of shallow geothermal resources and ground-source heat-pump applications in provincial capitals in the Yangtze River Basin, China. *Renew Sustain Energy Rev* 2019;111:392-421. <https://doi.org/10.1016/j.rser.2019.05.029>.
- [252] Meteotest. Meteonorm software: Worldwide irradiation data, <https://meteonorm.com/>; 2021 [accessed 8 April 2021].
- [253] Trimble. Sketchup, <https://www.sketchup.com/>; 2021 [accessed 8 April 2021].
- [254] Ministry of Housing and Urban-Rural Development of the People's Republic of China. Design standard for energy efficiency of residential buildings in severe cold and cold zones (JGJ 26-2018). Beijing: China Architecture & Building Press; 2018.
- [255] Ministry of Housing and Urban-Rural Development of the People's Republic of China. Design standard for energy efficiency of residential buildings in hot summer and cold winter zones (JGJ 134-2010). Beijing: China Architecture & Building Press; 2010.
- [256] Shah SK, Aye L, Rismanchi B. Simulated performance of a borehole-coupled heat pump seasonal solar thermal storage system for space heating in cold climate. *Sol Energy* 2020;202:365-85. <https://doi.org/10.1016/j.solener.2020.03.111>.
- [257] Yu CYM. Modeling the heating of the Green Energy Lab in Shanghai by the geothermal heat pump combined with the solar thermal energy and ground energy storage [dissertation]. Trondheim: Norwegian University of Science and Technology; 2012.
- [258] Ministry of Housing and Urban-Rural Development of the People's Republic of China. Technical standard for solar water heating system of civil buildings (GB 50364-2018). Beijing: China Architecture & Building Press; 2018.
- [259] Sibbitt B, McClenahan D, Djebbar R, Thornton J, Wong B, Carriere J, et al. The performance of a high solar fraction seasonal storage district heating system - Five years of operation. *Energy Procedia* 2012;30:856-65. <https://doi.org/10.1016/j.egypro.2012.11.097>.
- [260] Harbin Development and Reform Commission. Clean winter heating implementation plan in Harbin (2019-2021), http://www.harbin.gov.cn/art/2020/1/7/art_24978_863216.html; 2019 [accessed 8 April 2021].
- [261] Xue G, Song J, Kong X, Pan Y, Qi C, Li H. Prediction of natural gas consumption for city-level DHS based on attention GRU: A case study for a northern Chinese city. *IEEE Access* 2019;7:130685-99. <https://doi.org/10.1109/ACCESS.2019.2940210>.
- [262] Ascione F, Bianco N, De Stasio C, Mauro GM, Vanoli GP, 5.21 Energy management in hospitals, in: Dincer I editor. *Comprehensive energy systems*, Elsevier, Oxford, 2018, pp. 827-54.
- [263] Catolico N, Ge S, McCartney JS. Numerical modeling of a soil-borehole thermal energy storage system. *Vadose Zone J* 2016;15(1). <https://doi.org/10.2136/vzj2015.05.0078>.
- [264] Rad FM, Fung AS, Rosen MA. An integrated model for designing a solar community heating system with borehole thermal storage. *Energy Sustain Dev* 2017;36:6-15. <https://doi.org/10.1016/j.esd.2016.10.003>.
- [265] Lyu C, Leong WH, Zheng M, Jiang P, Yu F, Liu Y. Dynamic simulation and operating characteristics of ground-coupled heat pump with solar seasonal heat storage system. *Heat Transfer Eng* 2019;41(9-10):840-50. <https://doi.org/10.1080/01457632.2019.1576423>.

- [266] Rosato A, Ciervo A, Ciampi G, Scorpio M, Sibilio S. Impact of seasonal thermal energy storage design on the dynamic performance of a solar heating system serving a small-scale Italian district composed of residential and school buildings. *J Energy Storage* 2019;25:100889. <https://doi.org/10.1016/j.est.2019.100889>.
- [267] Zhang C, Song W, Sun S, Peng D. Parameter estimation of in-situ thermal response test with unstable heat rate. *Energy* 2015;88:497-505. <https://doi.org/10.1016/j.energy.2015.05.074>.
- [268] Metz B, Davidson O, Coninck Hd, Loos M, Meyer L. IPCC special report on carbon dioxide capture and storage. New York: Cambridge University Press; 2005.
- [269] Ming Z, Shaojie O, Yingjie Z, Hui S. CCS technology development in China: Status, problems and countermeasures—Based on SWOT analysis. *Renew Sustain Energy Rev* 2014;39:604-16. <https://doi.org/10.1016/j.rser.2014.07.037>.
- [270] National Bureau of Statistics of China. China national economic and social development statistics bulletin 2020 http://www.stats.gov.cn/tjsj/zxfb/202102/t20210227_1814154.html; 2021 [accessed 6 October 2021].
- [271] China Electricity Council. Research on the development plan of the electric power industry during the "14th Five-Year Plan", <https://cec.org.cn/detail/index.html?3-297199>; 2021 [accessed 6 October 2021].
- [272] Xu Y, Yang Z, Yuan J. The economics of renewable energy power in China. *Clean Technol Environ Policy* 2021;23(4):1341-51. <https://doi.org/10.1007/s10098-021-02031-0>.
- [273] Zhou K, Mao J, Li Y, Zhang H. Performance assessment and techno-economic optimization of ground source heat pump for residential heating and cooling: A case study of Nanjing, China. *Sustain Energy Technol Assess* 2020;40:100782. <https://doi.org/10.1016/j.seta.2020.100782>.
- [274] Xia ZH, Jia GS, Ma ZD, Wang JW, Zhang YP, Jin LW. Analysis of economy, thermal efficiency and environmental impact of geothermal heating system based on life cycle assessments. *Appl Energy* 2021;303:117671. <https://doi.org/10.1016/j.apenergy.2021.117671>.
- [275] Leckner M, Zmeureanu R. Life cycle cost and energy analysis of a Net Zero Energy House with solar combisystem. *Appl Energy* 2011;88(1):232-41. <https://doi.org/10.1016/j.apenergy.2010.07.031>.
- [276] Ma M, Ma X, Cai W, Cai W. Carbon-dioxide mitigation in the residential building sector: A household scale-based assessment. *Energy Convers Manag* 2019;198:111915. <https://doi.org/10.1016/j.enconman.2019.111915>.
- [277] Building Energy Research Center of Tsinghua University. Annual report of China building energy conservation 2022. Beijing, China: China Architecture & Building Press; 2022.
- [278] Hou X, Zhong S, Zhao Ja. A critical review on decarbonizing heating in China: Pathway exploration for technology with multi-sector applications. *Energies* 2022;15(3):1183. <https://doi.org/10.3390/en15031183>.
- [279] Itten A, Sherry-Brennan F, Hoppe T, Sundaram A, Devine-Wright P. Co-creation as a social process for unlocking sustainable heating transitions in Europe. *Energy Res Social Sci* 2021;74:101956. <https://doi.org/10.1016/j.erss.2021.101956>.
- [280] Yuan M, Thellufsen JZ, Sorknæs P, Lund H, Liang Y. District heating in 100% renewable energy systems: Combining industrial excess heat and heat pumps. *Energy Convers Manag* 2021;244:114527. <https://doi.org/10.1016/j.enconman.2021.114527>.

BIBLIOGRAPHY

- [281] López-Bernabé E, Linares P, Galarraga I. Energy-efficiency policies for decarbonising residential heating in Spain: A fuzzy cognitive mapping approach. *Energy Policy* 2022;171:113211. <https://doi.org/10.1016/j.enpol.2022.113211>.
- [282] Molar-Cruz A, Keim MF, Schifflachner C, Loewer M, Zosseder K, Drews M, et al. Techno-economic optimization of large-scale deep geothermal district heating systems with long-distance heat transport. *Energy Convers Manag* 2022;267:115906. <https://doi.org/10.1016/j.enconman.2022.115906>.
- [283] Xiong W, Wang Y, Mathiesen BV, Lund H, Zhang X. Heat roadmap China: New heat strategy to reduce energy consumption towards 2030. *Energy* 2015;81:274-85. <https://doi.org/10.1016/j.energy.2014.12.039>.
- [284] Zhang Y, Xia J, Fang H, Zuo H, Jiang Y. Roadmap towards clean heating in 2035: Case study of inner Mongolia, China. *Energy* 2019;189:116152. <https://doi.org/10.1016/j.energy.2019.116152>.
- [285] Zhang H, Zhou L, Huang X, Zhang X. Decarbonizing a large City's heating system using heat pumps: A case study of Beijing. *Energy* 2019;186:115820. <https://doi.org/10.1016/j.energy.2019.07.150>.
- [286] Zhang H, Zhao X, Zhang R. Synergistic development of heating system decarbonization transition and large-scale renewable energy penetration: A case study of Beijing. *Energy Convers Manag* 2022;269:116142. <https://doi.org/10.1016/j.enconman.2022.116142>.
- [287] Yuan M, Thellufsen JZ, Lund H, Liang Y. The first feasible step towards clean heating transition in urban agglomeration: A case study of Beijing-Tianjin-Hebei region. *Energy Convers Manag* 2020;223:113282. <https://doi.org/10.1016/j.enconman.2020.113282>.
- [288] Harbin Bureau of Statistics. Harbin statistical yearbook 2021. Beijing, China: China Statistics Press; 2022.
- [289] Zhang Y, Ma Q, Li B, Fan X, Fu Z. Application of an air source heat pump (ASHP) for heating in Harbin, the coldest provincial capital of China. *Energy Build* 2017;138:96-103. <https://doi.org/10.1016/j.enbuild.2016.12.044>.
- [290] Dai B, Qi H, Dou W, Liu S, Zhong D, Yang H, et al. Life cycle energy, emissions and cost evaluation of CO₂ air source heat pump system to replace traditional heating methods for residential heating in China: System configurations. *Energy Convers Manag* 2020;218:112954. <https://doi.org/10.1016/j.enconman.2020.112954>.
- [291] You T, Yang H. Feasibility of ground source heat pump using spiral coil energy piles with seepage for hotels in cold regions. *Energy Convers Manag* 2020;205:112466. <https://doi.org/10.1016/j.enconman.2020.112466>.
- [292] Wu W, You T, Wang B, Shi W, Li X. Evaluation of ground source absorption heat pumps combined with borehole free cooling. *Energy Convers Manag* 2014;79:334-43. <https://doi.org/10.1016/j.enconman.2013.11.045>.
- [293] Zou B. Simulation study of heating system of trough solar collectors combined with gas boiler [dissertation]. Harbin: Harbin Institute of Technology; 2014.
- [294] Yuan Y, Zhao J. Study on the supply capacity of crop residue as energy in rural areas of Heilongjiang province of China. *Renew Sustain Energy Rev* 2014;38:526-36. <https://doi.org/10.1016/j.rser.2014.06.009>.
- [295] Wang J-J, Xu Z-L, Jin H-G, Shi G-h, Fu C, Yang K. Design optimization and analysis of a biomass gasification based BCHP system: A case study in Harbin, China. *Renew Energy* 2014;71:572-83. <https://doi.org/10.1016/j.renene.2014.06.016>.
- [296] Hua C. Control system design of biomass boiler [dissertation]. Harbin: Harbin Institute of Technology; 2019.

- [297] Meng X. The combustion characteristics of blend biomass in a fixed bed reactor [dissertation]. Harbin: Harbin Institute of Technology; 2019.
- [298] Xu J, Lv T, Hou X, Deng X, Liu F. Provincial allocation of renewable portfolio standard in China based on efficiency and fairness principles. *Renew Energy* 2021;179:1233-45. <https://doi.org/10.1016/j.renene.2021.07.101>.
- [299] Ma X, Li P. Comparative test and analysis of various clean energy supply heating modes in harbin city. *Low Temp Archit Technol* 2020;42(10):138-41. <https://doi.org/10.13905/j.cnki.dwjz.2020.10.033>. (In Chinese).
- [300] Wang J. Heat and power synergic dispatch and optimal configuration of clean heat sources for district energy system [dissertation]. Harbin: Harbin Institute of Technology; 2019.
- [301] Jia Z, Bian J, Wang Y. Impacts of urban land use on the spatial distribution of groundwater pollution, Harbin City, Northeast China. *J Contam Hydrol* 2018;215:29-38. <https://doi.org/10.1016/j.jconhyd.2018.06.005>.
- [302] GenOpt. Generic optimization program, <https://simulationresearch.lbl.gov/GO/>; 2022 [accessed 2 May 2022].
- [303] Harbin Municipal People's Government. Harbin city heating measures, http://www.harbin.gov.cn/art/2011/10/25/art_4444_60616.html; 2011 [accessed 30 April 2022].
- [304] Ministry of Housing and Urban-Rural Development of the People's Republic of China. Design code for heating ventilation and air conditioning of civil buildings (GB 50736-2012). Beijing: China Architecture & Building Press; 2012.
- [305] Lund H, Werner S, Wiltshire R, Svendsen S, Thorsen JE, Hvelplund F, et al. 4th Generation District Heating (4GDH): Integrating smart thermal grids into future sustainable energy systems. *Energy* 2014;68:1-11. <https://doi.org/10.1016/j.energy.2014.02.089>.
- [306] Zhang Q, Chen W. Modeling China's interprovincial electricity transmission under low carbon transition. *Appl Energy* 2020;279:115571. <https://doi.org/10.1016/j.apenergy.2020.115571>.
- [307] China Electricity Council. China electricity statistical yearbook 2021. Beijing, China: China Statistics Press; 2021.
- [308] Lund H, Thellufsen JZ, Østergaard PA, Sorknæs P, Skov IR, Mathiesen BV. EnergyPLAN – Advanced analysis of smart energy systems. *Smart Energy* 2021;1:100007. <https://doi.org/10.1016/j.segy.2021.100007>.
- [309] Otanicar T, Taylor RA, Phelan PE. Prospects for solar cooling – An economic and environmental assessment. *Sol Energy* 2012;86(5):1287-99. <https://doi.org/10.1016/j.solener.2012.01.020>.
- [310] Teske S. Energy revolution: a sustainable pathway to a clean energy future for Europe. 2005. <http://eu.greenpeace.org/downloads/energy/EU25scenario2050.pdf>.
- [311] Luo S, Hu W, Liu W, Xu X, Huang Q, Chen Z, et al. Transition pathways towards a deep decarbonization energy system—A case study in Sichuan, China. *Appl Energy* 2021;302:117507. <https://doi.org/10.1016/j.apenergy.2021.117507>.
- [312] Hong L, Lund H, Mathiesen BV, Möller B. 2050 pathway to an active renewable energy scenario for Jiangsu province. *Energy Policy* 2013;53:267-78. <https://doi.org/10.1016/j.enpol.2012.10.055>.
- [313] He G, Lin J, Sifuentes F, Liu X, Abhyankar N, Phadke A. Rapid cost decrease of renewables and storage accelerates the decarbonization of China's power system. *Nat Commun* 2020;11(1):2486. <https://doi.org/10.1038/s41467-020-16184-x>.
- [314] Tan X, Li H, Guo J, Gu B, Zeng Y. Energy-saving and emission-reduction technology selection and CO₂ emission reduction potential of China's iron and steel industry under

BIBLIOGRAPHY

- energy substitution policy. *J Clean Prod* 2019;222:823-34. <https://doi.org/10.1016/j.jclepro.2019.03.133>.
- [315] Jang D, Kim K, Kim K-H, Kang S. Techno-economic analysis and Monte Carlo simulation for green hydrogen production using offshore wind power plant. *Energy Convers Manag* 2022;263:115695. <https://doi.org/10.1016/j.enconman.2022.115695>.
- [316] Sadeghi M, Kalantar M. Multi types DG expansion dynamic planning in distribution system under stochastic conditions using Covariance Matrix Adaptation Evolutionary Strategy and Monte-Carlo simulation. *Energy Convers Manag* 2014;87:455-71. <https://doi.org/10.1016/j.enconman.2014.07.010>.
- [317] Palisade. @RISK, <https://www.palisade.com/risk/>; 2022 [accessed 18 May 2022].
- [318] FRED Economic Data. Global price of LNG, Asia, <https://fred.stlouisfed.org/series/PNGASJPUSDM>; 2022 [accessed 18 May 2022].
- [319] ITC Trade Map. List of products imported by China, https://www.trademap.org/Product_SelCountry_TS.aspx?nvpm=1%7c156%7c%7c%7c%7c2711%7c%7c%7c4%7c1%7c1%7c1%7c2%7c1%7c1%7c3%7c1%7c1; 2022 [accessed 18 May 2022].
- [320] Heck N, Smith C, Hittinger E. A Monte Carlo approach to integrating uncertainty into the levelized cost of electricity. *Electr J* 2016;29(3):21-30. <https://doi.org/10.1016/j.tej.2016.04.001>.
- [321] Li B, Han Z, Meng X, Zhang H. Study on the influence of the design method of the ground source heat pump system with considering groundwater seepage. *Appl Therm Eng* 2019;160:114016. <https://doi.org/10.1016/j.applthermaleng.2019.114016>.
- [322] Wang E, Fung AS, Qi C, Leong WH. Performance prediction of a hybrid solar ground-source heat pump system. *Energy Build* 2012;47:600-11. <https://doi.org/10.1016/j.enbuild.2011.12.035>.
- [323] Dai L, Li S, DuanMu L, Li X, Shang Y, Dong M. Experimental performance analysis of a solar assisted ground source heat pump system under different heating operation modes. *Appl Therm Eng* 2015;75:325-33. <https://doi.org/10.1016/j.applthermaleng.2014.09.061>.
- [324] Wang W, Li F. Study on substitutable value of electric heating instead of coal heating in northern China under carbon constraints. *J Clean Prod* 2020;260:121155. <https://doi.org/10.1016/j.jclepro.2020.121155>.
- [325] Harbin Municipal People's Government. Measures for the administration of financial subsidy funds in Harbin for renovating coal-fired boilers and promoting clean energy use, http://www.harbin.gov.cn/art/2019/11/15/art_24408_812711.html; 2019 [accessed 4 July 2022].
- [326] Zhang Z, Zhou Y, Zhao N, Li H, Tohniyaz B, Mperejekumana P, et al. Clean heating during winter season in Northern China: A review. *Renew Sustain Energy Rev* 2021;149:111339. <https://doi.org/10.1016/j.rser.2021.111339>.
- [327] Thomson H, Liddell C. The suitability of wood pellet heating for domestic households: A review of literature. *Renew Sustain Energy Rev* 2015;42:1362-9. <https://doi.org/10.1016/j.rser.2014.11.009>.
- [328] Munawar MA, Khoja AH, Naqvi SR, Mehran MT, Hassan M, Liaquat R, et al. Challenges and opportunities in biomass ash management and its utilization in novel applications. *Renew Sustain Energy Rev* 2021;150:111451. <https://doi.org/10.1016/j.rser.2021.111451>.
- [329] Liu G, Dong X, Kong Z, Jiang Q, Li J. The role of China in the East Asian natural gas premium. *Energy Strategy Rev* 2021;33:100610. <https://doi.org/10.1016/j.esr.2020.100610>.

- [330] Ma C, Zhang Y, Li T. GIS-based evaluation of solar and biomass perspectives – Case study of China regions. *J Clean Prod* 2022;357:132013. <https://doi.org/10.1016/j.jclepro.2022.132013>.
- [331] Heilongjiang Bureau of Statistics. Heilongjiang statistical yearbook 2021. Beijing, China: China Statistics Press; 2022.
- [332] Chen Q, Xia M, Wang H, Liu W, Wang Z, Zhang X, et al. Evaluation indices set and decision-making method for regional "coal to electricity" optimal development mode. *AIP Conference Proceedings* 2019;2154(1):020003. <https://doi.org/10.1063/1.5125331>.
- [333] Pu L, Wang X, Tan Z, Wu J, Long C, Kong W. Feasible electricity price calculation and environmental benefits analysis of the regional nighttime wind power utilization in electric heating in Beijing. *J Clean Prod* 2019;212:1434-45. <https://doi.org/10.1016/j.jclepro.2018.12.105>.
- [334] Peng X, Tao X. Cooperative game of electricity retailers in China's spot electricity market. *Energy* 2018;145:152-70. <https://doi.org/10.1016/j.energy.2017.12.122>.
- [335] The State Council of the People's Republic of China. Working guidance for carbon dioxide peaking and carbon neutrality in full and faithful implementation of the new development philosophy, http://www.gov.cn/zhengce/2021-10/24/content_5644613.htm; 2021 [accessed 8 May 2022].
- [336] IEA. World energy outlook 2021. 2021. <https://www.iea.org/reports/world-energy-outlook-2021>.
- [337] Wang C, Chang Y, Zhang L, Pang M, Hao Y. A life-cycle comparison of the energy, environmental and economic impacts of coal versus wood pellets for generating heat in China. *Energy* 2017;120:374-84. <https://doi.org/10.1016/j.energy.2016.11.085>.
- [338] Mohamed U, Zhao Y-j, Yi Q, Shi L-j, Wei G-q, Nimmo W. Evaluation of life cycle energy, economy and CO₂ emissions for biomass chemical looping gasification to power generation. *Renew Energy* 2021;176:366-87. <https://doi.org/10.1016/j.renene.2021.05.067>.
- [339] Liu H, Andresen GB, Greiner M. Cost-optimal design of a simplified highly renewable Chinese electricity network. *Energy* 2018;147:534-46. <https://doi.org/10.1016/j.energy.2018.01.070>.
- [340] Lin J, He G, Yuan A. Economic rebalancing and electricity demand in China. *Electr J* 2016;29(3):48-54. <https://doi.org/10.1016/j.tej.2016.03.010>.
- [341] OECD. GDP long-term forecast, <https://data.oecd.org/gdp/gdp-long-term-forecast.htm>; 2018 [accessed 8 May 2022].
- [342] Liaoning Provincial Development and Reform Commission. Outline of the 14th five-year plan for economic and social development and long-range objectives through the year 2035 of Liaoning province. 2021.
- [343] Jilin Province Development and Reform Commission. Outline of the 14th five-year plan for economic and social development and long-range objectives through the year 2035 of Jilin province. 2021.
- [344] Heilongjiang Development and Reform Commission. Outline of the 14th five-year plan for economic and social development and long-range objectives through the year 2035 of Heilongjiang province. 2021.
- [345] China National Renewable Energy Centre (CNREC). China renewable energy outlook 2017. 2017.
- [346] Huber M, Weissbart C. On the optimal mix of wind and solar generation in the future Chinese power system. *Energy* 2015;90:235-43. <https://doi.org/10.1016/j.energy.2015.05.146>.
- [347] Electropaedia. Battery and energy technologies, https://www.mpoweruk.com/electricity_demand.htm; 2022 [accessed 8 May 2022].

BIBLIOGRAPHY

- [348] China National Renewable Energy Center (CNREC). Renewable energy data book. 2015.
- [349] Liu L, Wang Y, Wang Z, Li S, Li J, He G, et al. Potential contributions of wind and solar power to China's carbon neutrality. *Resour Conserv Recycl* 2022;180:106155. <https://doi.org/10.1016/j.resconrec.2022.106155>.
- [350] Campana PE, Li H, Zhang J, Zhang R, Liu J, Yan J. Economic optimization of photovoltaic water pumping systems for irrigation. *Energy Convers Manag* 2015;95:32-41. <https://doi.org/10.1016/j.enconman.2015.01.066>.
- [351] National Development and Reform Commission. Notice on matters concerning the 2021 renewable energy on-grid tariff policy, https://iam-sso.ndrc.gov.cn/gbssso/oauth/single?client_id=fgwportal&redirect_url=aHR0cHM6Ly93d3cubmRyYy5nb3YuY24veHhnaY96Y2ZiL3R6LzIwMjEwNi90MjAyMTA2MTFfMTI4MzA4OC5odG1s; 2021 [accessed 8 May 2022].
- [352] Global Energy Interconnection Development and Cooperation Organization (GEIDCO). Research on China's 14th five-year power development plan. 2020.
- [353] ERI China. China 2050 high renewable energy penetration scenario and roadmap study. 2015. <https://www.efchina.org/Attachments/Report/report-20150420/>.
- [354] IRENA. Renewable power generation costs in 2020. 2021. <https://www.irena.org/publications/2021/Jun/Renewable-Power-Costs-in-2020>.
- [355] IEA. Projected costs of generating electricity 2020. 2020. <https://www.iea.org/reports/projected-costs-of-generating-electricity-2020>.
- [356] National Bureau of Statistics of China. Average CO₂ emission factor of China's regional grids in 2011 and 2012, <https://www.ccchina.org.cn/archiver/ccchinacn/UpFile/Files/Default/20140923163205362312.pdf; 2013> [accessed 8 April 2021].
- [357] Ministry of Ecology and Environment of the People's Republic of China. Corporate greenhouse gas emissions accounting methods and reporting guidelines, https://www.mee.gov.cn/xxgk2018/xxgk/xxgk06/202203/t20220315_971468.html; 2022 [accessed 8 May 2022].
- [358] Li B, You L, Zheng M, Wang Y, Wang Z. Energy consumption pattern and indoor thermal environment of residential building in rural China. *Energy Built Environ* 2020;1(3):327-36. <https://doi.org/10.1016/j.enbenv.2020.04.004>.
- [359] EU. 2050 long-term strategy, https://climate.ec.europa.eu/eu-action/climate-strategies-targets/2050-long-term-strategy_en; 2020 [accessed 6 December 2022].
- [360] Terziotti LT, Sweet ML, McLeskey JT. Modeling seasonal solar thermal energy storage in a large urban residential building using TRNSYS 16. *Energy Build* 2012;45:28-31. <https://doi.org/10.1016/j.enbuild.2011.10.023>.
- [361] Durga S, Beckers KF, Taam M, Horowitz F, Cathles LM, Tester JW. Techno-economic analysis of decarbonizing building heating in Upstate New York using seasonal borehole thermal energy storage. *Energy Build* 2021;241:110890. <https://doi.org/10.1016/j.enbuild.2021.110890>.
- [362] Bird L, Lew D, Milligan M, Carlini EM, Estanqueiro A, Flynn D, et al. Wind and solar energy curtailment: A review of international experience. *Renew Sustain Energy Rev* 2016;65:577-86. <https://doi.org/10.1016/j.rser.2016.06.082>.
- [363] Bloess A, Schill W-P, Zerrahn A. Power-to-heat for renewable energy integration: A review of technologies, modeling approaches, and flexibility potentials. *Appl Energy* 2018;212:1611-26. <https://doi.org/10.1016/j.apenergy.2017.12.073>.

- [364] Hedegaard K, Münster M. Influence of individual heat pumps on wind power integration – Energy system investments and operation. *Energy Convers Manag* 2013;75:673-84. <https://doi.org/10.1016/j.enconman.2013.08.015>.
- [365] Liu D, Zhang G, Huang B, Liu W. Optimum electric boiler capacity configuration in a regional power grid for a wind power accommodation scenario. *Energies* 2016;9(3):144. <https://doi.org/10.3390/en9030144>.
- [366] Zhou J. Contraction Era, <https://card.weibo.com/article/m/show/id/2309634805261251706900>; 2022 [accessed 6 December 2022].
- [367] Yang T, Liu W, Sun Q, Hu W, Kramer GJ. Techno-economic-environmental analysis of seasonal thermal energy storage with solar heating for residential heating in China. *Energy* 2023;283:128389. <https://doi.org/10.1016/j.energy.2023.128389>.
- [368] Meha D, Pfeifer A, Duić N, Lund H. Increasing the integration of variable renewable energy in coal-based energy system using power to heat technologies: The case of Kosovo. *Energy* 2020;212. <https://doi.org/10.1016/j.energy.2020.118762>.
- [369] Kojima S, Asakawa K, Expectations for carbon pricing in Japan in the global climate policy context, in: Arimura TH, Matsumoto S (Eds.), *Carbon Pricing in Japan*, Springer Singapore, Singapore, 2021, pp. 1-21.
- [370] The World Bank. Population estimates and projections, <https://databank.worldbank.org/source/population-estimates-and-projections>; 2022 [accessed 5 October 2022].
- [371] Pupo-Roncallo O, Campillo J, Ingham D, Hughes K, Pourkashanian M. Large scale integration of renewable energy sources (RES) in the future Colombian energy system. *Energy* 2019;186:115805. <https://doi.org/10.1016/j.energy.2019.07.135>.
- [372] Pfeifer A, Krajačić G, Ljubas D, Duić N. Increasing the integration of solar photovoltaics in energy mix on the road to low emissions energy system – Economic and environmental implications. *Renew Energy* 2019;143:1310-7. <https://doi.org/10.1016/j.renene.2019.05.080>.
- [373] Pastore LM, Lo Basso G, Ricciardi G, de Santoli L. Synergies between Power-to-Heat and Power-to-Gas in renewable energy communities. *Renew Energy* 2022;198:1383-97. <https://doi.org/10.1016/j.renene.2022.08.141>.
- [374] Ishaku HP, Adun H, Jazayeri M, Kusaf M. Decarbonisation strategy for renewable energy integration for electrification of West African nations: a bottom-up EnergyPLAN modelling of West African power pool targets. *Sustainability* 2022;14(23):15933. <https://doi.org/10.3390/su142315933>.
- [375] Herc L, Pfeifer A, Duić N. Optimization of the possible pathways for gradual energy system decarbonization. *Renew Energy* 2022;193:617-33. <https://doi.org/10.1016/j.renene.2022.05.005>.
- [376] Qiu S, Lei T, Wu J, Bi S. Energy demand and supply planning of China through 2060. *Energy* 2021;234:121193. <https://doi.org/10.1016/j.energy.2021.121193>.
- [377] Liu W, Hu W, Lund H, Chen Z. Electric vehicles and large-scale integration of wind power – The case of Inner Mongolia in China. *Appl Energy* 2013;104:445-56. <https://doi.org/10.1016/j.apenergy.2012.11.003>.
- [378] Ma C, Hailu A, You C. A critical review of distance function based economic research on China's marginal abatement cost of carbon dioxide emissions. *Energy Econ* 2019;84:104533. <https://doi.org/10.1016/j.eneco.2019.104533>.
- [379] People's Government of Heilongjiang Province. Development Plan of New Energy and Renewable Energy Industry in Heilongjiang Province,

BIBLIOGRAPHY

- https://www.hlj.gov.cn/hlj/c108201/201101/c00_30643550.shtml; 2011 [accessed 6 December 2022].
- [380] Popovski E, Aydemir A, Fleiter T, Bellstädt D, Büchele R, Steinbach J. The role and costs of large-scale heat pumps in decarbonising existing district heating networks – A case study for the city of Herten in Germany. *Energy* 2019;180:918-33. <https://doi.org/10.1016/j.energy.2019.05.122>.
- [381] Novosel T, Ćosić B, Krajačić G, Duić N, Pukšec T, Mohsen MS, et al. The influence of reverse osmosis desalination in a combination with pump storage on the penetration of wind and PV energy: A case study for Jordan. *Energy* 2014;76:73-81. <https://doi.org/10.1016/j.energy.2014.03.088>.
- [382] Lu M, Guan J, Wu H, Chen H, Gu W, Wu Y, et al. Day-ahead optimal dispatching of multi-source power system. *Renew Energy* 2022;183:435-46. <https://doi.org/10.1016/j.renene.2021.10.093>.
- [383] Liu J, Guo T, Wang Y, Li Y, Xu S. Multi-technical flexibility retrofit planning of thermal power units considering high penetration variable renewable energy: The case of China. *Sustainability* 2020;12(9):3543. <https://doi.org/10.3390/su12093543>.
- [384] Yu S, Zhou S, Qin J. Layout optimization of China's power transmission lines for renewable power integration considering flexible resources and grid stability. *International Journal of Electrical Power & Energy Systems* 2022;135:107507. <https://doi.org/10.1016/j.ijepes.2021.107507>.
- [385] Gong L, Cao W, Liu K, Yu Y, Zhao J. Demand responsive charging strategy of electric vehicles to mitigate the volatility of renewable energy sources. *Renew Energy* 2020;156:665-76. <https://doi.org/10.1016/j.renene.2020.04.061>.
- [386] Ding N, Duan J, Xue S, Zeng M, Shen J. Overall review of peaking power in China: Status quo, barriers and solutions. *Renew Sustain Energy Rev* 2015;42:503-16. <https://doi.org/10.1016/j.rser.2014.10.041>.
- [387] Trading Economics. EU Carbon Permits, <https://tradingeconomics.com/commodity/carbon>; 2023 [accessed 11 April 2023].
- [388] Rockström J, Gaffney O, Rogelj J, Meinshausen M, Nakicenovic N, Schellnhuber HJ. A roadmap for rapid decarbonization. *Science* 2017;355(6331):1269-71. <https://doi.org/10.1126/science.aah3443>.
- [389] Ministry of Housing and Urban-Rural Development of the People's Republic of China. Planning and design standards for urban residential areas (GB50180-2018). Beijing: China Architecture & Building Press; 2018.

ACKNOWLEDGMENTS

Every story has an end. Doing my PhD in the Netherlands has been an exciting and challenging experience, both in my research career and in my personal life. The PhD journey is never a path that one takes alone. I would like to express my gratitude to all the people I have met and worked with. I am happy to have had you along the way.

First and foremost, I would like to thank my promoter, Prof. Gert Jan Kramer. I cannot ask for a better role model for being a real scientist. You let me know that it is meaningless to focus only on modeling and calculations; we researchers should give meaning to these numbers. You led me to see the bigger picture of my work rather than the quagmire of detail. You taught me to use simple and precise concepts to describe complicated issues and to be bold in making assumptions about future scenarios. Our fortnightly meeting was something that I always looked forward to. Your comments elevated the quality of my work and gave me the confidence to take the next step. Your visionary inspiration, critical guidance, and warm encouragement shaped me into a better researcher.

I am very grateful to my co-promoter, Dr. Wen Liu, for your help in both academic and private life. You picked me up and drove me to my studio on the first day I arrived in the Netherlands. You allayed all my anxieties about being alone in a strange environment. I remember and appreciate every effort you made to help me adapt quickly to working and living in the Netherlands. I am grateful for your numerous comments on each piece of my work for several rounds of revisions, even during the holidays. You were always available when I went for advice. You kept pulling me out of the struggle and back in the right direction. I have been very fortunate to have had you as my supervisor over the past years. Your instruction, support, and encouragement built my confidence and showed me the model of a great researcher and supervisor. It was you who escorted my PhD journey.

I would also like to express gratitude to those who have contributed to my work. Thanks to Dr. Renaldi Renaldi from the University of Oxford for sharing your knowledge on TRNSYS modeling, which answered my confusion. I want to thank Prof. Qie Sun from Shandong University and Prof. Weihao Hu from the University of Electronic Science and Technology of China for sharing data and valuable comments on Chapters 2 and 3. For Chapter 5, I thank Prof. Chris Spiersb at Utrecht University for your valuable and constructive feedback. Thanks to David Geerts for the Dutch translation.

I am also thankful for all the colleagues in the Energy & Resources Group of the Copernicus Institute of Sustainable Development at Utrecht University. Thank you for the welcoming working environment and amusing lunches and coffee breaks: Ana, Ivan, Matteo, Wina, Ernst, Blanca, Anand, Steven, Elena, Sara, Martin, Lucas, David, and all the others. I enjoyed drinking, gaming, and attending interesting workshops with you on the retreat days and away days. Special thanks go to my Chinese colleagues, Hui Yue, Jing Hu, Li Shen, Chenyue

ACKNOWLEDGMENTS

Zhang, Shiyu Ding, Zhi Gao, and Yun Wu. It was relaxing and warm to speak the mother tongue in a foreign country. I am so happy and proud to be part of the Energy & Resources Group. I collect every smile and remember every moment we spent together as a big family.

The financial support from the China Scholarship Council is gratefully acknowledged. Thank you for offering me the opportunity to pursue the PhD degree and explore the world.

I appreciate very much the examination committee: Prof. Ernst Worrell, Prof. Henrik Lund, Prof. Xiliang Zhang, Prof. Weihao Hu, and Dr. Wina Crijns-Graus. Thank you very much for taking the time to review and provide valuable comments on my dissertation.

My gratitude also goes to my supervisor, Prof. Qie Sun, during my master's period at Shandong University. Thank you for revising my papers and study abroad documents word by word and sparing no effort in providing various academic resources. From academic research to philosophy of life, I have greatly benefited from applying what I have learned. Without your support and encouragement, I would not have embarked on the journey to pursue PhD degree.

Great thanks are given to my lifelong friends: Hongli Cao, Yu Ma, Bing Han, Xuefei Lv, Yutong Han, Qianye Hui, Qiyao Rong, Song Liu, Yu Sun, Guochang Chen, Dewei Hou, Hao Wu, and Ruiwen Zhang. You have supported and encouraged me at each stage of my life since middle school. Although we have not met each other often since I went to the Netherlands, you always came to me and gave me a huge welcome every time I went back to China, no matter where you were. Your continuous company has made me never feel alone in tough times.

During the past years, I have been so lucky to chair the Association of Chinese Students and Scholars in Utrecht (ACSSNL-Utrecht) and then the Association of Chinese Students and Scholars in the Netherlands (ACSSNL). I enjoyed every moment of working together with you guys: Ding Ding, Qizhi Ren, Aiyi Li, Geng Chen, Quanxing Wan, Yuxin Liu, Yifan Chen, Yingying Geng, Xin Zhang, Wenrui Cao, Jiahang Li, Peijin Li, Ziyang Liu, Jiabin Li, Weichao Wang, and all the others. Special thanks go to Counselor Qingyu Meng, Counselor Ping Luo, Wei Bai, Haifeng Liu, Tao Sun, Ye Xu, and Yan Liang. Thank you for all the consideration and support for me.

I would like to thank all the colleagues in the PhD Network Utrecht (Prout) and the Utrecht PhD Party (UPP). It was my great honor to work with you to represent PhD candidates, to protect their rights, and to improve the quality of the PhD experience. Sincere thanks are given to Prof. Marijk van der Wende and Dr. Margreet de Lange for your support of my work. I would also like to thank the program board of the Netherlands-Asia Honours Summer School (NAHSS). Our yearly collaboration helps Dutch students gain knowledge of Southeast Asia and China.

ACKNOWLEDGMENTS

My deepest gratitude goes to my beloved parents. You never question or interfere with my choices but give endless and unconditional love, patience, support, and encouragement. You are my motivation to keep going, and I know that you are always there waiting to give me a big hug. I am so grateful to have a warm family. Although there were three years when I could not go home due to the lockdown during the COVID-19 pandemic, you made me feel surrounded by love and care and helped me get through the hard times.

Every story has an end, but every end is a new beginning. I will hold all your support and keep moving to live, experience, feel, and love.

纸短情长，伏惟珍重。

Tianrun Yang

October, 2023

Utrecht, the Netherlands

CURRICULUM VITAE

Tianrun Yang was born on July 11, 1992 in Fushun, China. From 2011 to 2015, he studied Energy and Environment System Engineering and Finance (dual degree) at Shandong University. After graduation, he started a master's program under the supervision of Prof. Ronald Wennersten and Prof. Qie Sun at the same university, majoring in Power Engineering and Engineering Thermophysics. In 2018, he completed his master's thesis, Design and Optimization of the Cold Energy Storage System Based on Phase Change Materials. After completing his master's degree, he joined the Energy & Resources Group of the Copernicus Institute of Sustainable Development of Utrecht University in October 2018 as a PhD candidate under the supervision of Prof. Gert Jan Kramer and Dr. Wen Liu. His research interests include seasonal thermal energy storage, energy system decarbonization, energy system modeling, and renewable energy utilization.

PUBLICATIONS

Yang T, Liu W, Kramer GJ, Sun Q. State of the art review of seasonal sensible heat storage. *Energy Proceedings* 2019;5:4255.

Yang T, Liu W, Kramer GJ, Sun Q. Seasonal thermal energy storage: A techno-economic literature review. *Renewable and Sustainable Energy Reviews* 2021;139:110732.

Yang T, Liu W, Sun Q, Hu W, Kramer GJ. Techno-economic-environmental analysis of seasonal thermal energy storage with solar heating for residential heating in China. *Energy* 2023;283:128389.

Yang T, Liu W, Kramer GJ. Integrated assessment on the implementation of sustainable heat technologies in the built environment in Harbin, China. *Energy Conversion and Management* 2023;279:116764.

Yang T, Liu W, Kramer GJ. Seasonal thermal energy storage employing solar heat: A case study of Heilongjiang, China exploring the transition to clean heating and renewable power integration. *Renewable Energy* 2023.